Study of Thermal Instability in Nanofluids

THESIS

Submitted to
Babasaheb Bhimrao Ambedkar University
(A Central University)
Lucknow

BABASAHEB
BHIMRAO
AMBEDKAR
UNIVERSITY

LUCKNOW
प्रज्ञा शील करूणा
ESTABLISHED 1996

for the award of the Degree of

Doctor of Philosophy

in

APPLIED MATHEMATICS

Under the supervision of
Prof. B.S. BHADAURIA

Research Scholar
VINEET KUMAR
Enrollment No. 056/13

DEPARTMENT OF APPLIED MATHEMATICS
SCHOOL FOR PHYSICAL SCIENCES
BABASAHEB BHIMRAO AMBEDKAR UNIVERSITY
(A CENTRAL UNIVERSITY)
VIDYA VIHAR, RAEBARELI ROAD, LUCKNOW-226 025
UTTAR PRADESH, INDIA

2018

Study of Thermal Instability in Nanofluids

THESIS

Submitted to
Babasaheb Bhimrao Ambedkar University
(A Central University)
Lucknow

BABASAHEB
BHIMRAO
AMBEDKAR
UNIVERSITY
LUCKNOW
प्रज्ञा शील करुणा
ESTABLISHED 1996

for the award of the Degree of

Doctor of Philosophy

in

APPLIED MATHEMATICS

Under the supervision of
Prof. B.S. BHADAURIA

Research Scholar
VINEET KUMAR
Enrollment No. 056/13

DEPARTMENT OF APPLIED MATHEMATICS
SCHOOL FOR PHYSICAL SCIENCES
BABASAHEB BHIMRAO AMBEDKAR UNIVERSITY
(A CENTRAL UNIVERSITY)
VIDYA VIHAR, RAEBARELI ROAD, LUCKNOW-226 025
UTTAR PRADESH, INDIA

2018

Dedicated

to

My Family Members

DECLARATION

I declare that the work embodied in this Ph.D. thesis entitled as "**Study of Thermal Instability in Nanofluid**" is carried out by me under the supervision of Prof. B.S. Bhadauria, Department of Applied Mathematics, Babasaheb Bhimrao Ambedkar University (A Central University) Lucknow, India. The information presented in this Ph.D. thesis has not been submitted for the award of any degree or diploma. I declare that I have faithfully acknowledged, given credit to and referred to the research workers whenever their works have been cited in the text and the body of the thesis. I further declare that I have not willful lifted up some others work, para, text, data, results, etc. reported in the journals, books, magazines, reports, dissertations, thesis, etc., or available at websites and included them in this thesis and cited my own work.

I also declare that the thesis is essentially free from all kinds of plagiarism.

Vineet Kumar

Date:03/10/2018

Vineet Kumar

(Research Scholar)

CERTIFICATE

This is to certify that the thesis titled **"Study of Thermal Instability in Nanofluids"** submitted by **Mr. Vineet Kumar** is an original research work and has not been previously submitted in part or full for the award of any other degree or diploma to this or any other university.

The thesis submitted to the Babasaheb Bhimrao Ambedkar University Lucknow satisfies all the requirements as stipulated in the *Doctor of Philosophy (Ph.D.) regulations -1999 as amended in 2008/2010/2013* and it is fit for submission and evaluation for the award of the degree of Doctor of Philosophy of the University.

Date: 03.10.2018

Supervisor 03.10.2018

Head of the Department 03.10.2018

Professor B. S. Bhadauria
Head
Department of Mathematics
B.B. Ambedkar University, Lucknow

Acknowledgements

First of all I express my gratitude to Almighty God who provided me enough strength, knowledge and health to do this research work. On the occasion of presenting my Ph.D. thesis, my sacred duty is to express my indebtedness from the inner core of the heart. This work could not have been completed without his blessings

I am extremely grateful to my eminent Supervisor, Prof. B.S. Bhadauria for his valuable guidance, scholarly inputs, constant encouragement and moral support, which I received during the entire period of my research work. This achievement was possible only because of the unconditional support provided by him. His devotion of duty would be a role model for me in the future, and his constructive criticism proved to be a boon in the study.

I am thankful to Dr. B.K. Singh, Dr. Mukesh Kumar Awasthi, Dr. Rahul Varshney, Dr. Maitri Verma for their kind cooperation, encouragement and valuable suggestion during the period of my study.

I express my deepest thanks from the bottom of my heart to all my dear friends Dr. Manoj Kumar Singh, Dr. Ajay Singh, Mr. Promod Kumar for making my stay in the campus a pleasant one with lively discussions and all supports. I thank all the staff members, Mr. Rakesh and Mr. Vinay Kumar Sahu of the Department for their cooperation and help during the course of my research work.

I would like to express my heart-felt and affectionate gratitude to my parents, my mother, Smt. Ram Bai Gupta and my father, Sri Sampat Lal Gupta, for the patience and encouragement shown by them during this period, I dedicate this thesis to them. Without them this thesis could never come to completion. My special thanks goes to my family members, faculty members of other department and my roommates for their support from behind the scenes during my studies without which I would not have achieved this work.

I gratefully acknowledge the funding agency, the University Grant Commission (UGC) of the Government of India, for providing financial support, to complete my thesis work, in the form of UGC-CSIR Junior Research Felloship(02-09-2013 to 01-09-2015) and Senior Research Felloship(02-09-2015 to 01-09-2018).

Vineet Kumar

Preface

The thesis entitled **"Study of Thermal Instability in Nanofluids"** comprising of analytical/numerical solutions of some problems related with the topic, is an outcome of the research work carried out by me during the course of investigations under the supervision of Dr. B.S. Bhadauria, Professor, Department of Mathematics, School of Physical and Decision Sciences, Babasaheb Bhimrao Ambedkar University, Lucknow, India.

Owing to the suspension of nanosize particles of metal in the base fluid, the nanofluids are being used as heat energy carriers due to their enhanced abilities over ordinary fluids. The presence of a few quantity of nanoparticles in base fluids causes a significant enhancement in the heat transfer. This heat transfer characteristic of nanofluids depends on both the thermo-physical properties of the base fluid and the suspended nanoparticles. The nanofluids found a wide range of applications in industrial, commercial, residential, medical and transportation sectors.

The **first chapter** consists of basic terminology used in thesis, definitions relevant to physical phenomenon, hydrodynamic equations and laws, applied analytical and numerical methods, literature review and real world applications in precise way.

In the **second chapter** the effect in thermal instability of nanofluid saturated porous layer confined between two horizontal surface in presence of internal heat source and rotation about vertical axis with revised boundary condition is studied. The revised boundary conditions are in practical because the value of temperature at boundaries can be adjusted but not the concentration in case of nanoparticles, and so at boundaries the nanoparticle flux is assumed to be constant. Further, linear stability analysis is performed subject to these boundary conditions. Darcy-Brinkman model is studied using Galarkin method to carried out linear stability analysis by depicting the behavior of Rayleigh number with respect to wave number taking different values of the other parameters. The effect of internal heat source is destabilising, the effect of rotation is stabilising the system whereas the instability of vertical throughflow depends on the direction of nanofluid flow.

The **third chapter** deals with the thermal instability of non-Newtonian power-law nanofluid saturated porous layer, confined between two horizontal surfaces in presence of throughflow. Extended Darcy's model together with the Oberbeck-Boussinesq approximation has been employed. Linear stability analysis is performed subject to various boundary conditions. The effect of parameters corresponding to the throughflow (Péclet number Pe), and the power-law index of the nanofluid has been investigated. These parameters shift the position of the neutral stability curve and also the value of critical Rayleigh number.

In the **fourth chapter** thermal instability in a nanofluid saturated porous medium under the effects of gravity modulation and internal heating is investigated. The non−uniform vertical vibrations of the system, which can be realized by oscillating the system vertically is considered to vary sinusoidally with time. Linear and nonlinear stability analyses have been performed to investigate onset of convection and heat/mass transfer in the system. Linear stability analysis is made using Venezian approach, however, for nonlinear stability analysis truncated Fourier series expansions is used. The effects of various physical parameters have been investigated on heat and mass transfer. Linear system shows that there is a particular range of frequency of modulation where the system is stabilizing and destabilizing. The duel effect of this nature is due to the presence of internal heating of the system. It is found that gravity modulation can be used effectively to regulate the stability of the system. Further, the effect of internal Rayleigh number is to destabilize the system

The **fifth chapter** deals with linear and non-linear stability analyses of the convective flow in a porous layer saturated by nanofluid, under rotational speed modulation rotating about a vertical axis. The revised boundary conditions are used as they are more realistic. Perturbation method has been adopted to execute the linear stability analysis, while a truncated Fourier series method has been used for weak non-linear analysis. The amendment in the critical Rayleigh number due to rotational speed modulation has been noticed using linear stability analysis. The concentration and thermal Nusselt numbers are obtained by performing a weak non-linear stability analysis, and their behavior is explored by solving

the time dependent(Non-autonomous in nature) finite amplitude equations using fourth order Runge-Kutta method. The obtained results are depicted graphically, and discussed in details. It is observed that the modulated rotational speed have stabilizing effect on the system for different values of the modulation frequency.

In the **sixth chapter**, the variation of thermal instability in an electrically conducting nanofluid layer under magnetic field modulation is studied. Time periodic magnetic field (i.e., magnetic field modulation) is associated in vertical direction together with certain boundary conditions. The perturbation technique has been adopted to perform both linear stability analysis and weak-nonlinear analysis. The non autonomous Ginzburg-Landau equation is derived under the assumptions of Boussinesq approximation and small-scale convective motion. In all convection measuring quantities (Nusselt number, nanoparticle concentration Nusselt number, Rayleigh number), the effect caused by magnetic field modulation has been obtained. Finally, the results have been discussed in detail, and depicted graphically.

In the **last chapter**, the heat transfer in a horizontal nanofluid layer is investigated by means of weakly non-linear stability analysis. A set of new boundary conditions for the nanoparticle fraction, which is physically more realistic has been considered. The new boundary condition is based on the assumption that the nanoparticle fraction adjusts itself so that the nanoparticle flux is zero on the boundaries. The governing equations for this problem are reduced to Ginzburg–Landau equation and solved by homotopy analysis method (HAM), and numerical method Mathematica NDSolve. The obtained results are valid for the whole solution domain with high accuracy. Nusselt number and Nanoparticle Nusselt number are calculated for different values of parameters. The results have been depicted graphically.

Contents

List of Figures

Nomenclature

Latin Symbols

c	Specific heat of material
d	Dimensional depth of fluid/porous layer
Da	Darcy number, $Da = \dfrac{\bar{\mu}K}{\mu d^2}$
D_B	Brownian diffusion coefficient
D_T	Thermophoretic diffusion coefficient
E	Energy field
E_R	Residual error
$\vec{g}$	Gravitational field
h	Controlling parameter
H	Magnetic field
K	Permeability of porous medium
k_B	Boltzmann constant
Le	Lewis number, $Le = \dfrac{\kappa_T}{D_B}$
n	Power law index
N_A	Modified diffusivity ratio, $N_A = \dfrac{D_T(T_h - T_c)}{D_B T_c(\phi_1 - \phi_0)}$
N_B	Modified particle-density increment, $N_B = \dfrac{\delta(\rho c)_p(\phi_1 - \phi_0)}{(\rho c)_f}$
Nu	Nusselt number
Nu_ϕ	Concentration Nusselt number
p	Pressure
Pe	Peclet number
Pm	Magnetic Pradtl number, $Pm = \dfrac{\nu_m\ (\rho c)_f}{\kappa_m}$

Pr	Pradtl number, $Pr = \dfrac{\mu}{\rho_f \ \kappa_T}$
q	Embedding parameter
Ra	Thermal Rayleigh-number
Ri	Internal Ryleigh number , $Ri = \frac{\eta d^2}{\kappa_T}$
Rn	Concentration Rayleigh number, $Rn = \dfrac{(\rho_p - \rho)(\phi_1 - \phi_0) g_0 K d}{\mu \kappa_T}$
Rm	Basic density Rayleigh number, $Rm = \dfrac{[\rho_p \phi_0 + \rho(1 - \phi_0)] g_0 K d}{\mu \kappa_T}$
t	Time
T	Temperature
T_c	Temperature at the upper wall
T_h	Temperature at the lower wall
Ta	Taylor number
$\mathbf{v}$	Fluid velocity(u, v, w)
V	Constant fluid velocity
$\mathbf{v}_D$	Darcy velocity
V_f	Volume of void
V_m	Volume of material
Va	Vadasz number, $Va = \frac{\varepsilon_p Pr}{Da}$
(x^*, y^*, z^*)	Cartesian coordinates

Greek symbols

α	Wave number
β	Proportionality factor
χ	Perturbation parameter
ε	Porosity
η	Internal heat source
γ/σ	Heat capacity ratio
$\dot{\gamma_m}$	Shear rate of power law nanofluid
κ	Thermal diffusivity of nanofluid
κ_m	Thermal diffusivity of porous medium

κ_p	Thermal diffusivity of nanoparticle
κ_T	Effective thermal conductivity of porous medium
μ	Viscosity
$\bar{\mu}$	Effective viscosity
ν	Magnetic viscosity
ω	Rotational frequency of modulation
Ω	Frequency of modulation
Ω_R	Rotational angular velocity
ϕ	Concentration of nanofluid
ψ	Stream function
ρ	Density of material
ρ_f	Density of base fluid
ρ_p	Density of nanoparticle
ρc	Heat capacity ratio
$(\rho c)_m$	Effective heat capacity of the porous medium
$(\rho c)_p$	Effective heat capacity of the nanoparticle material
τ	Time
τ_m	Shear stress of power law nanofluid
ξ	Amplitude of modulation

Subscripts

b	Basic solution
bf	Base fluid
p	Nanoparticle
nf	Nanofluid

Superscripts

’	Perturbation variable

Operators

∇^2	$\dfrac{\partial^2}{\partial x^2} + \dfrac{\partial^2}{\partial y^2} + \dfrac{\partial^2}{\partial z^2}$

Chapter 1

Introduction

Fluids that contain suspensions of nanometer size particles (usually 2-100 nm) in base fluids are termed as "nanofluids". Consequently very small quantities of nanoparticles(such as metal or metallic oxide: Cu, Cuo, Al_2O_3) submerged in the base fluids(commonly water and ethyl glycol), enhanced the effective thermal conductivity of these mixtures significantly. This technology is popular among the researchers since 1990's to first two decades of the 21st century. All those industries deal with heat transfer in some or the other way, have a strong need for improvement of heat transfer mediums. This could possibly be nanofluids, because of some potential benefits over normal fluids

- large surface area provided by nanoparticles for heat exchange.
- reduced pumping power due to enhanced heat transfer.
- minimal clogging.
- new innovation systems leading to savings of energy and cost.

1.1 Characteristics of Nanofluids

Enhancement of thermal conductivity is an important consideration for improving the heat transfer characteristics of regular liquids. Since the solid metal has a large thermal conductivity compared to the fluid, therefore the thermal conductivity of that base fluid is expected to improve with the suspension of solid particles in the base fluid.

1.2 Methods of Preparation and Processing

1.2.1 Production of Nanoparticles

Nanoparticles are made in two ways namely physical processes and chemical processes. Physical techniques include mechanical grinding and inert gas condensation technology while Chemical processes include spray pyrolysis, thermal spraying and chemical precipitation.

1.2.2 Preparation of Nanofluids

There are two ways to make a nanofluid, by one-step process or two step process. In the one-step process nanoparticles are simultaneously produce and disperses into the base fluid, whereas with the process of two steps, nanoparticles are made and then dispersed in the liquid. The main disadvantage of the two-step process is that nanoparticles can agglomerate before the nanoparticles to be suspended in the liquid. The one-step process is favorable among the researchers because it prevents oxidation of nanoparticles.

- In the one-step process the particles in the fluid are formed together and dispersed(Yu et. al., 2007). In this method the drying, storage, transport, and the dispersion of nanoparticles such types of process are avoided, hence the agglomeration of nanoparticles decreases, and the stability of the fluid increases. One-step processes can prepare nanoparticles evenly and the particles can be suspended in the base fluid. The method protects unwanted particle aggregation quite well. One-step physical method can not synthesize nanofluids extensively, and the cost is also high, so the one-step chemical method in industries is growing rapidly.

- The two-step method is the extensively used method(Lee et al., 1999) for preparation of nanofluids. The nanoparticles, nanofiibers, nanotubes used in this method are first produced in the form of dry powder by chemical or physical methods, then nanosized powder is dispersed in the liquid. The second processing phase is executed with the help of magnetic force movement, ultrasonic movement, high shear mixture, homogenizing machine and ball milling. Two-step method is the most economical method

of producing nanofluids on a large scale, because nanopowder synthesis technology is already being used to the industrial production level. Due to high surface area and surface activity, nanoparticles have total tendency to agglomerate each other. The use of surfactant is an important technique to increase the stability of nanoparticles in liquids. However, the efficiency of surfactant is also a major concern under high temperatures, especially for high temperature applications. Nanoparticles in most materials discussed are most commonly produced in the form of powders(Yu et al., 2007). Such a two-step process works well in some cases, such as nanofluids consisting of oxide nanoparticles dispersed in deionized water(Lee et al., 1999)].

1.3 Nanofluid Properties

Physical behavior of nanofluid is similar to normal fluid, so the nanofluids should be in accordance with the physical properties of a normal fluid such as thermal conductivity, specific heat, viscosity, etc. Nanofluid is the heterogeneous mixture of normal fluid and nanoparticles(up to 5%), so here theory of mixture will be effective. The nanofluids have been looked upon as flow and heat-transfer fluids of the future due to unprecedented combination of characteristic features desired in energy systems (fluid and thermal systems):

- Increased thermal conductivity at low nanoparticle concentrations.
- Strong temperature-dependent thermal conductivity.
- Non-linear increase in thermal conductivity with nanoparticle concentration.
- Increase in boiling critical heat flux (CHF).

1.3.1 Thermal Conductivity of Nanofluid

Thermal conductivity is a heat transport property of the material, which is defined as the ratio of energy flow through the surface and the local temperature gradient. Nanofluids have received high attention during the first decade of the twenty first century and all the research to evolve around these concepts are due to the experimental value of thermal conductivity.

High conductivity values of some nanofluids accomplish for future heat transfer media. There are so many method to measure the thermal conductivity of nanofluids some of them are as follows.

- Transient Hot Wire
- Transient Plate Source
- Steady Conduction Between Plates or Cylinders
- Laser Heating

Nanofluid thermal conductivity model has been proposed by Hamilton and Crosser (1962), which are effective for calculating thermal conductivities of fluids with nano-sized particles predict the enhanced thermal conductivities of the nanofluids because the models do not include any dependence on particle size. These superiority of nanofluids over the base fluids make nanofluids to be considered the next generation heat transfer fluids. Fluid thermal conductivity models have been proposed by Maxwell (1892) and Hamilton and Crosser (1962)

Hamilton-Crosser model for nanoparticles

$$\frac{\kappa_{nf}}{\kappa_{bf}} = \frac{\left(\frac{\kappa_p}{\kappa_{bf}} + 2\right) - 2\phi\left(1 - \frac{\kappa_p}{\kappa_{bf}}\right)}{\left(\frac{\kappa_p}{\kappa_{bf}} + 2\right) + \phi\left(1 - \frac{\kappa_p}{\kappa_{bf}}\right)} \tag{1.3.1}$$

Hamilton-Crosser model for nanotubes

$$\frac{\kappa_{nf}}{\kappa_{bf}} = \frac{\left(\frac{\kappa_p}{\kappa_{bf}} + 2.75\right) - 2.75\phi\left(1 - \frac{\kappa_p}{\kappa_{bf}}\right)}{\left(\frac{\kappa_p}{\kappa_{bf}} + 2.75\right) + \phi\left(1 - \frac{\kappa_p}{\kappa_{bf}}\right)} \tag{1.3.2}$$

1.3.2 Specific Heat Capacity of Nanofluid

The heat capacity term of the nanofluid has been incorporated into the energy equation, therefore it is important to be able to calculate it accurately. There are two types of correlations, which are commonly used by researchers given as follows

$$c_{nf} = (1 - \phi)c_{bf} + \phi c_p \tag{1.3.3}$$

simply the rule of mixtures applied to heat capacity

$$(\rho c)_{nf} = (1-\phi)(\rho c)_{bf} + \phi(\rho c)_{p} \tag{1.3.4}$$

Second one is the best specific heat correlation to use in predicting behavior in nanofluids.

1.3.3 Viscosity of Nanofluid

At a molecular scale, interaction between the different molecules in a fluid is a consequence of viscosity. It can also be interpreted as friction between the molecules in the fluid. Analogous to friction between moving solids, viscosity is determined by the sufficient energy required to make the fluid flow conveniently. The viscosity of nanofluids is highly dependent on the nanoparticle volume fraction. In case of nanofluids there are several techniques available in literature for the calibration of nanofluid viscosity. Models are to be used in various physical configuration suggested by Brinkman and Einstein (1999),

$$\mu = \frac{\mu_{bf}}{(1-\phi)^{2.5}} \tag{1.3.5}$$

$$\mu = \mu_{bf}(1+2.5\phi) \tag{1.3.6}$$

Table 1.1: Thermophysical properties of four base fluids at $300°K$

Base fluids	μ_{bf}	ρ_{bf}	κ_{bf}	$\beta_{bf} * 10^5$	c_{bf}
Water	0.00089	997	0.613	21	4179
Ethylene Glycol	0.0157	1114.4	0.252	65	2415
Engine Oil	0.486	884	0.144	70	1910
Glycerine	0.799	1259.9	0.286	48	2427

Table 1.2: Thermophysical properties of nanoparticles at $300°K$

Nanoparticles	ρ_p	κ_p	$\beta_p * 10^5$	c_p
Copper	8933	401	1.67	385
Copper Oxide	6320	76.5	1.8	531.8
Silver	10500	429	1.89	235
Alumina	3970	40	0.85	765
Titania	4250	8.9538	0.9	686.2

Table 1.3: Thermophysical properties of nanofluids for $\phi = 0.06$ at $300°K$

Nanofluids	ρ_{nf}	c_{nf}	$\beta_{nf} * 10^5$	κ_{nf}
W - Cu	1473.25	4123220.35	19.8402	0.72981
W-CuO	1316.47	4118526.61	19.8480	0.72743
W-Ag	1567.27	4064918.05	19.8534	0.72985
W-Al_2O_3	1175.47	4099091.05	19.7910	0.72483
W-TiO_2	1192.27	4091849.05	19.7940	0.70808
EG - Cu	1583.52	2736151.74	61.2002	0.30016
EG-CuO	1426.74	2731458.00	61.2080	0.29975
EG-Ag	1677.54	2677849.44	61.2134	0.30016
EG-Al_2O_3	1285.74	2712022.44	61.1510	0.29930
EG-TiO_2	1302.54	2704780.44	61.1540	0.29617
EO - Cu	1366.94	1793485.90	65.9002	0.17154
EO-CuO	1210.16	1788792.16	65.9080	0.17141
EO-Ag	1460.96	1735183.60	65.9134	0.17154
EO-Al_2O_3	1069.16	1769356.60	65.8510	0.17126
EO-TiO_2	1085.96	1762114.60	65.8540	0.17021
G - Cu	1720.29	3080662.96	45.2202	0.34064
G-CuO	1563.51	3075969.22	45.2280	0.34012
G-Ag	1814.31	3022360.66	45.2334	0.34065
G-Al_2O_3	1422.51	3056533.66	45.1710	0.33954
G-TiO_2	1439.31	3049291.66	45.1740	0.33555

1.4 Modes of Heat Transfer

The study of heat transfer is directed to assess the rate of flow of energy, both in the form of heat through the boundary of a system under the constant and transient conditions, and the determination of the temperature under the stable and transient conditions, the total information of system will be provided in terms of temperature gradient and rate of change in temperature with respect to time at different places and times.

1.4.1 Conduction

Conduction is a type of energy transfer mechanism, propagate in the form of heat occur due to temperature difference in any solid or any phase of material. This method of energy transfer recognize microscopically by movement of free electron flow from higher to low energy levels, lattice vibration and molecular collision. Although no macroscopic mass movement is involved.

1.4.2 Radiation

Thermal radiation is a type of heat transport phenomena in any phase of material, in which the electromagnetic wave propagate through the material and causes rise in temperature. Actually the electromagnetic spectrum of the limited wave length, is emitted at all surfaces, irrespective of the temperature. Such waves incident on surfaces of body is absorbed and therefore radiation heat transfer takes place between surfaces at different temperatures. No medium is required for such type of heat transfer, but the surfaces of material should be in visual contact for direct radiation.

1.4.3 Convection

In convection, it is estimated that the heat can be transferred at the flow of the fluid molecules. The energy transfer is by combined molecular diffusion and bulk flow. This mode is independent of the properties of the surface material and depends only on the fluid properties. The convective mechanism can be divided into the following types of convection.

- **Natural convection** is a practically possible mechanism in which energy can be transported in fluid caused by density differences, occurring due to temperature gradient without any external force. The examples are boiling of water, wind circulation, oceanic circulation and mantle convection etc.

- **Forced convection** is another form of heat transport in which fluid motion is controlled by external forces. This can be done with a suction machine, fan, pump, or other device. Forced convection occurs in air cooling of hot electrical components on a stack of printed circuit boards by use of fan.

- Convection and forced convection occurred simultaneously in the system, this physical phenomenon is known as **Mixed convection**. The result of mixed convection would be if a fan is used to force the air upward or downward through the circuit boards, thereby affecting the buoyancy flow.

1.5 Some Preliminaries

This section introduces some further distinctions and terminology for the ensuing discussion of action.

1.5.1 Newtonian and non-Newtonian fluids

In **Newtonian** fluid, viscosity is proportional to shear stress. Mineral oil, water and alcohol are some examples of Newtonian fluid. Some violated effect is found in **non-Newtonian** fluid i.e. there is no linear relation between viscosity and shear stress, for example honey, paint, glue, blood etc. Further, highly viscous fluid is also a kind of non-Newtonian fluid which is centre point of research and industrial applications.

1.5.2 Porous medium

A material which have solid matrix with interconnected void(pore) so that fluid molecules move easily in it, is known as porous material or porous medium. The example of porous medium are biological tissues (e.g. bones), rocks, foams, sand, human lung, wood, ceramics and soils. In a porous medium, the structure of pores with respect to shape and size is not similar.

1.5.3 Porosity

It is ratio of the volume of the voids to the total volume of the porous medium. The value of porosity of any porous domain lies in the unit interval. Let V_f denotes the volume of the fluid (voids), and V_m denotes the volume of the material (total volume), then the porosity ε is given by,

$$\varepsilon = \frac{V_f}{V_m} \tag{1.5.1}$$

1.5.4 Permeability

It is a measure of the convince with which a fluid can easily pass through a porous medium. The degree to which porous within the material is inter-connected is known as effective porosity. It is intrinsic property of the material.

1.5.5 Throughflow

Throughflow is the flow of a fluid into a system, or region forcibly without taking interest of pressure gradient between this region. System stability depends on the direction of throughflow due this stability of the system is affected. This concept is used to control the convective mechanism in engineering sciences, industries, geophysics etc.

A new convective parameter Pe (Péclet number) has come into existence which is responsible to govern the heat and mass transport in the system. According to direction of flow Pe is positive(i.e. upward throughflow) or Pe is negative(i.e. downward throughflow). Mathematical expression is as follows,

$$Pe = \frac{Vd}{\kappa}, \tag{1.5.2}$$

where V is the fluid velocity at basic state in z direction, κ is thermal diffusivity and d is depth of fluid layer.

1.5.6 Internal heating

Internal heating is a property, preserve by celestial bodies in the form of chemical reaction, nuclear fusion and decaying of radioactive materials, through which the celestial objects remains warm and active. The earth have thermal gradient between the interior core and exterior of the earth's crust due to the internally filled magma, helps convective flow. Therefore, the role of internal heat generation becomes very important in several applications that include geophysics, metal casting, reactor safety analyses. This term sits in the energy equation of convective problem. In this work, it is considerd as a convective parameter Ri, which is given by

$$Ri = \frac{\eta d^2}{\kappa}, \tag{1.5.3}$$

where η is the internal heat coefficient.

1.5.7 Modulation

In convective problem, a real challenges to regulate the convection as per the requirement, therefore modulation is required. It is a technique by which the stability of system can be controlled. This phenomenon becomes useful for industrial research to save money, energy and time etc. Scientists are postulating the theory and doing research with modulation effect in many practical problem. Many types of modulations are used by the authors in their studies such as **temperature**, **gravity**, **rotation** and **magnetic** field modulation. When modulation is applied to a problem, two additional parameters, amplitude and frequency of modulation appear in the system. These parameters provide control on convective mechanism either by increasing or decreasing their values.

Gravity Modulation

The variable gravitational field can be realized by vertically oscillating the system, many of the complex forces are responsible for it. One can easily see this phenomenon in space laboratory experiments, in areas of crystal growth, in atmospheric sciences etc. This idea has received much attention of the researchers using it as a tool to improve the heat and mass transfer rate. The controlling of convective instabilities by thermo-gravitational vibration is more interesting from the applications point of view.

The gravity modulation term sits in the momentum equation and involves the vertical time periodic vibrations of the system, is known as G-jitter in literature. Eq.(1.5.4) represents the mathematical form of gravity modulation as

$$\mathbf{g} = g_0(1 + \chi\xi cos(\Omega t)\hat{n}, \tag{1.5.4}$$

where g_0 is the constant gravity field and $\hat{n}$ is unit vector along $\mathbf{g}$.

Rotation modulation

In rotational modulation the system is rotating periodically about its axis. In particular, a time-periodic and sinusoidally varying angular velocity is to be considered. It has many application in automobile, medical, heat reservoirs and rotating celestial bodies etc. Rotation speed modulation is similar to gravity modulation, sits in momentum equation and gives the system, non-autonomous equations. Mathematical representation is as follows

$$\mathbf{\Omega_R} = \Omega_{R0}(1 + \chi\xi cos(\Omega t))\hat{e}, \tag{1.5.5}$$

where Ω_{R0} is the constant mean angular velocity & $\hat{e}$ is unit vector along $\mathbf{\Omega_R}$.

Magnetic modulation

Magnetic nanofluids gives birth to radical hydrodynamics in the system. The magneto convection is basically interaction of electrically conducting fluid flow and the applied magnetic field. According to Faraday's law, electromagnetic induction is responsible for convection, which can take place in fluids due to temperature dependence of their magnetization. This merit becomes more relevant where the gravity is absent. Where natural convection is not possible, the roll of magneto convection becomes crucial, magnetic force can be used to create circulation in system. The variable(periodic) magnetic field gives the variation in the magnetic force accordingly, since magnetization depends on the intensity of magnetic field, temperature and density. Hence, the modulated magnetic force governs convection of the fluid. Mathematically, it is defined as

$$\mathbf{H} = H_0(1 + \chi\xi \cos(\Omega t))\hat{e}, \tag{1.5.6}$$

where H_0 is the mean value of magnetic field.

1.6 Mathematical Model

The conservation equations formulated under certain assumption, such as the viscosity, density, thermal conductivity and specific heat of nanofluids may depend on the volume fraction of nanoparticles. To insight physics, the various effects on the order of magnitude estimated, all thermophysical properties of nanofluid except density shall be assumed constant in the analytical formulation.

1.6.1 Conservation of nanoparticle flux

The continuity equation for the nanofluid is formulated as follows

$$\left[\frac{\partial}{\partial t} + (v \cdot \nabla)\right] \phi = \frac{1}{\rho_p} \nabla \cdot \beth_p \tag{1.6.1}$$

where $\beth_p$ is the diffusion mass flux for the nanoparticles, given as the sum of two diffusion terms (Brownian motion and thermophoresis) by

$$\beth_p = -\rho_p \left[D_B \nabla \phi + \left(\frac{D_T}{T_c} \right) \nabla T \right] \tag{1.6.2}$$

where D_B is the Brownian diffusion coefficient and D_T is the thermophoretic diffusion coefficient of the nanoparticles given as

$D_B = \frac{k_B T}{3\pi \mu_{bf} d_p}, \qquad D_T = \left(\frac{\mu_{bf}}{\rho_{bf}}\right)\left(\frac{0.26\kappa_{bf}}{2\kappa_{bf}+\kappa_p}\right)\phi$

Here, k_B is Boltzmann's constant, μ_{bf} is the viscosity of the base fluid, d_p is the nanoparticle diameter, ρ_{bf} is the density of the base fluid, κ_{bf} and κ_p are the thermal conductivity of the base fluid and nanoparticles, respectively. From Eq.(1.6.2), it is clear that the sign of the Brownian diffusion coefficient and the thermophoretic diffusion coefficient of the nanoparticles are positive. Substituting the expression for $\beth_p$ into the conservation equation for the nanoparticles, Eq.1.6.1 yields

$$\left(\frac{\partial}{\partial t} + (v \cdot \nabla)\right) \phi = D_B \nabla^2 \phi + \frac{D_T}{T_c} \nabla^2 T \tag{1.6.3}$$

1.6.2 Energy equation

The energy equation for the nanofluid is

$$(\rho c)\left(\frac{\partial}{\partial t}+(v\cdot\nabla)\right)T=-\nabla\cdot\mathcal{F}+h_p\nabla\cdot\mathcal{J}_p \tag{1.6.4}$$

where, $h_p\nabla\cdot\mathcal{J}_p$ is the work needed to push the fluid into or out of the boundaries of a control volume, in the energy equation due to Brownian motion and thermophoresis of nanoparticles relative to the flow velocities and ρ is the density of the nanofluid, c is the fluid-specific heat (at constant pressure), and

$$\mathcal{F}=-\kappa\nabla T+h_p\mathcal{J}_p \tag{1.6.5}$$

where κ is the nanofluid thermal conductivity and h_p is the specific enthalpy of nanoparticles. Eq.(1.6.5) gives

$$\begin{aligned}\nabla\cdot\mathcal{F} &= -\kappa\nabla^2T+\nabla\cdot(h_p\mathcal{J}_p) &(1.6.6)\\ &= -\kappa\nabla^2T+h_p\nabla\cdot\mathcal{J}_p+\mathcal{J}_p\cdot\nabla h_p &(1.6.7)\\ &= -\kappa\nabla^2T+h_p\nabla\cdot\mathcal{J}_p+\mathcal{J}_p\cdot(c_p\nabla T) &(1.6.8)\end{aligned}$$

where ∇h_p is equal to $c_p\nabla T$ and c_p is the specific heat of the material constituting the nanoparticles. Using the expression for $\nabla\cdot\mathcal{F}$ and $\mathcal{J}_p$, the energy Eq.(1.6.4) becomes

$$(\rho c)\left(\frac{\partial}{\partial t}+(v\cdot\nabla)\right)T=\kappa\nabla^2T+(\rho c)_p\left[D_B\nabla\phi\cdot\nabla T+\frac{D_T}{T_c}\nabla T\cdot\nabla T\right] \tag{1.6.9}$$

1.6.3 Momentum equation

One can introduce a buoyancy force and the external force, under the Boussinesq approximation, the momentum equation can be written as

$$\rho_0\left(\frac{\partial}{\partial t}+(v\cdot\nabla)\right)v=-\nabla p+\mu\nabla^2v+\rho\overrightarrow{g}+\overrightarrow{F} \tag{1.6.10}$$

where p is the pressure, nanofluid density ρ and reference density of the nanofluid ρ_0 are given as

$$\rho = \phi\rho_p + (1-\phi)\rho_f \tag{1.6.11}$$

$$\rho_0 = \phi\rho_p + (1-\phi)\rho_{fo} \tag{1.6.12}$$

where ρ_p and ρ_f are the density of the nanoparticles and base fluid respectively, and ρ_{fo} is the base fluid density at the reference temperature T_c.

1.7 Methods of solution

There are variety of methods to establish set of solution of governing equations according to the kind of problem which has been taken. In some cases, analytical solution can be obtained but sometimes not, it depends upon the category of problem. If an analytical method is not applicable then the other way is numerical methods are used to find approximate solution of the problem under consideration.

1.7.1 Analytical methods

Analytical method uses well existing theorems and formulas to present solution in extent of precision. Some analytical methods used in present context are as follows

Energy method

The kinetic energy of the perturbations is calculated in this method, and if this kinetic energy increases along with time, then the flow is unstable, and if the system is dissipative with the volume in the phase-space contracting at a uniform rate given by with time then the flow is stable. This method fails to provide the information of unstable system, so it is rarely used for convective problems.

$$E(\tau) = E(0)exp[\lambda\tau] \tag{1.7.1}$$

Normal mode method

In this method, an arbitrary disturbance is expressed as a superposition of certain possible modes, and then the stability of the system with respect to each of these modes is investigated, based on oscillations theory. Mathematically, one can use the expression $exp[i(\alpha_x x+\alpha_y y)+st]$ for normal mode method, where s is the frequency of perturbation and $\alpha^2 = \alpha_x^2 + \alpha_y^2$ is the wave number. The stability analysis is performed by using frequency of perturbation (s). If $Re(s > 0)$, then the disturbance will grow exponentially with time, and it will represent an unstable system. If $Re(s = 0)$, then the system will be neutrally stable. If $Re(s < 0)$, then it shows a stable system as the disturbance reduces exponentially with time.

Perturbation method

Some time, people are facing difficulties in solving the engineering problems, mathematical non-linear governing equations in real life directly. In this method, the solution is represented by the initial few terms of an asymptotic expansion. The expansions may be carried out in terms of the introduced parameter, which appears in the considered equation, known as perturbation parameter. Here, it is assumed χ as a perturbation parameter such that the solution is available and reasonably simple for $\chi = 0$, this process known as regular perturbation method. There is one more kind of perturbation method, known as singular perturbation method, where the solution cannot be approximated by setting the parameter value to zero. Mathematically, to write an expression for approximation to the solution of P

$$P = P_0 + \chi P_1 + \chi^2 P_2 + ..., \tag{1.7.2}$$

where P_0 would be the known solution to the exactly solvable initial problem and $P_1, P_2, ..$ represent the higher-order terms, which may be found by successive iterations.

A truncated representation of Fourier series method

Linear stability analysis is sufficient to find the stability condition of the motionless solution and the corresponding eigenfunctions describing qualitatively the convective flow. However, it cannot provide any information related to the values of the convection amplitudes, nor regarding the rate of heat and mass transfer. In order to get this additional information, weakly non-linear stability analysis is performed, which helps to understand the physical mechanism with minimum amount of mathematical analysis in precise way.

$$\psi = \sum_{n=1}^{\infty}\sum_{m=1}^{\infty} A_{mn}(t)\sin(m\alpha x)\sin(n\pi z) \tag{1.7.3}$$

$$T = \sum_{n=1}^{\infty}\sum_{m=1}^{\infty} B_{mn}(t)\cos(m\alpha x)\sin(n\pi z) \tag{1.7.4}$$

$$\phi = \sum_{n=1}^{\infty}\sum_{m=1}^{\infty} C_{mn}(t)\cos(m\alpha x)\sin(n\pi z). \tag{1.7.5}$$

1.7.2 Numerical methods

Methods are constructed to find solution of mathematical problems by introducing numerical results, usually on a computer. A numerical method is a complete and unambiguous set of procedures for the approximate solution of a problem, together with error estimation. In selection of numerical methods, the main objective is minimum error and convergence rate is higher.

Galerkin method:

This method is used for converting a continuous operator problem to a discrete problem. Galerkin method is mainly a weighted residual method used to solve boundary value problems. Some basic steps of this method are given below:

1. Expand the unknown solution in a set of basis functions, with unknown coefficients or parameters; it is known as the trial solution.

2. Check whether the trial solution satisfy the boundary conditions as well as initial

conditions.

3. Define the residual, set the weighted residual to zero and solve the equations.

4. Find out the error by taking successive approximations, and show convergence as the number of basis functions increases.

Runge-Kutta method:

It is well known method of numerical analysis. The Runge-Kutta methods are used in family of implicit and explicit iterative methods for the approximation of solutions of ordinary differential equations. The mathematicians C. Runge and M.W. Kutta(1900) introduced this wonderful technique.

1.8 Application of Nanofluids

Nanofluids can be used in various engineering applications. These are following application of nanofluids.

1.8.1 Heat Transfer Applications

Industrial Cooling Applications

There are industries, using nanofluids as a closed loop cooling cycles in place of normal fluids and save large amount on energy consumption. When extracting energy from the earths crust that varies in length between 5 to 10 km and temperature between 5000C and 10000C, nanofluids can be employed to cool the pipes exposed to such high temperatures.

1.8.2 In Auto-mobile Sector

- **As a Coolant**: The use of nanofluids as coolants would allow for smaller size and better positioning of the radiators. Owing to the fact that there would be less fluid due to the higher efficiency, coolant pumps could be shrunk and truck engines could

be operated at higher temperatures allowing for more horsepower while still meeting stringent emission standards.

- **As a Lubricant**: In automotive lubrication applications, surface-modified nanoparticles stably dispersed in mineral oils are effective in reducing wear and enhancing load-carrying capacity.

1.8.3 Electronic Applications

A principal limitation on developing smaller microchips is the rapid heat dissipation. However, nanofluids can be used for liquid cooling of computer processors due to their high thermal conductivity.

1.8.4 Biomedical Applications

- **Nano-drug delivery**: Magnetic nanofluids are to be used to guide the particles up the bloodstream to a tumor with magnets. It will allow doctors to deliver high local doses of drugs or radiation without damaging nearby healthy tissue, which is a significant side effect of traditional cancer treatment methods.

- **Nano-cryosurgery** : Cryosurgery is a procedure that uses freezing to destroy undesired tissues. Intentional loading of nanoparticles with high thermal conductivity into the target tissues can reduce the final temperature, increase the maximum freezing rate .

1.9 Literature Review of Thermal Instability in Nanofluid

Several theoretical and experimental studies have been carried out on suspensions containing suspended particle(millimeter or micrometer sized), it was Maxwell who published theoretical work more than 100yrs ago and initiates the idea of suspensions. The earliest observation of such an experiment was performed by Masuda et. al. in 1993. Although these particles are use to improve the thermal conductivity of the fluid, but they created

lots of problems in terms of settling, producing drastic pressure drops, clogging channels, and premature wear on channels and components. There is challenge to produce nano-sized particle of metals and metal oxides in the years of nineties but it is possible in modern nanotechnology and provides extra opportunities to process and produce particles with average crystal size(below 50nm). Thus nanofluids were made by suspending the nanoparticles in the common fluids, called base fluids. Presence of these nanoparticles in the base fluids may increase the thermal conductivity of the fluids by 15-40%. Nanofluids are mixtures of base fluid such as water or ethylene-glycol along with small amount of nanoparticles such as metallic or metallic oxide particles (Cu, Cuo, Al_2O_3), having dimensions from 1 to 100nm. Natural convection or buoyancy driven convection, is the heat removal strategy adopted in a wide variety of industries ranging from transportation (heating, ventilation, and air conditioning), energy production and supply to electronics, textiles and paper production, geophysical problems, nuclear reactors to name a few. A large number of studies are available in the literature in which thermal instability in nanofluids have been investigated.

A significant feature of nanofluids is thermal conductivity enhancement which was first reported by Masuda et al. (1993). They have reported a 30% increase in the thermal conductivity of water with the addition of 4.3 vol.% Al_2O_3 nanoparticles. Choi (1995) was the first, who proposed this term "nanofluid". Choi (1999), in his work at Energy Technology Division, Argonne National Laboratory, supported by the U.S. Department of Energy, investigated the use of nanofluids in a wide variety of industries ranging from transportation , HVAC, and energy production and supply to electronics, textiles and paper production. Lee et al.(1999) studied the behavior of Al_2O_3 nanoparticles in water, observed 15% enhancement in thermal conductivity and also observed nanoparticle loading due to difference in the size of nanoparticles used.

The ballistic nature of heat transport within nanoparticles was analyzed by Chen (2001). Eastman et al. (2001) reported an increase of 40% in the effective thermal conductivity of ethylene-glycol with 0.3% volume of copper nanoparticles of 10 nm diameter. Further, 10-30% increase of the effective thermal conductivity in alumina/water nanofluids with 1-4% of alumina was reported by Das et al. (2003). These reports led Buongiorno and Hu (2005) to suggest the possibility of using nanofluids in advanced nuclear systems. Another

application of the nanofluid flow is in the delivery of nanodrug as suggested by Kleinstreuer et al. (2008).

Khanafer et al. (2003) reported an increase in concentration of suspended nanoparticles, is to increase in heat transfer in Cu-water nanofluids in a two-dimensional rectangular enclosures while Putra et al. (2003) reported that in natural convection, using Al_2O_3 and CuO nanofluids, the heat transfer coefficient was smaller than that in a clear fluid. Various studies have been conducted to determine the governing mechanisms in nanoscale, including a modified Maxwell model accounting for the ordered nanolayer near the particle fluid interface by Yu and Choi (2003), Brownian motion of nanoparticles in fluids by Jang and Choi (2004) and Kumar and Murthy (2005), ballistic nature of heat transport within nanoparticles by Keblinski and Cahill (2005) and thermal lagging in nanoparticles with a large surface area to volume ratio by Vadász (2006). A comprehensive review of heat transport in nanofluids is due to Eastman et al. (2004). In spite of several reported studies, it is a fact that no satisfactory explanation could be found so far, for abnormal enhancement in the thermal conductivity and viscosity of the fluid due to the presence of nano-particles. Wen and Ding (2006) reported a reduction in heat transfer after changing a clear fluid to a nanofluid while Abu-Nada et al. (2008) showed the enhancement of heat transfer in nanofluids at higher values of the Rayleigh number. Buongiorno (2006) has given an extensive study to account for the unusual behavior of nanofluids based on inertia, Brownian diffusion thermophoresis, diffusiophoresis, Magnus effects, fluid drainage and gravity settling, and proposed a model incorporating the effects of Brownian diffusion and the thermophoresis. With the help of these equations, studies were conducted by Kim et al. (2004), Tzou (2008a,b) and Nield and Kuznetsov (2010).

Kuznetsov and Nield both together have investigated a series of work on nanofluid as follows: the Horton Rogers Lapwood problem for the Darcy model in (2009), the onset of thermal instability in a porous medium saturated by a nanofluid using Brinkman model in (2010c), the effect of local thermal non-equilibrium using a three-temperature model in (2010a), the onset of double diffusive nanofluid convection in a layer of a saturated porous medium in (2010b), the effect of local thermal non-equilibrium (2011), the effect of vertical throughflow (2011) and a linear stability theory (2012) for Horton Rogers Lapwood problem

with thermal conductivity and viscosity dependent on the nanoparticle volume fraction.

Bhadauria and Agarwal (2011a,b) studied the effect of local thermal non equilibrium on linear and nonlinear thermal instability in a horizontal porous layer saturated by a nanofluid. Agarwal et al. (2011) and Agarwal and Bhadauria (2011) studied thermal instability in a rotating porous layer saturated by a nanofluid for top and bottom-heavy suspension for Darcy model. Agarwal et al. (2012) studied double diffusive convection in a horizontal porous layer saturated by a nanofluid, for the case where the base fluid of the nanofluid is itself a binary fluid such as salty water. Chand and Rana (2012) studied the onset of thermal convection in a rotating nanofluid saturated porous medium. Boundary and internal heat source effects on the onset of Darcy-Brinkman convection in a porous layer saturated by nanofluid was studied by Yadav et al. (2012). Umavathi (2013) studied temperature modulation, gravity modulation by Pranesh et al. (2014), of convection in a nanofluid saturated porous medium, using linear stability analysis with Venezian (1969) approach. Mohammed et al. (2015) investigated g-jitter mixed convective boundary layer flow of water-based nanofluids. For other related works on gravity modulation the reader may look at Bhadauria and Kiran (2014)a-b, (2015).

Chapter 2

Study of convective thermal instability in nanofluid saturated porous medium in presence of vertical throughflow, internal heat source and rotation

2.1 Introduction

For the last two decades, nanofluids are being used as heat transfer media due to their enhanced abilities over ordinary fluids as heat exchangers and transporters. The term nanofluid refers to the suspensions of nanometre size particles in the base fluid. The presence of very few quantity of nanoparticles in base fluids create a significant increment in the heat transfer characteristics. The convective heat transfer characteristics of nanofluids

This chapter is based on the research article: Study of convective thermal instability in nanofluid saturated porous medium in presence of vertical throughflow, internal heat source and rotation, Published in **VIJNANA BHARATHI, Bangalore University Journal of Science.** Vol. 1 No. 2 pp. 120-140, ISSN : 0971-6882.

depend on the thermo-physical properties of the base fluid and the suspended nanoparticles. The properties of nanofluids found a wide range of applications in industrial, commercial, residential and transportation sectors.

A significant feature of nanofluids is thermal conductivity enhancement, which was first introduced by Masuda et al. (1993). Nanofluids are mixtures of base fluid (like water or ethylene-glycol) along with small amount of nanoparticles (like metallic or metallic oxide: Cu, Cuo, Al_2O_3) having dimensions from 1nm to 100nm. Choi (1995) was the first who proposed the term "nanofluid". Chen (2001) analyzed the ballistic nature of heat transport within nanoparticles, Eastman et. al. (2001) reported that 40% thermal conductivity of ethylene-glycol increases with 0.3% volume of copper nanoparticles of 10nm diameter. Das et. al. (2003) found that $10 - 30\%$ increase of the effective thermal conductivity in alumina/water nanofluids with $1 - 4\%$ of alumina. These reports led Buongiorno and Hu (2005) to suggest the possibility of using nanofluids in advanced nuclear systems. Another application of the nanofluid flow due to Kleinstreuer et. al. (2008), is in the delivery of nano-drug.

Khanafer et. al. (2003) reported an increase in concentration of suspended nanoparticles, is to increase in heat transfer in Cu-water nanofluids in a two-dimensional rectangular enclosures, whereas Putra et. al. (2003) reported that in natural convection with Al_2O_3 and CuO nanofluids, the heat transfer coefficient was smaller than that in a regular fluid. A wide range of studies have been conducted to determine the governing mechanisms in nanoscale: Brownian motion of nanoparticles in fluids by Jang and Choi (2004), a modified Maxwell model accounting for the ordered nanolayer near the particle fluid interface by Yu and Choi (2003), ballistic nature of heat transport within nanoparticles by Keblinski and Cahill (2005), Vadász (2006) studied thermal lagging in nanoparticles with a large surface area to volume ratio. A comprehensive review of heat transport in nanofluids is due to Eastman et. al. (2004). It is a fact that in spite of several reported studies, no satisfactory explanation for abnormal enhancement in the thermal conductivity and viscosity of the fluid in the the presence of nano-particles, could be found so far. Wen and Ding (2006) reported a reduction in heat transfer after changing a regular fluid to a nanofluid whereas Abu-Nada et. al. (2008) have shown the enhancement of heat transfer in nanofluids at

higher values of the Rayleigh number.

First of all Buongiorno (2006) proposed a model for convective transport in nanofluids incorporating the effects of thermophoresis and Brownian diffusion. Tzou (2008a, 2008b) have studied the thermal instability problem by using this model and observed that nanofluid is less stable than base fluid. This problem was further revisited by Nield and Kuznetsov (2010) for different types of non-dimensional parameters. An extension to the porous medium of this model was studied by Nield and Kuznetsov (2009), Kuznetsov and Nield (2009) and Chand and Rana (2012). Yadav et al. (2012) examined the effect of internal heat source on the onset of nanofluid convection. In nanofluid saturated porous medium, Bhadauria and Agarwal (2011) studied the nonlinear two-dimensional convection.

The study of throughflow in various configuration is available in literature. For details refer articles due to: Wooding (1960), Shvartsblat (1968, 1969), Sutton (1970), Gershuni and Gershuni (1976), Jones and Persichetti (1986), Nield (1987), Siddheshwar (1995), Khalili and Shivakumara (1998, 2001, 2003), Shivakumara (1999), Barletta et. al (2010), Nield (2011), Nield and Kuznetsov (2011). Effect of rotation on thermal convection in an anisotropic porous medium with temperature-dependent viscosity was investigated by Vanishree and Siddheshwar (2010). The studies, concerning to rotating porous medium saturated by a nanofluid, were carried out by Veronis (1966), Rudraiah (1986) , Agarwal et al. (2011), Bhadauria and Agarwal (2011), Agarwal and Bhadauria (2011), and Chand and Rana (2012). There are several articles in which the effect of internal heating on convective flow has been investigated. For instance, see the article due to Roberts (1967), Tveitereid and Palm (19760), Tveitereid (1978), Yu and Shih (1980), Bhattacharya and Jena (1984), Takashima (1989), Tasaka and Takeda (2005), Joshi et al. (2006), Bhadauria et. al. (2011), Bhadauria (2012), Altawallbeh et al. (2013), Bhadauria et. al. (2013a-c) and Srivastava et. al. (2013).

Recently, Nield and Kuznetsov (2014) in their revised model subject to new set of boundary conditions, where it is assumed that there is no nanoparticle flux at the plate and the particle fraction value adjusts accordingly, In that case, the presence of oscillatory convection turns oblivious due to the absence of two opposing forces. Agarwal (2014) studied the thermal instability in a rotating porous layer saturated by a nanofluid based

on a new boundary condition for the nanoparticle fraction. Similar work has been done by Yadav et al. (2015) for free-free, rigid-rigid and free-rigid boundaries. Linear as well as non-linear study for Rayleigh-Bénard convection in a nanofluid under thermal non-equilibrium with new boundary condition is studied by Agarwal et. al. (2014). Nield and Kuznetsov (2015) has done tremendous work in the area of throughflow subject to another revised boundary conditions, considering the fact that the total nanoparticle flux is the sum of diffusive, convective and thermophoretic terms. Since the particles are transported in the fluid phase only, and so the intrinsic velocity is involved in the convective terms.

In the present chapter, the effect of throughflow, rotation and internal heat source on thermal instability in a porous medium saturated by a nanofluid has been studied. Horton-Rogers-Lapwood model based on the Brinkman model is used for the fluid flow. In place of fixed nanopartical fraction conditions, the thermo-nanopartical flux boundary conditions have been introduced. The study of the effect of the different parameters: namely Pe, Ta, Ri, Rn, Le, N_A, N_B, ϵ, α, and Da on thermal instability has been carried out. Effects of these parameters depicted graphically.

2.2 Governing Equation

Consider a densely packed porous layer saturated by a nanofluid, confined between two horizontal boundaries at $z = 0$ and $z = d$, heated from below. The boundaries are impermeable and perfectly thermally conducting. The porous layer is extended infinitely in x and y directions, with the z-axis extending vertically upward with the origin at the lower boundary. The porous layer is rotating uniformly about z-axis. The Coriolis effect has been taken into account by including the Coriolis force term in the momentum equation whereas the centrifugal force term can be realized as a gradient of a scalar, and hence has been absorbed into the pressure term. In addition, the local thermal equilibrium between the fluid and solid phase has been considered. The physical configuration of model has been described in Figure 2.1.

Employing the Oberbeck-Boussinesq approximation, the governing equations to study the thermal instability in a nanofluid-saturated rotating porous medium are [Buongiorno

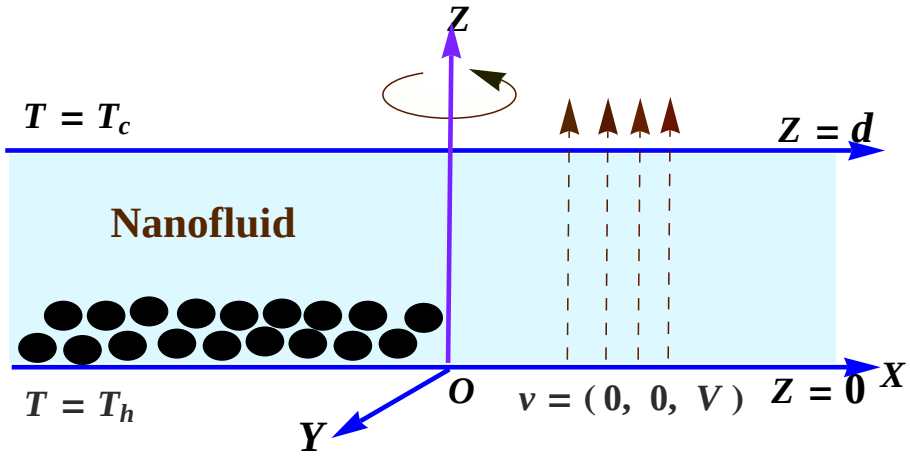

Figure 2.1: Physical configuration of the problem

(2006), Kuznetsov and Nield (2010) and Nield and Kuznetsov (2013), Nield and Kuznetsov (2014), Nield and Kuznetsov (2015)]

$$\nabla \cdot \mathbf{v_D} = \mathbf{0}, \tag{2.2.1}$$

$$\frac{\rho_f}{\varepsilon}\frac{\partial \mathbf{v_D}}{\partial t} + \nabla p = \bar{\mu}\nabla^2 \mathbf{v}_D - \frac{\mu}{K}\mathbf{v}_D + [\phi\rho_p + (1-\phi)\{\rho(1-\beta(T-T_c))\}]\vec{g} + \frac{2\rho_f}{\varepsilon}(\mathbf{v}_D \times \Omega_R), \tag{2.2.2}$$

$$(\rho c)_m \frac{\partial T}{\partial t} + (\rho c)_f \mathbf{v}_D \cdot \nabla T = \kappa_m \nabla^2 T + \varepsilon(\rho c)_p [D_B \nabla\phi - (\phi - \phi_0)\frac{\mathbf{v}_D}{\varepsilon} + \frac{D_T}{T_c}\nabla T] \cdot \nabla T + \eta(T - T_c), \tag{2.2.3}$$

$$\frac{\partial \phi}{\partial t} + \frac{1}{\varepsilon}\mathbf{v}_D \cdot \nabla\phi = D_B \nabla^2 \phi + \frac{D_T}{T_c}\nabla^2 T, \tag{2.2.4}$$

where $\mathbf{v}_D = (u, v, w)$ is the Darcy velocity, T_h and T_c are the temperature at lower and upper walls such that $T_h > T_c$.

In the above equations, both Brownian transport and thermophoresis coefficients are taken to be time-independent, in tune with the studies that neglect the effect of thermal transport attributed to the small size of the nanoparticles (as per arguments by Keblinski and Cahil 2005). Further, thermophoresis and Brownian transport coefficients are assumed to be temperature-independent due to the fact that the temperature ranges under consideration are not far away from the critical value. Assuming the temperature and the flux

of the nanoparticles to be constant at the boundaries, the boundary conditions are to be taken as

$$\mathbf{v} = (0,0,V),\ \ T = T_h,\ D_B\frac{\partial \phi}{\partial z} - (\phi - \phi_0)\frac{\mathbf{v}_D}{\varepsilon} + \frac{D_T}{T_c}\frac{\partial T}{\partial z} = 0 \text{ at } z = 0, \tag{2.2.5}$$

$$\mathbf{v} = (0,0,V),\ \ T = T_c,\ D_B\frac{\partial \phi}{\partial z} - (\phi - \phi_0)\frac{\mathbf{v}_D}{\varepsilon} + \frac{D_T}{T_c}\frac{\partial T}{\partial z} = 0 \text{ at } z = d, \tag{2.2.6}$$

The dimensionless variables are considered as given below:

$(x^*, y^*, z^*) = (x, y, z)/d,\ t^* = t\kappa_T/(\sigma d^2),\ (u^*, v^*, w^*) = (u, v, w)d/\kappa_T,\ p^* = pK/\mu\kappa_T, \phi^* = \dfrac{\phi - \phi_0}{\phi_0}$ and $T^* = \dfrac{T - T_c}{T_h - T_c}$, where $\kappa_T = \dfrac{\kappa_m}{(\rho c)_f}$, $\sigma = \dfrac{(\rho c_p)_m}{(\rho c_p)_f}$. ϕ_0 is reference value for nanoparticle volume fraction.

The non-dimensionalized governing equations along with boundary conditions are (after dropping the asterisk for simplicity)

$$\nabla \cdot \mathbf{v} = 0 \tag{2.2.7}$$

$$\frac{Da}{Pr}\frac{\partial \mathbf{v}}{\partial t} = -\nabla p - \mathbf{v} + Da\nabla^2\mathbf{v} - (Rm - Ra\ T + Rn\phi)\,\hat{k} + \sqrt{Ta}(\mathbf{v} \times \hat{k}) \tag{2.2.8}$$

$$\frac{\partial T}{\partial t} + \mathbf{v}\cdot\nabla T = \nabla^2 T - \frac{N_B}{\varepsilon}\phi\mathbf{v}\cdot\nabla T + \frac{N_B}{Le}\nabla\phi\cdot\nabla T + \frac{N_A N_B}{Le}\nabla T\cdot\nabla T + R_i T \tag{2.2.9}$$

$$\frac{1}{\sigma}\frac{\partial \phi}{\partial t} + \frac{1}{\varepsilon}\mathbf{v}\cdot\nabla\phi = \frac{1}{Le}\nabla^2\phi + \frac{N_A}{Le}\nabla^2 T \tag{2.2.10}$$

$$\left.\begin{aligned} &\mathbf{v} = (0,0,Pe),\ \ T = 1,\ \frac{\partial\phi}{\partial z} - \frac{PeLe}{\varepsilon}\phi + N_A\frac{\partial T}{\partial z} = 0 \ \text{ at } z = 0,\\ &\mathbf{v} = (0,0,Pe),\ \ T = 0,\ \frac{\partial\phi}{\partial z} - \frac{PeLe}{\varepsilon}\phi + N_A\frac{\partial T}{\partial z} = 0 \ \text{ at } z = 1, \end{aligned}\right\} \tag{2.2.11}$$

The non-dimensionlized parameters in the above equations are given below,

$$Da = \frac{\bar{\mu}K}{\mu d^2}, \qquad Ta = \left(\frac{2K\Omega_R}{\nu\varepsilon}\right)^2, \qquad Pr = \frac{\bar{\mu}\varepsilon(\rho c)_m}{\rho_f\kappa_m},$$

$$Ra = \frac{\rho_f g\beta K d(T_h - T_c)}{\mu\kappa_T}, \qquad Rn = \frac{(\rho_p - \rho_f)\phi_0 gKd}{\mu\kappa_T}, \qquad Rm = \frac{\left\{\rho_p\phi_0 + \rho_f(1-\phi_0)\right\}gKd}{\mu\kappa_T},$$

$$N_A = \frac{D_T(T_h - T_c)}{D_B T_c\phi_0}, \qquad N_B = \varepsilon\frac{(\rho_c)_p}{\rho_c)_f}\phi_0, \qquad Le = \frac{\kappa_T}{D_B},$$

$$Ri = \frac{\eta d^2}{\kappa_m}, \qquad Pe = \frac{dV}{\kappa_T},$$

N_A is the modified diffusivity ratio, which is similar to the Soret parameter that arises in cross diffusion in thermal instability.

2.3 Basic Solution

At the basic state, the nanofluid flow is only in z-direction, and so, it is assumed

$$\mathbf{v} = (0, 0, Pe), p = p_b(z), \quad T = T_b(z), \ \phi = \phi_b(z). \tag{2.3.1}$$

Using Eq.(2.3.1), Eq.(2.2.9) and Eq.(2.2.10) reduce to

$$\frac{d^2T_b}{dz^2} - Pe\frac{dT_b}{dz} + Pe\frac{N_B}{\varepsilon}\phi_b\frac{dT_b}{dz} + \frac{N_B}{Le}\frac{d\phi_b}{dz}\frac{dT_b}{dz} + \frac{N_AN_B}{Le}\left(\frac{dT_b}{dz}\right)^2 + R_iT_b = 0, \tag{2.3.2}$$

$$\frac{d^2\phi_b}{dz^2} - \frac{PeLe}{\varepsilon}\frac{d\phi_b}{dz} + N_A\frac{d^2T_b}{dz^2} = 0, \tag{2.3.3}$$

After integrating Eq.(2.3.3) subject to the boundary condition (2.2.11), to obtain

$$\frac{d\phi_b}{dz} - \frac{PeLe}{\varepsilon}\phi_b + N_A\frac{T_b}{dz} = 0, \tag{2.3.4}$$

Using Eq.(2.3.4), Eq.(2.3.2) reduces to

$$\frac{d^2T_b}{dz^2} - Pe\frac{dT_b}{dz} + R_iT_b = 0, \tag{2.3.5}$$

The solutions of Eq.(2.3.4) and Eq.(2.3.5) subject to the boundary condition (2.2.11) are as follows

$$T_b = \frac{e^{\frac{Pe}{2}z}\{e^{\frac{\xi_l}{2}(1-z)} - e^{\frac{-\xi_l}{2}(1-z)}\}}{\{e^{\frac{\xi_l}{2}} - e^{\frac{-\xi_l}{2}}\}}, \tag{2.3.6}$$

$$\phi_b = \frac{N_A}{e^{\frac{\xi_l}{2}} - e^{\frac{-\xi_l}{2}}}\left[\frac{(Pe-\xi_l)e^{\frac{\xi_l}{2}}(e^{\lambda_l z} - e^{\frac{(Pe-\xi_l)}{2}z})}{(Pe-\xi_l-2\lambda_l)} - \frac{(Pe+\xi_l)e^{\frac{-\xi_l}{2}}(e^{\lambda_l z} - e^{\frac{(Pe+\xi_l)}{2}z})}{(Pe+\xi_l-2\lambda_l)}\right], \tag{2.3.7}$$

where, for sort notation, can be written as follows

$$\xi_l = \sqrt{Pe^2 - 4R_i} \tag{2.3.8}$$

$$\lambda_l = \frac{PeLe}{\varepsilon} \tag{2.3.9}$$

2.4 Perturbation Solution

Now superimpose perturbations on the basic state as given below :

$$\mathbf{v} = (0, 0, Pe) + \mathbf{v}', \ p = p_b + p', \ T = T_b + T', \ \phi = \phi_b + \phi'. \tag{2.4.1}$$

Applying the perturbed values from (2.4.1) into model (2.2.7)-(2.2.11) and using (2.3.6) and (2.3.7), the following equations in linear form can be obtained(after neglecting the nonlinear terms)

$$\nabla \cdot \mathbf{v}' = 0 \tag{2.4.2}$$

$$\left[\frac{Da}{Pr}\frac{\partial}{\partial t} - Da\nabla^2 + 1\right]\mathbf{v}' = -\nabla p' + Ra\ T'\hat{k} - Rn\phi'\hat{k} + \sqrt{Ta}(\mathbf{v}' \times \hat{k}) \tag{2.4.3}$$

$$\frac{\partial T'}{\partial t} + Pe\frac{\partial T'}{\partial z} + \frac{dT_b}{dz}\mathbf{w}' = \nabla^2 T' - \frac{N_B}{\varepsilon}\left(Pe\frac{dT_b}{dz}\phi' + \phi_b\frac{dT_b}{dz}\mathbf{w}' + Pe\phi_b\frac{\partial T'}{\partial z}\right) + \frac{N_B}{Le}\left(\frac{d\phi_b}{dz}\frac{\partial T'}{\partial z} + \frac{dT_b}{dz}\frac{\partial \phi'}{\partial z}\right) + \frac{2N_A N_B}{Le}\left(\frac{dT_b}{dz}\frac{\partial T'}{\partial z}\right) + R_i T' \tag{2.4.4}$$

$$\frac{1}{\sigma}\frac{\partial \phi'}{\partial t} + \frac{Pe}{\varepsilon}\frac{\partial T'}{\partial z} + \frac{1}{\varepsilon}\frac{d\phi_b}{dz}\mathbf{w}' = \frac{1}{Le}\nabla^2\phi' + \frac{N_A}{Le}\nabla^2 T' \tag{2.4.5}$$

$$\mathbf{w}' = 0, \quad T' = 0, \ \frac{\partial \phi'}{\partial z} - \frac{PeLe}{\varepsilon}\phi' + N_A\frac{\partial T'}{\partial z} = 0 \ \text{ at } z = 0, \text{ and } \ at\ z = 1 \tag{2.4.6}$$

The parameter R_m is not carried over in the subsequent equations because it is part of the hydrostatic equilibrium. Differentiating Eq.(2.3.6) and Eq.(2.3.7) with respect to z, to obtain

$$\frac{dT_b}{dz} = \frac{e^{\frac{Pe}{2}z}\{(Pe - \xi_l)e^{\frac{\xi_l}{2}(1-z)} - (Pe + \xi_l)e^{\frac{-\xi_l}{2}(1-z)}\}}{2\{e^{\frac{\xi_l}{2}} - e^{\frac{-\xi_l}{2}}\}} \tag{2.4.7}$$

$$\frac{d\phi_b}{dz} = \lambda_l \phi_b - N_A \frac{dT_b}{dz} \tag{2.4.8}$$

Now, taking the curl of Eq.(2.4.3), to obtain

$$\left[\frac{Da}{Pr}\frac{\partial}{\partial t} - Da\nabla^2 + 1\right] \nabla \times \mathbf{v}' = \sqrt{Ta}\frac{\partial \mathbf{w}'}{\partial z} \tag{2.4.9}$$

Taking curl of Eq.(2.4.3) twice, and considering the vertical component, to obtain

$$\left[\frac{Da}{Pr}\frac{\partial}{\partial t} - Da\nabla^2 + 1\right] \nabla^2 \mathbf{w}' = Ra\nabla_1^2 T' - Rn\nabla_1^2 \phi' - \sqrt{Ta}\frac{\partial}{\partial z}\nabla \times \mathbf{v}' \tag{2.4.10}$$

From Eq.(2.4.9) and Eq.(2.4.10), it is obtained

$$\left[\frac{Da}{Pr}\frac{\partial}{\partial t} - Da\nabla^2 + 1\right]^2 \nabla^2 \mathbf{w}' = \left[\frac{Da}{Pr}\frac{\partial}{\partial t} - Da\nabla^2 + 1\right](Ra\nabla_1^2 T' - Rn\nabla_1^2 \phi') - Ta\frac{\partial^2 \mathbf{w}'}{\partial z^2} \tag{2.4.11}$$

Next, the normal mode technique is applied for finding the unknown fields in Eq.(2.4.11), Eq.(2.4.4) and Eq.(2.4.5). Let

$$(\mathbf{w}', T', \phi') = [W(z), \Theta(z), \Phi(z)]\, e^{st+ilx+imy} \tag{2.4.12}$$

and substitute it into the preceding differential equations, to obtain

$$\left(\left[\frac{Da}{Pr}s - Da(D^2-\alpha^2) + 1\right]^2 (D^2-\alpha^2) + TaD^2\right) W + Ra\alpha^2\left[\frac{Da}{Pr}s - Da(D^2-\alpha^2)+1\right]\Theta - Rn\alpha^2\left[\frac{Da}{Pr}s - Da(D^2-\alpha^2)+1\right]\Phi = 0 \tag{2.4.13}$$

$$-\left(\frac{dT_b}{dz} + \frac{N_B Pe}{\varepsilon}\phi_b\frac{dT_b}{dz}\right) W + \left(D^2 + \frac{N_B}{Le}\frac{d\phi_b}{dz}D + \frac{2N_A N_B}{Le}\frac{dT_b}{dz}D - \frac{N_B Pe}{\varepsilon}\phi_b D - PeD - \alpha^2 - s + Ri\right)\Theta + \left(\frac{N_B}{Le}\frac{dT_b}{dz}D - \frac{N_B Pe}{\varepsilon}\frac{dT_b}{dz}D\right)\Phi = 0 \tag{2.4.14}$$

$$\left(\frac{1}{\varepsilon}\frac{d\phi_b}{dz}\right) W - \left(\frac{N_A}{Le}(D^2-\alpha^2)\right)\Theta - \left(\frac{1}{Le}(D^2-\alpha^2) - \frac{Pe}{\varepsilon}D - \frac{s}{\sigma}\right)\Phi = 0 \tag{2.4.15}$$

$$W = 0, \quad \Theta = 0, \quad D\Phi - \frac{PeLe}{\varepsilon}\Phi + N_A D\Theta = 0 \quad \text{at} \quad z = 0, 1 \tag{2.4.16}$$

where

$$D = \frac{d}{dz} \text{ and at } \alpha = \sqrt{l^2 + m^2}, \tag{2.4.17}$$

and α is a horizontal wave number. The values of Pe is taken to be very small as compared with unity. The single-term Galerkin-type method is used to obtain an approximate solution of the system Eq.(2.4.4) to Eq.(2.4.16). For this, the trial functions are chosen in such a way that they satisfy the boundary conditions. Thus,

$$W_1 = \Theta_1 = \sin \pi z, \Phi_1 = -N_A \cos \wp \sin (\pi z - \wp), \tag{2.4.18}$$

where $\wp = \tan^{-1}\left(\frac{\lambda_l}{\pi}\right)$.

Using Eq.(2.4.18) in Eqs.(2.4.13)-(2.4.15), and under the orthogonality of the equations to each trial function, a system of 3 linear algebraic equations in the unknowns, namely A, B, C are obtained. To obtain a non-trivial solution for the equations in the system, the determinants of the coefficients of the linear equations must be zero, and so

$$\det \begin{bmatrix} M_{11} & M_{12} & M_{13} \\ M_{21} & M_{22} & M_{23} \\ M_{31} & M_{32} & M_{33} \end{bmatrix} = 0, \tag{2.4.19}$$

where

$$\begin{aligned}
M_{11} &= -\left\{ \left(\frac{Da}{Pr} s + Da(\pi^2 + \alpha^2) + 1 \right)^2 (\pi^2 + \alpha^2) + Ta\pi^2 \right\} \langle W_1 W_1 \rangle , \\
M_{12} &= Ra\alpha^2 \left\{ \left(\frac{Da}{Pr} s + Da(\pi^2 + \alpha^2) + 1 \right) \right\} \langle \Theta_1 W_1 \rangle , \\
M_{13} &= -Rn\alpha^2 \left\{ \left(\frac{Da}{Pr} s + Da(\pi^2 + \alpha^2) + 1 \right) \right\} \langle \Phi_1 W_1 \rangle , \\
M_{21} &= \left\langle \left[\left\{ - \left(1 + \frac{PeLe}{\varepsilon} \phi_b \right) \frac{dT_b}{dz} \right\} W_1 \right] \Theta_1 \right\rangle , \\
M_{22} &= \left\langle \left[\left\{ \left(D^2 + \frac{N_B}{Le} \frac{d\phi_b}{dz} D + \frac{2N_A N_B}{Le} \frac{dT_b}{dz} D - \frac{PeN_B}{\varepsilon} \phi_b D - PeD + \right. \right. \right. \right. \\
&\qquad \left. \left. \left. \left. \cdot (Ri - \alpha^2 - s) \right) \right\} \Theta_1 \right] \Theta_1 \right\rangle ,
\end{aligned}$$

$$M_{23} = \left\langle \left[\left\{ \left(\frac{N_B}{Le} \frac{dT_b}{dz} D - \frac{PeN_B}{\varepsilon} \frac{dT_b}{dz} \right) \right\} \Phi_1 \right] \Theta_1 \right\rangle,$$
$$M_{31} = \left\langle \left[\left\{ \left(\frac{1}{\varepsilon} \frac{d\phi_b}{dz} \right) \right\} W_1 \right] \Phi_1 \right\rangle,$$
$$M_{32} = \left\langle - \left[\left\{ \left(\frac{N_B}{Le} (D^2 - \alpha^2) \right) \right\} \Theta_1 \right] \Phi_1 \right\rangle,$$
$$M_{33} = \left\langle - \left[\left\{ \left(\frac{1}{Le} (D^2 - \alpha^2) - \frac{Pe}{\varepsilon} D - \frac{s}{\sigma} \right) \right\} \Phi_1 \right] \Phi_1 \right\rangle$$

and

$$\langle f(z) \rangle = \int_0^1 f(z) dz,$$

Ra as the eigenvalue of Eq.(2.4.19), found in terms of the other parameters as

$$Ra = \frac{M_{11}(M_{22}M_{33} - M_{32}M_{23}) + M_{13}(M_{21}M_{32} - M_{22}M_{31})}{\alpha^2 m_{12}(M_{21}M_{33} - M_{23}M_{31})}, \tag{2.4.20}$$

where

$$m_{12} \equiv M_{12}/Ra\alpha^2 = \left\{ \left(\frac{Da}{Pr} s + Da(\pi^2 + \alpha^2) + 1 \right) \right\} \langle \Theta_1 W_1 \rangle .$$

In the case of neutral stability, take $s = i\omega$ in the analysis. Further, for stationary convection to occur, ω must be zero(ie. $\omega = 0$). To get the value of Ra for stationary case one can restrict so that the system is linear in Pe. To evaluate the above integrals the software package MATHEMATICA 10.0 (Wolfram Research,Champaign, IL) is used and the following expression is obtained

$$\begin{aligned} Ra =& \frac{\delta^2(1 + Da\delta^2)^2 + \pi^2 Ta}{(1 + Da\delta^2)} \left(\frac{\delta^2}{\alpha^2} + \frac{PeN_AN_B(1 - \delta^2)}{2\alpha^2\varepsilon} + \frac{Ri}{4\delta^2} \left(\frac{N_AN_B}{\varepsilon} - \frac{\delta^2}{\pi^2} - 4 \right) \right) \\ & - RnN_ALe \left(\frac{1}{Le} + \frac{1}{\varepsilon} + \frac{Pe}{2\delta^2\varepsilon^2} \left(N_AN_B(1 - \delta^2) + \delta^2 Le \right) + \frac{Ri}{4\delta^2\varepsilon^2} \left(N_AN_B - 4\varepsilon \right) \right). \end{aligned} \tag{2.4.21}$$

The nanoparticle flux being zero at the boundaries implies the absence of the two opposing forces responsible for the occurrence of the oscillatory mode of convection hence oscillatory convection has been ruled out.

2.5 Result and discussion

Since oscillatory convection has not been taking into account due to absence of two opposing force, and so, concentrating on the study of stationary mode of convection in whole scenario. In absence of internal heat generation, Eq.(2.4.21) reduces to

$$\begin{aligned} Ra &= \frac{\delta^2(1+Da\delta^2)^2+\pi^2 Ta}{(1+Da\delta^2)}\left(\frac{\delta^2}{\alpha^2}+\frac{PeN_AN_B(1-\delta^2)}{2\alpha^2\varepsilon}\right) \\ &\quad -RnN_ALe\left(\frac{1}{Le}+\frac{1}{\varepsilon}+\frac{Pe}{2\delta^2\varepsilon^2}\left(N_AN_B(1-\delta^2)+\delta^2Le\right)\right) \end{aligned} \tag{2.5.1}$$

Further, in the absence of vertical throughflow (i.e., $Pe = 0$), the expression for Rayleigh number for stationary convection is obtained in Eq.2.5.2, which is same as obtained by Agarwal (2014)

$$Ra = \frac{\delta^4(1+Da\delta^2)^2+\pi^2\delta^2 Ta}{\alpha^2(1+Da\delta^2)} - RnN_ALe\left(\frac{1}{Le}+\frac{1}{\varepsilon}\right) \tag{2.5.2}$$

Also, for a regular fluid Ra attains its minimum when $\alpha = \pi$, that is, $\min\{Ra\} = 4\pi^2$. This value coincides with the well-known exact value for the Horton-Rogers-Lapwood problem as expected.

In the following plots, results in the plane (Ra, α) have been depicted for different values of the parameters. Figures 2.2–2.12 show the effect of various parameters on the neutral stability for stationary mode of convection.

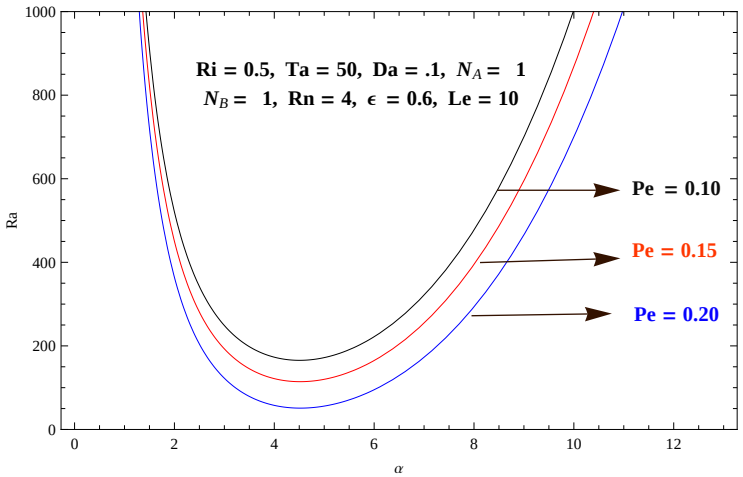

Figure 2.2: Ra versus α for different values of Pe

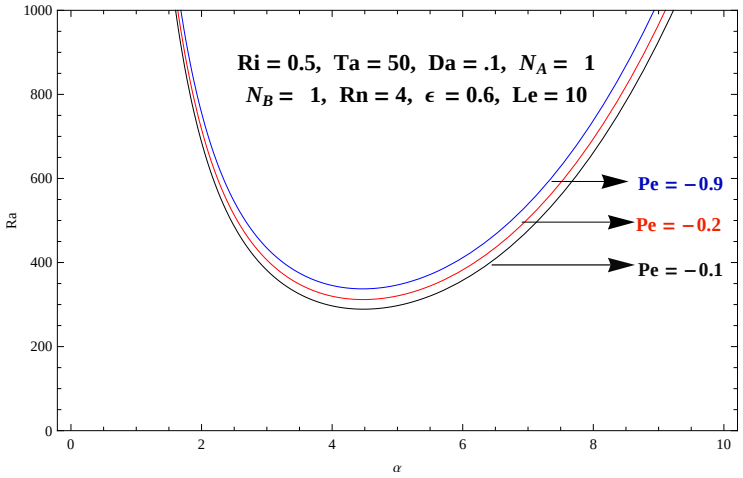

Figure 2.3: Ra versus α for different values of Pe

The effects of vertically upward throughflow $(+ve)$ and vertically downward throughflow $(-ve)$ on the thermal Rayleigh number is depicted in Figure 2.2 and Figure 2.3, respectively. It is found that vertically upward throughflow increase as Ra decreases, and so, Pe has a destabilizing effect on the stationary convection whereas vertically downward throughflow increase as Ra increases thus $-Pe$ have a stabilizing effect on the stationary convection in the system.

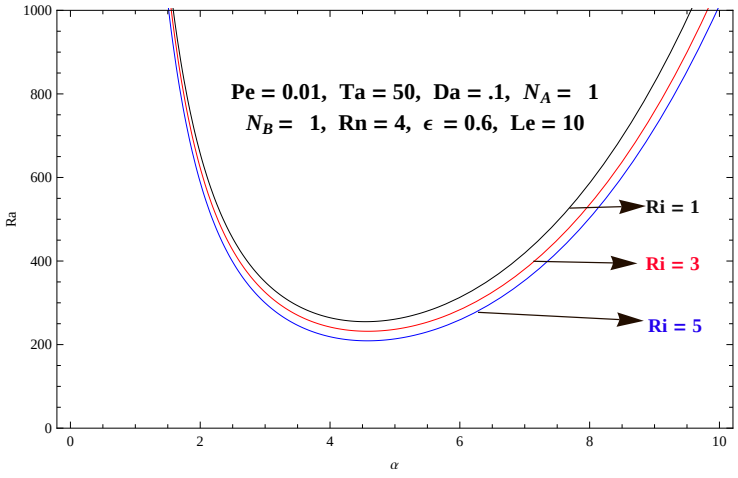

Figure 2.4: Ra versus α for different values of Ri

It is observed from Figure 2.4 and Figure 2.5 that Ri (internal heat Rayleigh number corresponding to heat source/sink) increases as thermal Rayleigh number Ra decreases. This means that the internal heat Rayleigh number Ri enhanced/delayed the onset of convection.

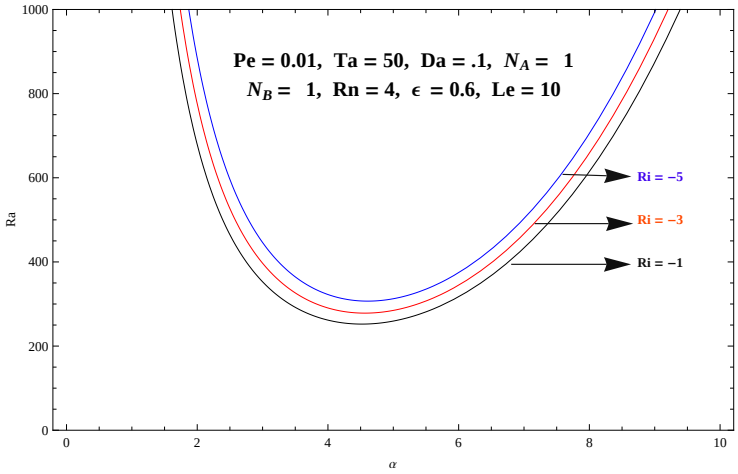

Figure 2.5: Ra versus α for different values of Ri

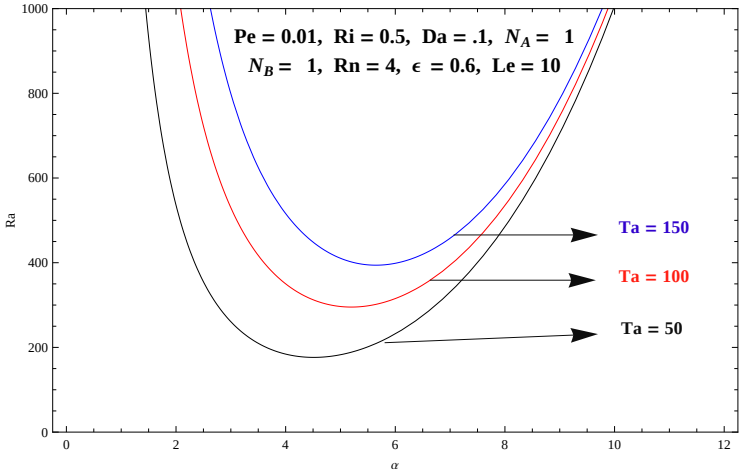

Figure 2.6: Ra versus α for different values of Ta

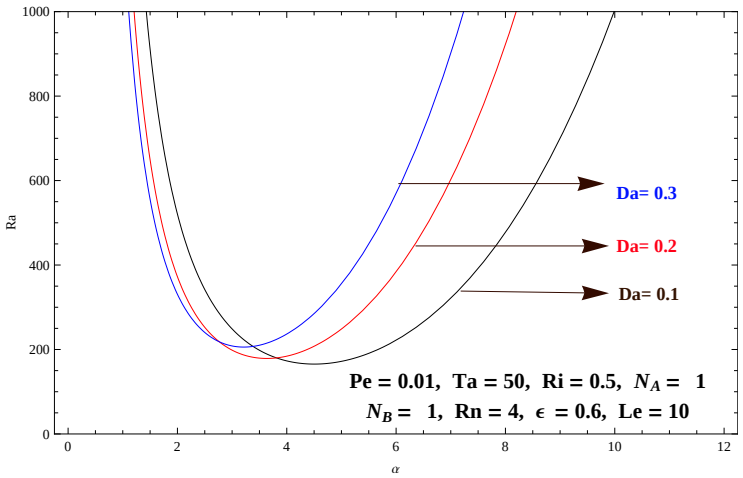

Figure 2.7: Ra versus α for different values of Da

Figure 2.6 depicts that the rotation parameter Ta delays the onset of convection and also it affect the critical wave number, and so the system will stabilised. Figure 2.7 depicts

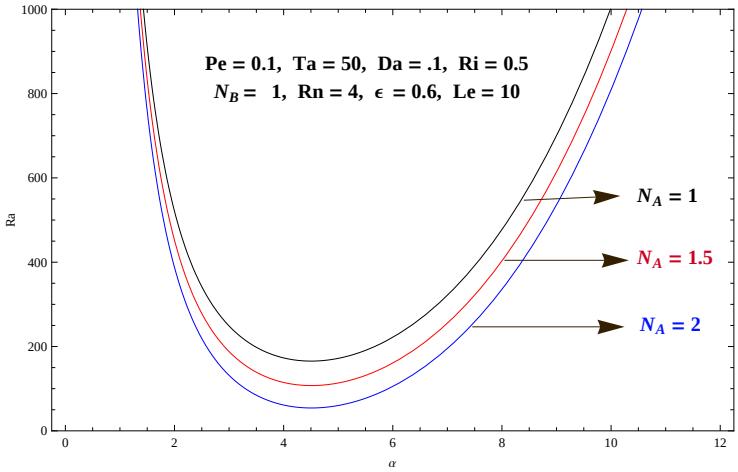

Figure 2.8: Ra versus α for different values of N_A

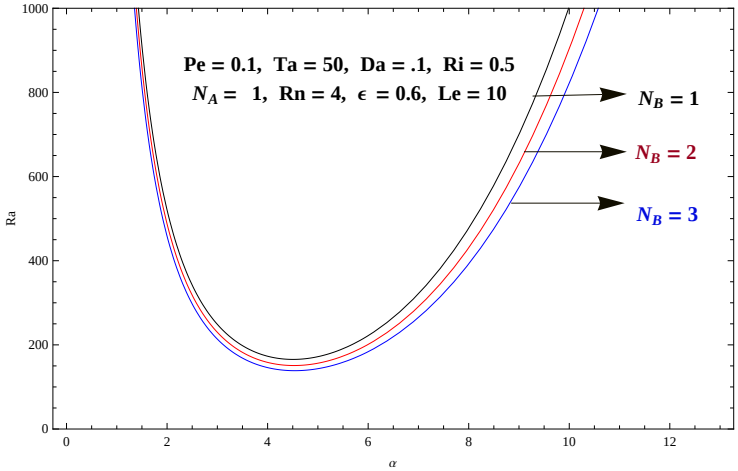

Figure 2.9: Ra versus α for different values of N_B

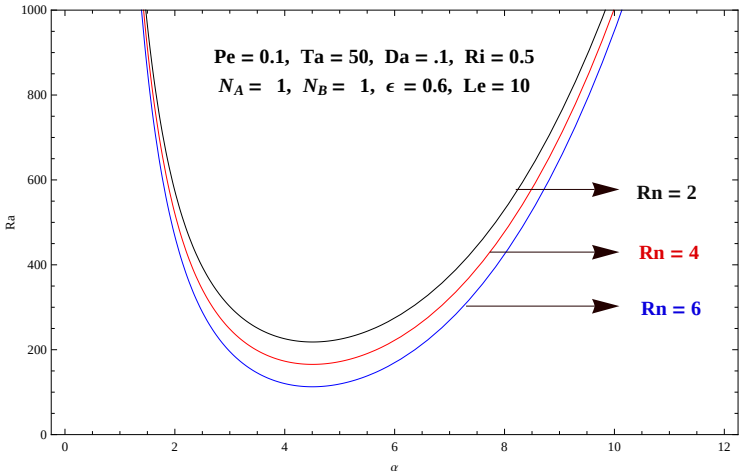

Figure 2.10: Ra versus α for different values of Rn

an interesting change that increase in the value of the Darcy number Da not only delays the onset of convection but also effects the critical wave number (the critical wave number

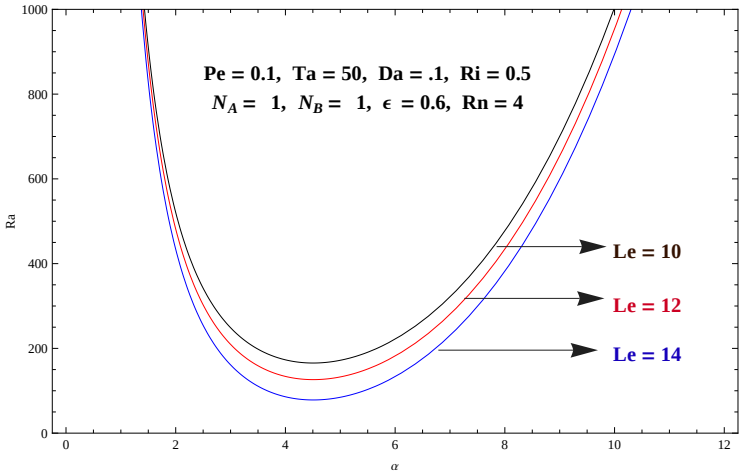

Figure 2.11: Ra versus α for different values of Le

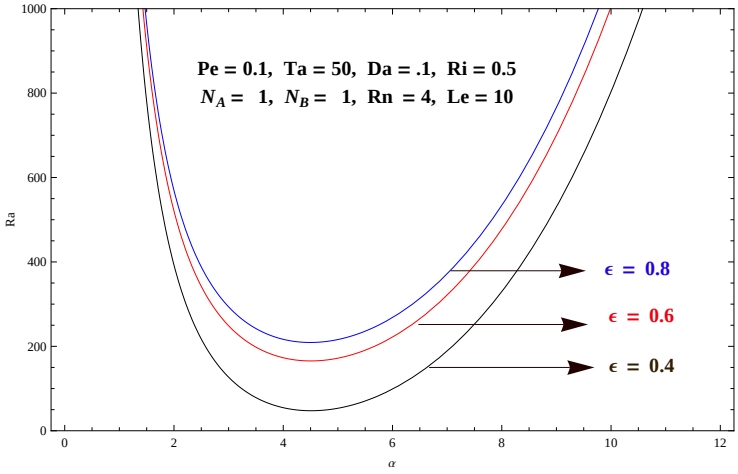

Figure 2.12: Ra versus α for different values of ε

decreases with increasing Darcy number).

It is noticed from Figures 2.8, 2.9, 2.10 and 2.11 that the modified diffusivity ratio (N_A), the modified particle-density increment (N_B), the concentration Rayleigh number (Rn) and Lewis number (Le) have destabilizing effects on the system, because an increase in the value of any of these parameters leads to decrease in the value of thermal Rayleigh number. It is evident from Figure 2.12 that the influence of porosity ε has a stabilizing effect on the system and increase in ε delays the onset of convection as expected.

2.6 Conclusion

Thermal instability has been studied in nanofluid-saturated porous layer for Brinkman model under throughflow, internal heat generation and rotation effect subject to the revised boundary conditions (at boundary nanoparticle flux is assumed to be zero). These convective boundary conditions are more reliable than the earlier boundary conditions, in the literature. Galerkin method has been introduced to solve the model. The expression for thermal Rayleigh number has been obtained by imposing linearity condition on the throughflow and internal heating term.

The numerical plots for stationary convection indicates that the parameters Ri, Pe, Rn, Le, N_A, N_B and Da destabilize the system where as the parameters Ta, $-Pe$, $-Ri$ and ε stabilize the system, and in the presence of throughflow and internal heat generation, the critical value of thermal Rayleigh number diminishes.

Chapter 3

The effect of vertical throughflow in a horizontal porous layer saturated by a power-law nanofluid

3.1 Introduction

Enhancement of heat transfer of liquids is a very challenging problem from energy efficiency point of view. To deal with this challenging problem, one can use tiny particle into the base fluid. In this context, nanofluids have replaced the ordinary base fluids as a heat transfer medium in industries due to their high thermal conductivity. Consequently, these properties of nanofluids have made them technically useful in many real world applications such as industries, commercial, residential and transportation sectors.

Nanofluids are mixtures of base fluid (like water or ethylene-glycol) along with small amount of nanoparticles (like metallic or metallic oxide: Cu, Cuo, Al_2O_3) having dimensions from 1nm to 100nm. Choi (1995) was the first who proposed the term "nanofluid". Chen (2001) analyzed the ballistic nature of heat transport within nanoparticles, Eastman et.

This chapter is based on the research article: The effect of vertical throughflow in a horizontal porous layer saturated by a power-law nanofluid, (Communicated).

al. (2001) reported that 40% thermal conductivity of ethylene-glycol increases with 0.3% volume of copper nanoparticles of 10nm diameter. Das et. al. (2003a) found $10-30\%$ increase of the effective thermal conductivity in alumina/water nanofluids with $1-4\%$ of alumina. The general topic of heat transfer in nanofluids has been surveyed in a book by Das et al. (2008). These reports led Buongiorno and Hu (2005) to suggest the possibility of using nanofluids in advanced nuclear systems. Another application of the nanofluid flow due to Kleinstreuer et. al. (2008) , is in the delivery of nano-drug. There are some more examples of heat transfer applications of nanofluids in engineering, like automotive and air-conditioning cooling, in domestic refrigerator and solar devices, are widely described by Gupta et al. (2013). First of all Buongiorno (2006) proposed a model for convective transport in nanofluids incorporating the effects of thermophoresis and Brownian diffusion. Tzou (2008 a, b) have studied the thermal instability problem by using this model and observed that nanofluid is less stable than base fluid. This problem was further revisited by Nield and Kuznetsov (2010) for different types of non-dimensional parameters. An extension to the porous medium of this model was studied by Nield and Kuznetsov (2009), Kuznetsov and Nield (2010a) and Chand and Rana (2012). Yadav et al. (2012) examined the effect of internal heat source on the onset of nanofluid convection. In nanofluid saturated porous medium, Bhadauria and Agarwal (2011a) studied the nonlinear two-dimensional convection.

The study of throughflow in various configuration is available in literature. For detail reference some articles due to: Wooding (1960), Shvartsblat (1968, 1969), Sutton (1970), Gershuni and Zhukhovitskii (1976), Jones and Persichetti (1986), Nield (1987), Siddheshwar (1995), Khalili and Shivakumara (2002, 2003), Shivakumara (1999, 2006), Barletta et. al (2010, 2011), Nield and Kuznetsov (2011). An exhaustive survey of the literature on this topic can be found in the book by Nield and Bejan (2013).

However, many practical problems cited above do not involve the power-law in the porous medium. Several studies have been published recently on convection of power-law fluids in porous media, see Barletta and Nield (2011), Nield (2011). Nield (2011) was pointed out that the onset of convection becomes singular when a Newtonian fluid is replaced by a standard power-law fluid. He has shown how this singularity can be removed and thermophoresis and Brownian motion become independent of the power-law index.

Hayat et al. (2016) have studied the flow of a power-law nanofluid past a vertical stretching sheet with a convective boundary condition. In this study, the nanoparticle concentration distribution is illustrated by Brownian motion parameter. Alves and Barletta (2013) and Barletta and Storesletten (2016) studied linear instability of the horizontal/vertical throughflow in a horizontal porous layer saturated by a power-law fluid.

The aim of this work is to extend the classical analysis of the onset of convective instability in a horizontal porous layer with vertical throughflow to a nanofluid of the power-law type under revised boundary condition[see. Nield and Kuznetsov (2015)]. In case of nanofluid of the power-law type, Nield (2011) concluded that the critical Rayleigh number is independent of the power-law index, this applies, whether or not the fluid is a nanofluid. Thus, all the results related to onset of convection, are independent of the index n. The present study deals with an additional convective regulator such as throughflow, thus the role of power law index n comes into existence. Nield and Kuznetsov (2014), Agarwal (2014a), Yadav et al. (2015), Agarwal et. al. (2015) and Nield and Kuznetsov (2015) have studied in their revised model subject to new set of boundary conditions, where they have considered the fact that the total nanoparticle flux is the sum of diffusive, convective and thermophoretic terms. Since the particles are transported in the fluid phase only, so the intrinsic velocity is involved in the convective terms only. The study of the effect of the different parameters: namely n, Pe, Rn, Le, N_A, N_B, and ε, on thermal instability has been carried out. Effect of these parameters depicted graphically.

3.2 Mathematical formulation

Particularly for this kind of non-Newtonian fluid, the shear stress τ_m (SI units are Pa) is a function of the shear rate $\dot{\gamma_m}$ (SI units are s^{-1}) given by

$$\tau_m = \mu_m \left(\dot{\gamma_m}\right)^n$$

where μ_m is the consistency factor and n is the power-law index. In the case of a Newtonian fluid($n = 1$), the consistency factor coincides with the dynamic viscosity. The SI measure-

ment units of the consistency factor are Pa s^n and, for a Newtonian fluid, the SI units of μ_m are Pa s. Pseudoplastic fluid behaviour is obtained with $n < 1$, while dilatant fluids are described by $n > 1$. When a power-law type nanofluid saturates a porous medium, the convective flow is comes into existence due to thermal buoyancy, classical Darcy's law can be further modelled and turned into modified Darcy's law. Under the Oberbeck-Boussinesq approximation one can consider as follows

$$\frac{\mu}{K}|\mathbf{v}^*|^{n-1}\mathbf{v}^* = -\nabla p + \phi^*\rho_p + (1-\phi^*)\{\rho(1-\beta(T^*-T_c^*))\}\vec{g}, \tag{3.2.1}$$

where μ is the effective consistency factor (SI units are Pa s^n m^{1-n}), K is the permeability (SI units are m^2) and p is the dynamic pressure (SI units are Pa), viz. the local difference between the pressure and the hydrostatic pressure. Moreover, in these equations, p^* is the pressure, t^* is the time, g is the gravitational acceleration acting in the negative vertical direction, $\mathbf{v}^* = (u^*, v^*, w^*)$ is the Darcy velocity, T^* is the nanofluid temperature, ϕ^* is the nanoparticle volume fraction and ϕ_0^* is a reference value of that nanoparticle fraction, ρ_p is the nanoparticle mass density at the reference temperature T_c^*, β is the thermal expansion coefficient of the base fluid, and $\vec{g}$ is the gravity acceleration whose modulus is denoted as g. The ratio $\frac{\mu}{K}$ depends on the consistency factor μ_m, power-law index n, permeability K, porosity ε, and on the tortuosity factor ζ through the relationship (see. Barletta and Storesletten (2016)).

$$\frac{\mu}{K} = 2\zeta\mu_m\left(\frac{3\varepsilon}{50K}\right)^{(n+1)/2}\left(\frac{3n+1}{n\varepsilon}\right)^n. \tag{3.2.2}$$

The tortuosity factor ζ is numerical constant independent of n.

Consider a porous medium whose porosity is denoted by ε and permeability by K. Use asterisks to denote dimensional variables. It is also consider a coordinate frame in which the z^*-axis is aligned vertically upward, and horizontal layer of a porous medium confined between the planes $z^* = 0$ and $z^* = d$. Each boundary wall is assumed to be permeable to the throughflow and perfectly thermally conducting. For simplicity, Darcy's law is assumed to hold and the OberbeckBoussinesq approximation is employed. Homogeneity and local thermal equilibrium in the porous medium is assumed. The conservation equations (for

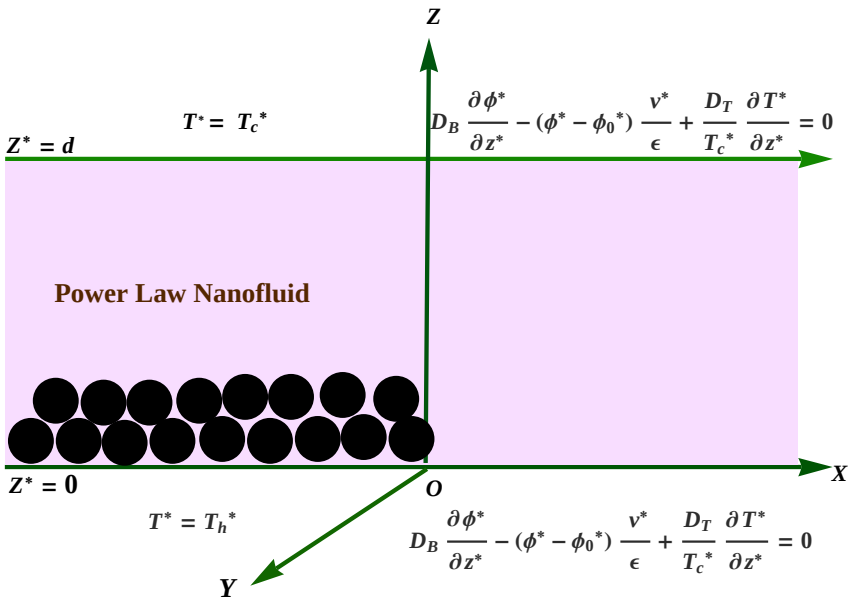

Figure 3.1: A sketch showing the physical configuration of the problem

total mass, momentum, thermal energy, and nanoparticles, respectively) are expressed in the form

$$\nabla \cdot \mathbf{v}^* = \mathbf{0}, \tag{3.2.3}$$

$$\frac{\mu}{K}|\mathbf{v}^*|^{n-1}\mathbf{v}^* = -\nabla p + \phi^* \rho_p + (1-\phi^*)\{\rho(1-\beta(T^* - T_c^*))\}\vec{g}, \tag{3.2.4}$$

$$(\rho c)_m \frac{\partial T^*}{\partial t^*} + (\rho c)_f \mathbf{v}^* \cdot \nabla T^* = \kappa_m \nabla^2 T^* + \varepsilon(\rho c)_p [D_B \nabla \phi^* - (\phi^* - \phi_0^*)\frac{\mathbf{v}^*}{\varepsilon} + \frac{D_T}{T_c^*}\nabla T^*] \cdot \nabla T^*, \tag{3.2.5}$$

$$\frac{\partial \phi^*}{\partial t^*} + \frac{1}{\varepsilon} \cdot \nabla \phi^* = D_B \nabla^2 \phi^* + \frac{D_T}{T_c^*} \nabla^2 T^*. \tag{3.2.6}$$

κ_m is the effective thermal conductivity of the porous medium, c_p is the specific heat of the material constituting the nanoparticles, D_B is the Brownian diffusion coefficient, and D_T is the thermophoretic diffusion coefficient, and introduced the effective heat capacity $(\rho c)_m$ and the effective thermal conductivity κ_m of the porous medium. Similarly, $(\rho c)_f$ is the heat capacity of the fluid. The reference temperature has been taken to be T_c^*. In the linear theory being applied here, the temperature change in the fluid has been assumed to be small in comparison with T_c^*. It is also assumed that the throughflow velocity has the

uniform value $(0, 0, V^*)$. Thus, the boundary conditions are

$$\mathbf{v}^* = (0,0,V^*),\ \ T^* = T_h^*,\ D_B\frac{\partial \phi^*}{\partial z^*} - (\phi^* - \phi_0^*)\frac{\mathbf{v}^*}{\varepsilon} + \frac{D_T}{T_c^*}\frac{\partial T^*}{\partial z^*} = 0 \text{ at } z = 0, \tag{3.2.7}$$

$$\mathbf{v}^* = (0,0,V^*),\ \ T^* = T_c^*,\ D_B\frac{\partial \phi^*}{\partial z^*} - (\phi^* - \phi_0^*)\frac{\mathbf{v}^*}{\varepsilon} + \frac{D_T}{T_c^*}\frac{\partial T^*}{\partial z^*} = 0 \text{ at } z = d. \tag{3.2.8}$$

The dimensionless variables are considered as given below: $(x, y, z) = (x^*, y^*, z^*)/d,\ t = t^*\alpha_m/(\sigma d^2),\ (u, v, w) = (u^*, v^*, w^*)d/\alpha_m,\ p = p^*K/\mu\alpha_m, \phi = \dfrac{\phi^* - \phi_0^*}{\phi_0^*}$ and $T = \dfrac{T^* - T_c^*}{T_h^* - T_c^*}$, where $\alpha_m = \dfrac{\kappa_m}{(\rho c)_f},\ \ \sigma = \dfrac{(\rho c_p)_m}{(\rho c_p)_f}$.

The non-dimensionalized governing equations along with boundary conditions are

$$\nabla \cdot \mathbf{v} = 0 \tag{3.2.9}$$

$$|\mathbf{v}|^{n-1}\mathbf{v} = -\nabla p - Rm\hat{e_z} + RaT\hat{e_z} - Rn\phi\hat{e_z} \tag{3.2.10}$$

$$\frac{\partial T}{\partial t} + \mathbf{v}\cdot\nabla T = \nabla^2 T - \frac{N_B}{\varepsilon}\phi\mathbf{v}\cdot\nabla T + \frac{N_B}{Le}\nabla\phi\cdot\nabla T + \frac{N_A N_B}{Le}\nabla T\cdot\nabla T \tag{3.2.11}$$

$$\frac{1}{\sigma}\frac{\partial \phi}{\partial t} + \frac{1}{\varepsilon}\mathbf{v}\cdot\nabla\phi = \frac{1}{Le}\nabla^2\phi + \frac{N_A}{Le}\nabla^2 T \tag{3.2.12}$$

$$\left.\begin{aligned} &\mathbf{v} = (0,0,Pe),\ \ T = 1,\ \frac{\partial\phi}{\partial z} - \frac{PeLe}{\varepsilon}\phi + N_A\frac{\partial T}{\partial z} = 0 \ \text{ at } z = 0,\\ &\mathbf{v} = (0,0,Pe),\ \ T = 0,\ \frac{\partial\phi}{\partial z} - \frac{PeLe}{\varepsilon}\phi + N_A\frac{\partial T}{\partial z} = 0 \ \text{ at } z = 1. \end{aligned}\right\} \tag{3.2.13}$$

The non-dimensionlized parameters in the above equations are given below,

$$Ra = \frac{\rho_f g\beta K d(T_h^* - T_c^*)}{\mu\alpha_m}, \qquad Rn = \frac{(\rho_p - \rho_f)\phi_0^* gKd}{\mu\alpha_m}, \qquad Rm = \frac{\left\{\rho_p\phi_0^* + \rho_f(1-\phi_0^*)\right\}gKd}{\mu\alpha_m},$$
$$N_A = \frac{D_T(T_h^* - T_c^*)}{D_B T_c^*\phi_0^*}, \qquad N_B = \varepsilon\frac{(\rho_c)_p}{\rho_c)_f}\phi_0^*, \qquad Le = \frac{\alpha_m}{D_B},$$
$$Pe = \frac{dV^*}{\alpha_m}.$$

Here, Pe is a Péclet number, Le is a Brownian motion Lewis number, and Ra is the familiar thermal Rayleigh-Darcy number. The parameters Rm and Rn may be regarded as basic-density Rayleigh number and concentration Rayleigh number, respectively. The parameter N_A is a modified diffusivity ratio, while N_B is a modified particle-density increment. It will be noted that the parameter Rm is not involved in these and subsequent equations. It is

just a measure of the basic static pressure gradient.

3.3 Basic Solution

At the basic state, the nanofluid flow is only in z-direction, and so, it is assumed

$$\mathbf{v} = (0, 0, Pe), p = p_b(z), \quad T = T_b(z), \ \phi = \phi_b(z). \tag{3.3.1}$$

Using Eq.(3.3.1), Eq.(3.2.11) and Eq.(3.2.12) reduce to

$$\frac{d^2T_b}{dz^2} - Pe\frac{dT_b}{dz} + Pe\frac{N_B}{\varepsilon}\phi_b\frac{dT_b}{dz} + \frac{N_B}{Le}\frac{d\phi_b}{dz}\frac{dT_b}{dz} + \frac{N_AN_B}{Le}\left(\frac{dT_b}{dz}\right)^2 = 0, \tag{3.3.2}$$

$$\frac{d^2\phi_b}{dz^2} - \frac{PeLe}{\varepsilon}\frac{d\phi_b}{dz} + N_A\frac{d^2T_b}{dz^2} = 0. \tag{3.3.3}$$

After integrating Eq.(3.3.3), subject to the boundary condition Eq.(3.2.13), to obtain

$$\frac{d\phi_b}{dz} - \frac{PeLe}{\varepsilon}\phi_b + N_A\frac{dT_b}{dz} = 0. \tag{3.3.4}$$

Using Eq.(3.3.4), Eq.(3.3.2) reduces to

$$\frac{d^2T_b}{dz^2} - Pe\frac{dT_b}{dz} = 0. \tag{3.3.5}$$

The solutions of Eq.(3.3.4) and Eq.(3.3.5) subject to the boundary condition Eq.(3.2.13) are as follow

$$T_b = \frac{e^{Pe} - e^{Pez}}{e^{Pe} - 1}, \tag{3.3.6}$$

$$\phi_b = N_A\left(\frac{(\lambda_l - Pe + N_APe)\left(1 - e^{\lambda_l z}\right)}{(Pe - \lambda_l)\left(e^{\lambda_l} - 1\right)} + \frac{N_APe\left(1 - e^{Pez}\right)}{(Pe - \lambda_l)\left(e^{Pe} - 1\right)}\right), \tag{3.3.7}$$

where, for sort notation, it is assumed

$$\lambda_l = \frac{PeLe}{\varepsilon}$$

In the limit as Pe tends to zero one obtains, as Nield and Kuznetsov (2014) obtained in their revised model, the linear expressions

$$T_b = 1 - z, \qquad \phi_b = N_A z,$$

3.4 Perturbation Solution

Perturb the basic solution, Eq.(3.3.1), Eq.(3.3.6) and Eq.(3.3.7), by defining the velocity, temperature and nanoparticle concentration disturbances, one can obtained

$$\mathbf{v} = (0, 0, Pe) + \chi \mathbf{v}', \; T = T_b + \chi T', \; \phi = \phi_b + \chi \phi'. \tag{3.4.1}$$

where χ is a positive perturbation parameter. Applying the perturbed values from Eq.(3.4.1) into model (3.2.9)-(3.2.13) and using Eq.(3.3.6) and Eq.(3.3.7), neglect terms of order higher than χ. Taking the curl of momentum Eq.(3.2.10) one can obtain along with the boundary conditions Eq.(3.2.13) as

$$\nabla \cdot \mathbf{v}' = 0 \tag{3.4.2}$$

$$\left(n\nabla_1^2 + \frac{\partial^2}{\partial z^2}\right)\mathbf{w}' = \frac{1}{|Pe|^{n-1}}(Ra\nabla_1^2 T' - Rn\nabla_1^2 \phi') \tag{3.4.3}$$

$$\frac{\partial T'}{\partial t} + Pe\frac{\partial T'}{\partial z} + \frac{dT_b}{dz}\mathbf{w}' = \nabla^2 T' - \frac{N_B}{\varepsilon}\left(Pe\frac{dT_b}{dz}\phi' + \phi_b\frac{dT_b}{dz}\mathbf{w}' + Pe\phi_b\frac{\partial T'}{\partial z}\right) + \frac{N_B}{Le}\left(\frac{d\phi_b}{dz}\frac{\partial T'}{\partial z} + \frac{dT_b}{dz}\frac{\partial \phi'}{\partial z}\right) + \frac{2N_A N_B}{Le}\left(\frac{dT_b}{dz}\frac{\partial T'}{\partial z}\right) \tag{3.4.4}$$

$$\frac{1}{\sigma}\frac{\partial \phi'}{\partial t} + \frac{QPe}{\varepsilon}\frac{\partial T'}{\partial z} + \frac{1}{\varepsilon}\frac{d\phi_b}{dz}\mathbf{w}' = \frac{1}{Le}\nabla^2\phi' + \frac{N_A}{Le}\nabla^2 T' \tag{3.4.5}$$

$$\mathbf{w}' = 0, \;\; T' = 0, \;\; \frac{\partial \phi'}{\partial z} - \lambda_l \phi' + N_A\frac{\partial T'}{\partial z} = 0 \;\; \text{at } z = 0, \text{ and } \; at \; z = 1. \tag{3.4.6}$$

Differentiating Eq.(3.3.6) and Eq.(3.3.7) with respect to z, to obtain

$$\frac{dT_b}{dz} = \frac{-Pee^{Pez}}{e^{Pe} - 1}, \tag{3.4.7}$$

$$\frac{d\phi_b}{dz} = \lambda_l \phi_b - N_A \frac{dT_b}{dz}. \tag{3.4.8}$$

Next, the normal mode technique is applied for finding the unknown fields in Eq.(3.4.3), Eq.(3.4.4) and Eq.(3.4.5). Let

$$(\mathbf{w}', T', \phi') = [W(z), \Theta(z), \Phi(z)]\, e^{st+ilx+imy}, \tag{3.4.9}$$

and substitute it into the preceding differential equations, one can obtain

$$(D^2 - n\alpha^2)W + \frac{Ra}{|Pe|^{n-1}}\alpha^2\Theta - \frac{Rn}{|Pe|^{n-1}}\alpha^2\Phi = 0 \tag{3.4.10}$$

$$-\left(\frac{dT_b}{dz} + \frac{N_B Pe}{\varepsilon}\phi_b \frac{dT_b}{dz}\right) W + \left(D^2 + \frac{N_B}{Le}\frac{d\phi_b}{dz}D + \frac{2N_A N_B}{Le}\frac{dT_b}{dz}D - \frac{N_B Pe}{\varepsilon}\phi_b D - PeD - \alpha^2 - s\right)\Theta + \left(\frac{N_B}{Le}\frac{dT_b}{dz}D - \frac{N_B Pe}{\varepsilon}\frac{dT_b}{dz}D\right)\Phi = 0 \tag{3.4.11}$$

$$\left(\frac{1}{\varepsilon}\frac{d\phi_b}{dz}\right) W - \left(\frac{N_A}{Le}(D^2 - \alpha^2)\right)\Theta - \left(\frac{1}{Le}(D^2 - \alpha^2) - \frac{Pe}{\varepsilon}D - \frac{s}{\sigma}\right)\Phi = 0 \tag{3.4.12}$$

$$W = 0, \quad \Theta = 0, \quad D\Phi - \lambda_l \Phi + N_A D\Theta = 0 \quad \text{at} \quad z = 0, 1. \tag{3.4.13}$$

where

$$D = \frac{d}{dz} \text{ and } \alpha = \sqrt{l^2 + m^2},$$

is a horizontal wave number. The values of Pe is taken to be very small as compared with unity. The single-term Galerkin-type method is used to obtain an approximate solution of the system Eq.(3.4.4) to Eq.(3.4.13). For this, the trial functions are chosen in such a way that they satisfy the boundary conditions. Thus, one can have

$$W_1 = \Theta_1 = \sin \pi z, \Phi_1 = -N_A \cos \wp \sin(\pi z - \wp), \tag{3.4.14}$$

where $\wp = \tan^{-1}\left(\frac{\lambda_l}{\pi}\right)$.

Using Eq.(3.4.14) in Eqs (3.4.10)-(3.4.12), and the orthogonality of the equations to each trial function, one can obtain a system of 3 linear algebraic equations in the unknowns, namely A, B, C. To obtain a non-trivial solution for the equations in the system, the

determinants of the coefficients of the linear equations must be zero, and so

$$\det \begin{bmatrix} M_{11} & M_{12} & M_{13} \\ M_{21} & M_{22} & M_{23} \\ M_{31} & M_{32} & M_{33} \end{bmatrix} = 0, \tag{3.4.15}$$

where

$$\begin{aligned}
M_{11} &= -(\pi^2 + n\alpha^2) \langle W_1 W_1 \rangle , \\
M_{12} &= \frac{Ra}{|Pe|^{n-1}} \alpha^2 \langle \Theta_1 W_1 \rangle , \\
M_{13} &= -\frac{Rn}{|Pe|^{n-1}} \alpha^2 \langle \Phi_1 W_1 \rangle , \\
M_{21} &= \left\langle \left[\left\{ -(1 + \lambda_l \phi_b) \frac{dT_b}{dz} \right\} W_1 \right] \Theta_1 \right\rangle , \\
M_{22} &= \left\langle \left[\left\{ \left(D^2 + \frac{N_B}{Le} \frac{d\phi_b}{dz} D + \frac{2N_A N_B}{Le} \frac{dT_b}{dz} D - \frac{PeN_B}{\varepsilon} \phi_b D - PeD - (\alpha^2 + s) \right) \right\} \Theta_1 \right] \Theta_1 \right\rangle , \\
M_{23} &= \left\langle \left[\left\{ \left(\frac{N_B}{Le} \frac{dT_b}{dz} D - \frac{PeN_B}{\varepsilon} \frac{dT_b}{dz} \right) \right\} \Phi_1 \right] \Theta_1 \right\rangle , \\
M_{31} &= \left\langle \left[\left\{ \left(\frac{1}{\varepsilon} \frac{d\phi_b}{dz} \right) \right\} W_1 \right] \Phi_1 \right\rangle , \\
M_{32} &= \left\langle - \left[\left\{ \left(\frac{N_B}{Le} (D^2 - \alpha^2) \right) \right\} \Theta_1 \right] \Phi_1 \right\rangle , \\
M_{33} &= \left\langle - \left[\left\{ \left(\frac{1}{Le} (D^2 - \alpha^2) - \frac{Pe}{\varepsilon} D - \frac{s}{\sigma} \right) \right\} \Phi_1 \right] \Phi_1 \right\rangle
\end{aligned}$$

and

$$\langle f(z) \rangle = \int_0^1 f(z) dz,$$

R_a as the eigenvalue of Eq.(3.4.15), its value is found in terms of the other parameters as

$$Ra = \frac{M_{11}(M_{22}M_{33} - M_{32}M_{23}) + M_{13}(M_{21}M_{32} - M_{22}M_{31})}{\alpha^2 m_{12}(M_{21}M_{33} - M_{23}M_{31})}, \tag{3.4.16}$$

where

$$m_{12} \equiv M_{12}/Ra\alpha^2 = \frac{1}{|Pe|^{n-1}} \langle \Theta_1 W_1 \rangle .$$

In the case of neutral stability, take $s = i\omega$ in the analysis. Further, for stationary convection to occur, ω must be zero(ie. $\omega = 0$). To get the value of Ra for stationary case one can restrict so that the system is linear in Pe. To evaluate the above integrals the software package MATHEMATICA 10.0 (Wolfram Research,Champaign, IL) is used and the following expression is obtained

$$\begin{aligned} Ra \ =& RnN_ALe\left\{-\left(\frac{1}{\varepsilon}+\frac{1}{Le}\right)+\frac{N_BN_APe}{2\left(\pi^2+\alpha^2\right)\varepsilon}\left\{\frac{\left(\pi^2+\alpha^2\right)-1}{\varepsilon}+\frac{1+N_A}{Le}\right\}\right\}+ \\ & |Pe|^{n-1}\left\{\frac{\left(\pi^2+n\alpha^2\right)\left(\pi^2+\alpha^2\right)}{\alpha^2}+\frac{N_BN_APe\left(\pi^2+n\alpha^2\right)}{\alpha^2}\left\{-\frac{(1+N_A)}{Le}+\frac{(1-(\pi^2+\alpha^2))}{2\varepsilon}\right\}\right\}. \end{aligned} \tag{3.4.17}$$

The nanoparticle flux being zero at the boundaries implies the absence of the two opposing forces responsible for the occurrence of the oscillatory mode of convection hence oscillatory convection has been ruled out.

3.5 Result and Discussion

Since oscillatory convection has not been taking into account due to absence of two opposing force, and so, concentrating on the study of stationary convection in whole scenario. For limiting case, one can assume that the fluid is regular (i.e. $Rn = N_A = 0$), therefore

$$Ra^{st} \ = \ |Pe|^{n-1}\left\{\frac{\left(\pi^2+n\alpha^2\right)\left(\pi^2+\alpha^2\right)}{\alpha^2}\right\}. \tag{3.5.1}$$

It is noticed that Eq.(3.5.1) coincides with the result of Barletta and Storesletten (2016).

Further, expression for Ra in Eq.(3.4.17) is valid for power law type nanofluid of index n, for Newtonian nanofluid(Power law index $n = 1$) Eq.(3.4.17) reduces to

$$\begin{aligned} Ra^{st} \ =& \ RnN_ALe\left\{-\left(\frac{1}{\varepsilon}+\frac{1}{Le}\right)+\frac{N_BN_APe}{2\left(\pi^2+\alpha^2\right)\varepsilon}\left\{\frac{\left(\pi^2+\alpha^2\right)-1}{\varepsilon}+\frac{1+N_A}{Le}\right\}\right\}+ \\ & \left\{\frac{\left(\pi^2+\alpha^2\right)^2}{\alpha^2}+\frac{N_BN_APe\left(\pi^2+\alpha^2\right)}{\alpha^2}\left\{-\frac{(1+N_A)}{Le}+\frac{(1-(\pi^2+\alpha^2))}{2\varepsilon}\right\}\right\} \end{aligned} \tag{3.5.2}$$

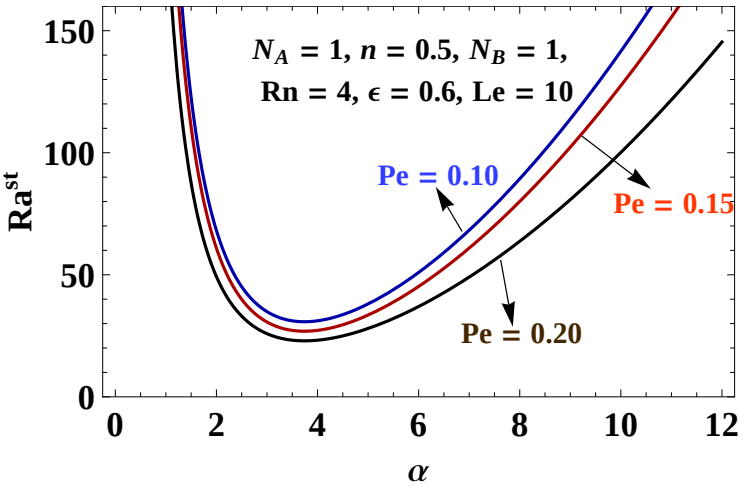

Figure 3.2: Ra^{st} versus α for different values of Pe

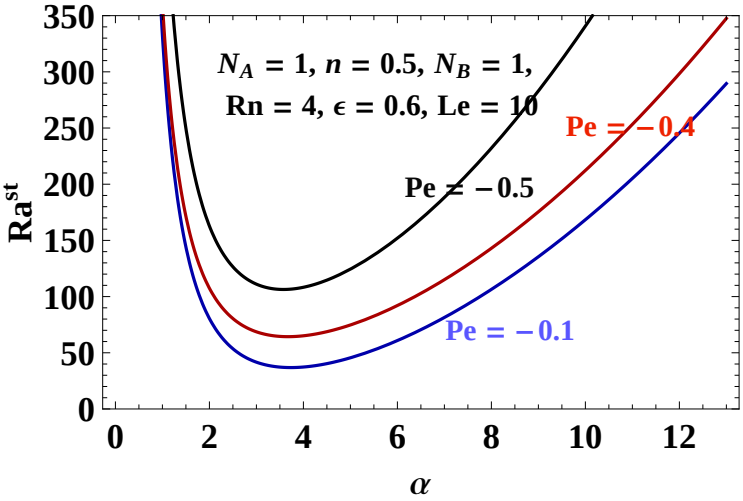

Figure 3.3: Ra^{st} versus α for different values of Pe

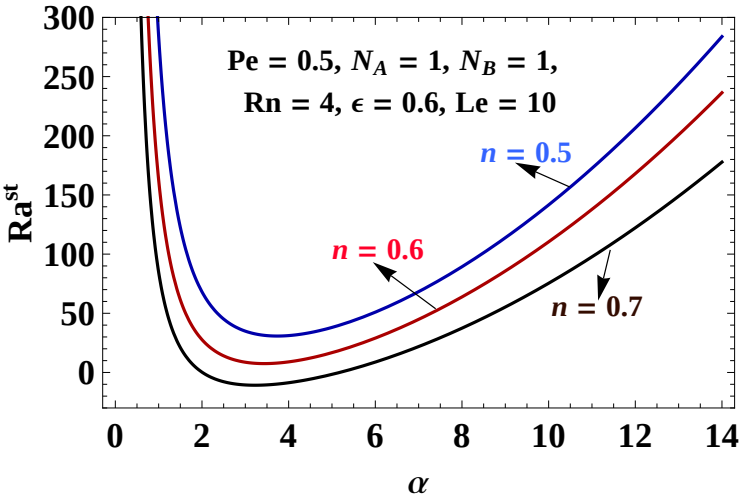

Figure 3.4: Ra^{st} versus α for different values of n

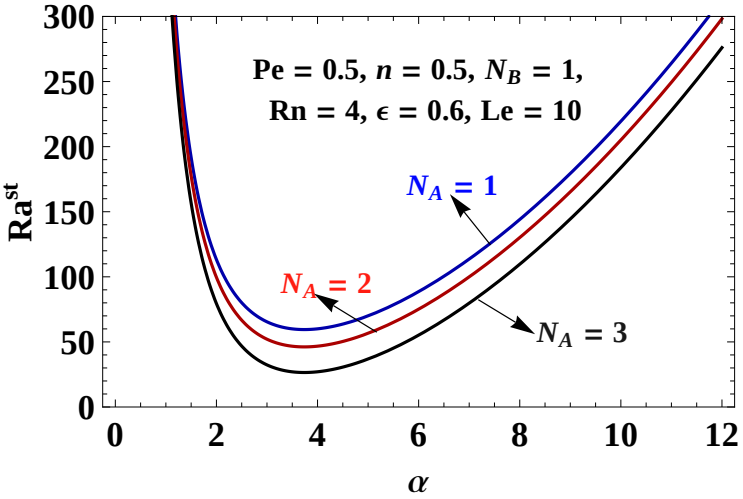

Figure 3.5: Ra^{st} versus α for different values of N_A

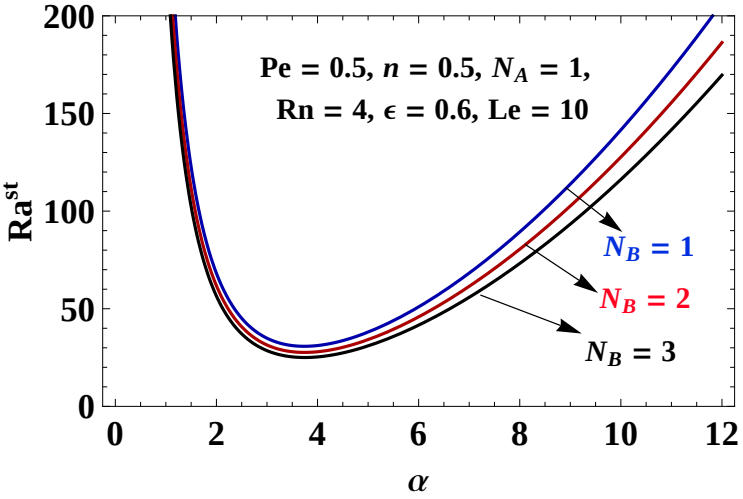

Figure 3.6: Ra^{st} versus α for different values of N_B

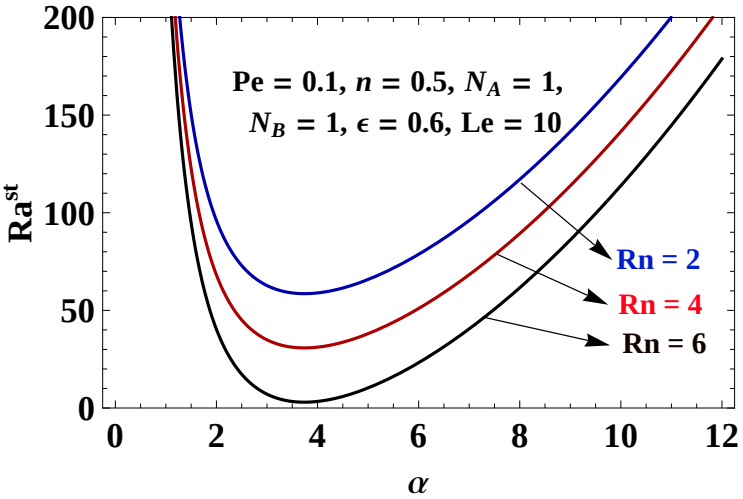

Figure 3.7: Ra^{st} versus α for different values of Rn

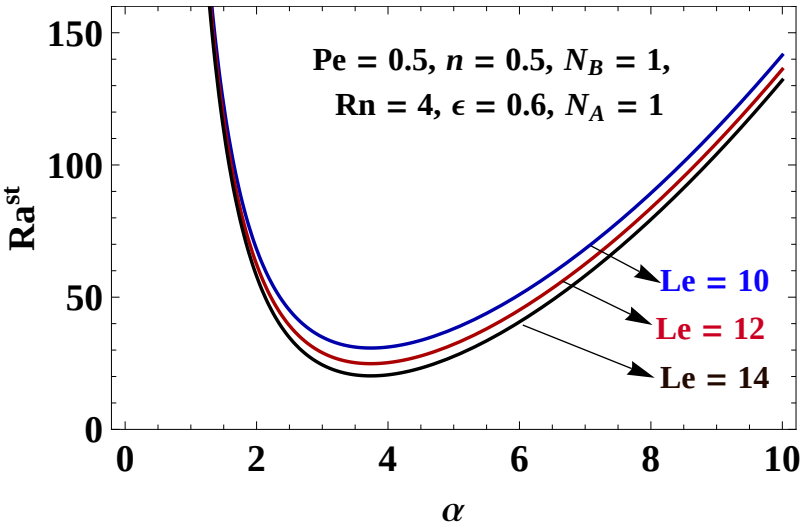

Figure 3.8: Ra^{st} versus α for different values of Le

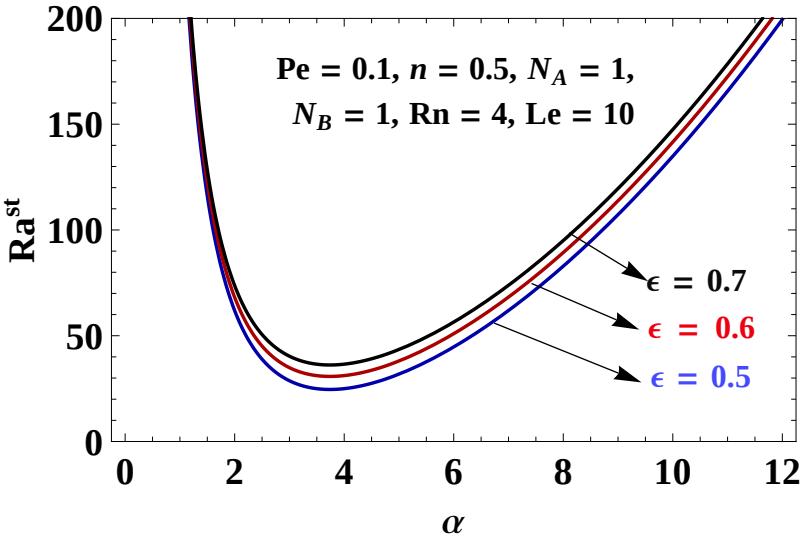

Figure 3.9: Ra^{st} versus α for different values of ε

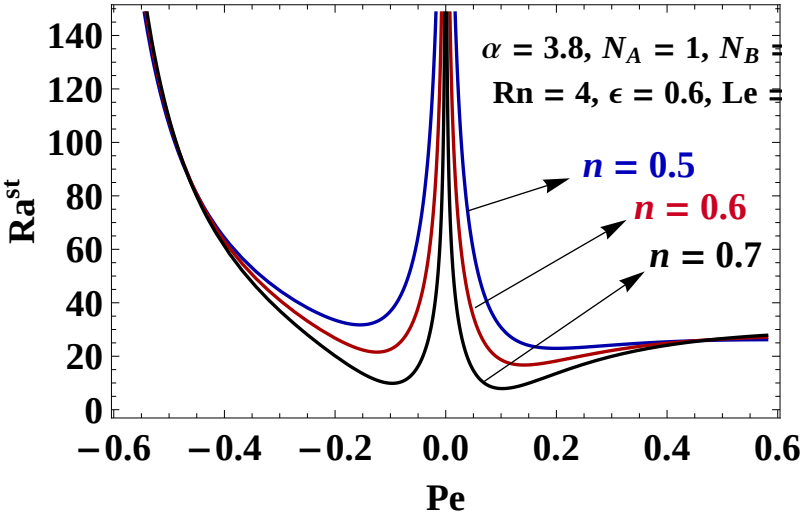

Figure 3.10: Ra^{st} versus Pe for different values of n

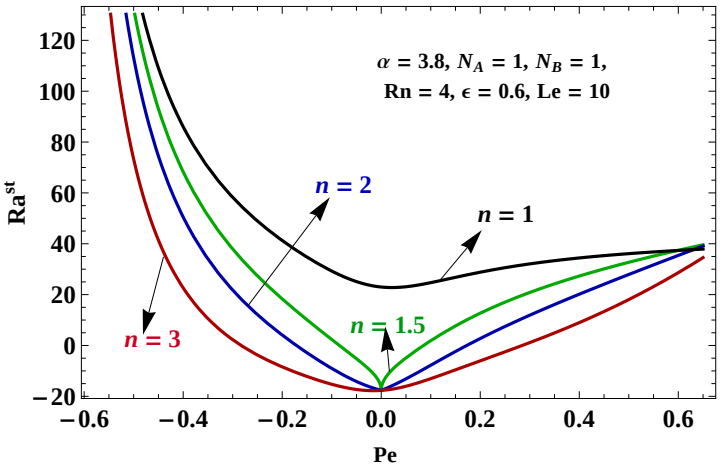

Figure 3.11: Ra^{st} versus Pe for different values of n

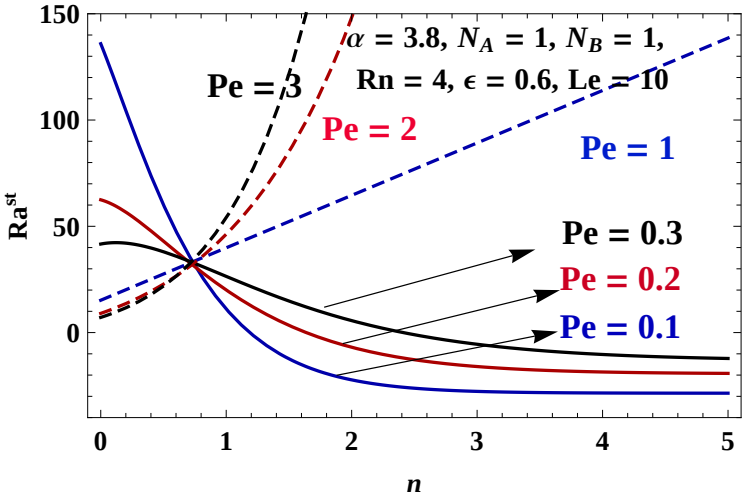

Figure 3.12: Ra^{st} versus n for different values of Pe

Consequently, in the absence of vertical throughflow (i.e., $Pe = 0$), the value of Rayleigh number for stationary convection is obtained as in Eq.3.5.3, which is same as obtained by Agarwal (2014a)

$$Ra^{st} = \frac{(\pi^2+\alpha^2)^2}{\alpha^2} - RnN_ALe\left(\frac{1}{\varepsilon}+\frac{1}{Le}\right). \tag{3.5.3}$$

Also, for a regular fluid Ra^{st} attains its minimum value when $\alpha = \pi$, that is, $\min\{Ra^{st}\} = 4\pi^2$. This result coincides with the well-known exact value for the Horton-Rogers-Lapwood problem.

Figures 3.2-3.9 depict neutral stability curves on the parametric plane (Ra^{st}, α) for different values of the parameters. In the cases considered, the Péclet number Pe ranges

from 0.1 to 1 and the power-law index n from 0.5 to 5 and other parameter values are fixed as $Rn = 4,\ N_A = 1,\ N_B = 1,\ \epsilon = 0.6$ and $Le = 10$. The neutral stability curve, in each case, confines the region of linear stability laying below the curve from the region of instability above the curve. The neutral stability curve is affected by both parameters Pe and n.

The effects of vertically upward throughflow and vertically downward throughflow on the thermal Rayleigh number are depicted in Figure 3.2 and Figure 3.3, respectively. It is found that as the vertically upward throughflow parameter Pe increases, the Rayleigh number Ra^{st} decreases, then, Pe has a destabilizing effect on the stationary convection. However for vertically downward throughflow paramet Pe has a stabilizing effect on the stationary convective system as Ra^{st} increases on increasing Pe. From Figure 3.4, it is observed that on decreasing the power law index n, thermal Rayleigh number Ra^{st} decreases. This means the power law index n enhances the onset of convection as it changes from pseudo-plastic nature to dilatant nature.

It is noticed from Figures (3.5, 3.6, 3.7 and 3.8) that the modified diffusivity ratio (N_A), the modified particle-density increment (N_B), the concentration Rayleigh number (Rn) and Lewis number (Le) have destabilizing effect on the system, because an increment in the value of any of these parameters leads to decrease in the value of thermal Rayleigh number. Further it is evident from Figure 3.9 that the influence of porosity ε has a stabilizing effect on the system, thus increase in ε delays the onset of convection as obtained by Agarwal (2014a).

The trends of Ra^{st} versus Pe for different values of n are reported in Figure 3.10 and Figure 3.11, respectively. Figure 3.10 shows the plots of Ra^{st} versus Pe for pseudo-plastic range of power law nanofluid whereas Figure 3.11 depicts the same for dilatancy range of power law nanofluid. The trajectories seem to be partially symmetric about $Pe = 0$ axis i.e. convective properties are not altered by the direction of throughflow .

Figure 3.12 shows the plots of Ra^{st} versus n for small and large values of Péclet number. Dotted line trajectories are for the large values of Péclet number where as solid line trajectories are used for small Péclet number. It is found that as power law index varies from pseudo-plasticity to dilatancy, the behaviour of instability change.

3.6 Conclusion

In the present chapter, it is considered the effects of the vertical throughflow of a non-Newtonian power-law nanofluid on the onset of convective instability in a horizontal porous layer heated from below. The extended Darcy's model of momentum diffusion is employed together with the Oberbeck-Boussinesq approximation. An analytical stationary basic solution is determined as analogous to Nield and Kuznetsov (2015).

The basic velocity, temperature and nanoparticle fraction fields turn out to be independent of the non-Newtonian rheology. A linear stability analysis is carried out by Galarkin method. The results have been obtained in terms of thermal Rayleigh number treated as eigen value of the problem. A numerical solution of the eigen value problem is employed to obtain the neutral stability curves and the critical Rayleigh number for the onset of instability. The concerning parameters of the transition to instability are the Péclet number associated with the throughflow, the power-law index of the nanofluid and parameter related to nanofluid. These parameters influence the position of the neutral stability curve and also the critical Rayleigh number and depicted graphically. The following findings are made:

1. The phase of power law nanofluid becomes significant in the presence of throughflow.

2. The effect of power law index is to increase (destabilizes) the heat transport as well as nanoparticle concentration transport in the system.

3. An analytical solution has been obtained under the regime of small Péclet numbers. It has been shown that simple analytical formulations for the neutral stability curve.

4. Convective motion is highly affected by pseudoplastic nanofluid and dilatant nanofluid.

5. Increment in concentration Rayleigh number Rn, modified diffusivity ratio N_A, modified particle density increment N_B and Lewis number Le enhances the heat and mass transfer.

6. Porosity ε of porous medium, diminishes the heat and concentration transport.

Chapter 4

G-jitter and internal heating effects on nanofluid convection in a porous media

4.1 Introduction

Common fluids have limited heat transfer capabilities while some of the metals have very high thermal conductivity in comparision to these fluids. Therefore, the basic idea behind nanofluids was to make a substance by combining these two, which would behave like a fluid and have thermal conductivity of a metal, thus nanofluids were made by suspending the nanoparticles in the common fluids, called base fluids. Presence of these nanoparticles in the base fluids may increase the thermal conductivity of the fluids by 15-40%. A large number of studies are available in the literature in which thermal instability in nanofluids have been investigated.

A significant feature of nanofluids is thermal conductivity enhancement which was first reported by Masuda et al. (1993). Nanofluids are mixtures of base fluid such as water

This chapter is based on the research article: G-jitter and internal heating effects on nanofluid convection in a porous media, Published in **Journal of Nanofluid, American Scientific Publisher.** Vol. 5 No. 3 pp. 328-339.

or ethylene-glycol along with small amount of nanoparticles such as metallic or metallic oxide particles (Cu, Cuo, Al_2O_3), having dimensions from 1 to 100nm. Choi (1995) was the first, who proposed this term "nanofluid". Natural convection or buoyancy driven convection, is the heat removal strategy adopted in a wide variety of industries ranging from transportation (heating, ventilation, and air conditioning), energy production and supply to electronics, textiles and paper production, geophysical problems, nuclear reactors to name a few (Choi 1999). The ballistic nature of heat transport within nanoparticles was analyzed by Chen (2001). Eastman et al. (2001) reported an increase of 40% in the effective thermal conductivity of ethylene-glycol with 0.3% volume of copper nanoparticles of 10 nm diameter. Further 10-30% increase of the effective thermal conductivity in alumina/water nanofluids with 1-4% of alumina was reported by Das et al. (2003). These reports led Buongiorno and Hu (2005) to suggest the possibility of using nanofluids in advanced nuclear systems. Another application of the nanofluid flow is in the delivery of nano-drug as suggested by Kleinstreuer et al. (2008).

Khanafer et al. (2003) reported an increase in concentration of suspended nanoparticles, is to increase in heat transfer in Cu-water nanofluids in a two-dimensional rectangular enclosures while Putra et al. (2003) reported that in natural convection, using Al_2O_3 and CuO nanofluids, the heat transfer coefficient was smaller than that in a clear fluid. Various studies have been conducted to determine the governing mechanisms in nanoscale, including a modified Maxwell model accounting for the ordered nanolayer near the particle fluid interface by Yu and Choi (2003), Brownian motion of nanoparticles in fluids by Jang and Choi (2004) and Kumar and Murthy (2005), ballistic nature of heat transport within nanoparticles by Keblinski and Cahill (2005) and thermal lagging in nanoparticles with a large surface area to volume ratio by Vadász (2006).

Kuznetsov and Nield both together have investigated a series of work on nanofluid as follows: the Horton Rogers Lapwood problem for the Darcy model in (2009), the onset of thermal instability in a porous medium saturated by a nanofluid using Brinkman model in (2010c), the effect of local thermal non-equilibrium using a three-temperature model in (2010a), the onset of double diffusive nanofluid convection in a layer of a saturated porous medium in (2010b), the effect of local thermal non-equilibrium (2011), the effect of vertical

throughflow (2011) and a linear stability theory (2012) for Horton Rogers Lapwood problem with thermal conductivity and viscosity dependent on the nanoparticle volume fraction.

It appears that all of the above studies deal with the case of uniform heating from below, and the case of internal heating has been largely neglected. There are numerous situations of great practical importance where the material offers its own source of heat. It is due to the internal heating of the earth that there exists a thermal gradient between the interior and exetior of the earth's crust, saturated by multicomponents fluids, which helps convective flow, thereby transferring the thermal energy towards the surface of the earth. Therefore, the role of internal heat generation becomes very important in several applications that include geophysics, reactor safety analyses, metal waste form development for spent nuclear fuel, fire and combustion studies, and storage of radioactive materials. However, there are relatively very few studies avalaible in which the effect of internal heating on convective flow has been investigated. Some of these studies are; Roberts (1967), Tveitereid and Palm (1976), Tveitereid (1978), Yu and Shih (1980), Bhattacharya and Jena (1984), Takashima (1989), Tasaka and Takeda (2005), Joshi et al. (2006), Bhadauria et al. (2011), Bhadauria (2012), Altawallbeh et al. (2013), Bhadauria et al. (2013a-c) and Srivastava et al. (2013).

Internal heating in porous media or gravity modulation of the system or a combination of both can be used as effective mechanism to control the convective flow by suppressing or advancing it. However, to the best of author's knowledge, no study is available in the literature in which the effect of vertical vibrations on the Darcy-Bénard convection in a nanofluid has been studied under internal heating effect using linear and nonlinear analysis. It is with this motive that linear and nonlinear analyses of thermal instability are made in a nanofluid saturated porous medium under gravity modulation, and studied the effect of internal heating on the system. For linear theory Venezian approach is followed, and five mode Lorenz model is considered for nonlinear theory, and in the process stability is discussed, heat and mass transport are quantified in terms of the Nusselt numbers.

4.2 Mathematical formulation

Consider a porous layer saturated by nanofluid, confined between two horizontal boundaries, respectively at z=0 and z=d, heated from below and cooled from above. The boundaries are impermeable and perfectly thermally conducting. The porous layer is extended infinitely in x and y-directions, and z-axis is taken vertically upward with the origin at the lower boundary. In addition, the local thermal equilibrium between the fluid and solid has been considered, thus the heat flow has been described using one equation model. T_h and T_c are the temperature at the lower and upper walls respectively such that $T_h > T_c$ (see Figure 4.1). Employing the Oberbeck-Boussinesq approximation, the governing equations to study the thermal instability in a nanofluid saturated porous medium are [Buongiorno (2006), Kuznetsov and Nield (2010a,b,c,) and Nield and Kuznetsov (2013)]:

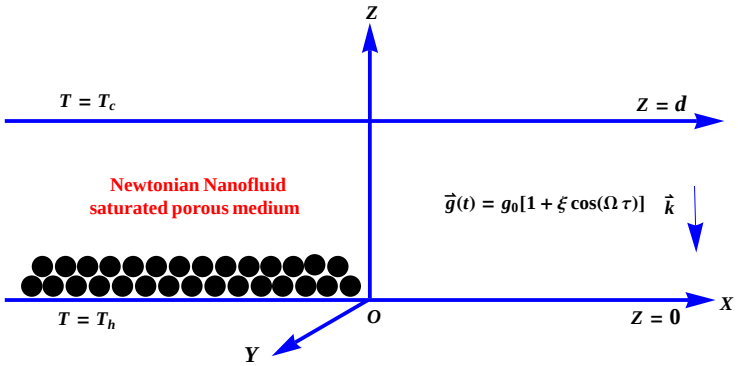

Figure 4.1: Physical configuration of the problem

$$\nabla \cdot \mathbf{v_D} = 0, \tag{4.2.1}$$

$$\frac{\rho_f}{\varepsilon}\frac{\partial \mathbf{v_D}}{\partial \tau} + \nabla p = -\frac{\mu}{K}\mathbf{v}_D + [\phi\rho_p + (1-\phi)\{\rho(1-\beta(T-T_c))\}]\vec{g} \tag{4.2.2}$$

$$\gamma\frac{\partial T}{\partial \tau} + \mathbf{v}_D \cdot \nabla T = \kappa_T \nabla^2 T + \varepsilon\frac{(\rho c)_p}{(\rho c)_f}[D_B \nabla\phi \cdot \nabla T + \frac{D_T}{T_c}\nabla T \cdot \nabla T] + \eta(T - T_c) \tag{4.2.3}$$

$$\frac{\partial \phi}{\partial \tau} + \frac{1}{\varepsilon}\mathbf{v}_D \cdot \nabla\phi = D_B\nabla^2\phi + \frac{D_T}{T_c}\nabla^2 T \tag{4.2.4}$$

$$\vec{g} = g_0\,(1 + \xi\cos(\Omega\tau))\,\vec{k} \tag{4.2.5}$$

where $\mathbf{v}_D$ is the Darcy velocity. The physical variables have their usual meanings, given in the nomenclature. Assuming temperature and volumetric fraction of the nanoparticles to be constant at the stress-free boundaries, one may take the boundary conditions on T and ϕ as:

$$\mathbf{v} = 0, \quad T = T_h, \ \phi = \phi_0 \text{ at } z = 0, \tag{4.2.6}$$

$$\mathbf{v} = 0, \quad T = T_c, \ \phi = \phi_1 \text{ at } z = d, \tag{4.2.7}$$

where ϕ_1 is greater than ϕ_0. The dimensionless variables are considered as given below: $(x^*, y^*, z^*) = (x, y, z)/d$, $\tau^* = \tau\kappa_T/\gamma d^2$, $(u^*, v^*, w^*) = (u, v, w)d/\kappa_T$, $p^* = pK/\mu\kappa_T, \phi^* = \dfrac{\phi - \phi_0}{\phi_1 - \phi_0}$ and $T^* = \dfrac{T - T_c}{T_h - T_c}$, where $\kappa_T = \dfrac{k_m}{(\rho c)_f}$, $\gamma = \dfrac{(\rho c_p)_m}{(\rho c_p)_f}$. The non-dimensionalized governing equations along with boundary conditions are (after dropping the asterisk for simplicity)

$$\nabla \cdot \mathbf{v} = 0 \tag{4.2.8}$$

$$\frac{1}{Va}\frac{\partial \mathbf{v}}{\partial \tau} = -\nabla p - \mathbf{v} - \mathrm{g}_m \left(Rm - Ra\ T + Rn\phi\right) \hat{e_z} \tag{4.2.9}$$

$$\gamma\frac{\partial T}{\partial \tau} + \mathbf{v} \cdot \nabla T = (\nabla^2 + Ri)T + \frac{N_B}{Le}\nabla\phi \cdot \nabla T + \frac{N_A N_B}{Le}\nabla T \cdot \nabla T \tag{4.2.10}$$

$$\frac{\partial \phi}{\partial \tau} + \mathbf{v} \cdot \nabla \phi = \frac{1}{Le}\nabla^2\phi + \frac{N_A}{Le}\nabla^2 T \tag{4.2.11}$$

$$\mathbf{v} = 0, \quad T = 1, \ \phi = 0 \text{ at } z = 0, \text{ and } \mathbf{v} = 0, \quad T = 0, \ \phi = 1 \text{ at } z = 1, \tag{4.2.12}$$

where $\mathrm{g}_m = (1 + \xi\cos(\Omega t))$. The non-dimensionlized parameters in the above equations are given in nomenclature, N_A is the modified diffusivity ratio, which is similar to the Soret parameter that arises in cross diffusion in thermal instability.

4.2.1 Conduction state

At the basic state, the nanofluid is assumed to be at rest, therefore the quantities at the basic state will vary only in z-direction, and are given by:

$$\mathbf{v} = 0, p = p_b(z), \quad T = T_b(z), \ \phi = \phi_b(z). \tag{4.2.13}$$

Substituting Eq.(4.2.13) in Eq.(4.2.10) and Eq.(4.2.11), to get:

$$\frac{d^2T_b}{dz^2} + RiT_b + \frac{N_B}{Le}\frac{d\phi_b}{dz}\frac{dT_b}{dz} + \frac{N_AN_B}{Le}(\frac{dT_b}{dz})^2 = 0, \tag{4.2.14}$$

Using order magnitude analysis, Kuznetsov and Nield (2009) and Tzou (2008a,b) showed that the second and third terms in equation Eq.(4.2.14) are small, and hence

$$\frac{d^2T_b}{dz^2} + RiT_b = 0, \quad \frac{d^2\phi_b}{dz^2} = 0. \tag{4.2.15}$$

The boundary conditions for solving Eq.(4.2.15) can be obtained from Eq.(4.2.12) as:

$$T_b = 1, \ \phi_b = 0 \ at \ z = 0, \tag{4.2.16}$$

$$T_b = 0, \ \phi_b = 1 \ at \ z = 1. \tag{4.2.17}$$

Solving Eq.(4.2.15), subject to the conditions, Eq.(4.2.16) and Eq.(4.2.17), one can obtain:

$$T_b = \frac{\sin\sqrt{Ri}(1-z)}{\sin\sqrt{Ri}}, \tag{4.2.18}$$

$$\phi_b = z. \tag{4.2.19}$$

4.2.2 Perturbed state/Dimensionless governing equations

Now superimpose perturbations on the basic state given in equation (4.2.13):

$$\mathbf{v} = \mathbf{v}', \ p = p_b + p', \ T = T_b + T', \ \phi = \phi_b + \phi'. \tag{4.2.20}$$

Substituting the above expression (4.2.20) in Eqs.(4.2.8)-(4.2.11) and using the expressions (4.2.18) and (4.2.19), eliminating the pressure term and introducing the stream functions, one can obtain:

$$\frac{1}{Va}\frac{\partial}{\partial\tau}(\nabla^2\psi) + \nabla^2\psi = \left(Rn\frac{\partial\phi}{\partial x} - Ra\frac{\partial T}{\partial x}\right)\mathrm{g}_m\vec{k}, \tag{4.2.21}$$

$$-\frac{\partial T_b}{\partial z}\frac{\partial \psi}{\partial x} - (\nabla^2 + Ri)T = -\frac{\partial T}{\partial \tau} + \frac{\partial(\psi, T)}{\partial(x, z)}, \tag{4.2.22}$$

$$-\frac{\partial \psi}{\partial x} - \frac{N_A}{Le}\nabla^2 T = \frac{1}{Le}\nabla^2\phi - \frac{1}{\gamma}\frac{\partial \phi}{\partial \tau} + \frac{\partial(\psi, \phi)}{\partial(x, z)}. \tag{4.2.23}$$

4.3 Linear stability

Here linear stability analysis considering marginal and over-stable states is studied. To perform linear stability analysis, nonlinear terms in Eq.(4.2.21) to Eq.(4.2.23) are neglected thus a linear system of equations is obtained as.

$$\frac{1}{Va}\frac{\partial}{\partial \tau}(\nabla^2\psi) + \nabla^2\psi = \left(Rn\frac{\partial \phi}{\partial x} - Ra\frac{\partial T}{\partial x}\right) \mathrm{g}_m\vec{k}, \tag{4.3.1}$$

$$-\frac{\partial T_b}{\partial z}\frac{\partial \psi}{\partial x} - (\nabla^2 + Ri)T = -\frac{\partial T}{\partial \tau}, \tag{4.3.2}$$

$$-\frac{\partial \psi}{\partial x} - \frac{N_A}{Le}\nabla^2 T = \frac{1}{Le}\nabla^2\phi. \tag{4.3.3}$$

Eliminating T and ϕ from Eq.(4.3.1) to Eq.(4.3.3) a single equation for ψ is obtained in the following form

$$\left(\frac{1}{Va}\frac{\partial}{\partial t} + 1\right)\left(\nabla^2 + Ri - \frac{\partial}{\partial t}\right)\left(\frac{1}{Le}\nabla^2 - \frac{1}{\gamma}\frac{\partial}{\partial t}\right)\nabla^2\psi = -\frac{\partial^2}{\partial x^2}Rn\left[\left(\nabla^2 + Ri - \frac{\partial}{\partial t}\right) - \frac{NA}{Le}\nabla^2\frac{\partial T_b}{\partial z}\right] g_m\psi + Ra\frac{\partial^2}{\partial x^2}\left[\left(\frac{1}{Le}\nabla^2 - \frac{1}{\gamma}\frac{\partial}{\partial t}\right)\frac{\partial T_b}{\partial z}\right] g_m\psi. \tag{4.3.4}$$

4.3.1 Method of Solution

Perturbation technique is used to obtain eigen functions ψ and eigen values Ra by introducing a small perturbation parameter ξ.

$$\begin{cases} \psi = \psi_0 + \xi\psi_1 + \xi^2\psi_2 + \dots \\ \\ Ra = Ra_0 + \xi^2 Ra_2 + \dots \end{cases} \tag{4.3.5}$$

Substitute the Eq.(4.3.5) into Eq.(4.3.4) and equate the like powers of ξ on both sides, to obtain

$$\begin{aligned} L\psi_0 &= 0, \qquad (4.3.6)\\ L\psi_1 &= Rn\frac{\partial^2}{\partial x^2}\left[-\left(\nabla^2 + Ri - \frac{\partial}{\partial t}\right) + \frac{NA}{Le}\nabla^2\frac{\partial T_b}{\partial z}.\right]\psi_0\cos(\Omega t),\\ &+ Ra_0\frac{\partial^2}{\partial x^2}\left[\left(\frac{1}{Le}\nabla^2 - \frac{1}{\gamma}\frac{\partial}{\partial t}\right)\frac{\partial T_b}{\partial z}.\right]\psi_0\cos(\Omega t), \qquad (4.3.7)\end{aligned}$$

$$\begin{aligned} L\psi_2 &= Rn\frac{\partial^2}{\partial x^2}\left[-\left(\nabla^2 + Ri - \frac{\partial}{\partial t}\right) + \frac{NA}{Le}\nabla^2\frac{\partial T_b}{\partial z}.\right]\psi_1\cos(\Omega t),\\ &+ \frac{\partial^2}{\partial x^2}\left[\left(\frac{1}{Le}\nabla^2 - \frac{1}{\gamma}\frac{\partial}{\partial t}\right)\frac{\partial T_b}{\partial z}.\right](Ra_0\psi_1\cos(\Omega t) + Ra_2\psi_0), \qquad (4.3.8)\end{aligned}$$

where

$$L = \left(\frac{1}{Va}\frac{\partial}{\partial t} + 1\right)\left(\nabla^2 + Ri - \frac{\partial}{\partial t}\right)\left(\frac{1}{Le}\nabla^2 - \frac{1}{\gamma}\frac{\partial}{\partial t}\right)\nabla^2 - \frac{\partial^2}{\partial x^2}Rn\left[-\left(\nabla^2 + Ri - \frac{\partial}{\partial t}\right) + \frac{NA}{Le}\nabla^2\frac{\partial T_b}{\partial z}.\right] - Ra_0\frac{\partial^2}{\partial x^2}\left[\left(\frac{1}{Le}\nabla^2 - \frac{1}{\gamma}\frac{\partial}{\partial t}\right)\frac{\partial T_b}{\partial z}.\right] \qquad (4.3.9)$$

4.3.2 Zeroth Order System

The marginally stable solutions for Eq.(4.3.6) are assumed in the form

$$\psi_0 = \sin(\alpha x)\sin(\pi z) \qquad (4.3.10)$$

Since ψ is independent of y, therefore α is the wave number in x direction, the corresponding eigen values are given by

$$Ra_0 = \left(\frac{\delta^2(\delta^2 - Ri)(4\pi^2 - Ri)}{4\pi^2\alpha^2}\right) - Rn\left(\frac{Le(\delta^2 - Ri)(4\pi^2 - Ri)}{4\pi^2\delta^2} + NA\right) \qquad (4.3.11)$$

where $\delta^2 = \pi^2 + \alpha^2$.

4.3.3 First Order System

Use Eq.(4.3.10) in Eq.(4.3.7) to get,

$$L\psi_1 = Rn\alpha^2\left[\left(Ri-\delta^2+\frac{NA}{Le}I_1\delta^2\right)\cos(\Omega t)+\Omega\sin(\Omega t)\right]\sin(\alpha x)\sin(\pi z) + Ra_0\alpha^2 I_1\left[\left(\frac{\delta^2}{Le}\cos(\Omega t)-\frac{\Omega}{\gamma}\sin(\Omega t)\right)\right]\sin(\alpha x)\sin(\pi z), \tag{4.3.12}$$

where $I_1 = \int_0^1\int_0^{\frac{\pi}{\alpha}}\frac{\partial T_b}{\partial z}\sin^2(\alpha x)\sin^2(\pi z)dxdz = -\frac{\pi^3/\alpha}{(4\pi^2-Ri)}$.

For the solution of the homogeneous equation corresponding to the Eq.(4.3.12), one must have a term which is orthogonal to $\sin(\alpha x)\sin(\pi z)$. Using Eq.(4.3.9) one can obtain

$$L[\sin(\pi z)\exp^{(i\alpha x-i\Omega t)}] = L(\Omega)\sin(\pi z)\exp^{(i\alpha x-i\Omega t)}, \tag{4.3.13}$$

where

$$\begin{aligned}
&L(\Omega) = A+iB\\
&A = \Omega^2\left(\frac{\delta^2}{\gamma}\left(1+\frac{\delta^2-Ri}{Va}\right)+\frac{\delta^4}{LeVa}\right)+Rn\alpha^2\left(\delta^2-Ri-\frac{NA}{Le}I_1\delta^2\right)-Ra_0\alpha^2\frac{1}{Le}I_1\delta^2\\
&\quad-\frac{\delta^4}{Le}\left(\delta^2-Ri\right)\\
&B = \Omega\left[Ra_0\alpha^2\frac{I_1}{\gamma}-Rn\alpha^2+\frac{\delta^2}{\gamma}\left(\delta^2-Ri-\frac{\Omega^2}{Va}\right)+\frac{\delta^4}{Le}\left(1+\frac{\delta^2-Ri}{Va}\right)\right]
\end{aligned}$$

Hence, ψ_1 is obtained by inverting the operator L in the following form

$$\psi_1 = Re\left[\frac{L^*(\Omega)}{|L(\Omega)|^2}F_1(t)\sin(\alpha x)\sin(\pi z),\right] \tag{4.3.14}$$

where

$$F_1(t) = Rn\alpha^2\left\{\left(Ri-\delta^2+\frac{NA}{Le}I_1\delta^2\right)\cos(\Omega t)+\Omega\sin(\Omega t)\right\} + Ra_0\alpha^2 I_1\left\{\left(\frac{\delta^2}{Le}\cos(\Omega t)-\frac{\Omega}{\gamma}\sin(\Omega t)\right)\right\}.$$

4.3.4 Second Order System

From the Eq.(4.3.8) it is obtained

$$L\psi_2 = \left[Ra_0\alpha^2 I_1\frac{\delta^2}{Le} - Rn\alpha^2\left(\delta^2 - Ri - \frac{NA}{Le}I_1\delta^2\right)\right]\psi_1\cos(\Omega t)$$

$$+\left[Ra_0\alpha^2\frac{1}{\gamma} - Rn\alpha^2\right](\psi_1\cos(\Omega t))' + Ra_2\alpha^2 I_1\frac{\delta^2}{Le}\psi_0. \tag{4.3.15}$$

It is not required to solve the Eq.(4.3.15), but use it to determine Ra_2. For the existence of a solution of the Eq.(4.3.15), it is necessary that, the steady part of its right hand side must be orthogonal to $\sin(\alpha x)\sin(\pi z)$. This gives,

(4.3.16)

$$\int_0^1\int_0^{\frac{\pi}{\alpha}}\left[\left\{Ra_0\alpha^2 I_1\frac{\delta^2}{Le} - Rn\alpha^2\left(\delta^2 - Ri - \frac{NA}{Le}I_1\delta^2\right)\right\}\overline{\psi_1\cos(\Omega t)} + \left\{Ra_0\alpha^2\frac{1}{\gamma} - Rn\alpha^2\right\}\overline{(\psi_1\cos(\Omega t))'} + Ra_2\alpha^2 I_1\frac{\delta^2}{Le}\psi_0\right] sin(\alpha x)\sin(\pi z)dxdz, \tag{4.3.17}$$

where the upper bar denotes the time average.

$$Ra_2 = -\frac{LeA\alpha^2\left[Ra_0 I_1\frac{\delta^2}{Le} - Rn\left(\delta^2 - Ri - \frac{NA}{Le}I_1\delta^2\right)\right]^2}{2I_1\delta^2(A^2+B^2)}. \tag{4.3.18}$$

4.4 Nonlinear stability

Assuming Fourier expressions for the physical variables such as stream function, temperature and nanoparticle fraction, a local nonlinear stability analysis is performed, and hence take the following:

$$\psi = \sum_{n=1}^{\infty}\sum_{m=1}^{\infty}A_{mn}(\tau)\sin(m\alpha x)\sin(n\pi z) \tag{4.4.1}$$

$$T = \sum_{n=1}^{\infty}\sum_{m=1}^{\infty}B_{mn}(\tau)\cos(m\alpha x)\sin(n\pi z) \tag{4.4.2}$$

$$\phi = \sum_{n=1}^{\infty}\sum_{m=1}^{\infty}C_{mn}(\tau)\cos(m\alpha x)\sin(n\pi z). \tag{4.4.3}$$

In what follows, take the modes $(1,1)$ for stream function, and $(0,2)$ and $(1,1)$ for temperature and nanoparticle concentration, thus using a severely truncated representation of Fourier series for stream function, temperature and nanoparticle concentration, as used by Veronis (1966), Rudraiah (1986). This study will help in understanding the physics of the problem with minimum mathematical expressions. Further, the results can be used as starting point to generalize it for full nonlinear problem. Also, it is to be noted that the effect of nonlinearity is to distort the temperature and concentration fields through the interaction of ψ and T, and ψ and ϕ respectively. As a result a component of the form $sin(2\pi z)$ will be generated. Therefore the minimal expression which describes the finite amplitude convection is of the form

$$\psi = A_{11}(\tau)\sin(\alpha x)\sin(\pi z) \tag{4.4.4}$$

$$T = B_{11}(\tau)\cos(\alpha x)\sin(\pi z) + B_{02}(\tau)\sin(2\pi z) \tag{4.4.5}$$

$$\phi = C_{11}(\tau)\cos(\alpha x)\sin(\pi z) + C_{02}(\tau)\sin(2\pi z), \tag{4.4.6}$$

where the amplitudes $A_{11}(\tau), B_{11}(\tau), B_{02}(\tau), C_{11}(\tau)$ and $C_{02}(\tau)$ are functions of time and to be determined. Substituting expressions (4.4.4) - (4.4.6) in Eqs.(4.2.21) - (4.2.23), using the orthogonality condition for the eigenfunctions associated with the considered minimal mode, to get:

$$\frac{dA_{11}(\tau)}{d\tau} = \frac{Va}{\delta^2}\{\alpha\,(1+\xi\cos(\Omega t))\,[RnC_{11}(\tau) - RaB_{11}(\tau)] - \delta^2 A_{11}(\tau)\} \tag{4.4.7}$$

$$\frac{dB_{11}(\tau)}{d\tau} = -[\frac{4\pi^2 a}{(4\pi^2 - Ri)}A_{11}(\tau) + (\delta^2 - Ri)B_{11}(\tau) + \pi\alpha A_{11}(\tau)B_{02}(\tau)] \tag{4.4.8}$$

$$\frac{dB_{02}(\tau)}{d\tau} = \frac{\pi\alpha}{2}A_{11}(\tau)B_{11}(\tau) - (4\pi^2 - Ri)B_{02}(\tau) + \frac{8\pi^2 Ri}{9\pi^4 - 10\pi^2 Ri - Ri^2}A_{11}(\tau) \tag{4.4.9}$$

$$\frac{1}{\gamma}\frac{dC_{11}(\tau)}{d\tau} = -[\alpha A_{11}(\tau) + \frac{1}{Le}\delta^2 C_{11}(\tau) + \pi\alpha A_{11}(\tau)C_{02}(\tau) + \frac{N_A}{Le}\delta^2 B_{11}(\tau)] \tag{4.4.10}$$

$$\frac{1}{\gamma}\frac{dC_{02}(\tau)}{d\tau} = \frac{\pi\alpha}{2}A_{11}(\tau)C_{11}(\tau) - \frac{4\pi^2}{Le}[C_{02}(\tau) + N_A B_{02}(\tau)] \tag{4.4.11}$$

The above system of simultaneous autonomous ordinary differential equations can be subsequently solved numerically using Mathematica NDSolve.

4.5 Heat and nanoparticle concentration transport

The thermal Nusselt number, $Nu(\tau)$ is defined as

$$Nu(\tau) = \frac{\text{Heat transport by (conduction + convection)}}{\text{Heat transport by conduction}} = 1 + \left[\frac{\int_0^{2\pi/\alpha_c} \left(\frac{\partial T}{\partial z} \right) dx}{\int_0^{2\pi/\alpha_c} \left(\frac{\partial T_b}{\partial z} \right) dx} \right]_{z=0}. \tag{4.5.1}$$

Substituting equations (4.2.18) and (4.4.5) in Eq.(4.5.1), to get

$$Nu(\tau) = 1 - 2\pi B_{02}(\tau) \tag{4.5.2}$$

The nanoparticle concentration Nusselt number, $Nu_\phi(\tau)$ is defined similar to the thermal Nusselt number.

$$\text{Nu}_\phi(\tau) = \frac{\text{Mass transport by (molecular diffusion+advection)}}{\text{Mass transfer by molecular diffusion}}, \tag{4.5.3}$$

$$= (1 - 2\pi C_{02}(\tau)) + N_A(1 - 2\pi B_{02}(\tau)). \tag{4.5.4}$$

4.6 Results and discussion

The nanofluids have an enhanced magnitude of thermal conductivity than normal fluids or metals, being attributed to the presence of nanoparticles in them. Nanofluids being combinations of base fluids with some metallic nano-scale sized particles or fibers, suspended in them, combined the thermal properties of both, leading to an enhanced rate of thermal conductivity. This has been experimentally verified by many researchers in the past decade.

Here in this Chapter the effect of gravity modulation and internal heat generation on the onset of Darcy-Bénard nanofluid convection is investigated. The linear stability solution is obtained using Venezian approach. The expressions for the critical Rayleigh number for different realistic values of the non dimensional parameters such as Lewis number, concentration Rayleigh number, Vadász number, heat capacity ratio, internal Rayleigh

number and modified diffusivity ratio are computed, and the results are depicted in Figures 4.2–4.7.

Using Darcy model and considering top heavy porus layer, a nonlinear stability analysis is performed to study heat and concentration transport. Linear theory has been investigated by Umavathi (2013), concerning temperature modulation, Pranesh et al. (2014) performed gravity modulation using Venezian model and Mohammed et al (2015) studied g-jitter induced magnetoconvection with boundary layer flow. It is well known that a nonlinear theory is needed to analyze heat/mass transport, which is not possible by linear stability theory. Moreover external regulations of convection is important in the study of thermal instability, therefore, in this Chapter gravity modulation has been consider for either enhancing or inhibiting the convective heat transport as is required for a real life application. It is to be noted that according to Buongiorno (2006) Le is large for most nanofluids investigated so far, but as per Bhadauria and Agarwal (2011b) and Umavathi (2013) $Le = 10$ is considered in the case of nanopartical concentration Rayleigh number. The effect of gravity modulation on heat transport has been depicted in Figures 4.8–4.22. The following parameters $Va, Rn, N_A, Le, \gamma, \xi$ and Ω occuring in the present study, influence the convective heat transport. The first five parameters are related to the porous layer and the next two parameters concern the external mechanism of controlling convection. Because of small amplitude of modulation, the values of ξ are considered to be small. Further, the gravity modulation assumed to be of low frequency, as at low range of frequencies, the effect of frequency on onset of convection as well as on heat transport is maximum. The coefficient of heat transport, i.e. thermal Nusselt number and the coefficient of nanoparticle concentration transport, i.e. concentration Nusselt number are calculated as functions of time and other parameters of the system. The obtained results are depicted in the Figures 4.8–4.22 for $Nu(\tau)$ and $Nu_\phi(\tau)$ verses time τ. In the figures, the values of $Nu(\tau)$ and $Nu_\phi(\tau)$ start with 1 and 2 respectively, and remain constant for a quite some time, showing the conduction state. Then the values of $Nu(\tau)$ and $Nu_\phi(\tau)$ increase as time passes, thus showing that the convection is taking place. These values oscillate and then approach constant values thus showing that the steady state has been achieved.

For the results corresponding to linear stability, graphs Ra_2 versus Ω are ploted. In

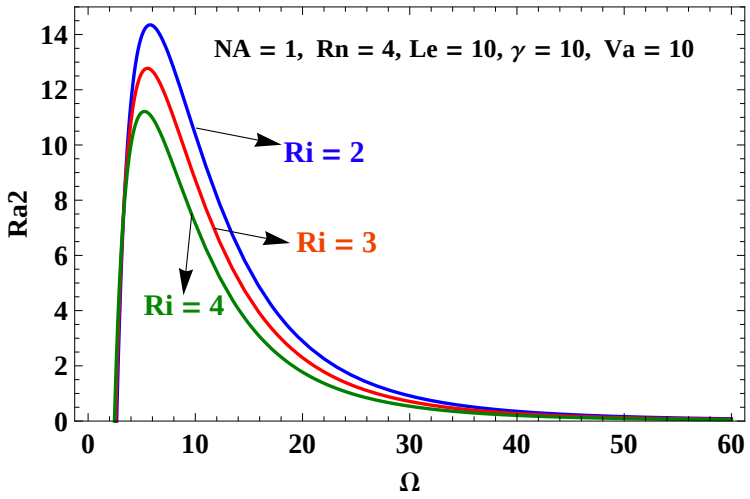

Figure 4.2: Ra_2 versus Ω for different values of Ri

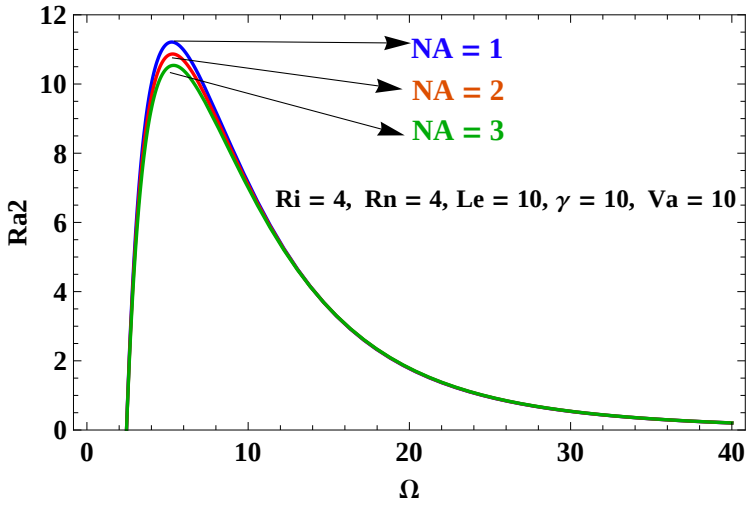

Figure 4.3: Ra_2 versus Ω for different values of N_A

Figure 4.2 it is observed that, as Ri increases, $|Ra_2|$ decreases. The increase in Ri implies that the entropy of the system will increase. Thus, increase in Ri destabilizes the system. Figure 4.3 is the plot of Ra_2 versus Ω for different values of modified diffusivity ratio N_A. Increase in N_A signifies that thermophoresis effect will increase, it is observed that $|Ra_2|$ decreases as N_A increases, thus destabilize the system.

Figure 4.4 shows the effect of Rn. An increment in Rn represents an increment in concentration of suspended nanoparticles. It is found as Rn increases $|Ra_2|$ increases, thereby it stabilizes the system. This means that the fluids with suspended nanoparticles are more helpful for stabilization than ordinary fluids. Figure 4.5 is the plot of Ra_2 versus Ω for different values of Lewis number Le. From the figure it is found that as Le increases

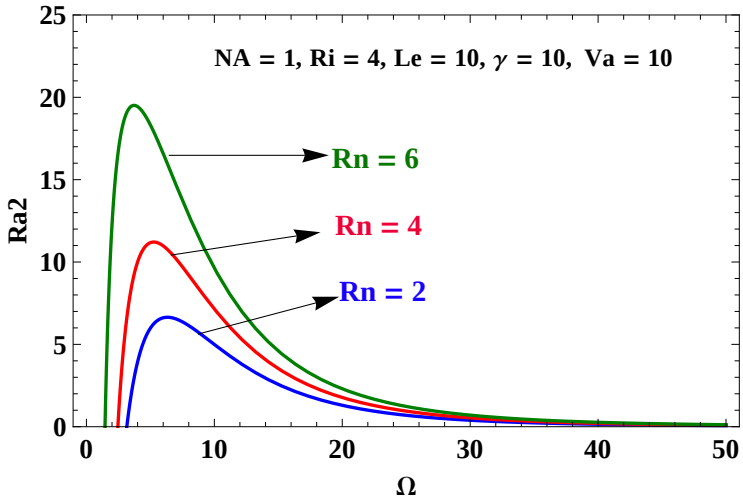

Figure 4.4: Ra_2 versus Ω for different values of Rn

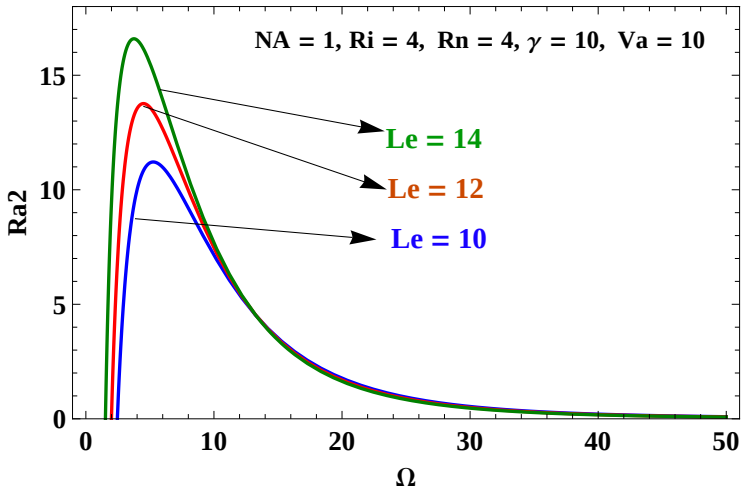

Figure 4.5: Ra_2 versus Ω for different values of Le

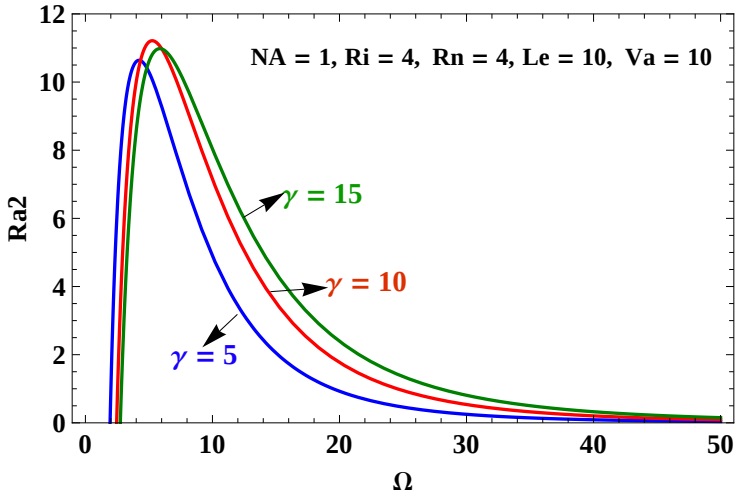

Figure 4.6: Ra_2 versus Ω for different values of γ

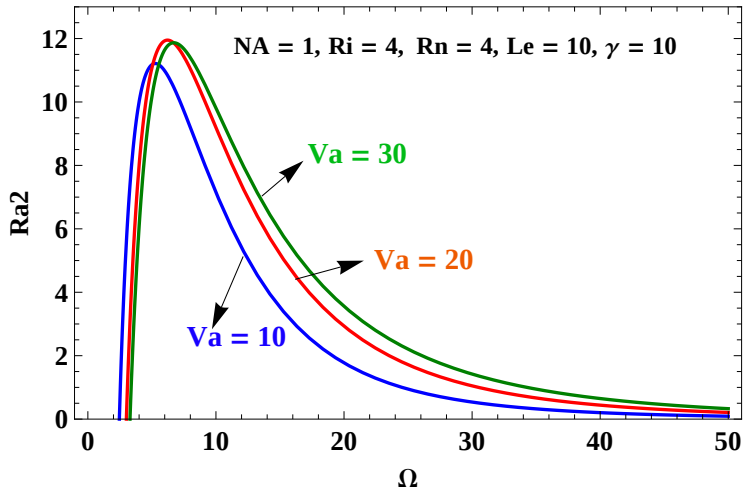

Figure 4.7: Ra_2 versus Ω for different values of Va

$|Ra_2|$ increases, thus the system is stabilized.

From the Figure 4.6 it is observed that, for certain range of modulation frequency as γ increases Ra_2 increases but out of that range the effect is reversed. For higher value of Ω the variation in heat capacity ratio is small and hence it stabilizes the system. Figure 4.7 is the plot of Ra_2 versus Ω for different values of Vadász number Va. It is observed that the effect of Vadász number is similar to γ. It can be inferred that it destabilizes the system for lower values of Ω and stabilizes the system for larger values of Ω.

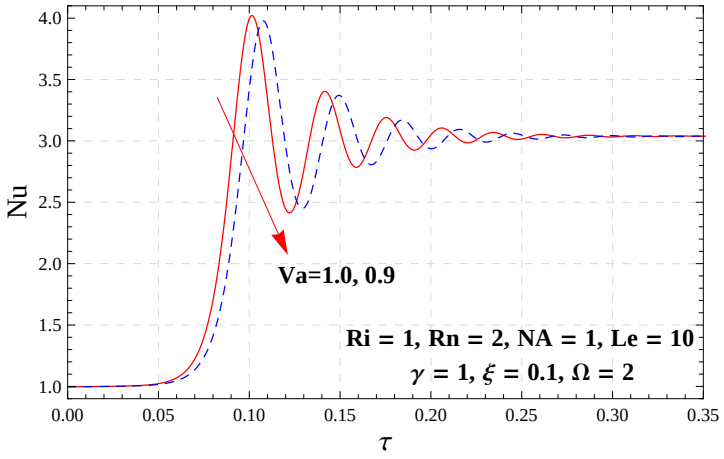

Figure 4.8: Nu verses τ for different values of Va

Now it is found the results related to nonlinear system are discussed. From the Figure 4.8 and 4.9, it is found that initially when time τ is small, the vibrations become of high amplitudes as the value of Va increases, and so thermal Nusselt and concentration Nusselt

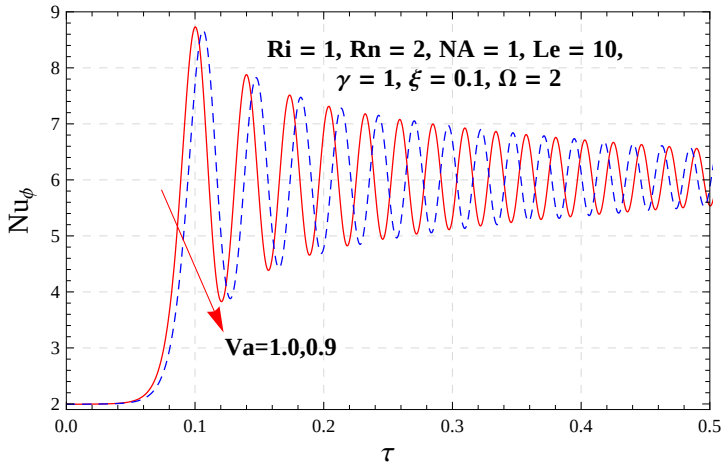

Figure 4.9: Nu_ϕ verses τ for different values of Va

numbers increase, thus increasing the rate of heat and nanoparticle concentration transport. But at large values of time τ, the vibrations become smaller and subsequently the values of Nu and Nu_ϕ approach steady state values.

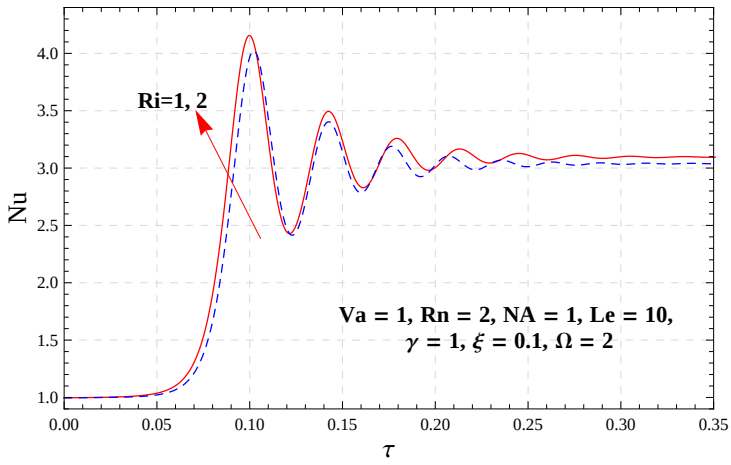

Figure 4.10: Nu verses τ for different values of Ri

From the Figure 4.10 and Figure 4.11, it is observed that the effect of internal Rayleigh number Ri is to enhance the heat transport and nanoparticle concentration as well. This confirms the results obtained most recently by Bhadauria (2012) and Bhadauria et al. (2011b, 2012, 2013).

However, from Figure 4.12 and 4.13, it is found that as the value of thermal capacity ratio γ increases, the values of thermal Nusselt and concentration Nusselt numbers decrease, thus decreasing the rate of heat and concentration transport. Further, the influence of

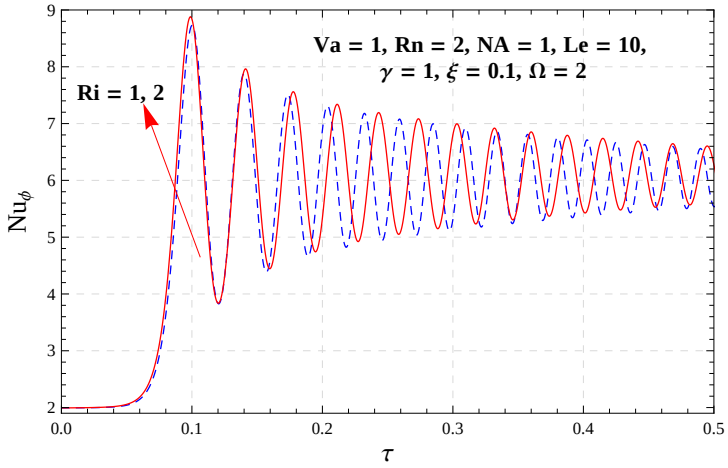

Figure 4.11: Nu_ϕ verses τ for different values of Ri

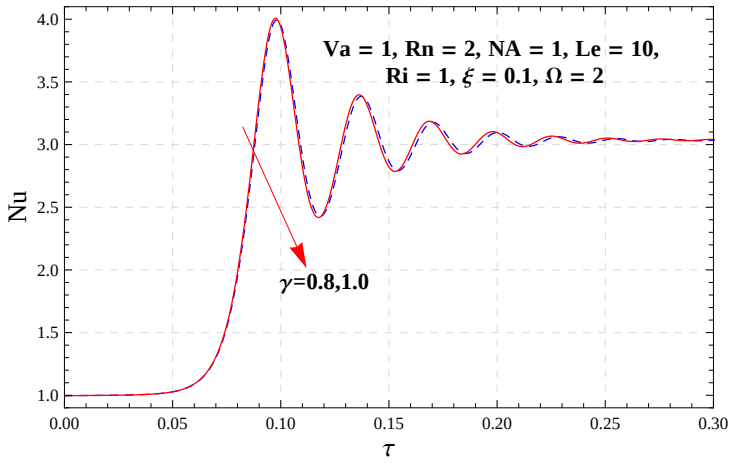

Figure 4.12: Nu verses τ for different values of γ

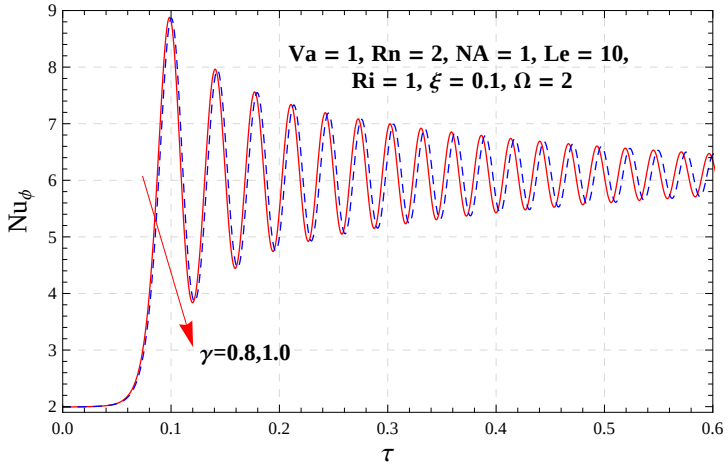

Figure 4.13: Nu_ϕ verses τ for different values of γ

concentration Rayleigh number Rn on both thermal Nusselt number as well as on concentration Nusselt number is found to be similar that is to enhance the heat and concentration transport as given in Figure 4.14 and 4.15 respectively, which is due to the fact that the nanoparticle concentration is more at the top.

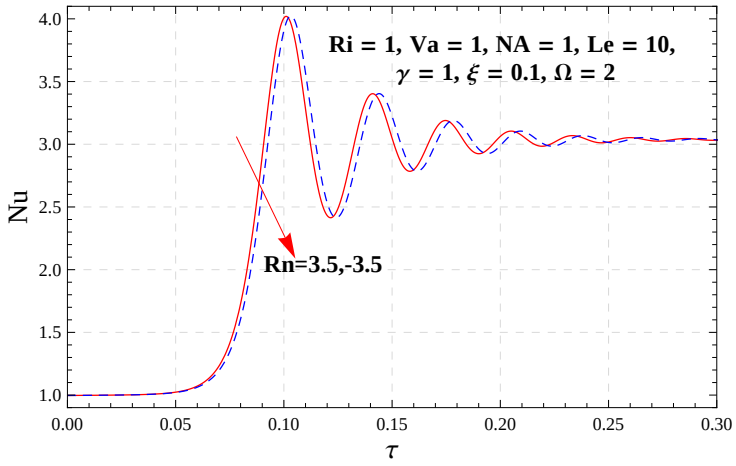

Figure 4.14: Nu verses τ for different values of Rn

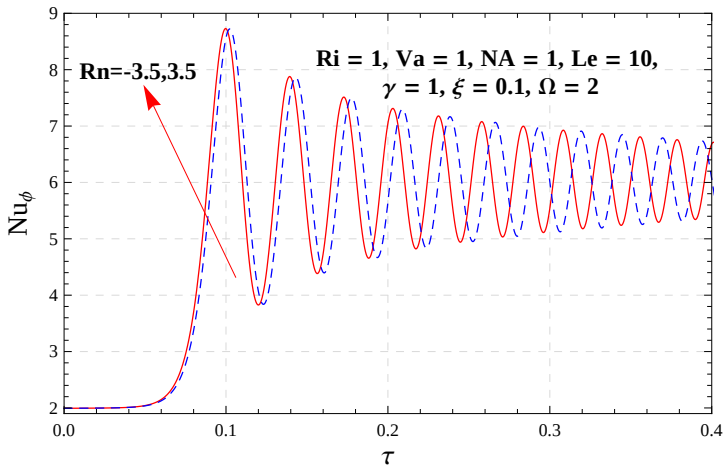

Figure 4.15: Nu_ϕ verses τ for different values of Rn

Figure 4.16 shows that N_A and Le do not have significant effect on thermal Nusselt number as reported earlier by Bhadauria and Agarwal (2011). On the contrary in the case of concentration Nusselt number both Le and N_A have increasing effect as given in the Figure 4.17 and 4.18 respectively.

Figure 4.19 and 4.20 show that the effect of increase in the amplitude of gravity modulation on heat and nanoparticle concentration transport is to increase the values of Nu and

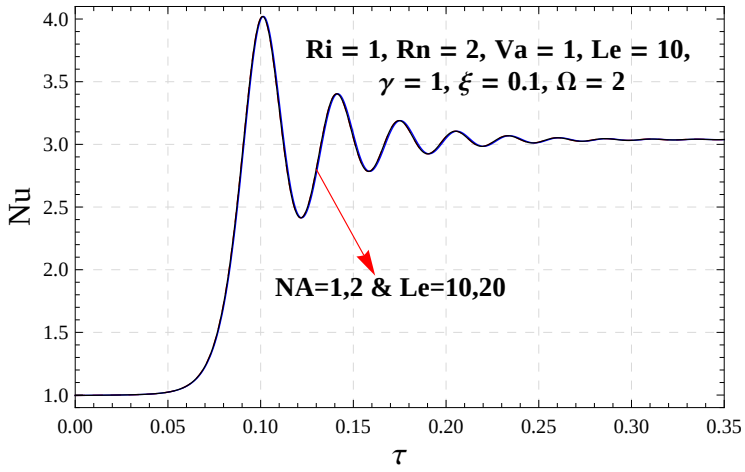

Figure 4.16: Nu verses τ for different values of N_A and Le

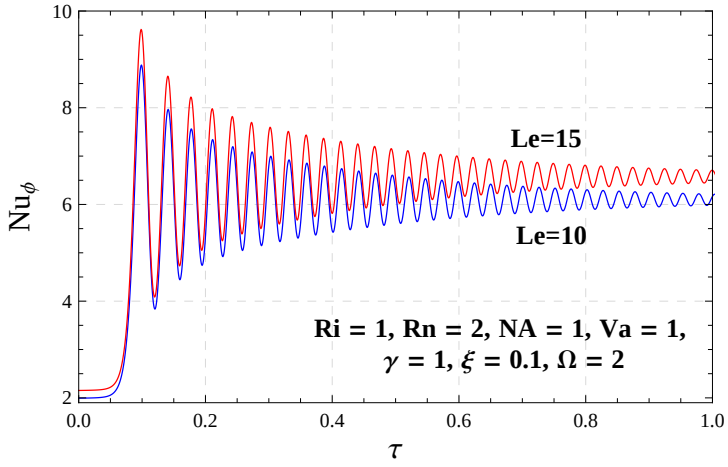

Figure 4.17: Nu_ϕ verses τ for different values of Le

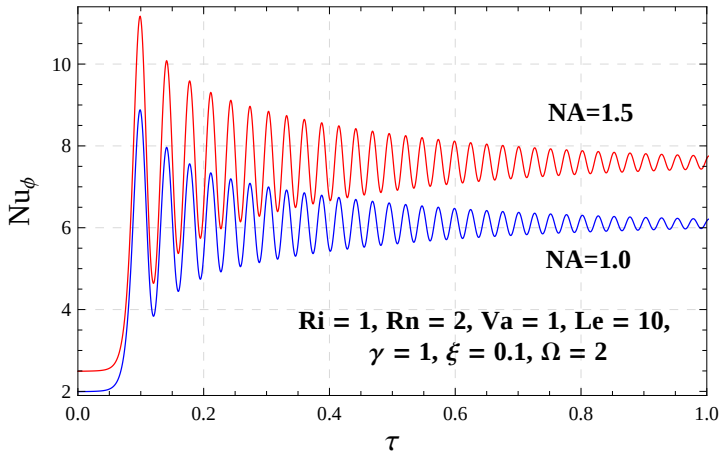

Figure 4.18: Nu_ϕ verses τ for different values of N_A

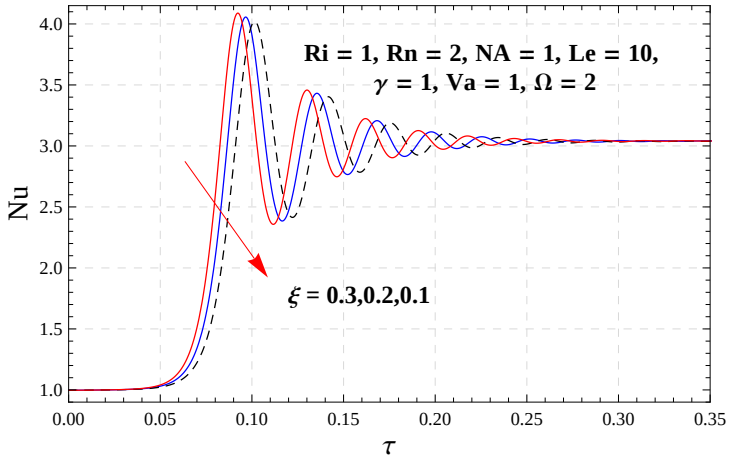

Figure 4.19: Nu verses τ for different values of ξ

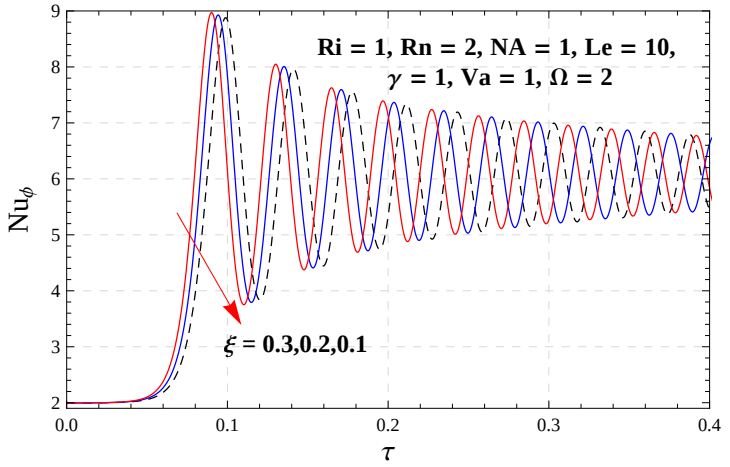

Figure 4.20: Nu_ϕ verses τ for different values of ξ

Nu_ϕ and hence transport phenomena in both the cases. Figure 4.21 and 4.22 show that the effect of increasing frequency of gravity modulation on heat and nanoparticle concentration transport is to decrease the values of Nu and Nu_ϕ, and hence stabilize the system. Thus, the classical results as per Gresho and Sani (1970) and Bhadauria and Kiran (2014) are found.

It is observed in most of the cases that there is much effect of parameters on Nu and Nu_ϕ at small values of time, but less effect at large time, since vibrations become smaller in magnitude, and disappears as Nu, Nu_ϕ reach steady state values. Finally, the parameters Va, Rn, ξ have destabilizing effects on the system, while γ, Ω have stabilizing effects. The parameters N_A, Le do not show any effect on Nu, but increases the value of Nu_ϕ.

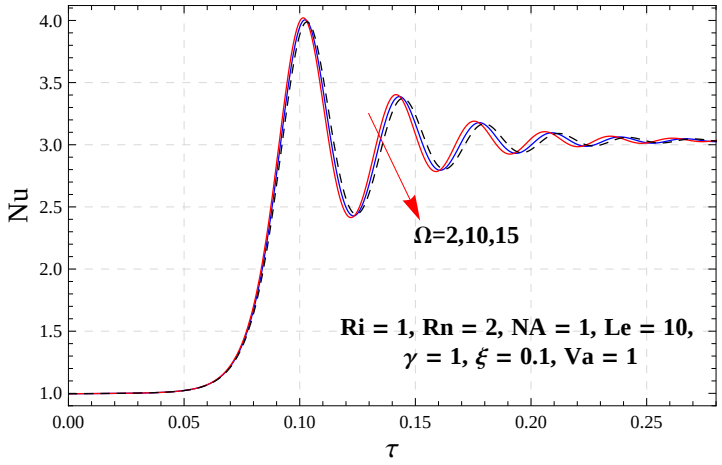

Figure 4.21: Nu verses τ for different values of Ω

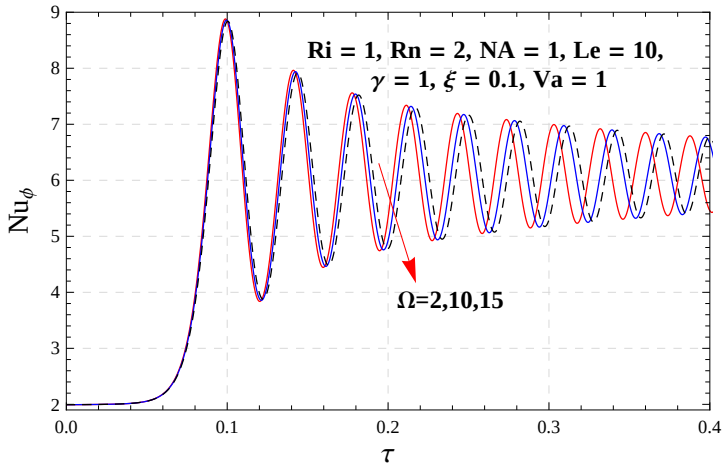

Figure 4.22: Nu_ϕ verses τ for different values of Ω

4.7 Conclusions

In the present chapter, the combined effect of internal heating and gravity modulation is considered on Bénard−Darcy convection in a horizontal porous layer saturated by a nanofluid, which is heated from below and cooled from above. Further, the effect of Brownian motion along with thermophoresis is incorporated. The top heavy suspension of nano particles has been considered. Linear stability results obtained in terms of correction in critical Rayleigh number. The results have been obtained in terms of the concentration and thermal Nusselt numbers with the help of the finite amplitude equations. The effect of various parameters has been obtained, and depicted graphically. The following observations are made

1. Low frequency of modulation shows destabilization effect but high frequencies stabilize the system for Va and γ.

2. The effect of internal heating is to increase (destabilizes) the heat transport as well as nanoparticle concentration transport in the system.

3. Increment in concentration Rayleigh number Rn, modified diffusivity ratio N_A and Lewis number Le increases the effect of gravity modulation.

4. An increment in Va is to increase the values of $Nu(\tau)$ and $Nu_\phi(\tau)$ at small values of time τ but no effect at large time τ.

5. The effect of increased nanoparticle concentration Rn is to enhance the heat and concentration transport.

6. There is no significant effect of N_A and Le on thermal Nusselt number.

7. Increasing Le, ξ, N_A and Rn is to increase the concentration Nusselt number, whereas an increase in Ω decreases the same, and so the concentration transport.

8. The effect of time on Nusselt numbers is found to be oscillatory, when τ is small. However, when time τ becomes very large, Nusselt numbers approached the respective steady values.

9. Gravity modulation can be used to regulate the system effectively, whereas internal heating destabilize the system.

Chapter 5

Effect of rotational speed modulation on thermal instability in a nanofluid saturated porous medium

5.1 Introduction

During the last two decades, the nanofluids (the suspensions of nanometre size particles in the base fluid) are being used as heat transfer media due to their enhanced abilities over ordinary fluids as heat exchangers and transporters. The presence of very little quantity of nanoparticles in base fluids creates a significant enhancement in the heat transfer characteristics of the fluids. This characteristics of nanofluids depends on the thermo-physical properties of the base fluid and the suspended nanoparticles. The nanofluids find a wide range of applications in industrial, commercial, residential and transportation sectors.

A significant feature of nanofluids is the thermal conductivity enhancement, which was first introduced by Masuda et al. (1993). Nanofluids are mixtures of base fluid (like water or ethylene-glycol) along with small amount of nanoparticles (like metallic or metallic oxide:

This chapter is based on the research article: Convective motion in nanofluid under variable rotational speed, Published in **Advanced Science Engineering and Medicine, American Scientific Publisher.** Vol. 10 No. 7/8 pp. 717-723.

Cu, Cuo, Al_2O_3) having dimensions from 1nm to 100nm. Choi (1995) was the first to propose the term "nanofluid". Chen (2001) analyzed the ballistic nature of heat transport within nanoparticles, Eastman et al. (2001) reported that 40% thermal conductivity of ethylene-glycol increases with 0.3% volume of copper nanoparticles of 10nm diameter. Das et al. (2003) found $10-30\%$ increase of the effective thermal conductivity in alumina/water nanofluids with $1-4\%$ of alumina. These reports led Buongiorno and Hu (2005) to suggest the possibility of using nanofluids in advanced nuclear systems. Another application of the nanofluid flow due to Kleinstreuer et al. (2008), is in the delivery of nano-drug.

Khanafer et al. (2003) reported an increase in concentration of suspended nanoparticles, is to increase in heat transfer in Cu-water nanofluids in a two-dimensional rectangular enclosures whereas Putra et al. (2003) reported that in natural convection with Al_2O_3 and CuO nanofluids, the heat transfer coefficient was smaller than that in a regular fluid. A wide range of studies have been conducted to determine the governing mechanisms in nanoscale such as the Brownian motion of nanoparticles in fluids by Jang and Choi (2004), a modified Maxwell model accounting for the ordered nanolayer near the particle fluid interface by Yu and Choi (2003), ballistic nature of heat transport within nanoparticles by Keblinski and Cahill (2005). Vadász (2006) studied thermal lagging in nanoparticles with a large surface area to volume ratio. A comprehensive review of heat transport in nanofluids is due to Eastman et al. (2004). It is a fact that in spite of several reported studies, no satisfactory explanation for abnormal enhancement in the thermal conductivity and viscosity of the fluid in the presence of nano-particles, could be found so far. Wen and Ding (2006) reported a reduction in heat transfer after changing a regular fluid to a nanofluid. Abu-Nada et al. (2008) have shown the enhancement of heat transfer in nanofluids at higher values of the Rayleigh number.

It was Buongiorno (2006), who first proposed a model for convective heat transport in nanofluids incorporating the effects of thermophoresis and Brownian diffusion. Tzou (2008a, 2008b) studied the thermal instability problem by using Buongiorno (2006) model, and observed that nanofluid is less stable than base fluid. This problem was further revisited by Nield and Kuznetsov (2010) for different types of non-dimensional parameters. An extension to the porous medium of this model was studied by Nield and Kuznetsov (2009),

Kuznetsov and Nield (2009) and Chand and Rana (2012). Yadav et al. (2012) examined the effect of internal heat source on the onset of nanofluid convection. Two-dimensional nonlinear convection in nanofluid saturated porous medium have been studied by Bhadauria and Agarwal (2011).

Combined effect of thermal modulation and rotation on the onset of convection in a rotating fluid layer was studied, in brief, by Rauscher and Kelly (1975). Liu and Ecke (1997) analyzed heat transport of turbulent Rayleigh-Bénard convection under rotational effect. Malashetty and Swamy (2008) investigated thermal instability in a rotating fluid layer subjected to both boundary temperature modulation, and found that by proper tuning of the modulation frequency, Taylor number and Prandtl number, the onset of convection can be advanced/delayed. Kloosterziel and Carnevale (2003) investigated the effect of rotation on the stability of thermally modulated system, and determined the critical points analytically for the marginal stability boundary, above which an increment either in viscosity or in diffusivity is destabilizing. They also showed that for a non-viscous fluid, the system will always be unstable, contradicting Chandrasekhar's (1961) conclusion. Malashetty and Swamy (2007) studied the effect of rotation on the stability of thermally modulated system, and found that the symmetric modulation destabilizes the system at low frequencies, while it stabilizes at moderate and high frequencies. Asymmetric modulation is the most stable situations at all frequencies. Bhadauria (2007) studied the fluid convection in a rotating porous layer under modulated temperature on the boundaries considering rigid-rigid boundaries. Bhadauria (2008) investigated rotational influence on Darcy convection, and found that both rotation and permeability suppress the onset of thermal instability. Bhadauria et al. (2012) investigated the nonlinear thermal instability in a rotating viscous fluid layer under temperature/gravity Modulation. They found that by suitably adjusting the frequency or amplitude of modulation one can control the convective flow.

Although rotation speed modulation was the induced concept of the temperature-gravity modulation, but only scarce research material is available in the literature. The effect of temperature modulation on the Rayleigh-Bénard instability and the effect of rotational speed modulation in the Taylor-Couette instability have been studied theoretically and experimentally by Niemela and Donnelly (1986), Kumar et al. (1986), Walsh and Donnelly

(1988). While studying the rotational speed modulation effect, one more parameter in the form of rotational speed appears which affects the stability of convective flow. In the literature, the relevant study is due to Bhattacharjee (1989), who found that the effect of modulation is stabilizing in various physical configurations. Suthar et al. (2009) studied the effect of the rotation speed modulation. Effect of rotation on thermal convection in a porous medium was studied by Veronis (1966), Rudraiah (1986), Vanishree and Siddheshwar (2010). The studies, concerning the rotating porous media saturated with a nanofluid, were carried out by Agarwal et al. (2011), Bhadauria and Agarwal (2011), Agarwal and Bhadauria (2011) and Chand and Rana (2012).

Recently, Nield and Kuznetsov (2014) in their revised model adopted a new set of boundary conditions, where it was assumed that there is no nanoparticle flux at the boundaries, and the particle fraction value adjusts accordingly. In this case, the oscillatory mode of convection was ruled out due to the absence of two opposing forces. Agarwal (2014) studied the thermal instability in a rotating porous layer saturated by a nanofluid, considering new boundary conditions for nanoparticle fraction. Similar work has been done by Yadav et al. (2015) for free-free, rigid-rigid and free-rigid boundaries. Linear as well as nonlinear stability analysis for Rayleigh-Bénard convection in a nanofluid under thermal non-equilibrium with new boundary condition is done by Agarwal et al. (2015).

The present chapter is concerned with the study of the effect of rotational speed modulation on thermal instability in a porous medium saturated by a nanofluid. Horton-Rogers-Lapwood model based on the Brinkman model is used for the fluid flow, and in place of fixed nanopartical fraction boundary conditions, the thermo-nanopartical flux boundary conditions have been introduced. The effect of the different parameters such as ω, ξ, Pr, Ta, Rn, Le, N_A, N_B, ε, and Da on thermal instability has been studied, and the correction in the critical Rayleigh number due to rotational speed modulation has been investigated. The physical behavior of these parameters has been depicted graphically. Further, using non-linear analysis, it is found that the rotational speed modulation can be used to regulate the heat and mass transports effectively.

5.2 Governing Equation

Consider a nanofluid saturated porous layer, confined between two horizontal boundaries at $z = 0$ and $z = d$, heated from below. The boundaries are assumed to be impermeable and perfectly thermally conducting. The porous layer is extended infinitely in x and y directions, while the z-axis is extending vertically upward with the origin at the lower boundary. The porous layer is rotating about z-axis periodically with angular velocity Ω_R. The Coriolis effect has been taken into account by including the Coriolis force term in the momentum equation whereas the centrifugal force term can be realized as a gradient of a scalar, and hence has been absorbed into the pressure term. In addition, the local thermal equilibrium between the fluid and solid has been considered. Employing the Oberbeck-Boussinesq approximation, the governing equations to study the thermal instability in a nanofluid-saturated rotating porous medium are [Buongiorno (2006), Kuznetsov and Nield (2010a,b,c,) and Nield and Kuznetsov (2013), Nield and Kuznetsov (2014)]

$$\begin{cases} \nabla \cdot \mathbf{v_D} = \mathbf{0}, \\ \frac{\rho_f}{\varepsilon}\frac{\partial \mathbf{v_D}}{\partial t} + \nabla p = \bar{\mu}\nabla^2 \mathbf{v}_D - \frac{\mu}{K}\mathbf{v}_D + [\phi\rho_p + (1-\phi)\{\rho(1-\beta(T-T_c))\}]\vec{g} + \frac{2\rho_f}{\varepsilon}(\mathbf{v}_D \times \Omega_R), \\ (\rho c)_m \frac{\partial T}{\partial t} + (\rho c)_f \mathbf{v}_D \cdot \nabla T = \kappa_m \nabla^2 T + \varepsilon(\rho c)_p [D_B \nabla\phi + \frac{D_T}{T_c}\nabla T] \cdot \nabla T, \\ \frac{\partial \phi}{\partial t} + \frac{1}{\varepsilon}\mathbf{v}_D \cdot \nabla\phi = D_B \nabla^2 \phi + \frac{D_T}{T_c}\nabla^2 T, \end{cases} \tag{5.2.1}$$

where $\mathbf{v}_D = (u, v, w)$ is the Darcy velocity, T_h and T_c are the temperatures at the lower and upper walls such that $T_h > T_c$. The considered rotational speed, which is varying sinusoidally with respect to time, is defined as:

$$\mathbf{\Omega_R} = \Omega_{R0}(1 + \xi\cos(\omega t))\hat{k}. \tag{5.2.2}$$

The constants and variables, used in the above Eqs.(5.2.1) and (5.2.2), have their usual meanings, and are given in the nomenclature.

In Eq.(5.2.1), both Brownian transport and thermophoresis coefficients are time-independent, in tune with the studies that neglect the effect of thermal transport attributed to the small size of the nanoparticles (as per arguments by Keblinski and Cahil 2005). Further, thermophoresis and Brownian transport coefficients are assumed to be temperature-independent due to the fact that the temperature ranges under consideration are not far away from the critical value. Let the temperature and flux of volumetric fraction of the nanoparticles to be constant at the boundaries, the boundary conditions are taken as

$$\mathbf{v} = 0, \quad T = T_h, \; D_B \frac{\partial \phi}{\partial z} + \frac{D_T}{T_c} \frac{\partial T}{\partial z} = 0 \text{ at } z = 0, \tag{5.2.3}$$

$$\mathbf{v} = 0, \quad T = T_c, \; D_B \frac{\partial \phi}{\partial z} + \frac{D_T}{T_c} \frac{\partial T}{\partial z} = 0 \text{ at } z = d. \tag{5.2.4}$$

The dimensionless variables are considered as given below:
$(x^*, y^*, z^*) = (x, y, z)/d, \; t^* = t\kappa_T/(\sigma d^2), \; (u^*, v^*, w^*) = (u, v, w)d/\kappa_T, \; p^* = pK/\mu\kappa_T, \phi^* = \dfrac{\phi - \phi_0}{\phi_0}$ and $T^* = \dfrac{T - T_c}{T_h - T_c}$, where $\kappa_T = \dfrac{\kappa_m}{(\rho c)_f}, \quad \sigma = \dfrac{(\rho c_p)_m}{(\rho c_p)_f}$ and ϕ_0 is the reference value for nanoparticle volume fraction. The non-dimensionalized governing equations along with boundary conditions are (after dropping the asterisk for simplicity)

$$\nabla \cdot \mathbf{v} = 0 \tag{5.2.5}$$

$$\frac{Da}{Pr} \frac{\partial \mathbf{v}}{\partial t} = -\nabla p - \mathbf{v} + Da \nabla^2 \mathbf{v} - (Rm - Ra\; T + Rn\phi)\, \hat{k} + \sqrt{Ta}(1 + \xi \cos(\omega t))(\mathbf{v} \times \hat{k}) \tag{5.2.6}$$

$$\frac{\partial T}{\partial t} + \mathbf{v} \cdot \nabla T = \nabla^2 T + \frac{N_B}{Le} \nabla \phi \cdot \nabla T + \frac{N_A N_B}{Le} \nabla T \cdot \nabla T \tag{5.2.7}$$

$$\frac{1}{\sigma} \frac{\partial \phi}{\partial t} + \frac{1}{\varepsilon} \mathbf{v} \cdot \nabla \phi = \frac{1}{Le} \nabla^2 \phi + \frac{N_A}{Le} \nabla^2 T \tag{5.2.8}$$

$$\left.\begin{aligned} &\mathbf{v} = 0, \quad T = 1, \; \tfrac{\partial \phi}{\partial z} + N_A \tfrac{\partial T}{\partial z} = 0 \;\; \text{at } z = 0, \\ &\mathbf{v} = 0, \quad T = 0, \; \tfrac{\partial \phi}{\partial z} + N_A \tfrac{\partial T}{\partial z} = 0 \;\; \text{at } z = 1. \end{aligned}\right\} \tag{5.2.9}$$

The non-dimensionlized parameters in the above equations are as given below:

$$Da = \frac{\bar{\mu}K}{\mu d^2}, \qquad Ta = \left(\frac{2K\Omega_{R0}}{\nu\varepsilon}\right)^2, \qquad Pr = \frac{\bar{\mu}\varepsilon(\rho c)_m}{\rho_f \kappa_m},$$
$$Ra = \frac{\rho_f g\beta Kd(T_h - T_c)}{\mu\kappa_T}, \qquad Rn = \frac{(\rho_p - \rho_f)\phi_0 gKd}{\mu\kappa_T}, \qquad Rm = \frac{\left\{\rho_p\phi_0 + \rho_f(1-\phi_0)\right\}gKd}{\mu\kappa_T},$$
$$N_A = \frac{D_T(T_h - T_c)}{D_B T_c \phi_0}, \qquad N_B = \varepsilon\frac{(\rho_c)_p}{\rho_c)_f}\phi_0, \qquad Le = \frac{\kappa_T}{D_B}.$$

5.3 Basic Solution

At the basic state, the nanofluid is at rest, and are given by:

$$\mathbf{v} = 0, p = p_b(z), \quad T = T_b(z), \ \phi = \phi_b(z). \tag{5.3.1}$$

Using Eq.(5.3.1), Eq.(5.2.7) and Eq.(5.2.8) reduce to

$$\frac{d^2T_b}{dz^2} + \frac{N_B}{Le}\frac{d\phi_b}{dz}\frac{dT_b}{dz} + \frac{N_A N_B}{Le}\left(\frac{dT_b}{dz}\right)^2 = 0, \tag{5.3.2}$$

$$\frac{d^2\phi_b}{dz^2} + N_A\frac{d^2T_b}{dz^2} = 0. \tag{5.3.3}$$

After integrating Eq.(5.3.3), subject to the boundary condition Eq.(5.2.9), obtained as follows

$$\frac{d\phi_b}{dz} + N_A\frac{dT_b}{dz} = 0, \tag{5.3.4}$$

Using Eq.(5.3.4), Eq.(5.3.2) reduces to

$$\frac{d^2T_b}{dz^2} = 0. \tag{5.3.5}$$

The solutions of Eq.(5.3.4) and Eq.(5.3.5) subject to the boundary condition (5.2.9) are as follows

$$T_b = 1 - z, \tag{5.3.6}$$

$$\phi_b = \phi_0 + N_A z. \tag{5.3.7}$$

5.4 Stability Analysis

Now superimpose perturbations on the basic state as given below :

$$\mathbf{v} = \mathbf{v}',\ p = p_b + p',\ T = T_b + T',\ \phi = \phi_b + \phi'. \tag{5.4.1}$$

Substituting the expressions (5.4.1) into the Eqs.(5.2.5)-(5.2.9), and using (5.3.6) and (5.3.7), to obtain

$$\nabla \cdot \mathbf{v}' = 0 \tag{5.4.2}$$

$$\left[\frac{Da}{Pr}\frac{\partial}{\partial t} - Da\nabla^2 + 1\right]\mathbf{v}' = -\nabla p' + Ra\ T'\hat{k} - Rn\phi'\hat{k} + \sqrt{Ta}(\mathbf{v}' \times \hat{k}) \tag{5.4.3}$$

$$\frac{\partial T'}{\partial t} + \frac{dT_b}{dz}\mathbf{w}' + \mathbf{v}'.\nabla T' = \nabla^2 T' + \frac{N_B}{Le}\left(N_A \nabla(T' + T_b).\nabla(T' + T_b) + \nabla(T' + T_b).\nabla(\phi' + \phi_b)\right) \tag{5.4.4}$$

$$\frac{1}{\sigma}\frac{\partial \phi'}{\partial t} + \frac{d\phi_b}{dz}\mathbf{w}' + \mathbf{v}'.\nabla\phi' = \frac{1}{Le}\nabla^2\phi' + \frac{N_A}{Le}\nabla^2 T' \tag{5.4.5}$$

$$\mathbf{v}' = 0,\quad T' = 0,\ \frac{\partial \phi'}{\partial z} + N_A\frac{\partial T'}{\partial z} = 0 \ \text{ at } z = 0, \text{ and at } z = 1. \tag{5.4.6}$$

The parameter R_m is not carried over in the subsequent equations because it is part of the hydrostatic equilibrium. The nanoparticle flux being zero at the boundaries implies the absence of the two opposing forces responsible for the occurrence of the oscillatory mode of convection, hence oscillatory convection has been ruled out.

Consider the case of two-dimensional rolls, assuming all physical quantities to be independent of y. For two-dimensional convection, the stream function ψ is introduced as $u = \frac{\partial \psi}{\partial z}$; $w = -\frac{\partial \psi}{\partial x}$, and eliminate the pressure term by taking curl of the momentum equation twice, the system of nonlinear perturbed equations is obtained as

$$\left(\frac{Da}{Pr}\frac{\partial}{\partial t} - Da\nabla^2 + 1\right)^2 \nabla^2\left(-\frac{\partial \psi}{\partial x}\right) = \left(\frac{Da}{Pr}\frac{\partial}{\partial t} - Da\nabla^2 + 1\right)\nabla_1^2(RaT - Rn\phi)$$
$$+Ta(1 + \xi\cos(\omega t))^2\frac{\partial^2}{\partial z^2}\left(\frac{\partial \psi}{\partial x}\right) \tag{5.4.7}$$

$$\frac{\partial T}{\partial t}+\frac{\partial \psi}{\partial x}=\nabla^2 T+\frac{\partial(\psi,T)}{\partial(x,z)} \tag{5.4.8}$$

$$\frac{1}{\sigma}\frac{\partial \phi}{\partial t}-\frac{N_A}{\varepsilon}\frac{\partial \psi}{\partial x}=\frac{1}{Le}\nabla^2\phi+\frac{N_A}{Le}\nabla^2 T+\frac{1}{\varepsilon}\frac{\partial(\psi,\phi)}{\partial(x,z)} \tag{5.4.9}$$

$$\psi=\frac{\partial^2\psi}{\partial z^2}=0,\quad T=0,\quad \frac{\partial\phi}{\partial z}+N_A\frac{\partial T}{\partial z}=0 \ \text{ at } z=0, \text{ and at } z=1. \tag{5.4.10}$$

5.4.1 Linear Stability Analysis

The linear stability analysis is done to study the marginal states. For performing linear stability analysis, Neglect nonlinear terms in Eqs.(5.4.7)-(5.4.9), thus, get a linear system of equations

$$\left(\frac{Da}{Pr}\frac{\partial}{\partial t}-Da\nabla^2+1\right)^2\nabla^2\left(-\frac{\partial\psi}{\partial x}\right)=\left(\frac{Da}{Pr}\frac{\partial}{\partial t}-Da\nabla^2+1\right)\nabla_1^2(RaT-Rn\phi)$$
$$+Ta(1+\xi\cos(\omega t))^2\frac{\partial^2}{\partial z^2}\left(\frac{\partial\psi}{\partial x}\right) \tag{5.4.11}$$

$$\frac{\partial T}{\partial t}+\frac{\partial\psi}{\partial x}=\nabla^2 T \tag{5.4.12}$$

$$\frac{1}{\sigma}\frac{\partial\phi}{\partial t}-\frac{N_A}{\varepsilon}\frac{\partial\psi}{\partial x}=\frac{1}{Le}\nabla^2\phi+\frac{N_A}{Le}\nabla^2 T' \tag{5.4.13}$$

$$\psi=\frac{\partial^2\psi}{\partial z^2}=0,\quad T'=0,\quad \frac{\partial\phi'}{\partial z}+N_A\frac{\partial T'}{\partial z}=0 \ \text{ at } z=0, \text{ and at } z=1. \tag{5.4.14}$$

Eliminating T and ϕ from Eqs.(5.4.11)-(5.4.13), one can obtain a single equation for ψ in the form

$$\left(\frac{\partial}{\partial t}-\nabla^2\right)\left(\frac{1}{\sigma}\frac{\partial}{\partial t}-\frac{1}{Le}\nabla^2\right)\left(\frac{Da}{Pr}\frac{\partial}{\partial t}-Da\nabla^2+1\right)^2\nabla^2\left(\frac{\partial\psi}{\partial x}\right)=Ra\left(\frac{Da}{Pr}\frac{\partial}{\partial t}-Da\nabla^2+1\right)$$
$$\left(\frac{1}{\sigma}\frac{\partial}{\partial t}-\frac{1}{Le}\nabla^2\right)\nabla_1^2\left(\frac{\partial\psi}{\partial x}\right)+RnN_A\left(\frac{Da}{Pr}\frac{\partial}{\partial t}-Da\nabla^2+1\right)\left(\frac{1}{\varepsilon}\frac{\partial}{\partial t}-\nabla^2\left(\frac{1}{Le}+\frac{1}{\varepsilon}\right)\right)\times$$
$$\nabla_1^2\left(\frac{\partial\psi}{\partial x}\right)-Ta\left(\frac{\partial}{\partial t}-\nabla^2\right)\left(\frac{1}{\sigma}\frac{\partial}{\partial t}-\frac{1}{Le}\nabla^2\right)(1+\xi\cos(\omega t))^2\frac{\partial^2}{\partial z^2}\left(\frac{\partial\psi}{\partial x}\right). \tag{5.4.15}$$

Replacing $\left(-\frac{\partial\psi}{\partial x}\right)$ by w in the above equation, to obtain

$$\left(\frac{\partial}{\partial t}-\nabla^2\right)\left(\frac{1}{\sigma}\frac{\partial}{\partial t}-\frac{1}{Le}\nabla^2\right)\left(\frac{Da}{Pr}\frac{\partial}{\partial t}-Da\nabla^2+1\right)^2\nabla^2 w=Ra\left(\frac{Da}{Pr}\frac{\partial}{\partial t}-Da\nabla^2+1\right)$$
$$\left(\frac{1}{\sigma}\frac{\partial}{\partial t}-\frac{1}{Le}\nabla^2\right)\nabla_1^2 w+RnN_A\left(\frac{Da}{Pr}\frac{\partial}{\partial t}-Da\nabla^2+1\right)\left(\frac{1}{\varepsilon}\frac{\partial}{\partial t}-\nabla^2\left(\frac{1}{Le}+\frac{1}{\varepsilon}\right)\right)\nabla_1^2 w$$
$$-Ta\left(\frac{\partial}{\partial t}-\nabla^2\right)\left(\frac{1}{\sigma}\frac{\partial}{\partial t}-\frac{1}{Le}\nabla^2\right)(1+\xi\cos(\omega t))^2\frac{\partial^2}{\partial z^2}w. \tag{5.4.16}$$

The perturbation technique is applied to obtain eigen functions w and the corresponding eigen values Ra by introducing a small perturbation parameter ξ as follows [Venezian (1969)]

$$\begin{aligned} w &= w_0 + \xi w_1 + \xi^2 w_2 + \dots \\ Ra &= Ra_0 + \xi Ra_1 + \xi^2 Ra_2 + \dots \end{aligned} \tag{5.4.17}$$

Using expressions (5.4.17) into Eq.(5.4.16), and then equating the like powers of ξ on both sides, it is obtained

$$\xi^0 : \; Lw_0 = 0 \tag{5.4.18}$$

$$\begin{aligned} \xi^1 : \; Lw_1 =& Ra_1 \left(\frac{Da}{Pr}\frac{\partial}{\partial t} - Da\nabla^2 + 1\right)\left(\frac{1}{\sigma}\frac{\partial}{\partial t} - \frac{1}{Le}\nabla^2\right)\nabla_1^2 w_0 - \\ & 2Ta\left(\frac{\partial}{\partial t} - \nabla^2\right)\left(\frac{1}{\sigma}\frac{\partial}{\partial t} - \frac{1}{Le}\nabla^2\right)\cos(\omega t)\frac{\partial^2}{\partial z^2} w_0 \end{aligned} \tag{5.4.19}$$

$$\begin{aligned} \xi^2 : \; Lw_2 =& Ra_2 \left(\frac{Da}{Pr}\frac{\partial}{\partial t} - Da\nabla^2 + 1\right)\left(\frac{1}{\sigma}\frac{\partial}{\partial t} - \frac{1}{Le}\nabla^2\right)\nabla_1^2 w_0 - \\ & Ta\left(\frac{\partial}{\partial t} - \nabla^2\right)\left(\frac{1}{\sigma}\frac{\partial}{\partial t} - \frac{1}{Le}\nabla^2\right)\cos^2(\omega t)\frac{\partial^2}{\partial z^2} w_0 \\ & + Ra_1\alpha^2\left(\frac{Da}{Pr}\frac{\partial}{\partial t} - Da\nabla^2 + 1\right)\left(\frac{1}{\sigma}\frac{\partial}{\partial t} - \frac{1}{Le}\nabla^2\right) w_1 - \\ & 2Ta\left(\frac{\partial}{\partial t} - \nabla^2\right)\left(\frac{1}{\sigma}\frac{\partial}{\partial t} - \frac{1}{Le}\nabla^2\right)\cos(\omega t)\frac{\partial^2}{\partial z^2} w_1, \end{aligned} \tag{5.4.20}$$

where

$$\begin{aligned} L =& \left(\frac{\partial}{\partial t} - \nabla^2\right)\left(\frac{1}{\sigma}\frac{\partial}{\partial t} - \frac{1}{Le}\nabla^2\right)\left(\frac{Da}{Pr}\frac{\partial}{\partial t} - Da\nabla^2 + 1\right)^2\nabla^2 - \\ & Ra_0\left(\frac{Da}{Pr}\frac{\partial}{\partial t} - Da\nabla^2 + 1\right)\left(\frac{1}{\sigma}\frac{\partial}{\partial t} - \frac{1}{Le}\nabla^2\right)\nabla_1^2 \\ & - RnN_A\left(\frac{Da}{Pr}\frac{\partial}{\partial t} - Da\nabla^2 + 1\right)\left(\frac{1}{\varepsilon}\frac{\partial}{\partial t} - \nabla^2\left(\frac{1}{Le} + \frac{1}{\varepsilon}\right)\right)\nabla_1^2 + \\ & Ta\left(\frac{\partial}{\partial t} - \nabla^2\right)\left(\frac{1}{\sigma}\frac{\partial}{\partial t} - \frac{1}{Le}\nabla^2\right)\frac{\partial^2}{\partial z^2}. \end{aligned} \tag{5.4.21}$$

In the following sections, the above system is solved for different orders of ξ.

Lowest order system

Since, two dimensional dynamics is assumed to be independent of y direction, so, taking $w_0 = \sin(\alpha x)\sin(\pi z)$ for the marginally stable solutions, and the corresponding eigen values are obtained by using Eq.(5.4.18)

$$Ra_0 = \left(\frac{\delta^4(Da\delta^2+1)^2 + Ta\pi^2\delta^2}{\alpha^2(Da\delta^2+1)}\right) - RnN_ALe\left(\frac{1}{Le}+\frac{1}{\varepsilon}\right) \tag{5.4.22}$$

where $\delta^2 = \pi^2 + \alpha^2$.

First order system

Use expression for w_0 and Eq.(5.4.19) to get

$$Lw_1 = -Ra_1\left(Da\delta^2+1\right)\left(\frac{\delta^2}{Le}\right)\alpha^2 w_0 + 2Ta\pi^2\left(h_1\cos(\omega t) - h_2\sin(\omega t)\right)w_0 \tag{5.4.23}$$

where $h_1 = \left(\frac{\delta^4}{Le} - \frac{\omega^2}{\sigma}\right)$ and $h_2 = \delta^2\omega\left(\frac{1}{Le}+\frac{1}{\sigma}\right)$.

The solution of the homogeneous equation corresponding to Eq.(5.4.23) must have a term orthogonal to null space of operator L. Now, apply the theory of minimal Rayleigh number, taking $R_1 = 0$, so that time dependent term on right hand side of equation Eq.(5.4.19) is complete orthogonal function to $\sin(\alpha x)\sin(\pi z)$. Using $w_0 = \sin(\alpha x)\sin(\pi z)$, to obtain

$$L[\sin(\pi z)\exp^{(i\alpha x - i\omega t)}] = L(\omega)\sin(\pi z)\exp^{(i\alpha x - i\omega t)}, \tag{5.4.24}$$

where

$$L(\omega) = S_1 + iS_2, \tag{5.4.25}$$

$$\begin{aligned} S_1 =& \frac{\delta^2}{Le}\left\{(Da\delta^2+1)\left(+RnN_ALe\left(\frac{1}{Le}+\frac{1}{\varepsilon}\right)\right) - \delta^4(Da\delta^2+1)^2 - Ta\pi^2\delta^2\right\} + \\ & \omega^2\left\{\frac{Da^2}{Pr^2}\frac{\delta^6}{Le} + (Da\delta^2+1)^2\frac{\delta^2}{\sigma} + \frac{Ta\pi^2}{\sigma} + 2\delta^2(Da\delta^2+1)\frac{Da}{Pr}\left(\frac{1}{Le}+\frac{1}{\varepsilon}\right) - \right. \\ & \left.\alpha^2\frac{Da}{Pr}\left(\frac{Ra_0}{\sigma}+\frac{RnN_A}{\varepsilon}\right)\right\} \end{aligned} \tag{5.4.26}$$

$$
\begin{aligned}
S_2 \;=&\omega\left[\left(\delta^4(Da\delta^2+1)+Ta\pi^2\delta^2\right)\left(\frac{1}{Le}+\frac{1}{\sigma}\right)+2\frac{Da}{Pr}\frac{\delta^6}{Le}(Da\delta^2+1)-\right.\\
&Ra_0\alpha^2\left(\frac{(Da\delta^2+1)}{\sigma}+\frac{Da}{Pr}\frac{\delta^2}{Le}\right)-RnN_A\alpha^2\left(\frac{Da\delta^2}{Pr}\left(\frac{1}{Le}+\frac{1}{\varepsilon}\right)+\frac{Da\delta^2+1}{\varepsilon}\right)+\\
&\left.\omega^2\left\{\frac{(Da^2\delta^2)}{Pr^2}\left(\frac{1}{Le}+\frac{1}{\sigma}\right)+2\frac{Da}{Pr}\frac{Da\delta^2+1}{\sigma}\right\}\right] \qquad (5.4.27)
\end{aligned}
$$

Now, w_1 is obtained by inverting the operator L term by term as follows

$$
w_1 = 2Ta\pi^2\mathbf{Re}\left[\frac{L^*(\omega)}{|L(\omega)|^2}\left\{h_1\cos(\omega t)-h_2\sin(\omega t)\right\}\sin(\alpha x)\sin(\pi z)\right]. \qquad (5.4.28)
$$

Second order system

From Eq.(5.4.20), it is obtained

$$
\begin{aligned}
Lw_2 \;=&-Ra_2\alpha^2(Da\delta^2+1)\frac{\delta^2}{Le}\sin(\alpha x)\sin(\pi z)+Ta\pi^2\left(\frac{\delta^4}{Le}\cos^2(\omega t)+\right.\\
&\left.\frac{\omega^2}{\sigma}\cos(2\omega t)-2\omega\delta^2\left(\frac{1}{Le}+\frac{1}{\sigma}\right)\sin(2\omega t)\right)\sin(\alpha x)\sin(\pi z)\\
&+2Ta\pi^2\left[H_1\frac{\delta^4}{Le}+\left\{H_2\left(\frac{\delta^4}{Le}-\frac{4\omega^2}{\sigma}\right)+2H_1\delta^2\omega\left(\frac{1}{Le}+\frac{1}{\sigma}\right)\right\}\sin(2\omega t)\right.\\
&\left.+\left\{H_1\left(\frac{\delta^4}{Le}-\frac{4\omega^2}{\sigma}\right)-2H_2\delta^2\omega\left(\frac{1}{Le}+\frac{1}{\sigma}\right)\right\}\cos(2\omega t)\right]\sin(\alpha x)\sin(\pi z), \qquad (5.4.29)
\end{aligned}
$$

where $H_1 = Ta\pi^2\mathbf{Re}\left[\frac{L^*(\omega)}{|L(\omega)|^2}h_1\right]$, $H_2 = -Ta\pi^2\mathbf{Re}\left[\frac{L^*(\omega)}{|L(\omega)|^2}h_2\right]$.

It is not required to solve the Eq.(5.4.29), but use it to determine Ra_2. For the existence of the solution of Eq.(5.4.29), it is necessary that the steady part of its right hand side is orthogonal to $\sin(\alpha x)\sin(\pi z)$, which yields

$$
\begin{aligned}
\int_0^1\int_0^{\frac{\pi}{\alpha}}&\left[-Ra_2\alpha^2(Da\delta^2+1)\frac{\delta^2}{Le}\sin(\alpha x)\sin(\pi z)+Ta\pi^2\left(\frac{\delta^4}{Le}\overline{\cos^2(\omega t)}+\frac{\omega^2}{\sigma}\overline{\cos(2\omega t)}-\right.\right.\\
&\left.2\omega\delta^2\left(\frac{1}{Le}+\frac{1}{\sigma}\right)\overline{\sin(2\omega t)}\right)\sin(\alpha x)\sin(\pi z)+2Ta\pi^2\left[H_1\frac{\delta^4}{Le}+\left\{H_2\left(\frac{\delta^4}{Le}-\frac{4\omega^2}{\sigma}\right)+\right.\right.\\
&\left.2H_1\delta^2\omega\left(\frac{1}{Le}+\frac{1}{\sigma}\right)\right\}\overline{\sin(2\omega t)}+\left\{H_1\left(\frac{\delta^4}{Le}-\frac{4\omega^2}{\sigma}\right)-2H_2\delta^2\omega\left(\frac{1}{Le}+\frac{1}{\sigma}\right)\right\}\times\\
&\left.\left.\overline{\cos(2\omega t)}\right]\sin(\alpha x)\sin(\pi z)\cdot\right]sin(\alpha x)\sin(\pi z)dxdz=0, \qquad (5.4.30)
\end{aligned}
$$

where $\overline{f(t)}$ denotes the time average of $f(t)$. Simplifying the above equation, to obtain

$$Ra_2 = \frac{Ta\pi^2\delta^2}{2\alpha^2(Da\delta^2+1)}\left(1+2Ta\pi^2\left(\frac{\delta^4}{Le}-\frac{\omega^2}{\sigma}\right)\mathbf{Re}\left[\frac{L^*(\omega)}{|L(\omega)|^2}\right]\right). \tag{5.4.31}$$

5.4.2 Weakly Nonlinear Stability Analysis

To perform a local nonlinear stability analysis, one can use the following Fourier expressions

$$\psi = \sum_{n=1}^{\infty}\sum_{m=1}^{\infty} A_{mn}(t)\sin(m\alpha x)\sin(n\pi z) \tag{5.4.32}$$

$$T = \sum_{n=1}^{\infty}\sum_{m=1}^{\infty} B_{mn}(t)\cos(m\alpha x)\sin(n\pi z) \tag{5.4.33}$$

$$\phi = \sum_{n=1}^{\infty}\sum_{m=1}^{\infty} C_{mn}(t)\cos(m\alpha x)\sin(n\pi z). \tag{5.4.34}$$

In what follows, take the modes $(1,1)$ for stream function, and $(0,2)$ and $(1,1)$ for temperature and nanoparticle concentration, thus using a severely truncated representation of Fourier series for stream function, temperature and nanoparticle concentration [Veronis (1966), Rudraiah (1986)]. This study will help in understanding the physics of the problem with minimum mathematical expressions. Further, the results can be used as starting point to generalize it for full nonlinear problem. Also, it is to be noted that the effect of nonlinearity is to distort the temperature and concentration fields through the interaction of ψ and T, and ψ and ϕ respectively. As a result a component of the form $sin(2\pi z)$ will be generated. Therefore, the minimal expression which describes the finite amplitude convection is of the form

$$\psi = A_{11}(t)\sin(\alpha x)\sin(\pi z) \tag{5.4.35}$$

$$T = B_{11}(t)\cos(\alpha x)\sin(\pi z) + B_{02}(t)\sin(2\pi z) \tag{5.4.36}$$

$$\phi = C_{11}(t)\cos(\alpha x)\sin(\pi z) + C_{02}(t)\sin(2\pi z), \tag{5.4.37}$$

where the amplitudes $A_{11}(t), B_{11}(t), B_{02}(t), C_{11}(t)$ and $C_{02}(t)$ are functions of time and to be determined. Using Eqs. (5.4.35)-(5.4.37) in Eqs. (5.4.7)-(5.4.10) with the orthogonality

condition for the eigenfunctions associated with the considered minimal mode, to get

$$\frac{dA_{11}(t)}{dt} = D_{11}(t) \tag{5.4.38}$$

$$\frac{dD_{11}(t)}{dt} = -\frac{Pr^2}{Da^2\delta^2}\Big[(Da\delta^2+1)^2\{\delta^2+Ta\pi^2(1+\xi\cos(\omega t))^2\}A_{11}(t)+\alpha(Da\delta^2+1)[RaB_{11}(t) - RnC_{11}(t)]+2\frac{Da}{Pr}\delta^2(Da\delta^2+1)D_{11}(t)+\alpha\frac{Da}{Pr}\left[Ra\frac{dB_{11}(t)}{dt}-Rn\ \frac{dC_{11}(t)}{dt}\right]\Big] \tag{5.4.39}$$

$$\frac{dB_{11}(t)}{dt} = -\left[\alpha A_{11}(t)+\delta^2 B_{11}(t)+\pi\alpha A_{11}(t)B_{02}(t)\right] \tag{5.4.40}$$

$$\frac{dB_{02}(t)}{dt} = \frac{\pi\alpha}{2}A_{11}(t)B_{11}(t)-4\pi^2 B_{02}(t) \tag{5.4.41}$$

$$\frac{dC_{11}(t)}{dt} = \sigma\left[\frac{N_A}{\varepsilon}\alpha A_{11}(t)-\frac{\pi\alpha}{\varepsilon}A_{11}(t)C_{02}(t)-\frac{\delta^2}{Le}(N_A B_{11}(t)+C_{11}(t))\right] \tag{5.4.42}$$

$$\frac{dC_{02}(t)}{dt} = \frac{\sigma}{2}\left[\frac{\pi\alpha}{\varepsilon}A_{11}(t)C_{11}(t)-\frac{8\pi^2}{Le}[N_A B_{02}(t)+C_{02}(t)]\right]. \tag{5.4.43}$$

The above system of simultaneous autonomous ordinary differential equations has been solved numerically using the function NDSolve(Wolfram Mathematica 8.0), and results are depicted graphically.

5.5 Heat and Nanoparticle Concentration Transport

The thermal Nusselt number, $Nu(t)$ is defined as

$$\begin{aligned} Nu(t) &= \frac{\text{Heat transport by (conduction + convection)}}{\text{Heat transport by conduction}} \\ &= 1+\left(\frac{\int_0^{2\pi/\alpha_c}\left(\frac{\partial T}{\partial z}\right)dx}{\int_0^{2\pi/\alpha_c}\left(\frac{\partial T_b}{\partial z}\right)dx}\right)_{z=0}. \end{aligned} \tag{5.5.1}$$

The value of $Nu(t)$ is now obtained by using Eqs. (5.3.6) and (5.4.36) in Eq.(5.5.1), to get

$$Nu(t) = 1-2\pi B_{02}(t) \tag{5.5.2}$$

Proceeding in the similar fashion to obtain the nanoparticle concentration Nusselt number ($Nu_\phi(t)$) or Sherwood number, as it is more commonly known in double diffusive convection problem of normal fluids, to get

$$\begin{aligned} \mathrm{Nu}_\phi(\tau) &= \frac{\text{Mass transport by (molecular diffusion+advection)}}{\text{Mass transfer by molecular diffusion}}, \qquad (5.5.3) \\ &= 1 + \left[\frac{\int_0^{2\pi/\alpha_c} \left(\frac{1}{Le} \frac{\partial \phi}{\partial z} + \frac{N_A}{Le} \frac{\partial T}{\partial z} \right) dx}{\int_0^{2\pi/\alpha_c} \left(\frac{1}{Le} \frac{\partial \phi_b}{\partial z} \right) dx} \right]_{z=0}, \\ &= 1 \qquad (5.5.4) \end{aligned}$$

which corresponds to the pure conduction stage, and represents no mass being transferred.

5.6 Result and discussion

In this chapter, the effect of rotational speed modulation on the onset of thermal convection has been studied, by performing a linear stability analysis, and calculated heat transport in a nanofluid saturated porous medium by means of a weakly nonlinear stability analysis. The rotational speed modulation with revised boundary conditions has been considered for either enhancing or inhibiting the convective flow and heat transport as it is required in many real life applications in different fields of sciences and engineering.

The variation of correction in the critical thermal Rayleigh number, Ra_2 with frequency ω for different values of parameters, is depicted in Figures 5.1–5.8. From the figures, it is found that the effect of rotation speed modulation is less at low frequency as the value of Ra_2 is small. The value of Ra_2 increases for intermediate values of ω, so the effect of modulation is more at intermediate values of the frequency. Thus, at intermediate values of the frequency, the onset of convection takes place a little late, and so the system is stabilized more in this range of frequency. Further, as the frequency ω increases, the effect of modulation diminishes and disappears altogether at very large values of ω. These results are compatible with the results of Venezian (1969), in which the effect of temperature modulation of the boundaries on thermal stability has been studied, and where the correction in

the critical value of the Rayleigh number due to temperature modulation becomes almost zero at high frequencies.

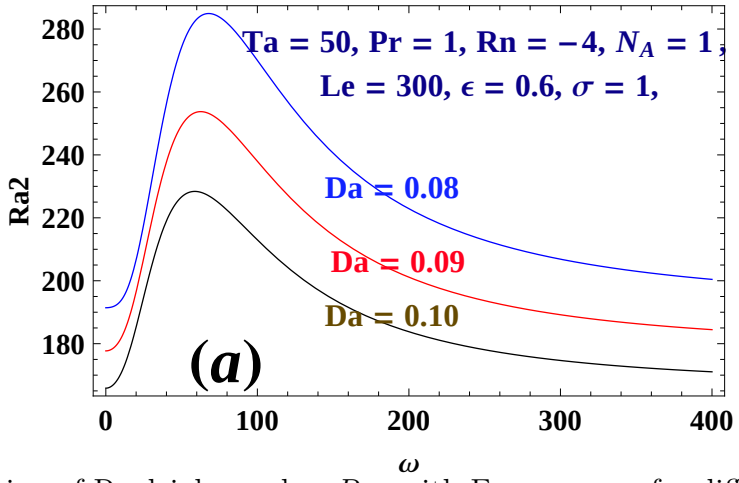

Figure 5.1: Variation of Rayleigh number Ra_2 with Frequency ω for different values of Da

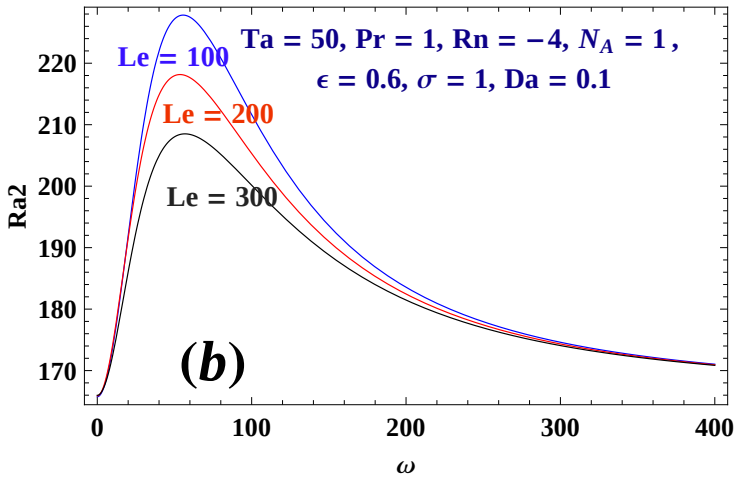

Figure 5.2: Variation of Rayleigh number Ra_2 with Frequency ω for different values of Le

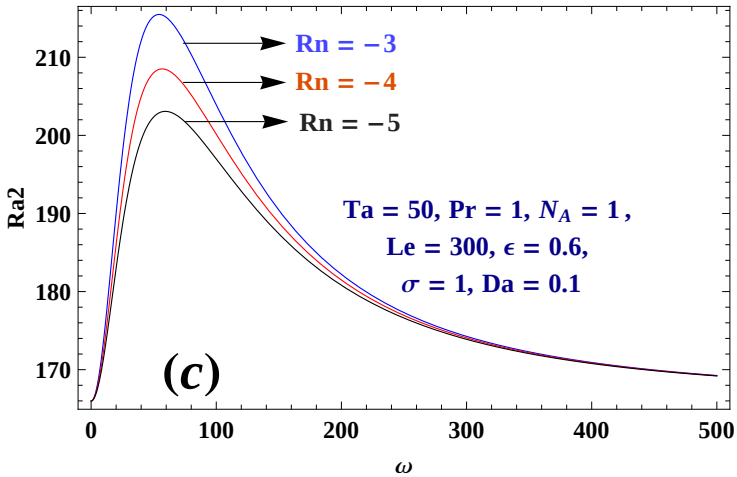

Figure 5.3: Variation of Rayleigh number Ra_2 with Frequency ω for different values of Rn

Figure 5.1 is the plot of Ra_2 versus ω for different values of Darcy number Da. It shows that Ra_2 decreases as Da increases, thereby the critical Rayleigh number decreases, and the onset of convection takes place a little early. Thus the system becomes less stabilized on increasing Da. Figure 5.2 is the plot of Ra_2 versus ω for different values of Lewis number Le. It evident that as the value of Lewis number increases, the correction to thermal Rayleigh number decreases, so the onset of convection takes place at lower value of Ra, thus system is less stabilized. But this effect diminishes for the large number of frequency of modulation. Figure 5.3 depicts graph of Ra_2 versus ω for different values of nanoparticle Rayleigh number Rn. It is clear that as Rn increases, the concentration of suspended nanoparticles will increase, so the onset of convection will take place at higher value of Ra. Thus, it is found that an increment in Rn increases Ra_2, thereby stabilizes the system more. This means that the fluids with suspended nanoparticles are more helpful to stabilization than ordinary fluids. Figure 5.4 is the plot for Ra_2 versus ω for different values of

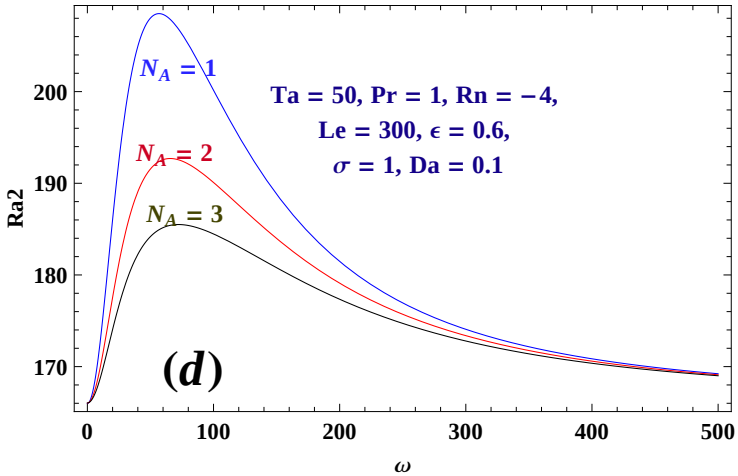

Figure 5.4: Variation of Rayleigh number Ra_2 with Frequency ω for different values of N_A

modified diffusivity ratio N_A. Increase in N_A signifies that the thermophoresis effect will increase. Now, when the thermophoresis effect increases, the onset of convection will occur early and so Ra_2 decreases as N_A increases, thus the system becomes less stabilizing. Figure 5.5 depicts variation of Ra_2 with ω for different values of the Prandtl number Pr. This figure confirms that Ra_2 decreases as Prandtl number increases, thus onset of convection is advanced due to higher thermal conductivity. In Figure 5.6, Ra_2 versus ω is shown for different values of heat capacity ratio σ. As there is no significant change in the value of

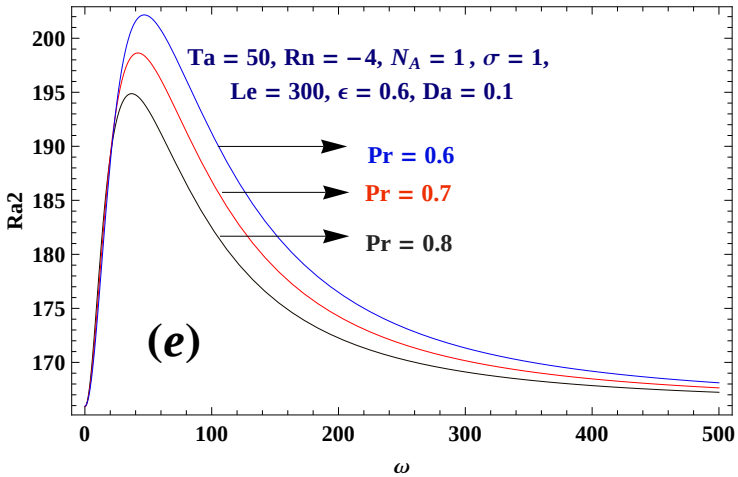

Figure 5.5: Variation of Rayleigh number Ra_2 with Frequency ω for different values of Pr

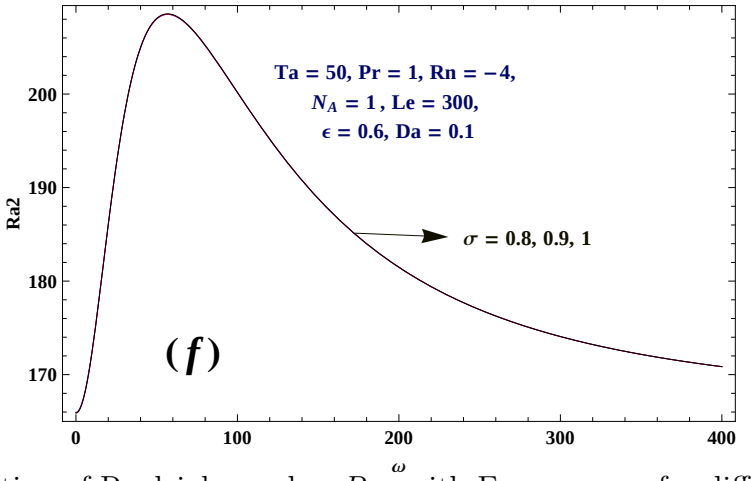

Figure 5.6: Variation of Rayleigh number Ra_2 with Frequency ω for different values of σ

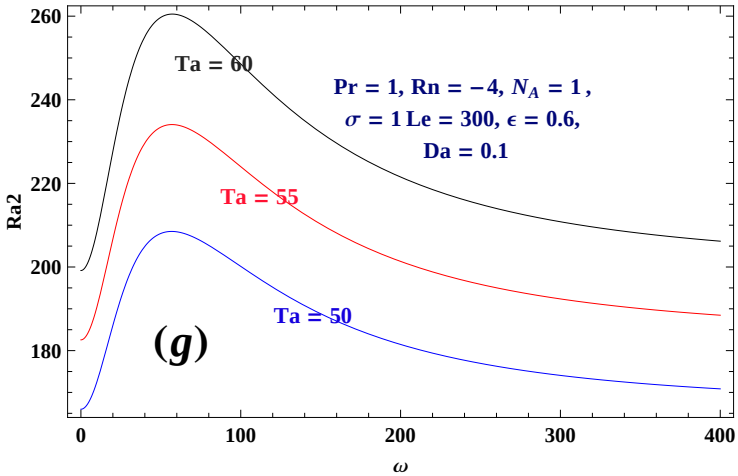

Figure 5.7: Variation of Rayleigh number Ra_2 with Frequency ω for different values of Ta

Ra_2, on increasing heat capacity ratio, therefore, the system is not much effected by this parameter. Figure 5.7 depicts Ra_2 versus ω for different values of Taylor number Ta. It is evident that as Taylor number Ta increases, the correction in thermal Rayleigh number,

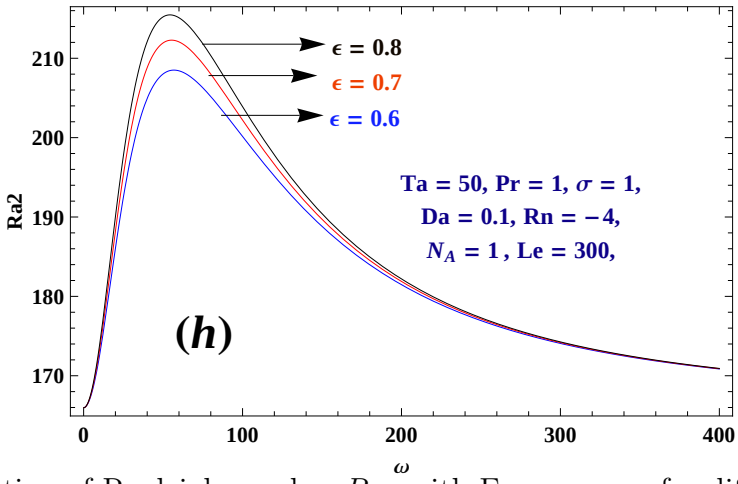

Figure 5.8: Variation of Rayleigh number Ra_2 with Frequency ω for different values of ε

Ra_2 also increases, implying that the effect of an increment in Ta is more stabilising on the system. Figure 5.8 depicts the plot of Ra_2 versus ω for different values of porosity ε, which confirms that as porosity of the system increases, the thermal Rayleigh number also increases, so the onset of convection takes place a little late, and the system is stabilized.

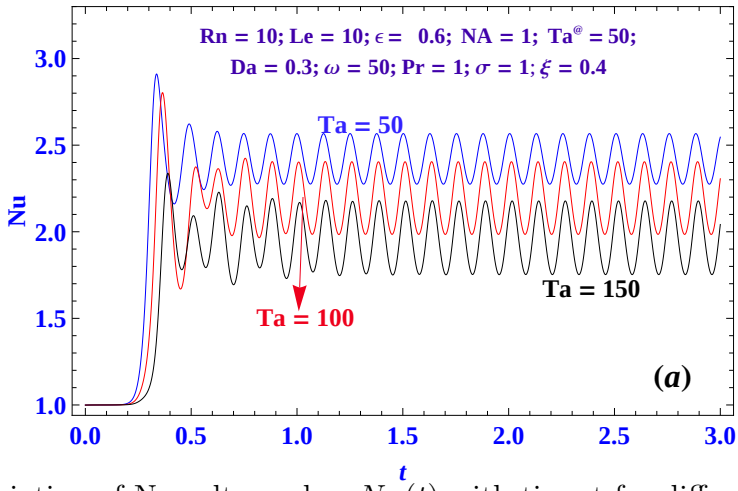

Figure 5.9: Variation of Nusselt number $Nu(t)$ with time t for different values of Ta

Figure 5.9 depicts the effect of Taylor number Ta on $Nu(t)$ for fixed values of other parameters. Similar to linear theory, it can be seen that as Ta increases, the value of Nusselt number decreases, and so is the heat transport. Further, as the value of Taylor number Ta increases, the amplitude of modulation increases, and so, the effect of Ta is reflecting on amplitude of modulation as well. From Eq.5.4.7, it is clear that the rotation is multiple of amplitude of rotation speed modulation, it means that the amplitude of rotation speed modulation is dependant of rotation. Generally, if there is no rotation

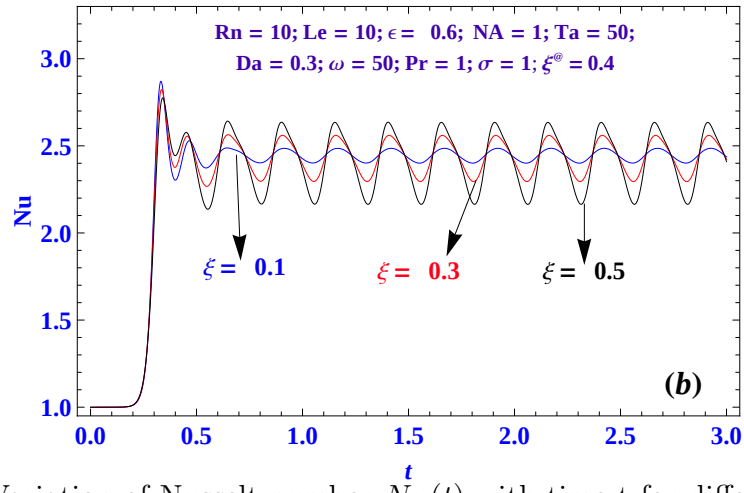

Figure 5.10: Variation of Nusselt number $Nu(t)$ with time t for different values of ξ

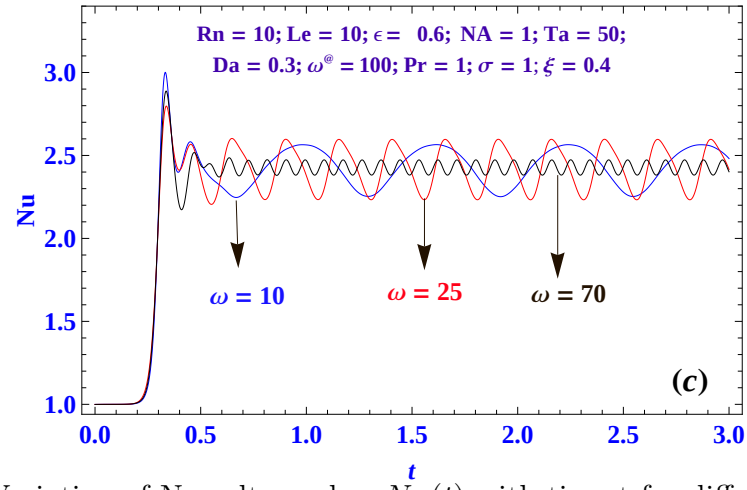

Figure 5.11: Variation of Nusselt number $Nu(t)$ with time t for different values of ω

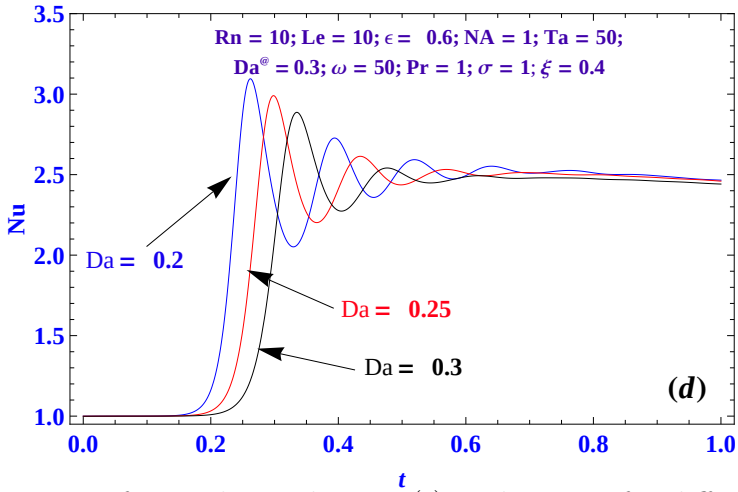

Figure 5.12: Variation of Nusselt number $Nu(t)$ with time t for different values of Da

$Ta = 0$, it is meaningless to talk about rotation speed modulation. Moreover, for no rotation $Ta = 0$, the effect of frequency of modulation will vanish, so the effect of frequency

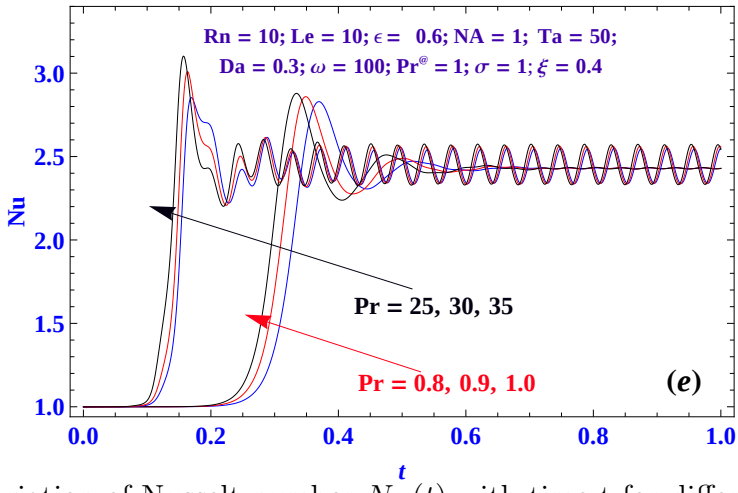

Figure 5.13: Variation of Nusselt number $Nu(t)$ with time t for different values of Pr

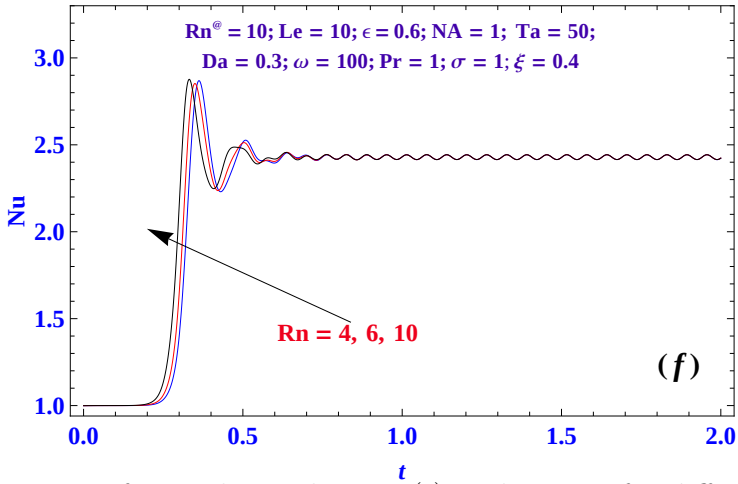

Figure 5.14: Variation of Nusselt number $Nu(t)$ with time t for different values of Rn

of modulation can not be seen in absence of the rotation. Here, results are follow as $Nu_{Ta=0} > Nu_{Ta=50} > Nu_{Ta=100} > Nu_{Ta=150}$

The effect of amplitude of modulation for moderate values of Ta, keeping fixed the values of other parameters, is depicted in Figure 5.10. It shows that the Nusselt number $Nu(t)$ increases upon increasing the value of ξ. Hence advancing the convection, it means that the heat transfer increases as ξ increase. Unmodulated system (i.e., $\xi = 0$) shows no influence on heat transport for larger values of time t. i.e. $Nu_{\xi=0.1} < Nu_{\xi=0.3} < Nu_{\xi=0.5}$

It is evident from Figure 5.11 that the effect of frequency of modulation for small values of ω heat transport is more. As the value of ω increases, the magnitude of $Nu(t)$ decreases and shortens the wavelength of oscillations. As the frequency increases from 10 to 100, the magnitude of $Nu(t)$ decreases, and the effect of modulation on heat transport

diminishes. On further increasing the value of ω, the effect of modulation on thermal instability disappears altogether. Hence, the effect of ω is to stabilize the system. i.e. $Nu_{\omega=10} > Nu_{\omega=25} > Nu_{\omega=70}$

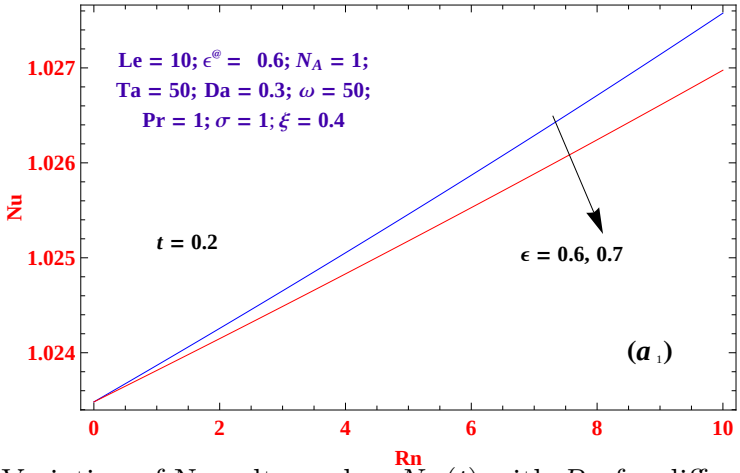

Figure 5.15: Variation of Nusselt number $Nu(t)$ with Rn for different values of ε

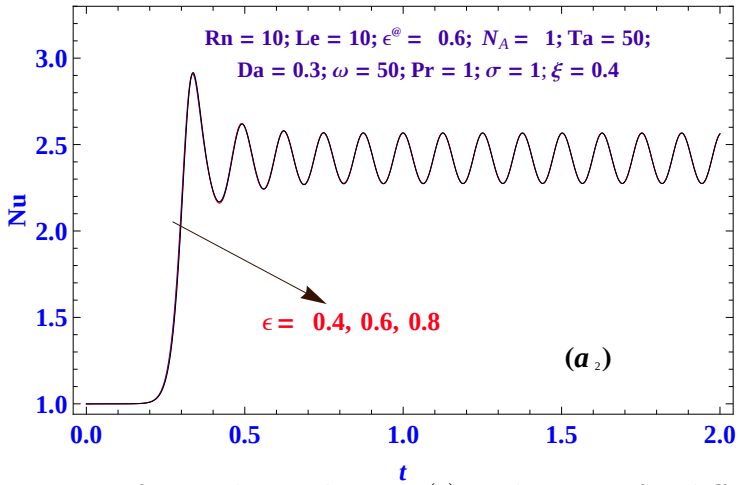

Figure 5.16: Variation of Nusselt number $Nu(t)$ with time t for different values of ε

Figure 5.12 confirms that the Nusselt number $Nu(t)$ increases upon decreasing Darcy number Da for keeping fixed the other parameters. Thus, an increment in Darcy number diminishes the rate of heat transfer. Figure 5.13 confirms that the Nusselt number $Nu(t)$ increases upon increasing Prandtl number Pr for fixed the other parameters. This may happen due to the dominating role of thermal diffusivity κ_m over kinematic viscosity μ. As Prandtl number Pr increases, then for no change in kinematic viscosity, probably there is a large decrement in thermal diffusivity, and this makes sudden increase in the temperature gradient, results the convection takes place early, and there is an enhancement in

heat transfer. Hence, the effect of an increment in Prandtl number Pr is to advance the convection. It is evident from Figure 5.14 that upon increasing the nanoparticle concentration Rayleigh number Rn, the Nusselt number $Nu(t)$ increases. This implies that the heat transfer advances due to increment in thermal conductivity of nanofluid.

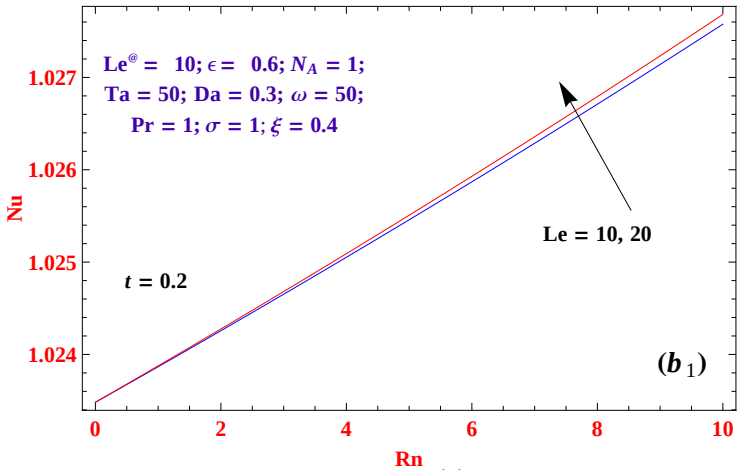

Figure 5.17: Variation of Nusselt number $Nu(t)$ with Rn for different values of Le

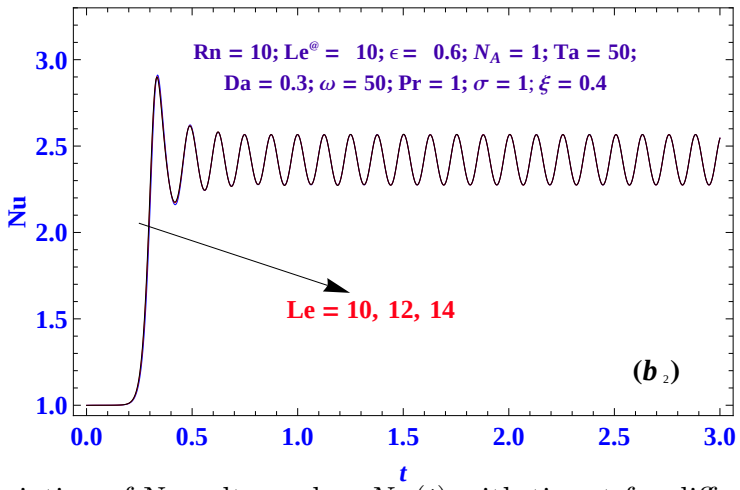

Figure 5.18: Variation of Nusselt number $Nu(t)$ with time t for different values of Le

The effect in Nusselt number $Nu(t)$ with respect to time t, and that with respect to Rn for $t = 0.2$ and different values of ε, Le and σ, is depicted in Figures 5.15–5.20. Corresponding to porosity(ε) there is no effect in Figure 5.16 realized while Figure 5.15 shows a stabilising effect for time $t = 0.2$. Corresponding to the Lewis number Le, no effect occurs in Figure 5.18 while Figure 5.17 shows the destabilising effect for time $t = 0.2$. Similar effect is found for heat capacity ratio σ as in Figure 5.20 no effect while in Figure 5.19 again the destabilising effect for the same time.

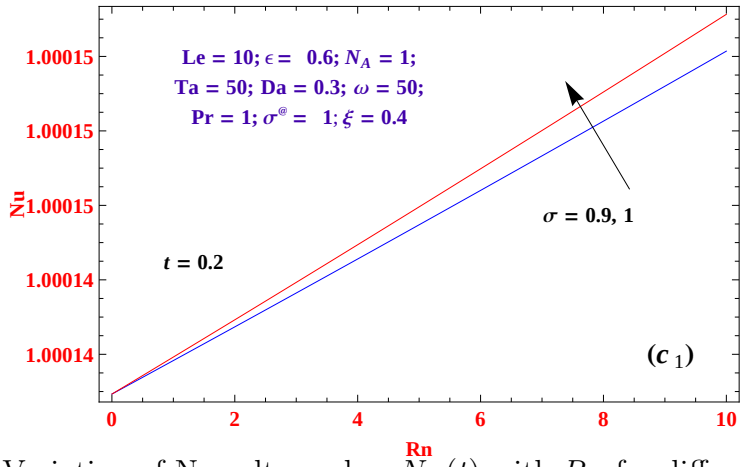

Figure 5.19: Variation of Nusselt number $Nu(t)$ with Rn for different values of σ

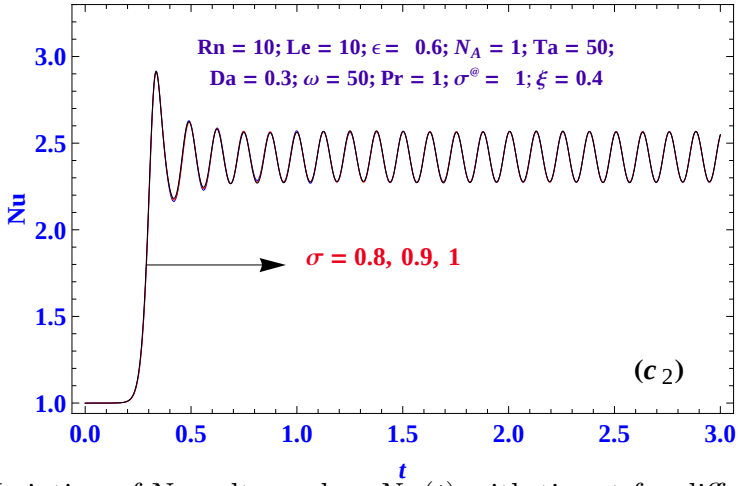

Figure 5.20: Variation of Nusselt number $Nu(t)$ with time t for different values of σ

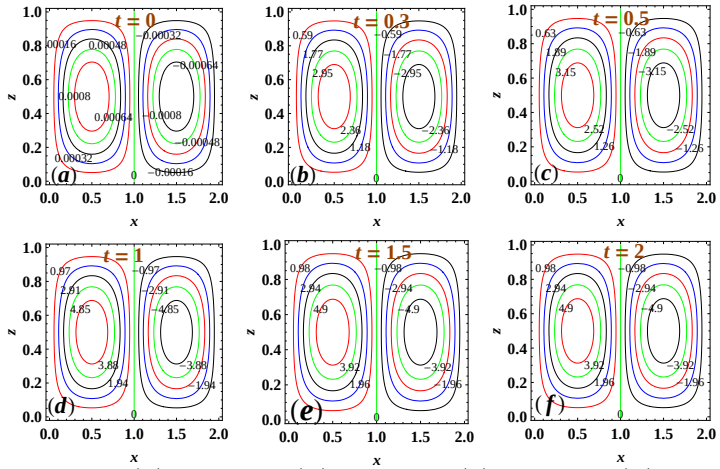

Figure 5.21: Streamlines at (a) $t = 0.0$, (b) $t = 0.3$, (c) $t = 0.5$, (d) $t = 1.0$, (e) $t = 1.5$, (f) $t = 2.0$

In Figure 5.21 and Figure 5.22 the stream lines and the corresponding isotherms are depicted respectively for rotation speed modulation at different time levels with the pa-

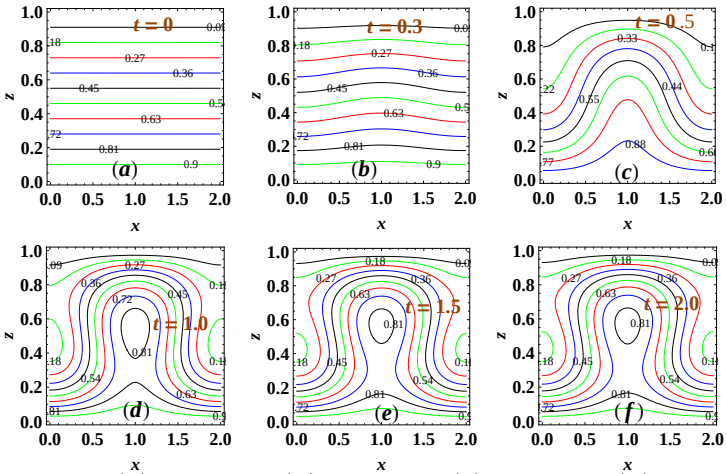

Figure 5.22: Isotherms at (a) $t = 0.0$, (b) $t = 0.3$, (c) $t = 0.5$, (d) $t = 1.0$, (e) $t = 1.5$, (f) $t = 2.0$

rameter values as $Rn = 10$, $Pr = 1$, $\sigma = 1$, $Le = 10$, $\varepsilon = 0.6$, $\omega = 50$, $\xi = 0.4$, $Ta = 100$, $Da = 0.3$. It is observed from the figures that initially for small values of time, the magnitude of stream lines is also small (Figure 5.21 *a* and *b*), and isotherms are straight that is the system is in conduction state (Figure 5.22 *a* and *b*). However, as time increases, the magnitude of stream lines increases and the isotherms lose their evenness, upto $t = 1.5$. This shows that the convection is taking place in the system. Convection becomes faster upon further increasing the value of time t. However, the system achieves the steady state beyond $t = 1.5$, as there is no change in the values of stream lines and isotherms.

5.7 Conclusion

In this chapter, thermal instability in a horizontal porous layer saturated by a nanofluid have studied, rotating about z-axis with time periodic angular velocity Ω_R. Darcy-Brinkman model with more realistic boundary conditions is considered, which incorporates the effects of Brownian motion along with thermophoresis. The results have been obtained in terms of thermal Rayleigh number, Nusselt number and nanoparticle Nusselt number using perturbation technique and truncated Fourier series method. The effect of various parameters have been obtained and depicted graphically. The following findings are made:

1. It is found that the rotational speed modulation can be used to regulate the heat and mass transports effectively.

2. The new boundary conditions has significant role on heat and mass transport due to this nanoparticle Nusselt number become constant during the entire time domain.

3. The effect of the concentration Rayleigh number Rn, Lewis number Le, modulation amplitude ξ, heat capacity ratio σ, modified diffusivity ratio N_A and Prandtl number Pr, is to destabilize the system.

4. The effect of the porosity ε, modulation frequency ω, Taylor number Ta, and Darcy number Da is to stabilize the system.

5. The effect of time t on Nusselt number is found to be oscillatory for small values of t, however, for very large values of time t, Nusselt number approaches the steady value.

6. There is no significant effect of N_A on thermal Nusselt number, but destabilising effect occur in linear theory.

Chapter 6

Onset of convection and heat transfer in a nanofluid layer under magnetic field modulation

6.1 Introduction

Owing to the suspension of nanosize particles of metal in the base fluid, the nanofluids are being used as heat energy carriers due to their enhanced abilities over ordinary fluids. The presence of a few quantity of nanoparticles in base fluids causes a significant enhancement in the heat transfer. This heat transfer characteristic of nanofluids depends on both the thermo-physical properties of the base fluid and the suspended nanoparticles. The nanofluids found a wide range of applications in industrial, commercial, residential, medical and transportation sectors.

An important virtue of nanofluids is the thermal conductivity enhancement, introduced first by Masuda et al. (1993). Choi (1995) was the first to propose the term "nanofluid".

This chapter is based on the research article: Weak nonlinear stability analysis of thermal convection in an electrically conducting nanofluid layer under magnetic field modulation, Published in **Recent Advances in Mathematical & Computational Science, Book Chapter in BBAU conference proceedings** Vol. 1 No. 1, ISBN : 9789384337674.

The ballistic nature of heat transport within nanoparticles was studied by Chen (2001), Eastman et al. (2001) found that 40% thermal conductivity of ethylene-glycol increases with 0.3% volume of copper nanoparticles of size 10nm, and Das et al. (2003) found $(10-30)\%$ increase of the effective thermal conductivity in alumina-water nanofluids with $(1-4)\%$ of alumina. Based on the above study Buongiorno and Hu (2005) suggested the possibility of the use of nanofluids in advanced nuclear systems as a coolant. The nanofluid flow can be used in the delivery of nano-drug, due to Kleinstreuer et al. (2008).

At first, Buongiorno (2006) proposed a mathematical model for convective transport in nanofluids incorporating the effects of thermophoresis and Brownian diffusion. The thermal instability problem, using the above model has been studied by Tzou (2008a,2008b) who found that the nanofluids are less stable in comparison to the base fluid, an analogous study has been carried out by Nield and Kuznetsov (2010) for different types of non-dimensional parameters. An extension to the porous medium of this model was studied by Nield and Kuznetsov (2009), Kuznetsov and Nield (2010). Two-dimensional nonlinear convection in nanofluid saturated porous medium have been studied by Bhadauria and Agarwal (2011).

The effect of magnetic field on nanofluid convection finds importance in geophysics. In particular, in the study of Earth's core at Earth's mantle consisting of conducting fluid. The magnetic field has a key role in science, engineering and industrial applications. Chandrasekhar (1961) studied in detail the thermal convection in under a magnetic field. Some of the researchers who have studied the problem of magneto-convection in a porous medium are: Patil and Rudraiah (1973), Rudraiah and Vortmeyer (1978), Alchaar et al. (1995a,b) and Bian et al. (1996a,b) who studied the magneto-convection in a porous medium for various physical models and boundary conditions. Sekar et al. (1993), Bhadauria (2006) and Bhadauria et al. (2008a,b,2010) studied the effect of magnetic field on thermal modulated convection. Matura and Lucke (2009) investigated the influence of a time-periodic and spatially homogeneous magnetic field on the linear stability properties and on the nonlinear response of a ferrofluid layer heated from below and from above. Bhadauria and Kiran (2014) made an analytic study of heat transport in an electrically conducting fluid layer under a non-uniform time-dependent magnetic field by performing a weakly nonlinear analyais. Gupta et al. (2013) found that magnetic field stabilizes the nanofluid layer for

both stationary and oscillatory convection cases. Chand and Rana (2015) studied the double diffusive convection in a horizontal layer of nanofluid in the presence of uniform vertical magnetic field with Soret effect, considering more realistic boundary conditions.

Recently, Nield and Kuznetsov (2014) in their revised model subject to new set of boundary conditions, assumed that there is no nanoparticle flux at the plate and the particle fraction value adjusts accordingly. In this case, they ruled out the possibility of oscillatory convection due to absence of two opposing forces. Agarwal (2014a) studied the thermal instability in a rotating porous layer saturated by a nanofluid based on a new boundary condition for the nanoparticle fraction. Similar work has been done by Yadav et al. (2015) for free-free, rigid-rigid and free-rigid boundaries. Linear as well as non-linear study for Rayleigh-Bénard convection in a nanofluid under thermal non-equilibrium with new boundary condition is studied by Agarwal et. al. (2014b). Nield and Kuznetsov (2015) has done a study with throughflow subjecting to another revised boundary conditions, where they considered the fact that the total nanoparticle flux is the sum of diffusive, convective and thermophoretic terms.

To best of my knowledge, the effect of magnetic field modulation with revised boundary conditions in nanofluids has not been studied, in the literature till date. The present chapter concerned with the study of the effect of magnetic field modulation on thermal instability in an electrically conducting nanofluid layer. A perturbation approach has been adopted to perform the stability analysis. Instead of fixed nanopartical fraction boundary conditions, the thermo-nanopartical flux boundary conditions have been introduced. Time periodic magnetic field is associated in vertical direction with convective boundary condition. The effect of magnetic field modulation on critical Rayleigh number and Nusselt number has been studied for different parameters, namely- Ω, ξ, Pr, Q, Rn, Le, and N_A. The numerical computation has been done to study the effect of each parameter, and depicted the behavior graphically.

6.2 Governing Equation

Considered the nanofluid layer is confined between two horizontal boundaries, $z = 0$ and $z = d$, and heated from below. The boundaries are assumed to be impermeable and perfectly thermally conducting. The nanofluid layer is extended infinitely in x and y directions, with the z-axis extending vertically upward and the origin lying at the lower boundary $z = 0$. A periodic magnetic field is applied externally in vertical upward direction. In addition, the local thermal equilibrium between the fluid and the nanoparticles has been considered. The physical configuration is as shown in the Figure 6.1. Employing the Oberbeck-Boussinesq approximation, the governing equations to study the thermal instability in a nanofluid layer are [Buongiorno (2006), Kuznetsov and Nield (2010a,b,) and Nield and Kuznetsov (2013), Nield and Kuznetsov (2014)]

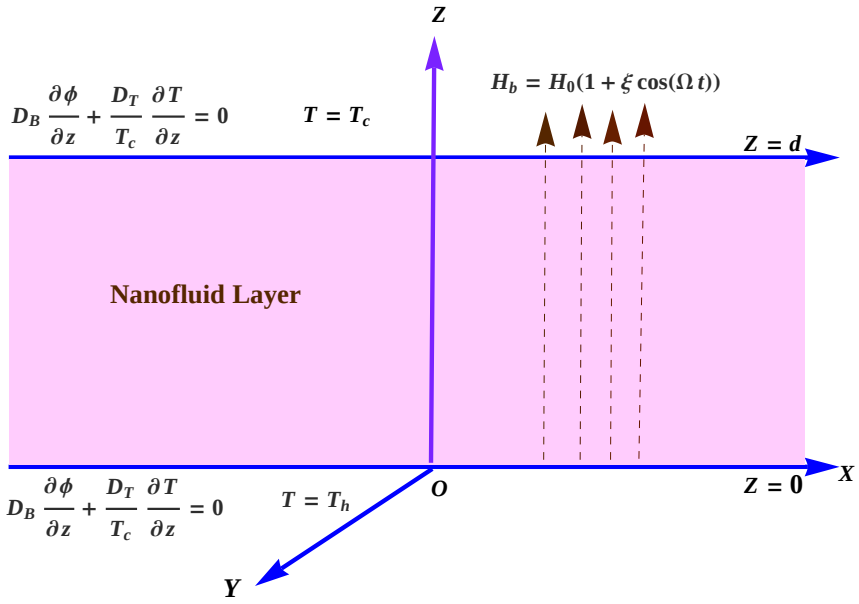

Figure 6.1: Sketch showing the physical configuration of the problem

$$
\begin{cases}
\nabla \cdot \mathbf{v} = \mathbf{0}, \\
\rho_f \left(\frac{\partial \mathbf{v}}{\partial t} + \mathbf{v} \cdot \nabla \mathbf{v} \right) + \nabla p = \mu \nabla^2 \mathbf{v} + [\phi \rho_p + (1 - \phi)\{\rho(1 - \beta(T - T_c))\}]\vec{g} + \mu_m (H \cdot \nabla H), \\
(\rho c)_f \left(\frac{\partial T}{\partial t} + \mathbf{v} \cdot \nabla T \right) = \kappa_f \nabla^2 T + (\rho c)_p [D_B \nabla \phi + \frac{D_T}{T_c} \nabla T] \cdot \nabla T, \\
\frac{\partial \phi}{\partial t} + \mathbf{v} \cdot \nabla \phi = D_B \nabla^2 \phi + \frac{D_T}{T_c} \nabla^2 T,
\end{cases}
\tag{6.2.1}
$$

The modified Maxwell equations are [Chandrasekhar (1961), Gupta et al. (2013), Bhadauria and Kiran (2014)]

$$\begin{cases} \nabla \cdot H = 0, \\ \\ \dfrac{\partial H}{\partial t} + \mathbf{v} \cdot \nabla H = H \cdot \nabla \mathbf{v}_D + \nu_m \nabla^2 H, \end{cases} \tag{6.2.2}$$

where T_h and T_c are the temperatures at the lower and upper walls such that $T_h > T_c$. The constants and variables used in the above equations have their usual meanings, and given in the nomenclature.

The magnetic field at basic state, which is varying sinusoidally with respect to time, is defined as:

$$\vec{H_b} = H_0(1 + \xi \cos(\Omega t)\hat{k} \tag{6.2.3}$$

where H_0 is the mean value of the magnetic field.

In Eq.(6.2.1) both Brownian transport and thermophoresis coefficients are time-independent, in tune with the studies that neglect the effect of thermal transport attributed to the small size of the nanoparticles (Keblinski and Cahil 2005). Further, thermophoresis and Brownian transport coefficients are assumed to be temperature-independent due to the fact that the temperature ranges under consideration are not far away from the critical value. Let the temperature and flux of volumetric fraction of the nanoparticles to be constant at the boundaries. The boundary conditions are taken as

$$\mathbf{v} = 0, \quad T = T_h, \; D_B \frac{\partial \phi}{\partial z} + \frac{D_T}{T_c} \frac{\partial T}{\partial z} = 0 \text{ at } z = 0, \tag{6.2.4}$$

$$\mathbf{v} = 0, \quad T = T_c, \; D_B \frac{\partial \phi}{\partial z} + \frac{D_T}{T_c} \frac{\partial T}{\partial z} = 0 \text{ at } z = d. \tag{6.2.5}$$

The dimensionless variables are considered as given below:
$(x^*, y^*, z^*) = (x, y, z)/d$, $t^* = t\alpha_f/(d^2)$, $(u^*, v^*, w^*) = (u, v, w)d/\alpha_f$, $p^* = p/\mu\alpha_f, \phi^* = \dfrac{\phi - \phi_0}{\phi_0}, H^* = \dfrac{H}{H_0}$ and $T^* = \dfrac{T - T_c}{T_h - T_c}$, where $\alpha_f = \dfrac{\kappa_f}{(\rho c)_f}$ and ϕ_0 is reference value for nanoparticle volume fraction. The non-dimensionalized governing equations along with boundary conditions are (after dropping the asterisk for simplicity)

$$\nabla \cdot \mathbf{v} = 0 \tag{6.2.6}$$

$$\frac{1}{Pr}\left(\frac{\partial \mathbf{v}}{\partial t} + \mathbf{v}\cdot\nabla\mathbf{v}\right) = -\nabla p + \nabla^2\mathbf{v} - (Rm - Ra\ T + Rn\phi)\,\hat{k} + Pm\ Q\ (H\cdot\nabla H) \tag{6.2.7}$$

$$\frac{\partial T}{\partial t} + \mathbf{v}\cdot\nabla T = \nabla^2 T + \frac{N_B}{Le}\nabla\phi\cdot\nabla T + \frac{N_A N_B}{Le}\nabla T\cdot\nabla T \tag{6.2.8}$$

$$\frac{\partial \phi}{\partial t} + \mathbf{v}\cdot\nabla\phi = \frac{1}{Le}\nabla^2\phi + \frac{N_A}{Le}\nabla^2 T \tag{6.2.9}$$

$$\nabla \cdot H = 0, \tag{6.2.10}$$

$$\frac{\partial H}{\partial t} + \mathbf{v}\cdot\nabla H = H\cdot\nabla\mathbf{v} + Pm\nabla^2 H \tag{6.2.11}$$

$$\left.\begin{aligned} &\mathbf{v} = 0,\quad T = 1,\ \frac{\partial\phi}{\partial z} + N_A\frac{\partial T}{\partial z} = 0 \ \text{ at } z = 0,\\ &\mathbf{v} = 0,\quad T = 0,\ \frac{\partial\phi}{\partial z} + N_A\frac{\partial T}{\partial z} = 0 \ \text{ at } z = 1. \end{aligned}\right\} \tag{6.2.12}$$

The non-dimensionlized parameters in the above equations are as given below,

$$Pm = \frac{\nu_m}{\alpha_f}, \qquad Q = \left(\frac{\mu_m H_0^2 d^2}{\mu\nu_m}\right), \qquad Pr = \frac{\mu(\rho c)_f}{\rho_f \kappa_f},$$
$$Ra = \frac{\rho_f g\beta d(T_h - T_c)}{\mu\alpha_f}, \qquad Rn = \frac{(\rho_p - \rho_f)\phi_0 g d}{\mu\alpha_f}, \qquad Rm = \frac{\{\rho_p\phi_0 + \rho_f(1-\phi_0)\}gd}{\mu\alpha_f},$$
$$N_A = \frac{D_T(T_h - T_c)}{D_B T_c \phi_0}, \qquad N_B = \frac{(\rho_c)_p}{\rho_c)_f}\phi_0, \qquad Le = \frac{\alpha_f}{D_B},$$

6.3 Basic Solution

At the basic state, the nanofluid layer is at rest, so that physical quantities to be assumed

$$\mathbf{v} = 0, p = p_b(z),\quad T = T_b(z),\ \phi = \phi_b(z)\ \ H = \vec{H}_b. \tag{6.3.1}$$

Using Eq.(6.3.1), Eq.(6.2.8) and Eq.(6.2.9) reduce to

$$\frac{d^2 T_b}{dz^2} + \frac{N_B}{Le}\frac{d\phi_b}{dz}\frac{dT_b}{dz} + \frac{N_A N_B}{Le}\left(\frac{dT_b}{dz}\right)^2 = 0, \tag{6.3.2}$$

$$\frac{d^2\phi_b}{dz^2} + N_A \frac{d^2T_b}{dz^2} = 0. \tag{6.3.3}$$

After integrating Eq.(6.3.3) subject to the boundary condition Eq.(6.2.12), it is obtain

$$\frac{d\phi_b}{dz} + N_A \frac{dT_b}{dz} = 0, \tag{6.3.4}$$

Using Eq.(6.3.4), Eq.(6.3.2) reduces to

$$\frac{d^2T_b}{dz^2} = 0. \tag{6.3.5}$$

The solutions of Eq.(6.3.4) and Eq.(6.3.5) subject to the boundary condition (6.2.12) are as follow

$$T_b = 1 - z, \tag{6.3.6}$$

$$\phi_b = \phi_0 + N_A z. \tag{6.3.7}$$

6.4 Stability Analysis

Superimposing perturbations on the basic state as given below :

$$\mathbf{v} = \mathbf{v}',\ p = p_b + p',\ T = T_b + T',\ \phi = \phi_b + \phi',\quad H = \vec{H}_b + H'. \tag{6.4.1}$$

Since the case of two-dimensional rolls is being considered, therefore all physical quantities are assumed to be independent of y. For two-dimensional convection, the stream function ψ and magnetic potential Φ are introduced as $(u, v, w) = (\frac{\partial\psi}{\partial z}, 0, -\frac{\partial\psi}{\partial x})$, $(H_x, H_y, H_z) = (\frac{\partial\Phi}{\partial z}, 0, -\frac{\partial\Phi}{\partial x})$. The pressure term in Eq.(6.2.7) has been removed by taking twice curl of momentum equation. Now using the expression Eq.(6.4.1) in Eqs.(6.2.6)-(6.2.12), and also using Eq.(6.3.6) and Eq.(6.3.7), the system of nonlinear perturbed equa-

tions is obtained as

$$\left(\frac{1}{Pr}\frac{\partial}{\partial t}-\nabla^2\right)\nabla^2\psi=-Ra\frac{\partial T}{\partial x}+Rn\frac{\partial \phi}{\partial x}+Q\ Pm\ (1+\xi\cos(\Omega t))\frac{\partial}{\partial z}\nabla^2\Phi- Q\ Pm\ \frac{\partial(\Phi,\nabla^2\Phi)}{\partial(x,z)}+\frac{1}{Pr}\frac{\partial(\psi,\nabla^2\psi)}{\partial(x,z)} \tag{6.4.2}$$

$$\frac{\partial T}{\partial t}+\frac{\partial \psi}{\partial x}=\nabla^2 T-\frac{N_A N_B}{Le}\frac{\partial T}{\partial z}+\frac{N_B}{Le}\frac{\partial \phi}{\partial z}+\frac{\partial(\psi,T)}{\partial(x,z)}+\frac{N_B}{Le}\left(\nabla\phi.\nabla T+N_A\nabla T.\nabla T\right) \tag{6.4.3}$$

$$\frac{\partial \phi}{\partial t}-N_A\frac{\partial \psi}{\partial x}=\frac{1}{Le}\nabla^2\phi+\frac{N_A}{Le}\nabla^2 T+\frac{\partial(\psi,\phi)}{\partial(x,z)} \tag{6.4.4}$$

$$\left(\frac{\partial}{\partial t}-Pm\nabla^2\right)\Phi=(1+\xi\cos(\Omega t))\frac{\partial \psi}{\partial z}+\frac{\partial(\psi,\Phi)}{\partial(x,z)} \tag{6.4.5}$$

$$\psi=\frac{\partial^2\psi}{\partial z^2}=0,\ \Phi=\frac{\partial \Phi}{\partial z}=0,\ T=0,\ \frac{\partial \phi}{\partial z}+N_A\frac{\partial T}{\partial z}=0\ \text{ at } z=0,\ \text{and at } z=1. \tag{6.4.6}$$

The parameter R_m is not carried over in the subsequent equations because it is a part of the hydrostatic equilibrium. Primes " $'$ " have been dropped in the above system.

6.4.1 Linear Stability Analysis

The linear stability analysis is studied by considering marginal and over-stable states. To perform linear stability analysis, the nonlinear terms are neglected from the Eqs.(6.4.2)−(6.4.6), so the linear system of equations is obtained as.

$$\left(\frac{1}{Pr}\frac{\partial}{\partial t}-\nabla^2\right)\nabla^2\psi=-Ra\frac{\partial T}{\partial x}+Rn\frac{\partial \phi}{\partial x}+Q\ Pm\ (1+\xi\cos(\Omega t))\frac{\partial}{\partial z}\nabla^2\Phi \tag{6.4.7}$$

$$\frac{\partial T}{\partial t}+\frac{\partial \psi}{\partial x}=\nabla^2 T-\frac{N_A N_B}{Le}\frac{\partial T}{\partial z}+\frac{N_B}{Le}\frac{\partial \phi}{\partial z} \tag{6.4.8}$$

$$\frac{\partial \phi}{\partial t}-N_A\frac{\partial \psi}{\partial x}=\frac{1}{Le}\nabla^2\phi+\frac{N_A}{Le}\nabla^2 T \tag{6.4.9}$$

$$\left(\frac{\partial}{\partial t}-Pm\nabla^2\right)\Phi=(1+\xi\cos(\Omega t))\frac{\partial \psi}{\partial z} \tag{6.4.10}$$

$$\psi=\frac{\partial^2\psi}{\partial z^2}=0,\ \ T=0,\ \frac{\partial \phi}{\partial z}+N_A\frac{\partial T}{\partial z}=0\ \text{ at } z=0,\ \text{and }\ at\ z=1 \tag{6.4.11}$$

Eliminating T, ϕ and Φ from Eqs.(6.4.7)−(6.4.10) under orthogonality condition, single equation for ψ is obtained in the form

$$\begin{aligned}
&\left(\frac{\partial}{\partial t}-\nabla^2\right)\left(\frac{\partial}{\partial t}-\frac{1}{Le}\nabla^2\right)\left(\frac{1}{Pr}\frac{\partial}{\partial t}-\nabla^2\right)\left(\frac{\partial}{\partial t}-Pm\nabla^2\right)\nabla^2\psi \\
&\quad = Ra\left(\frac{\partial}{\partial t}-\frac{1}{Le}\nabla^2\right)\left(\frac{\partial}{\partial t}-Pm\nabla^2\right)\left(\frac{\partial^2\psi}{\partial x^2}\right)+RnN_A\times \\
&\quad \left(\frac{\partial}{\partial t}-\nabla^2\left(\frac{1}{Le}+1\right)\right)\left(\frac{\partial}{\partial t}-Pm\nabla^2\right)\left(\frac{\partial^2\psi}{\partial x^2}\right)+ \\
&\quad PmQ\left(\frac{\partial}{\partial t}-\nabla^2\right)\left(\frac{\partial}{\partial t}-\frac{1}{Le}\nabla^2\right)(1+\xi\cos(\Omega t))^2\nabla^2\frac{\partial^2\psi}{\partial z^2}
\end{aligned} \tag{6.4.12}$$

The perturbation technique is applied to obtain eigen functions ψ and corresponding eigen values Ra by introducing a small perturbation parameter χ, suitably small amplitude of modulation is also considered as perturbation parameter as following Venezian (1969)

$$\begin{aligned}
\psi &= \psi_0+\chi\psi_1+\chi^2\psi_2+\ldots \\
Ra &= Ra_0+\chi Ra_1+\chi^2 Ra_2+\ldots
\end{aligned} \tag{6.4.13}$$

Using expressions in Eq.(6.4.13) into Eq.(6.4.12), and equating the like powers of χ on both sides, it is obtained

$$\chi^0: \; L\psi_0 = 0 \tag{6.4.14}$$

$$\begin{aligned}
\chi^1: \; L\psi_1 &= Ra_1\left(\frac{\partial}{\partial t}-Pm\nabla^2\right)\left(\frac{\partial}{\partial t}-\frac{1}{Le}\nabla^2\right)\frac{\partial^2}{\partial x^2}\psi_0+ \\
&\quad 2PmQ\left(\frac{\partial}{\partial t}-\nabla^2\right)\left(\frac{\partial}{\partial t}-\frac{1}{Le}\nabla^2\right)\cos(\Omega t)\frac{\partial^2}{\partial z^2}\nabla^2\psi_0
\end{aligned} \tag{6.4.15}$$

$$\begin{aligned}
\chi^2: \; L\psi_2 &= Ra_2\left(\frac{\partial}{\partial t}-Pm\nabla^2\right)\left(\frac{\partial}{\partial t}-\frac{1}{Le}\nabla^2\right)\frac{\partial^2\psi_0}{\partial x^2}+ \\
&\quad PmQ\left(\frac{\partial}{\partial t}-\nabla^2\right)\left(\frac{\partial}{\partial t}-\frac{1}{Le}\nabla^2\right)\cos^2(\Omega t)\frac{\partial^2}{\partial z^2}\nabla^2\psi_0 \\
&\quad +Ra_1\alpha^2\left(\frac{\partial}{\partial t}-Pm\nabla^2\right)\left(\frac{\partial}{\partial t}-\frac{1}{Le}\nabla^2\right)\psi_1+ \\
&\quad 2PmQ\left(\frac{\partial}{\partial t}-\nabla^2\right)\left(\frac{\partial}{\partial t}-\frac{1}{Le}\nabla^2\right)\cos(\Omega t)\frac{\partial^2}{\partial z^2}\nabla^2\psi_1,
\end{aligned} \tag{6.4.16}$$

where

$$\begin{aligned} L \;=\; & \left(\frac{\partial}{\partial t}-\nabla^2\right)\left(\frac{\partial}{\partial t}-\frac{1}{Le}\nabla^2\right)\left(\frac{1}{Pr}\frac{\partial}{\partial t}-\nabla^2\right)\left(\frac{\partial}{\partial t}-Pm\nabla^2\right)\nabla^2 - \\ & Ra_0\left(\frac{\partial}{\partial t}-Pm\nabla^2\right)\left(\frac{\partial}{\partial t}-\frac{1}{Le}\nabla^2\right)\frac{\partial^2}{\partial x^2} \\ & -RnN_A\left(\frac{\partial}{\partial t}-Pm\nabla^2\right)\left(\frac{\partial}{\partial t}-\nabla^2\left(\frac{1}{Le}+1\right)\right)\frac{\partial^2}{\partial x^2} - \\ & PmQ\left(\frac{\partial}{\partial t}-\nabla^2\right)\left(\frac{\partial}{\partial t}-\frac{1}{Le}\nabla^2\right)\frac{\partial^2}{\partial z^2}\nabla^2. \end{aligned} \tag{6.4.17}$$

In the following section, the above system is solved for different orders of χ.

Lowest order system

Since, two dimensional dynamics is assumed to be independent of y direction, so $\psi_0 = \sin(\alpha x)\sin(\pi z)$ is taken for the marginally stable solutions, and the corresponding eigen values are obtained by using Eq.(6.4.14)

$$Ra_0 = \left(\frac{\delta^6 + Q\ \pi^2\delta^2}{\alpha^2}\right) - RnN_A\left(1+Le\right), \tag{6.4.18}$$

where $\delta^2 = \pi^2 + \alpha^2$. In the absence of magnetic field, the expression of Ra_0 coincide with the result of Nield and Kuznetsov (2014).

First order system

$$L\psi_1 = -Ra_1 Pm\delta^2\left(\frac{\delta^2}{Le}\right)\alpha^2\psi_0 + 2PmQ\delta^2\pi^2\left(h_1\cos(\Omega t) - h_2\sin(\Omega t)\right)\psi_0 \tag{6.4.19}$$

where $h_1 = \left(\frac{\delta^4}{Le} - \Omega^2\right)$ and $h_2 = \delta^2\Omega\left(\frac{1}{Le}+1\right)$. The solution of the homogeneous equation corresponding to Eq.(6.4.19) must have a term orthogonal to null space of operator L. Now applying the theory of minimal Rayleigh number and taking $R_1 = 0$, so that the time dependent term on right hand side of equation Eq.(6.4.15) is complete orthogonal function

to $\sin(\alpha x)\sin(\pi z)$. Use $\phi_0 = \sin(\alpha x)\sin(\pi z)$, to obtain

$$L[\sin(\pi z)\exp^{(i\alpha x - i\Omega t)}] = L(\Omega)\sin(\pi z)\exp^{(i\alpha x - i\Omega t)}, \tag{6.4.20}$$

where

$$L(\Omega) = S_1 + iS_2, \tag{6.4.21}$$

$$\begin{aligned} S_1 = & -\frac{Pm\delta^4}{Le}\left\{\left(Ra_0\alpha^2 + Rn\alpha^2 N_A Le\left(\frac{1}{Le}+1\right)\right) - \delta^6) + Pm\ Q\ \pi^2\delta^2\right\} \\ & + \Omega^2\left\{\frac{\delta^6}{Pr}\left(\frac{1+Pm}{Le}+1\right) + \delta^6\left(\frac{1}{Le}+1+Pm\right) + RnN_A\alpha^2 + Ra_0\alpha^2 + Pm\ Q\ \pi^2\right\} \\ & - \Omega^4\frac{\delta^2}{Pr} \end{aligned} \tag{6.4.22}$$

$$\begin{aligned} S_2 = & \ \Omega\left[\delta^8\left(\frac{1+Pm}{Le}+1\right) + Pm\ Q\ \pi^2\delta^2\left(\frac{1}{Le}+1\right) + Pm\frac{1}{Pr}\frac{\delta^6}{Le} + Ra_0\alpha^2\delta^2\left(\frac{Pm}{1}+\frac{1}{Le}\right)\right. \\ & \left. + RnN_A\alpha^2\delta^2\left(\frac{1}{Le}+1+Pm\right) + \Omega^2\left\{\frac{(\delta^4)}{Pr}\left(\frac{1}{Le}+1+Pm\right)+\delta^4\right\}\right]. \end{aligned} \tag{6.4.23}$$

Now, ψ_1 is obtained by inverting the operator L term by term as follows

$$\psi_1 = 2Pm\ Q\ \delta^2\pi^2\mathbf{Re}\left[\frac{L^*(\Omega)}{|L(\Omega)|^2}\left\{h_1\cos(\Omega t) - h_2\sin(\Omega t)\right\}\sin(\alpha x)\sin(\pi z)\right], \tag{6.4.24}$$

where L^* is complex conjugate of L.

Second order system

From equation Eq.(6.4.16), it is obtained

$$\begin{aligned} L\psi_2 = & -Ra_2\alpha^2(Pm\delta^2)\frac{\delta^2}{Le}\sin(\alpha x)\sin(\pi z) + Pm\ Q\ \delta^2\pi^2\left(\frac{\delta^4}{Le}\cos^2(\Omega t) + \Omega^2\cos(2\Omega t) - 2\Omega\delta^2\times\right. \\ & \left.\left(\frac{1}{Le}+1\right)\sin(2\Omega t)\right)\sin(\alpha x)\sin(\pi z) + 2\ Pm\ Q\ \delta^2\pi^2\left[H_1\frac{\delta^4}{Le} + \left\{H_2\left(\frac{\delta^4}{Le} - 4\Omega^2\right) + \right.\right. \\ & \left.\left. 2H_1\delta^2\Omega\left(\frac{1}{Le}+1\right)\right\}\sin(2\Omega t) + \left\{H_1\left(\frac{\delta^4}{Le} - 4\Omega^2\right) - 2H_2\delta^2\Omega\left(\frac{1}{Le}+1\right)\right\}\cos(2\Omega t)\right]\times \\ & \sin(\alpha x)\sin(\pi z), \end{aligned} \tag{6.4.25}$$

where $H_1 = \ Pm\ Q\ \pi^2\mathbf{Re}\left[\frac{L^*(\Omega)}{|L(\Omega)|^2}h_1\right]\ H_2 = -\ Pm\ Q\ \pi^2\mathbf{Re}\left[\frac{L^*(\Omega)}{|L(\Omega)|^2}h_2\right]$.

Here the Eq.(6.4.25) is not solved but used to determine Ra_2. For the existence of solution of the Eq.(6.4.25), it is necessary that the steady part of its right hand side is orthogonal to $\sin(\alpha x)\sin(\pi z)$, which yields

$$\int_0^1\int_0^{\frac{\pi}{\alpha}}\left[-Ra_2\alpha^2(Pm\delta^2)\frac{\delta^2}{Le}\sin(\alpha x)\sin(\pi z)+PmQ\delta^2\pi^2\left(\frac{\delta^4}{Le}\overline{\cos^2(\Omega t)}+\Omega^2\overline{\cos(2\Omega t)}-2\Omega\delta^2\times\right.\right.$$
$$\left(\frac{1}{Le}+1\right)\overline{\sin(2\Omega t)}\Big)\sin(\alpha x)\sin(\pi z)+2PmQ\delta^2\pi^2\left[H_1\frac{\delta^4}{Le}+\left\{H_2\left(\frac{\delta^4}{Le}-4\Omega^2\right)+\right.\right.$$
$$\left.\left.2H_1\delta^2\Omega\left(\frac{1}{Le}+1\right)\right\}\overline{\sin(2\Omega t)}+\left\{H_1\left(\frac{\delta^4}{Le}-4\Omega^2\right)-2H_2\delta^2\Omega\left(\frac{1}{Le}+1\right)\right\}\overline{\cos(2\Omega t)}\right]\times$$
$$\left.\sin(\alpha x)\sin(\pi z)\right]sin(\alpha x)\sin(\pi z)dxdz=0, \tag{6.4.26}$$

where $\overline{f(t)}$ denotes the time average of $f(t)$. Simplifying the above equation, the expression for critical Rayleigh number is obtained as

$$Ra_2=\frac{Q\pi^2\delta^2}{2\alpha^2}\left(1+2\ Pm\ Q\ \pi^2\left(\frac{\delta^4}{Le}-\Omega^2\right)\mathbf{Re}\left[\frac{L^*(\Omega)}{|L(\Omega)|^2}\right]\right). \tag{6.4.27}$$

6.4.2 Weakly nonlinear Analysis

Now introduce the following asymptotic expansion

$$\mathrm{Ra} = \mathrm{Ra}_{0,c}+\chi^2\mathrm{Ra}_2+\chi^4\mathrm{Ra}_4+..., \tag{6.4.28}$$
$$\psi = \chi\psi_1+\chi^2\psi_2+\chi^3\psi_3+..., \tag{6.4.29}$$
$$T = \chi T_1+\chi^2T_2+\chi^3T_3+..., \tag{6.4.30}$$
$$\phi = \chi\phi_1+\chi^2\phi_2+\chi^3\phi_3+..., \tag{6.4.31}$$
$$\Phi = \chi\Phi_1+\chi^2\Phi_2+\chi^3\Phi_3+..., \tag{6.4.32}$$

where $\mathrm{Ra}_{0,c}$ is the critical value of the Rayleigh number at which the onset of convection takes place.

Now assume the variation of time only at the slow time scale $\tau=\chi^2t$ and arranging the systems at different order of χ.

At the lowest order, the system is

$$\begin{pmatrix} -\nabla^2 & \mathrm{Ra}_{0,c}\frac{\partial}{\partial x} & -\mathrm{Rn}\frac{\partial}{\partial x} & -QPm\frac{\partial}{\partial z}\nabla^2 \\ \frac{\partial}{\partial x} & -\nabla^2+\frac{N_AN_B}{\mathrm{Le}}\frac{\partial}{\partial z} & \frac{N_B}{\mathrm{Le}}\frac{\partial}{\partial z} & 0 \\ -N_A\frac{\partial}{\partial x} & -\frac{N_A}{\mathrm{Le}}\nabla^2 & -\frac{1}{\mathrm{Le}}\nabla^2 & 0 \\ -\frac{\partial}{\partial z} & 0 & 0 & -Pm\nabla^2 \end{pmatrix}\begin{pmatrix} \psi_1 \\ T_1 \\ \phi_1 \\ \Phi_1 \end{pmatrix} = 0 \tag{6.4.33}$$

solution at the lowest order subject to the boundary conditions in Eq.(6.4.6), are given by

$$\psi_1 = A[\tau]\mathrm{Sin}\,(k_cx)\,\mathrm{Sin}(\pi z), \tag{6.4.34}$$

$$T_1 = -\frac{k_c}{\delta^2}A[\tau]\ \mathrm{Cos}\,(k_cx)\,\mathrm{Sin}(\pi z), \tag{6.4.35}$$

$$\phi_1 = \frac{k_cN_A\,(\mathrm{Le}+1)}{\delta^2}A[\tau]\ \mathrm{Cos}\,(k_cx)\,\mathrm{Sin}(\pi z), \tag{6.4.36}$$

$$\Phi_1 = \frac{\pi}{Pm\delta^2}A[\tau]\ \mathrm{Sin}\,(k_cx)\,\mathrm{Cos}(\pi z), \tag{6.4.37}$$

where $\delta^2 = k_c^2+\pi^2$.

The critical value of the Rayleigh number and the corresponding wave number for the onset of stationary convection is calculated numerically and the expression for critical Rayleigh number is given by

$$\mathrm{Ra}_{0,c} = \frac{\delta^2(\delta^4+\pi^2Q)}{k_c^2} - N_A\mathrm{Rn}\,(\mathrm{Le}+1)\,, \tag{6.4.38}$$

and the critical wave number is $k_c = \frac{\pi}{\sqrt{2}}$.

6.5 Amplitude equation and Heat and Mass Transport for Stationary Instability

At the second order, the system is

$$\begin{pmatrix} -\nabla^2 & \mathrm{Ra}_{0,c}\frac{\partial}{\partial x} & -\mathrm{Rn}\frac{\partial}{\partial x} & -QPm\frac{\partial}{\partial z}\nabla^2 \\ \frac{\partial}{\partial x} & -\nabla^2+\frac{N_AN_B}{\mathrm{Le}}\frac{\partial}{\partial z} & \frac{N_B}{\mathrm{Le}}\frac{\partial}{\partial z} & 0 \\ -N_A\frac{\partial}{\partial x} & -\frac{N_A}{\mathrm{Le}}\nabla^2 & -\frac{1}{\mathrm{Le}}\nabla^2 & 0 \\ -\frac{\partial}{\partial z} & 0 & 0 & -Pm\nabla^2 \end{pmatrix}\begin{pmatrix} \psi_2 \\ T_2 \\ \phi_2 \\ \Phi_2 \end{pmatrix} = \begin{pmatrix} R_{21} \\ R_{22} \\ R_{23} \\ R_{24} \end{pmatrix}, \tag{6.5.1}$$

where

$$
\begin{aligned}
R_{21} &= 0, && (6.5.2)\\
R_{22} &= \frac{-{k_c}^2\pi}{2\delta^2}A[\tau]^2\mathrm{Sin}(2\pi z) - \frac{{k_c}^2 N_A N_B}{\delta^4}\left({k_c}^2\mathrm{Sin}^2(k_c x)\mathrm{Sin}^2(\pi z)\right.\\
&\quad \left.+\pi^2\mathrm{Cos}^2(k_c x)\mathrm{Cos}^2(\pi z)\right)A[\tau]^2, && (6.5.3)\\
R_{23} &= \frac{\pi {k_c}^2 N_A\,(\mathrm{Le}+1)}{2\delta^2}A[\tau]^2\mathrm{Sin}(2\pi z). && (6.5.4)\\
R_{24} &= -\frac{\pi^2 {k_c}^2}{2Pm\delta^2}A[\tau]^2\mathrm{Sin}(2k_c x). && (6.5.5)
\end{aligned}
$$

The second order solutions subject to the boundary conditions in Eq.(6.4.6), are given by

$$
\begin{aligned}
\psi_2 &= 0, && (6.5.6)\\
T_2 &= \frac{-{k_c}^2}{8\pi\delta^2}A[\tau]^2\mathrm{Sin}(2\pi z), && (6.5.7)\\
\phi_2 &= \frac{{k_c}^2 N_A \mathrm{Le}}{8\pi\delta^2}\left((\mathrm{Le}+1)+\frac{1}{\mathrm{Le}}\right)A[\tau]^2\mathrm{Sin}(2\pi z). && (6.5.8)\\
\Phi_2 &= -\frac{\pi^2}{8k_c Pm^2\delta^2}A[\tau]^2\mathrm{Sin}(2k_c x). && (6.5.9)
\end{aligned}
$$

The thermal Nusselt number, is defined as:

$$
\begin{aligned}
Nu[\tau] &= \frac{\text{Heat transport by (conduction + convection)}}{\text{Heat transport by conduction}}\\
&= \frac{\left[\frac{k_c}{2\pi}\int_0^{\frac{2\pi}{k_c}}(1-z+T_2)_z\,dx\right]_{z=0}}{\left[\frac{k_c}{2\pi}\int_0^{\frac{2\pi}{k_c}}(1-z)_z\,dx\right]_{z=0}}, && (6.5.10)
\end{aligned}
$$

The nanoparticle concentration Nusselt number (Sherwood number), is defined as

$$
\begin{aligned}
Nu_\phi[\tau] &= \frac{\text{Mass transport by (molecular diffusion + molecular advection)}}{\text{Mass transport by molecular diffusion}}\\
&= \frac{\left[\frac{k_c}{2\pi}\int_0^{\frac{2\pi}{k_c}}(\phi_0+N_A z+\phi_2)_z\,dx\right]_{z=0}}{\left[\frac{k_c}{2\pi}\int_0^{\frac{2\pi}{k_c}}(\phi_0+N_A z)_z\,dx\right]_{z=0}}. && (6.5.11)
\end{aligned}
$$

Substituting expressions of T_2 and ϕ_2 in the above Eqs.(6.5.10 and 6.5.11) and simplifying, it is obtained

$$\begin{aligned} \mathrm{Nu}[\tau] &= 1+\frac{k_c^2}{4\delta^2}(A[\tau])^2, && (6.5.12)\\ \mathrm{Nu}_\phi[\tau] &= 1+\left(\frac{{k_c}^2\mathrm{Le}}{4\delta^2}\left((\mathrm{Le}+1)+\frac{1}{\mathrm{Le}}\right)\right)(A[\tau])^2. && (6.5.13)\end{aligned}$$

At the third order, the system is

$$\begin{pmatrix} -\nabla^2 & \mathrm{Ra}_{0,c}\frac{\partial}{\partial x} & -\mathrm{Rn}\frac{\partial}{\partial x} & -QPm\frac{\partial}{\partial z}\nabla^2 \\ \frac{\partial}{\partial x} & -\nabla^2+\frac{N_AN_B}{\mathrm{Le}}\frac{\partial}{\partial z} & \frac{N_B}{\mathrm{Le}}\frac{\partial}{\partial z} & 0 \\ -N_A\frac{\partial}{\partial x} & -\frac{N_A}{\mathrm{Le}}\nabla^2 & -\frac{1}{\mathrm{Le}}\nabla^2 & 0 \\ -\frac{\partial}{\partial z} & 0 & 0 & -Pm\nabla^2 \end{pmatrix}\begin{pmatrix}\psi_3\\ T_3\\ \phi_3\\ \Phi_3\end{pmatrix}=\begin{pmatrix}R_{31}\\ R_{32}\\ R_{33}\\ R_{34}\end{pmatrix} \qquad (6.5.14)$$

where

$$\begin{aligned} R_{31} &= -\frac{1}{Pr}\frac{\partial\nabla^2\psi_1}{\partial\tau}-\mathrm{Ra}_2\frac{\partial T_1}{\partial x}+Q\ Pm\ \xi Cos\left(\Omega\tau\right)\frac{\partial\nabla^2\Phi_1}{\partial z}-Q\ Pm\times \\ &\quad \left[\frac{\partial\Phi_1}{\partial x}\frac{\partial\nabla^2\Phi_2}{\partial z}-\frac{\partial\nabla^2\Phi_1}{\partial x}\frac{\partial\Phi_2}{\partial z}\right]+\frac{1}{Pr}\left[\frac{\partial\psi_1}{\partial x}\frac{\partial\nabla^2\psi_2}{\partial z}-\frac{\partial\nabla^2\psi_1}{\partial x}\frac{\partial\psi_2}{\partial z}\right], && (6.5.15)\\ R_{32} &= \frac{\partial\psi_1}{\partial x}\frac{\partial T_2}{\partial z}+\frac{N_B}{\mathrm{Le}}\left[\frac{\partial\phi_1}{\partial z}\frac{\partial T_2}{\partial z}+\frac{\partial\phi_2}{\partial z}\frac{\partial T_1}{\partial z}\right]+2\frac{N_AN_B}{\mathrm{Le}}\left[\frac{\partial\phi_1}{\partial z}\frac{\partial T_2}{\partial z}\right]-\frac{\partial T_1}{\partial\tau}, && (6.5.16)\\ R_{33} &= \frac{\partial\psi_1}{\partial x}\frac{\partial\phi_2}{\partial z}-\frac{\partial\phi_1}{\partial\tau}, && (6.5.17)\\ R_{34} &= \xi Cos\left(\Omega\tau\right)\frac{\partial\psi_1}{\partial z}+\frac{\partial\psi_1}{\partial x}\frac{\partial\Phi_2}{\partial z}-\frac{\partial\Phi_1}{\partial\tau}, && (6.5.18)\end{aligned}$$

Substituting the value of $\psi_1,\ T_1,\ T_2,\ \phi_1,\phi_2,\ \Phi_1$ and Φ_2 in the above equations to get the expressions of $R_{31}, R_{32}, R_{33}, R_{34}$.

Applying the solvability condition for the existence of third order solution, the non-autonomous Ginzburg–Landau equation with time periodic coefficients is obtained in the form

$$A_1A'[\tau]+A_2A[\tau]+A_3(A[\tau])^3=0 \qquad (6.5.19)$$

where $A_1=\left(\frac{\pi^2}{Pm\delta^4}+\frac{{k_c}^2}{\delta^4}\left(1+(1+Le)^2{N_A}^2\right)-\frac{\delta^2}{Pr}\right)$

$A_2=-\left(-\frac{{k_c}^2}{\delta^2}\mathrm{Ra}_2+\frac{\pi^2}{Pm\delta^2}\left(1+Pm\ Q\delta^2\right)\xi\cos(\Omega\tau)\right)$

$A_3 = \left(\frac{{k_c}^4}{8\delta^4}\left(1+(1+Le)(1+Le+Le^2){N_A}^2\right)+\frac{\pi^4}{Pm^2\delta^4}\left(1+(\delta^2-4{k_c}^2)\right)\right)$.

The Ginzburg–Landau equation given by Eq.(6.5.19) is a non–autonomous Bernoulli equation and to obtained its solution Mathematica function NDSolve has been used, subject to the initial condition $A[0] = a_0$, where a_0 is the chosen initial amplitude of convection. It is assumed $\mathrm{Ra}_2 = \mathrm{Ra}_{0,c}$ to keep the parameters to the minimum.

6.6 Result and discussion

In the present chapter, the effect of time-periodic magnetic field on the onset of magneto-convection in a nanofluid layer is analyzed by performing linear and weakly nonlinear stability analyses. The magnetic field modulation has been used as an external regulator for the onset of magneto-convection. Magnetic field modulation with revised boundary conditions has been considered for either enhancing or inhibiting the onset of magneto-convection, and consequently, it is a tool for controlling the convective flow as required in many real life applications in various fields of sciences and engineering. The physical variables which appear in the present analysis are Ω, ξ, Pr, Pm, Q, Rn, Le and N_A. The effect of any of these parameters has been studied keeping fixed the other parameters. The parameter values are fixed as $Q = 100$, $Pm = .6$, $Pr = 1$, $Rn = 10$, $N_A = 1$ and $Le = 10$. The range of each parameter is considered as in Gupta et al. (2013) and Chand and Rana (2015), $Ra < 10^5$(thermal Rayleigh number), $4 \leq Rn \leq 15$ (nanoparticle Rayleigh number), $50 \leq Q \leq 200$ (Chandrasekhar number), $10 \leq Le \leq 300$ (Lewis number), $0.5 < N_A \leq 10$ (modified diffusivity ratio), $1 \leq Pr \leq 5$ (Prandtl number), and $0 \leq Pm \leq 1$ (magnetic Prandtl number).

If one desires to quantify heat and mass transfer in presence of modulation, one has to use nonlinear stability analysis because the linear stability analysis is not sufficient to give information regarding heat and mass transfer. Since, it is difficult to control the nanoparticle fraction at the boundaries, therefore, new set of boundary conditions have been taken by assuming that the normal component of the nanoparticle flux on boundaries is zero. This assumption is more realistic and suitable for the real world problems. In the following, the results have been discussed for each parameter involved in the system.

Frequency of modulation Ω

The Nusselt number $Nu(\tau)$ or nanoparticle concentration Nusselt number $Nu_\phi(\tau)$ with respect to time τ has been plotted for magnetic modulation. It is evident from all figures that for lower value of time τ, the values of $Nu(t)$ and $Nu_\phi(t)$ do not alter and remain almost constant. the values increase as the time τ increases and finally for the large values of τ they become oscillatory due to frequency of modulation. Also, $Nu(\tau)$ starts with value one, showing that initially the system is in conduction state. The effect of frequency of modulation is shown in Figure 6.2 and Figure 6.3 and for the increasing value of frequency of modulation heat and mass transfer decreases.

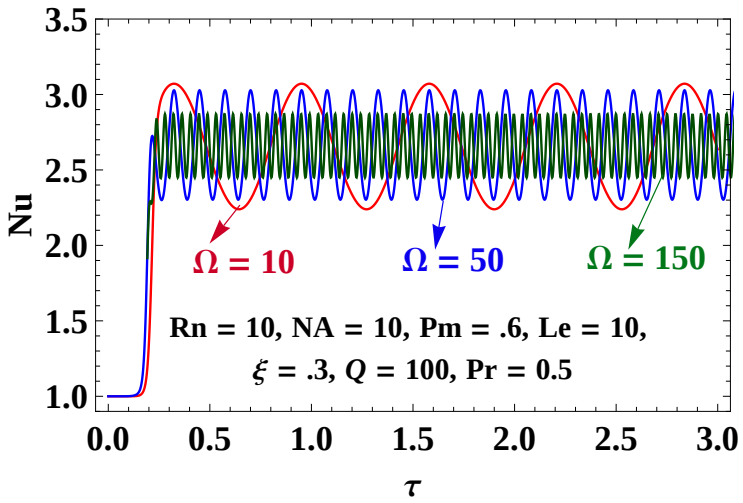

Figure 6.2: Nu versus τ for different values of Ω

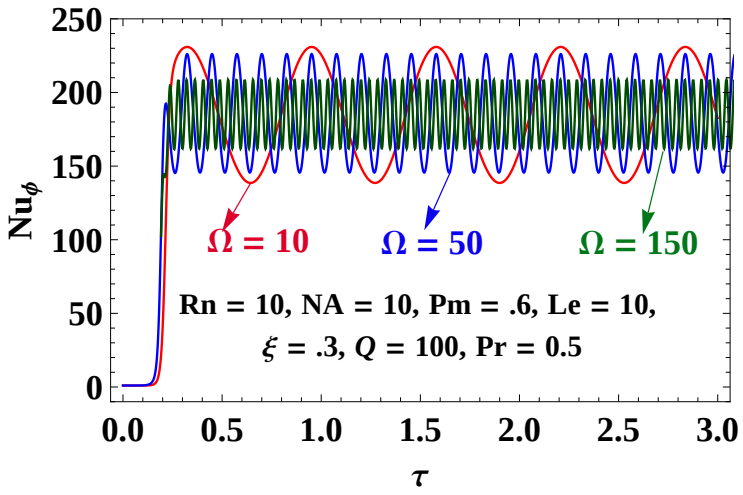

Figure 6.3: Nu_ϕ versus τ for different values of Ω

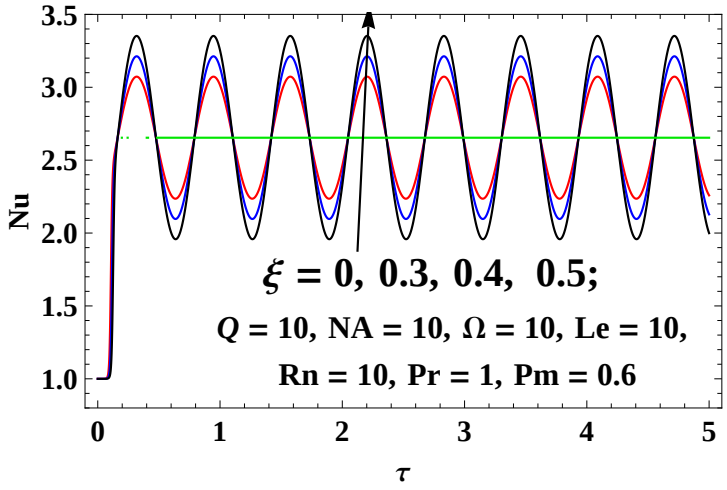

Figure 6.4: Nu versus τ for different values of ξ

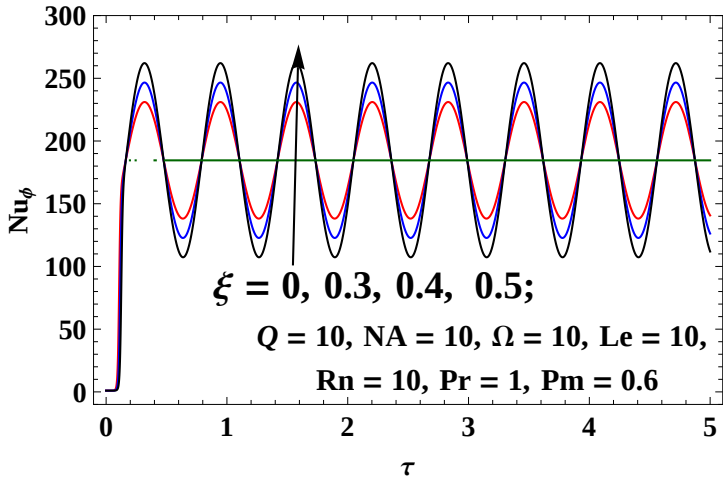

Figure 6.5: Nu_ϕ versus τ for different values of ξ

Amplitude of modulation ξ

Figure 6.4 and Figure 6.5 depict the effect of amplitude of modulation ξ, which is small in magnitude. If $\xi = 0$, the effect of modulation vanishes as shown in Figure 6.4 and Figure 6.5. However, on increasing the value of ξ concern Nusselt numbers are increasing, thus it advances the heat and mass transfer effectively.

Chandrasekhar number Q

The correction, Ra_2, in the critical thermal Rayleigh number due to magnetic field modulation in a nanofluid layer, has been depicted as function of the frequency Ω for different values of parameters. Figure 6.6 and Figure 6.7 are the plots of Ra_2 versus Ω for vari-

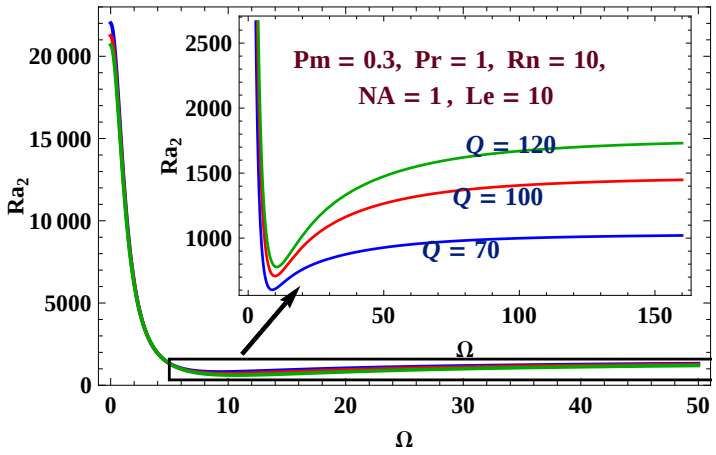

Figure 6.6: Variation of Ra_2 with Frequency Ω for different values of Q,

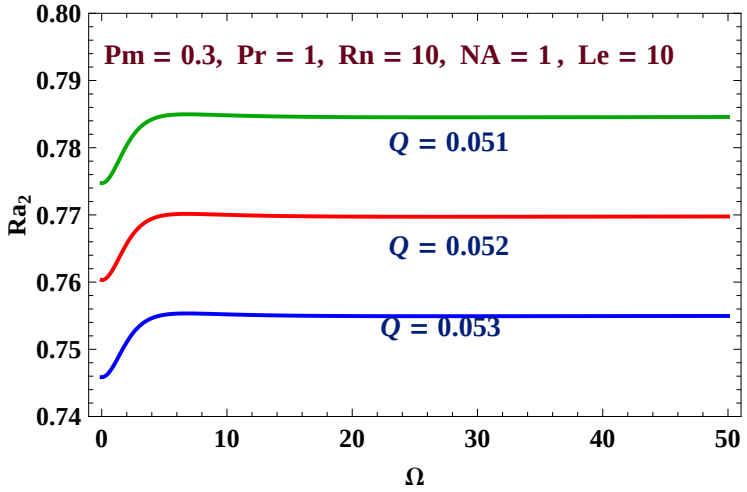

Figure 6.7: Variation of Ra_2 with Frequency Ω for different values of Q,

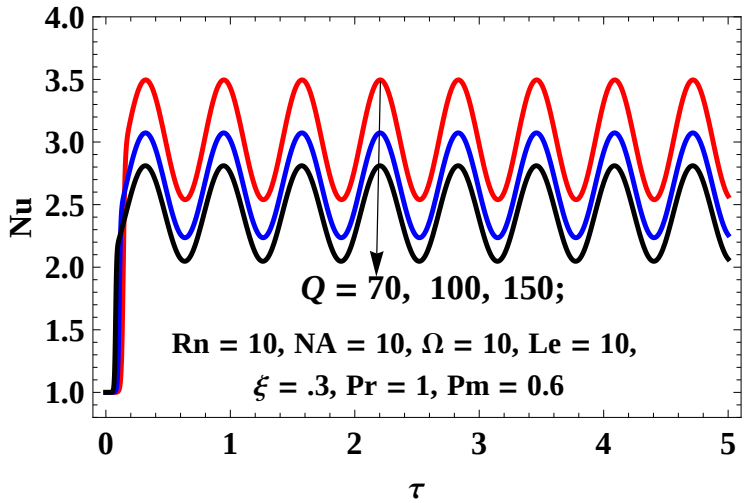

Figure 6.8: Nu versus τ for different values of Q

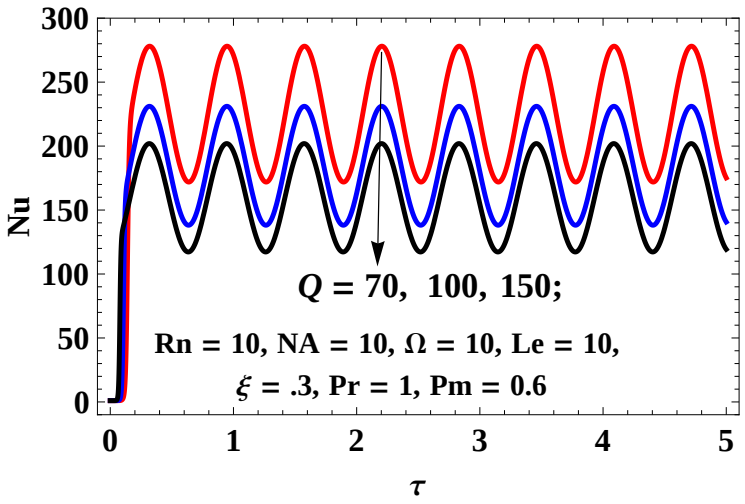

Figure 6.9: Nu_ϕ versus τ for different values of Q

ous values of Chandrasekhar number Q. It is evident from the Figure 6.6 and Figure 6.7 that the value of Ra_2 increases as Q increases whether Q is small or sufficient large, thus thermal critical Rayleigh number increases. Figure 6.8 and Figure 6.9 show the effect of Chandrashekhar number Q. It is found that on increasing value of Chandrashekhar number Nusselt numbers are decrease, thus heat/mass transfer decreases in the system. These four figures shows that the effect of Chandrasekhar number, which represents the ratio of the Lorentz force to the viscous force, on the onset of convection in a nanofluid layer is stabilizing. This happens due to the fact that the Lorentz force, which is due to the combination of electric and magnetic force, opposes the convective motion of nanofluid, thus nanofluid can not move in vertical direction as easily as without magnetic field.

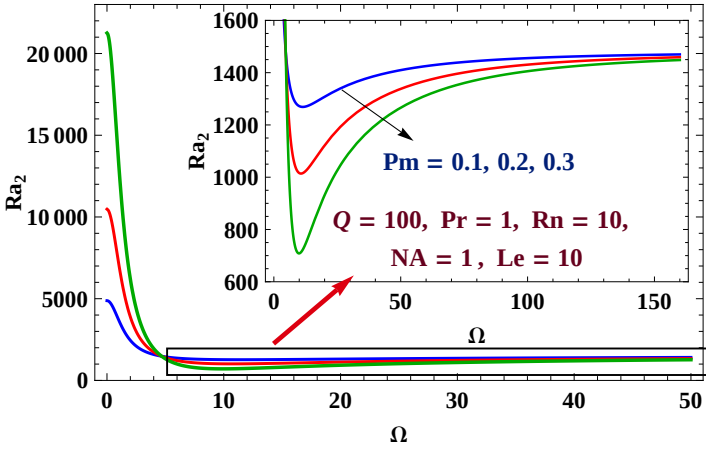

Figure 6.10: Variation of Ra_2 with Frequency Ω for different values of magnetic Pm,

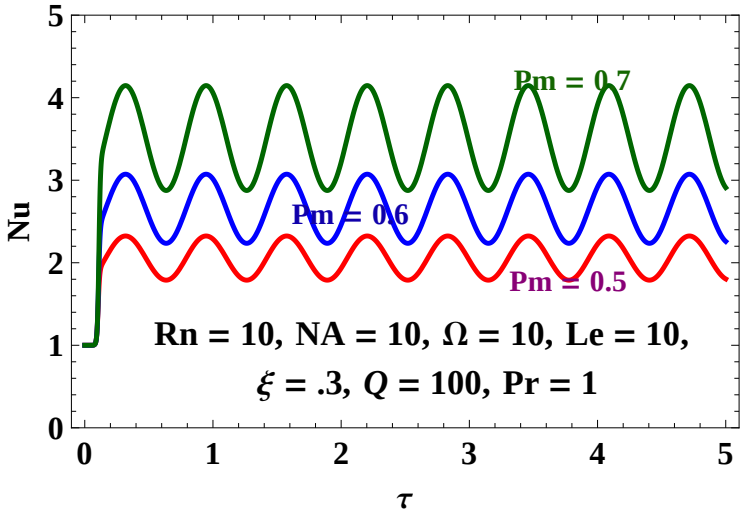

Figure 6.11: Nu versus τ for different values of magnetic Pm

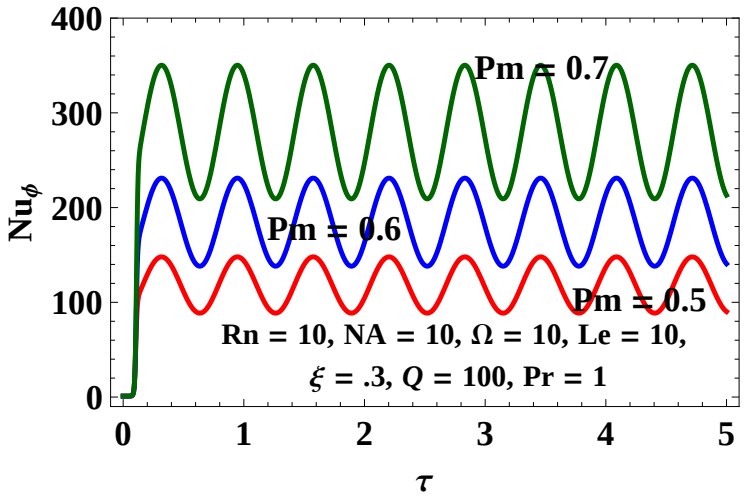

Figure 6.12: Nu_ϕ versus τ for different values of magnetic Pm

Magnetic Prandtl number Pm

Figure 6.10 is the plot of Ra_2 versus Ω for different values of magnetic Prandtl number Pm. It confirms that Ra_2 decreases as Pm increases, and so, the system will be destabilized. From Figure 6.11 and Figure 6.12, it is evident that for the increasing the value of magnetic Prandtl number Pm heat and mass transfer increases then it advances the onset of convection. It can be concluded that the effect of magnetic Prandtl number Pm, which is the ratio of viscous diffusion rate to the magnetic diffusion rate, is to enhance the heat transfer. When Pm increases, then either the viscous diffusion rate may increase or the magnetic diffusion rate may decrease and in both cases heat transfer increases.

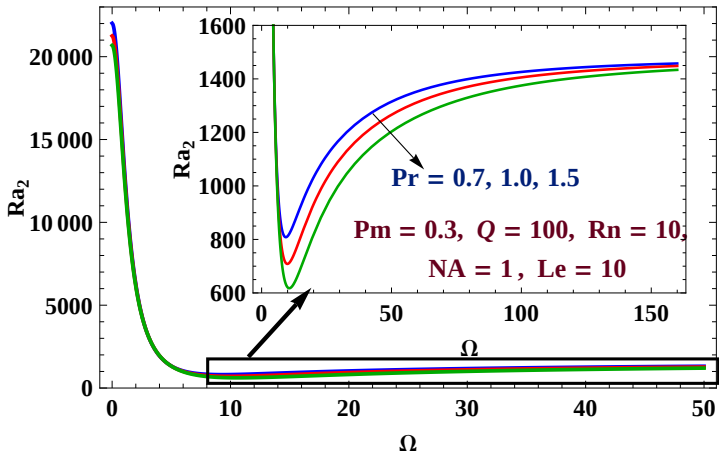

Figure 6.13: Variation of Ra_2 with Frequency Ω for different values of Pr.

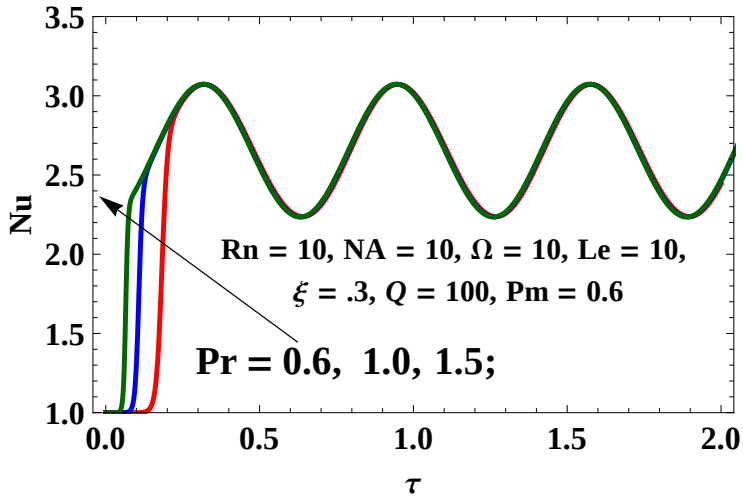

Figure 6.14: Nu versus τ for different values of Pr.

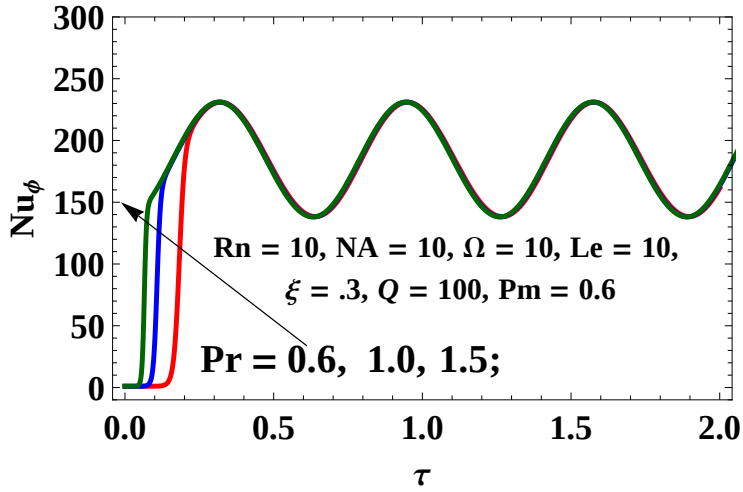

Figure 6.15: Nu_ϕ versus τ for different values of Pr.

Prandtl number Pr

It is clear from Figure 6.13 that the effect of Prandtl number Pr is similar to magnetic Prandtl number Pm, that is, Pr advances the onset of magneto-convection, thus enhances the heat transfer in the system. Values of Nusselt numbers are increasing as the value of Pr is increased, as shown in Figure 6.14 and Figure 6.15. It is observed that the effect of Prandtl number, which is ratio of kinematic viscosity and thermal diffusivity, is to enhance the heat and mass transport. It is clear that when Pr increases, then either kinematic viscosity increases or thermal diffusivity decreases, which means in both the cases that heat transfer increases. The values of Pr are taken small so as to include the time-derivative term in momentum equation. Also, it is found that there is a small variation in the values of Ra_2 in case of Prandtl number Pr.

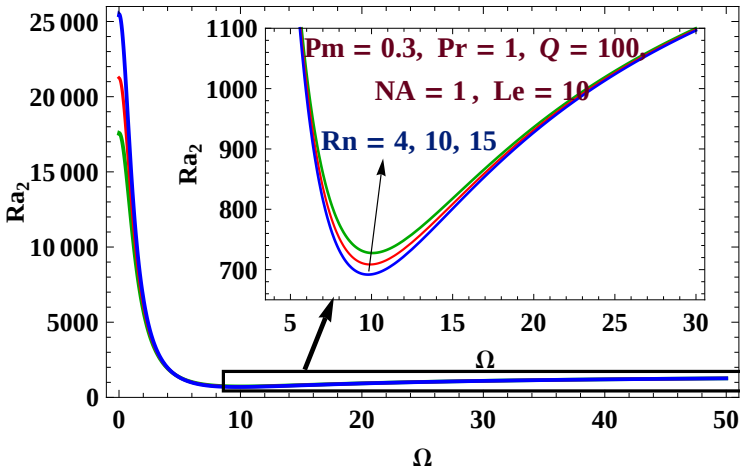

Figure 6.16: Variation of Ra_2 with Frequency Ω for different values of Rn

Nanoparticle Rayleigh number Rn

Figure 6.16 is the plot of Ra_2 versus Ω for different values of nanoparticle Rayleigh number Rn. It is found that an increment in Rn increases Ra_2, thereby stabilizing the system. Further on increasing the value of concentration Rayleigh number Rn, heat/mass transfer decreases as shown in Figure 6.17 and Figure 6.18. This means that the fluids with suspended nanoparticles are more helpful than ordinary fluids to adjust the heat transfer by modulation. Since, here it is considered the revised boundary conditions, therefore unable to determine whether system is top heavy or bottom heavy.

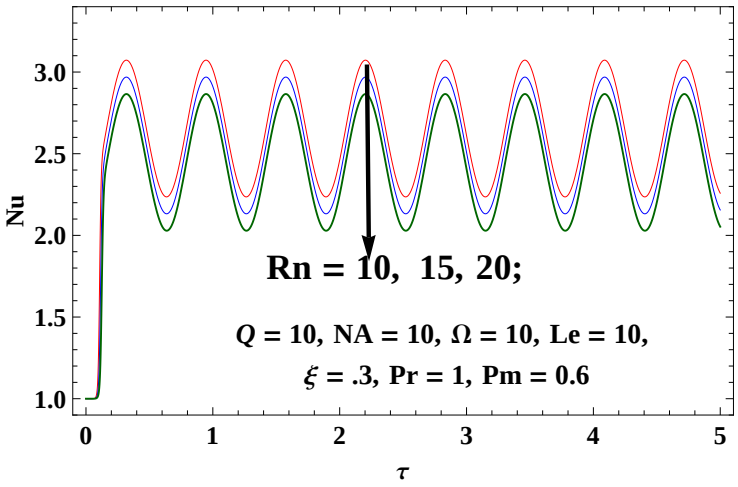

Figure 6.17: Nu versus τ for different values of Rn

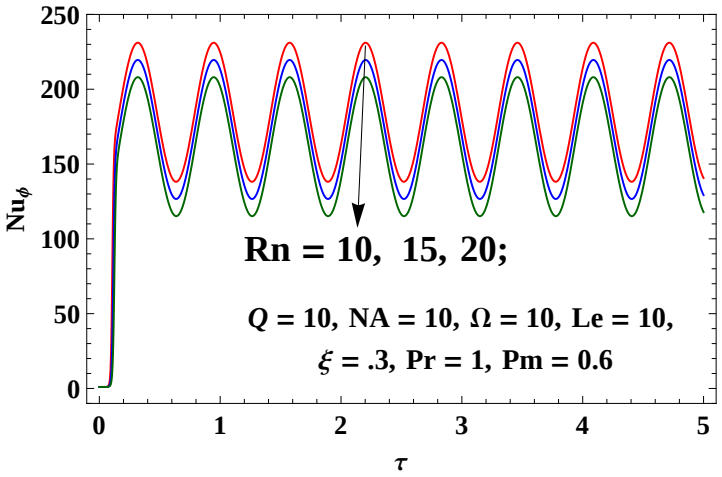

Figure 6.18: Nu_ϕ versus τ for different values of Rn

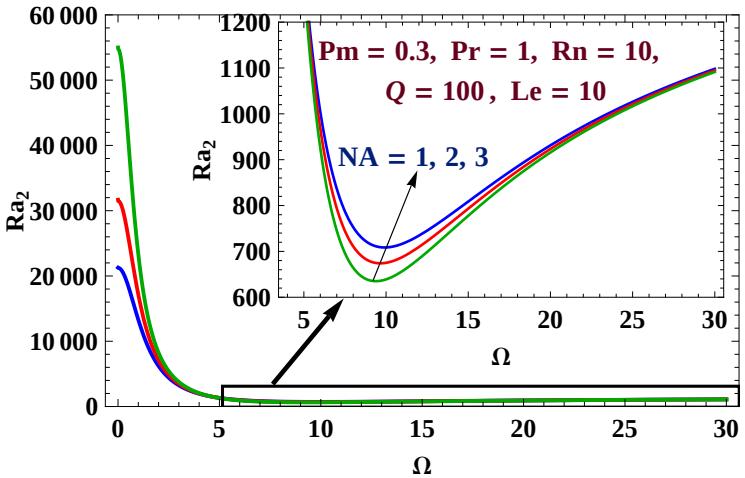

Figure 6.19: Variation of Ra_2 with Frequency Ω for different values of N_A,

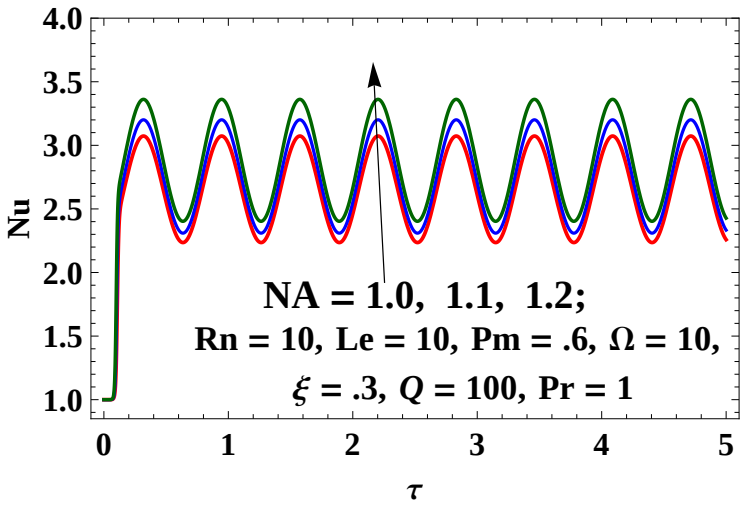

Figure 6.20: Nu versus τ for different values of N_A

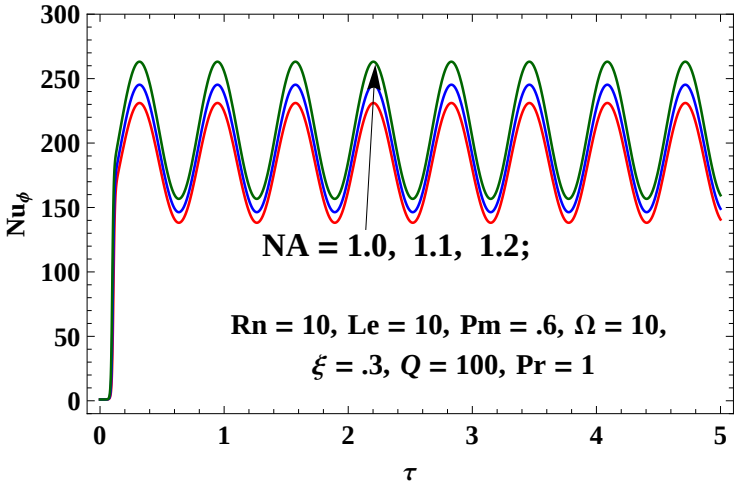

Figure 6.21: Nu_ϕ versus τ for different values of N_A

Modified diffusivity ratio N_A

Figure 6.19 shows the plot of Ra_2 versus Ω for different values of modified diffusivity ratio N_A. It is noticed that an increment in N_A signifies that thermophoresis effect will increase which means entropy of system increases. It is clear from Figure 6.19 that Ra_2 decreases as N_A increases, thus, it destabilizes the system. Same results have also been obtained from the Figure 6.20 and Figure 6.21 in case of heat and mass transfer.

Lewis number Le

For most of the nanofluids investigated so far, Lewis number is large, Gupta et. al. (2013). Figure 6.22 is the plot of Ra_2 versus Ω for different values of Lewis number Le. It is evident

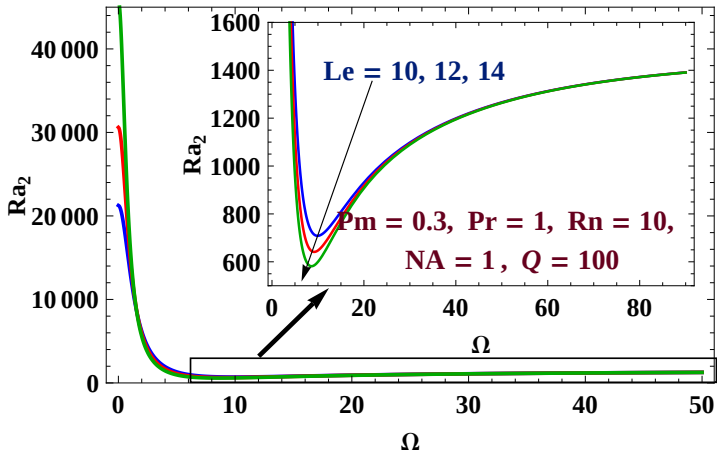

Figure 6.22: Variation of Ra_2 with Frequency Ω for different values of Le

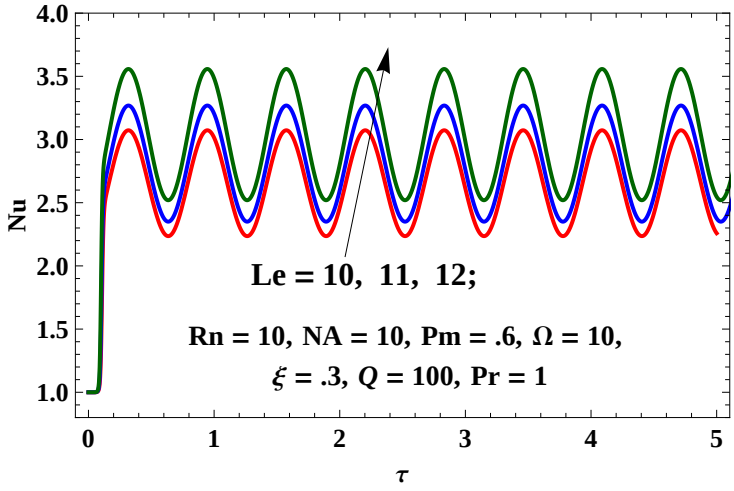

Figure 6.23: Nu versus τ for different values of Le

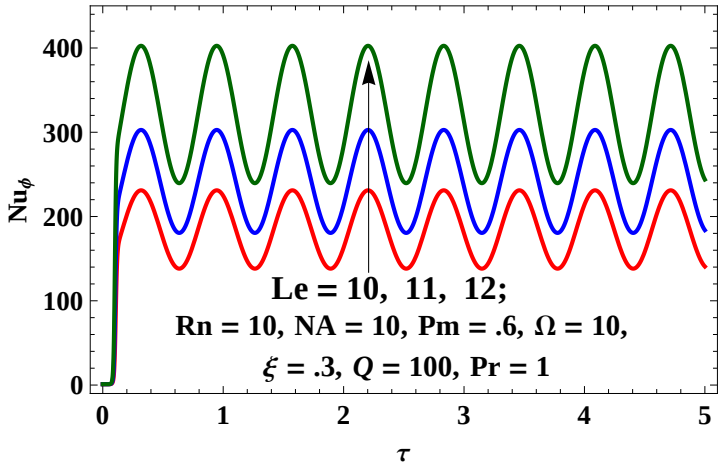

Figure 6.24: Nu_ϕ versus τ for different values of Le

that as the value of Lewis number increases, the value of Ra_2 decreases, thus it destabilizes the system and so enhances the heat transfer. Thus effect of increasing Lewis number Le

is to advance heat/mass transfer as found in Figure 6.23 and Figure 6.24. Further, it is noticed that this effect diminishes at high frequency of modulation.

6.7 Conclusion

In this chapter, magneto-convection in a horizontal nanofluid layer is studied under magnetic field modulation with more realistic boundary conditions, which incorporates the effects of Brownian motion along with thermophoresis. The results have been obtained in terms of the correction to the critical thermal Rayleigh number, thermal Nusselt number and nanoparticle concentration Nusselt number using perturbation method. The effect of various parameters have been obtained and depicted graphically. The following findings are made:

1. The magnetic modulation can be used to regulate the heat and mass transports effectively.

2. The new boundary conditions which are more realistic, have significant effect on heat and mass transport.

3. The effects of the Lewis number Le, Prandtl number Pm, modified diffusivity ratio N_A and Prandtl number Pr are to destabilize the system.

4. The effect of Chandrashekhar number Q and concentration Rayleigh number Rn are to stabilize the system.

5. The values of $Nu(t)$ and $Nu_\phi(t)$ remain almost constant for the small values of τ. The values of $Nu(t)$ and $Nu_\phi(t)$ increased as the time τ increased and finally they become oscillatory for the large values of τ.

6. Effect of magnetic field modulation is high at intermediate values of the frequency, but low at high frequencies.

Chapter 7

An analytical study of the heat transfer of nanofluid convection in an horizontal fluid layer

7.1 Introduction

Enhancement in heat transfer of conventional fluid by using nanoparticles is one of the rapidly growing research area in fluid dynamics. The impact of nanoparticles on the enhancement of convective heat transfer is its marvellous property and its importance. It is well known that by using nanoparticles the heat transfer of conventional fluid increases considerably high and suits many applications where rapid heat transportation is required. Growing technology demands high class energy efficient devices, which needs rapid heat exchangers, where nanofluids can be used as a coolant. Saidur et al. (2011) enlighten some special features of the nanofluids from the application point of view. The documented works on convective heat transfer based on the experimental and theoretical results which ensures that the efficiency of nanofluids to enhance the heat transfer are provided by Wen

This chapter is based on the research article: Study of the heat transfer of nanofluid convection in an horizontal fluid layer, Published in **International Journal of Science, Technology and Society, BBAU.** Vol 3, No. 1&2, pp. 27-39, ISSN : 2395-7395.

et al. (2009), Eastman et al. (2001), Wang and Mujumdar (2007), Daungthongsuk and Wongwises (2007), Trisaksria and Wongwises (2007), Godson et al. (2010), Kakaç and Pramuanjaroenkij (2009), Robert et al. (2013).

Natural convection between horizontal fluid layer attracts considerable interest due to its application in many engineering branches, atmospheric sciences, geophysical problems. The buoyancy induced convection arises due to temperature gradient between fluid layer with nanofluid finds its application in solar collector, nuclear reactors. The documented work in this area has been done by, Kim et al. (2004) studied the buoyancy driven instability of nanofluids using Bruggeman model, Buongiorno (2006) derived the equations for nanofluid convection and found that only Brownian diffusion and thermophoresis are important slip mechanisms in nanofluids convection, Tzou (2008a, 2008b) studied the nanofluid instability caused by natural convection and found that the critical Rayleigh number was significantly low, by one to two orders of magnitude, as compared to that for regular fluids, Nield and Kuznetsov (2010) studied the onset of convection and predicted that oscillatory convection was possible with bottom heavy nanoparticles fluid layer, Abu-Nada (2011) studied the effect of variable thermal conductivity and variable viscosity of nanofluids on heat transfer in natural convection using CuO-water nanofluids, Agarwal and Bhadauria (2015) studied the thermal instability of nanofluid layer under local thermal non-equilibrium. Recently, Nield and Kuznetsov (2014) considered a physically more realistic model for the thermal instability by taking a new set of boundary conditions, which is based on the assumption that the normal component of the nanoparticle flux on boundaries is zero. Therefore, in this chapter, an attempt has been made to study the heat transfer of nanofluid-saturated porous medium with the assumption that there is no nanoparticle flux at the boundaries, which is physically a more realistic condition.

The homotopy analysis method (HAM) is the renowned methods to solve non-linear differential equations and there is no constrains on parameters involved in governing equations. This method has been introduced by Liao in 1992. This innovative technique has been used by several authors in a field of science and engineering to solve different types of governing differential equations: linear and non-linear, This method offers highly accurate successive approximations of the solution. Some relevant studies are referred in following

references Liao (2004), Hayat et. al. (2004), Domairry and Nadim (2008).

7.2 Governing Equations

Consider an infinitely extended horizontal fluid layer saturated by nanofluid, confined between the planes $z = 0$ and $z = d$. Cartesian frame of reference has been taken with origin at the lower boundary and the z-axis in vertically upward direction. The gravitational force is acting in vertically downward direction. T_h and T_c are the lower and upper plate temperature respectively with the condition that $T_h > T_c$, T_c is taken as reference temperature. Moreover, it is assumed that there is no nanoparticle flux at the boundaries and that the particle fraction value there adjusts accordingly. Further, the density variation is considered under Boussinesq approximation. Then using the approximated buoyancy term, the governing equations under the above considerations incorporating the Brownian diffusion and thermophoresis are as follows:

$$\nabla.\mathbf{v} = 0, \tag{7.2.1}$$

$$\rho_f \left(\frac{\partial \mathbf{v}}{\partial t} + \mathbf{v}.\nabla\mathbf{v} \right) = -\nabla p + \mu\nabla^2\mathbf{v} + (\phi\rho_p + (1-\phi)\rho_f \left[1 - \beta\left(T - T_c\right)\right])\mathbf{g} \tag{7.2.2}$$

$$(\rho c)_f \left(\frac{\partial T}{\partial t} + \mathbf{v}.\nabla T \right) = \kappa\nabla^2 T + (\rho c)_p \left[D_B \nabla\phi.\nabla T + \left(\frac{D_T}{T_c} \right) \nabla T.\nabla T \right] \tag{7.2.3}$$

$$\frac{\partial \phi}{\partial t} + \mathbf{v}.\nabla\phi = D_B\nabla^2\phi + \left(\frac{D_T}{T_c} \right) \nabla^2 T, \tag{7.2.4}$$

where $\mathbf{v} = (u, v, w)$. It is assumed that the boundaries are held at constant temperature and the nanoparticle flux is zero on the boundaries therefore, the boundary conditions are taken as follows:

$$w = 0, \quad T = T_h, \quad D_B \frac{\partial \phi}{\partial z} + \frac{D_T}{T_c} \frac{\partial T}{\partial z} = 0 \quad \text{at} \quad z = 0, \tag{7.2.5}$$

$$w = 0, \quad T = T_c, \quad D_B \frac{\partial \phi}{\partial z} + \frac{D_T}{T_c} \frac{\partial T}{\partial z} = 0 \quad \text{at} \quad z = d. \tag{7.2.6}$$

Introducing the dimensionless variables by using the following transformations:

$$(x^*, y^*, z^*) = (x, y, z)/d, t^* = t\alpha_f/d^2, (u^*, v^*, w^*) = (u, v, w)d/\alpha_f \,,$$
$$T^* = (T - T_c)/(T_h - T_c), p^* = pd^2/\mu\alpha_f, \tag{7.2.7}$$
$$\phi^* = (\phi - \phi_0)/\phi_0, \alpha_f = \frac{\kappa}{(\rho c)_f}$$

where ϕ_0 is a reference scale for the nanoparticle fraction.

The nondimensionlized equations (after dropping the asterisks for simplicity) are:

$$\nabla.\mathbf{v} = 0, \tag{7.2.8}$$

$$\frac{1}{\mathrm{Pr}}\left(\frac{\partial \mathbf{v}}{\partial t} + \mathbf{v}.\nabla\mathbf{v}\right) = -\nabla p + \nabla^2\mathbf{v} - \mathrm{Rm}\hat{k} + \mathrm{Ra}T\hat{k} - \mathrm{Rn}\phi\hat{k}, \tag{7.2.9}$$

$$\frac{\partial T}{\partial t} + \mathbf{v}.\nabla T = \nabla^2 T + \left[\frac{N_B}{\mathrm{Le}}\nabla\phi.\nabla T + \frac{N_A N_B}{\mathrm{Le}}\nabla T.\nabla T\right], \tag{7.2.10}$$

$$\frac{\partial \phi}{\partial t} + \mathbf{v}.\nabla\phi = \frac{1}{\mathrm{Le}}\nabla^2\phi + \frac{N_A}{\mathrm{Le}}\nabla^2 T \tag{7.2.11}$$

$$w = 0, \quad T = 1, \quad \frac{\partial \phi}{\partial z} + N_A\frac{\partial T}{\partial z} = 0 \quad \text{at} \quad z = 0 \tag{7.2.12}$$

$$w = 0, \quad T = 0, \quad \frac{\partial \phi}{\partial z} + N_A\frac{\partial T}{\partial z} = 0 \quad \text{at} \quad z = 1. \tag{7.2.13}$$

The nondimensional parameters, which appeared in the above equations are defined as follow:

$\mathrm{Pr} = \frac{\mu}{\rho\alpha_f}$ is the Prandtl number, $\mathrm{Le} = \frac{\alpha_f}{D_B}$ is the Lewis number, $\mathrm{Ra} = \frac{\rho_{\mathrm{fo}} g\beta d^3(T_h - T_c)}{\mu\alpha_f}$ is the Rayleigh number, $\mathrm{Rm} = \frac{[\rho_p\phi_0 + \rho_{\mathrm{fo}}(1-\phi_0)]gd^3}{\mu\alpha_f}$ basic-density Rayleigh number, $\mathrm{Rn} = \frac{(\rho_p - \rho_{\mathrm{fo}})\phi_0 g d^3}{\mu\alpha_f}$ is the concentration Rayleigh number, $N_A = \frac{D_T(T_h - T_c)}{D_B T_c \phi_0}$ is the modified diffusivity ratio and $N_B = \frac{(\rho c)_p}{(\rho c)_f}\phi_0$ is the modified particle density increment.

7.2.1 Basic solution

The basic state of the nanofluid is assumed to be quiescent thus, temperature field and nanoparticle volume fraction vary in the z-direction only. This the gives basic state solution

of the form

$$u = v = w = 0, \quad T = T_b(z), \quad \phi = \phi_b(z), \tag{7.2.14}$$

satisfying the following equations

$$\frac{d^2T_b}{dz^2} + \frac{N_B}{\mathrm{Le}}\frac{d\phi_b}{dz}\frac{dT_b}{dz} + \frac{N_A N_B}{\mathrm{Le}}\left(\frac{dT_b}{dz}\right)^2 = 0, \tag{7.2.15}$$

$$\frac{d^2\phi_b}{dz^2} + N_A\frac{d^2T_b}{dz^2} = 0. \tag{7.2.16}$$

Using the boundary conditions (7.2.12–7.2.13), Eq.(7.2.16) may be integrated to give

$$\frac{d\phi_b}{dz} + N_A\frac{dT_b}{dz} = 0. \tag{7.2.17}$$

Use the Eq.(7.2.17) in the Eq.(7.2.15), to get

$$\frac{d^2T_b}{dz^2} = 0. \tag{7.2.18}$$

The solution of the Eq.(7.2.18), subject to the boundary conditions (7.2.12–7.2.13), is given by

$$T_b = 1 - z, \tag{7.2.19}$$

also the Eq.(7.2.16) has been solved subjected to the boundary conditions (7.2.12–7.2.13) using (7.2.19), it is obtained

$$\phi_b = \phi_0 + N_A z. \tag{7.2.20}$$

7.2.2 Perturbation state

Introducing the stream function ψ, eliminating the pressure term and then imposing finite amplitude perturbations on the basic quiescent state as

$$\psi = \Psi, \; T = 1 - z + \Theta \text{ and } \phi = \phi_0 + N_A z + \Phi, \tag{7.2.21}$$

the following set of equations are obtained

$$\frac{1}{\mathrm{Pr}}\left(\frac{\partial}{\partial t}\nabla^2-\nabla^4\right)\Psi+\mathrm{Ra}\frac{\partial\Theta}{\partial x}-\mathrm{Rn}\frac{\partial\Phi}{\partial x}=\frac{1}{\mathrm{Pr}}\frac{\partial\left(\Psi,\nabla^2\Psi\right)}{\partial(x,z)}, \tag{7.2.22}$$

$$\frac{\partial\Psi}{\partial x}+\left(\frac{\partial}{\partial t}-\nabla^2+\frac{N_AN_B}{\mathrm{Le}}\frac{\partial}{\partial z}\right)\Theta+\frac{N_B}{\mathrm{Le}}\frac{\partial\Phi}{\partial z}=\frac{\partial(\Psi,\Theta)}{\partial(x,z)}+\left[\frac{N_B}{\mathrm{Le}}\nabla\Phi.\nabla\Theta+\frac{N_AN_B}{\mathrm{Le}}\nabla\Theta.\nabla\Theta\right], \tag{7.2.23}$$

$$-N_A\frac{\partial\Psi}{\partial x}-\frac{N_A}{\mathrm{Le}}\nabla^2\Theta+\left(\frac{\partial}{\partial t}-\frac{1}{\mathrm{Le}}\nabla^2\right)\Phi=\frac{\partial(\Psi,\Phi)}{\partial(x,z)}. \tag{7.2.24}$$

Boundary conditions to solve Eqs.(7.2.22–7.2.24) are

$$\Psi=0,\quad \Theta=0,\quad \frac{\partial\Phi}{\partial z}+N_A\frac{\partial\Theta}{\partial z}=0\quad \text{at}\quad z=0,1 \tag{7.2.25}$$

Now the following asymptotic expansions are introduced

$$\mathrm{Ra} = \mathrm{Ra}_{0,c}+\chi^2\mathrm{Ra}_2+\chi^4\mathrm{Ra}_4+..., \tag{7.2.26}$$

$$\Psi = \chi\Psi_1+\chi^2\Psi_2+\chi^3\Psi_3+..., \tag{7.2.27}$$

$$\Theta = \chi\Theta_1+\chi^2\Theta_2+\chi^3\Theta_3+..., \tag{7.2.28}$$

$$\Phi = \chi\Phi_1+\chi^2\Phi_2+\chi^3\Phi_3+..., \tag{7.2.29}$$

where $\mathrm{Ra}_{0,c}$ is the critical value of the Rayleigh number at which the onset of convection takes place.

It is assumed that the variation of time is only at the slow time scale, $\tau=\chi^2t$ so the systems has been arranged at different orders of χ.

At the lowest order,

$$\begin{pmatrix} -\nabla^4 & \mathrm{Ra}_{0,c}\frac{\partial}{\partial x} & -\mathrm{Rn}\frac{\partial}{\partial x} \\ \frac{\partial}{\partial x} & \left(-\nabla^2+\frac{N_AN_B}{\mathrm{Le}}\frac{\partial}{\partial z}\right) & \frac{N_B}{\mathrm{Le}}\frac{\partial}{\partial z} \\ -N_A\frac{\partial}{\partial x} & -\frac{N_A}{\mathrm{Le}}\nabla^2 & -\frac{1}{\mathrm{Le}}\nabla^2 \end{pmatrix}\begin{pmatrix}\Psi_1\\ \Theta_1\\ \Phi_1\end{pmatrix}=0. \tag{7.2.30}$$

The solution at the lowest order subject to the boundary conditions (7.2.25), are given by

$$\Psi_1 = A[\tau]\mathrm{Sin}\,(\alpha_c x)\,\mathrm{Sin}(\pi z), \tag{7.2.31}$$

$$\Theta_1 = -\frac{\alpha_c}{\delta^2}A[\tau]\ \mathrm{Cos}\,(\alpha_c x)\,\mathrm{Sin}(\pi z), \tag{7.2.32}$$

$$\Phi_1 = \frac{\alpha_c N_A}{\delta^2}A[\tau]\ \mathrm{Cos}\,(\alpha_c x)\,\mathrm{Sin}(\pi z), \tag{7.2.33}$$

where $\delta^2 = \alpha_c^2 + \pi^2$ and α_c is the critical wave number.

The expression for thermal Rayleigh number is given by

$$\mathrm{Ra} = \frac{\delta^6}{\alpha^2} - N_A\mathrm{Rn}(\mathrm{Le}+1), \tag{7.2.34}$$

where α is the wave number.

The critical value of the Rayleigh number and the corresponding wave number for the onset of stationary convection is calculated numerically and the expression for critical Rayleigh number is given by

$$\mathrm{Ra}_{0,c} = \frac{\delta^6}{{\alpha_c}^2} - N_A\mathrm{Rn}(\mathrm{Le}+1), \tag{7.2.35}$$

and the critical wave number is $\alpha_c = \frac{\pi}{\sqrt{2}}$.

7.3 Amplitude equation and Heat and Mass Transport for Stationary Instability

At the second order

$$\begin{pmatrix} -\nabla^4 & \mathrm{Ra}_{0,c}\frac{\partial}{\partial x} & -\mathrm{Rn}\frac{\partial}{\partial x} \\ \frac{\partial}{\partial x} & -\nabla^2 + \frac{N_A N_B}{\mathrm{Le}}\frac{\partial}{\partial z} & \frac{N_B}{\mathrm{Le}}\frac{\partial}{\partial z} \\ -N_A\frac{\partial}{\partial x} & -\frac{N_A}{\mathrm{Le}}\nabla^2 & -\frac{1}{\mathrm{Le}}\nabla^2 \end{pmatrix} \begin{pmatrix} \Psi_2 \\ \Theta_2 \\ \Phi_2 \end{pmatrix} = \begin{pmatrix} R_{21} \\ R_{22} \\ R_{23} \end{pmatrix}, \tag{7.3.1}$$

where

$$R_{21} = 0, \tag{7.3.2}$$

$$R_{22} = \frac{-{\alpha_c}^2\pi}{2\delta^2}A[\tau]^2\mathrm{Sin}(2\pi z) - \frac{\pi{\alpha_c}^2 N_A N_B}{2\delta^4}\left({\alpha_c}^2\mathrm{Sin}^2(\alpha_c x)\,\mathrm{Sin}^2(\pi z) + \pi^2\mathrm{Cos}^2(\alpha_c x)\mathrm{Cos}^2(\pi z)\right)A[\tau]^2, \tag{7.3.3}$$

$$R_{23} = \frac{\pi{\alpha_c}^2 N_A}{2\delta^2}A[\tau]^2\mathrm{Sin}(2\pi z). \tag{7.3.4}$$

The second order solution subject to the boundary conditions (7.2.25), are given by

$$\Psi_2 = 0, \tag{7.3.5}$$

$$\Theta_2 = \frac{-{\alpha_c}^2}{8\pi\delta^2}A[\tau]^2\mathrm{Sin}(2\pi z), \tag{7.3.6}$$

$$\Phi_2 = \frac{{\alpha_c}^2 N_A \mathrm{Le}}{8\pi\delta^2}\left((\mathrm{Le}+1)+\frac{1}{\mathrm{Le}}\right)A[\tau]^2\mathrm{Sin}(2\pi z). \tag{7.3.7}$$

The horizontally averaged Nusselt number and Sherwood number, Nu and Nu^{Φ}, for stationary mode of convection (the mode considered in this problem) is given by:

$$\mathrm{Nu}[\tau] = \frac{\left[\frac{\alpha_c}{2\pi}\int_0^{\frac{2\pi}{\alpha_c}}(1-z+\Theta_2)_z\,dx\right]_{z=0}}{\left[\frac{\alpha_c}{2\pi}\int_0^{\frac{2\pi}{\alpha_c}}(1-z)_z\,dx\right]_{z=0}}, \tag{7.3.8}$$

$$\mathrm{Nu}_{\Phi}[\tau] = \frac{\left[\frac{\alpha_c}{2\pi}\int_0^{\frac{2\pi}{\alpha_c}}(\phi_0+N_A z+\Phi_2)_z\,dx\right]_{z=0}}{\left[\frac{\alpha_c}{2\pi}\int_0^{\frac{2\pi}{\alpha_c}}(\phi_0+N_A z)_z\,dx\right]_{z=0}}. \tag{7.3.9}$$

Substituting expressions of Θ_2 and Φ_2 in the above Eqs.(7.3.8 and 7.3.9) and simplifying, it is obtained

$$\mathrm{Nu}[\tau] = 1+\frac{\alpha_c^2}{4\delta^2}(A[\tau])^2, \tag{7.3.10}$$

$$\mathrm{Nu}_{\Phi}[\tau] = 1+\left(\frac{{\alpha_c}^2\mathrm{Le}}{4\delta^2}\left((\mathrm{Le}+1)+\frac{1}{\mathrm{Le}}\right)\right)(A[\tau])^2. \tag{7.3.11}$$

At the third order

$$\begin{pmatrix} -\nabla^4 & \mathrm{Ra}_{0,c}\frac{\partial}{\partial x} & -\mathrm{Rn}\frac{\partial}{\partial x} \\ \frac{\partial}{\partial x} & -\nabla^2+\frac{N_A N_B}{\mathrm{Le}}\frac{\partial}{\partial z} & \frac{N_B}{\mathrm{Le}}\frac{\partial}{\partial z} \\ -N_A\frac{\partial}{\partial x} & -\frac{N_A}{\mathrm{Le}}\nabla^2 & -\frac{1}{\mathrm{Le}}\nabla^2 \end{pmatrix}\begin{pmatrix}\Psi_3\\ \Theta_3\\ \Phi_3\end{pmatrix} = \begin{pmatrix}R_{31}\\ R_{32}\\ R_{33}\end{pmatrix} \tag{7.3.12}$$

where

$$R_{31} = -\frac{1}{\mathrm{Pr}}\frac{\partial}{\partial\tau}\left(\nabla^2\Psi_1\right) - \mathrm{Ra}_2\frac{\partial\Theta_1}{\partial x}, \tag{7.3.13}$$

$$R_{32} = \frac{\partial\Psi_1}{\partial x}\frac{\partial\Theta_2}{\partial z} + \frac{N_B}{\mathrm{Le}}\left\{\frac{\partial\Phi_1}{\partial z}\frac{\partial\Theta_2}{\partial z} + \frac{\partial\Phi_2}{\partial z}\frac{\partial\Theta_1}{\partial z}\right\} + 2\frac{N_A N_B}{\mathrm{Le}}\left\{\frac{\partial\Phi_1}{\partial z}\frac{\partial\Theta_2}{\partial z}\right\} - \frac{\partial\Theta_1}{\partial\tau}, \tag{7.3.14}$$

$$R_{33} = \left\{\frac{\partial\Psi_1}{\partial x}\frac{\partial\Phi_2}{\partial z}\right\} - \frac{\partial\Phi_1}{\partial\tau}, \tag{7.3.15}$$

Substituting the value of $\Psi_1, \Theta_1, \Theta_2, \Phi_1$ and Φ_2 in the above equations to get the expressions of R_{31}, R_{32}, R_{33}.

Applying the solvability condition for the existence of third order solution, the Ginzburg–Landau equation with constant coefficients has been obtained in of the form

$$a_1 A'[\tau] + a_2 A[\tau] + a_3 (A[\tau])^3 = 0 \tag{7.3.16}$$

where

$a_1 = \frac{\delta^2}{\mathrm{Pr}} + \frac{{\alpha_c}^2}{\delta^4}\left(\mathrm{Ra}_{0,c} + \mathrm{Rn}N_A\right) + \frac{{\alpha_c}^2}{\delta^4}\mathrm{LeRn}N_A(\mathrm{Le}+1),$

$a_2 = -\frac{{\alpha_c}^2}{\delta^2}\mathrm{Ra}_2$

$a_3 = \frac{{\alpha_c}^4}{8\delta^4}\left(\mathrm{Ra}_{0,c} + \mathrm{Rn}N_A\right) + \left(\frac{{\alpha_c}^4 N_A \mathrm{Le}}{8\delta^4}\right)\ \mathrm{LeRn}\left((\mathrm{Le}+1) + \frac{1}{\mathrm{Le}}\right).$

The Ginzburg–Landau equation given by Eq.(7.3.16) is a Bernoulli equation and to obtained its solution HAM method has been employed, under subject to the initial condition $A[0] = a_0$, where a_0 is the chosen initial amplitude of convection. In the calculations, $\mathrm{Ra}_2 = \mathrm{Ra}_{0,c}$ has been assumed to keep the parameters to the minimum.

7.4 Method Description

Assume the following non-linear differential equation in the form of

$$N\left[A(t)\right] = 0 \tag{7.4.1}$$

where N is a non-linear operator, t is an independent variable and $A(t)$ is the solution of equation. A function, $\varphi(t,q)$ is defined as follow.

$$\lim_{q\to 0}\varphi(t,q) = A_0(t) \tag{7.4.2}$$

where, $q : [0,1]$ and $A_0(t)$ is the initial guess which satisfies initial or boundary conditions and

$$\lim_{q\to 1}\varphi(t,p) = A(t) \tag{7.4.3}$$

Now by using the generalized homotopy method, Liao's so-called zero-order deformation (Eq.(7.4.1)) is

$$(1-q)L\left[\varphi(t,q) - A_0(t)\right] = qhN\left[\varphi(t,q)\right] \tag{7.4.4}$$

where h is the auxiliary parameter which helps in increasing the convergence of the results, L is the linear operator. It should be noted that there is a great freedom to choose the auxiliary parameter h, the initial guess $A_0(t)$ and the auxiliary linear operator L. This freedom plays an important role in establishing the keystone of validity and flexibility of HAM as shown in this chapter. Thus, when q increases from 0 to 1, the solution $\varphi(t,q)$ changes between the initial guess $A_0(t)$ and the solution $A(t)$ The Taylor series expansion of $\varphi(t,q)$ with respect to q is

$$\varphi(t,q) = A_0(t) + \sum_{m=i}^{+\infty} A_m(t)q^m \tag{7.4.5}$$

and

$$A_0^{[m]}(t) = \frac{\partial^m\varphi(t,q)}{\partial q^m}|_{q=0} \tag{7.4.6}$$

where $A_0^{[m]}(t)$ for briefly is called the mth-order of deformation derivation which reads

$$A_m(t) = \frac{A_0^{[m]}(t)}{m!} = \frac{1}{m!}\frac{\partial^m\varphi(t,q)}{\partial q^m}|_{q=0} \tag{7.4.7}$$

Indeed, in homotopy analysis method(HAM) the non-linear differential equation is solved by separating any Taylor expansion term. Now, the vector is defined as

$$\vec{A_m} = \{\vec{A_1}, \vec{A_2}, \vec{A_3}, ..., \vec{A_n}\} \tag{7.4.8}$$

According to the definition in Eq.(7.4.7), the governing equation and corresponding initial conditions of $A_m(t)$ can be deduced from zero-order deformation [Eq.(7.4.1)]. Differentiating Eq.(7.4.1) m times with respect to the embedding parameter q and setting $q = 0$ and finally dividing by $m!$, will give the so called mth-order deformation equation in the form:

$$L\left[A_m(t) - \chi_m A_{m-1}(t)\right] = hR\left(A_{m-1}\right) \tag{7.4.9}$$

where $R\left(A_{m-1}\right) = \frac{1}{(m-1)!}\frac{\partial^{m-1}N[\varphi(t,q)]}{\partial q^{m-1}}|_{q=0}$

and

$$\chi_m = \begin{cases} 0 & m \leq 1 \\ 1 & m > 1 \end{cases}$$

So by applying inverse linear operator to both sides of the linear equation, Eq.(7.4.1), one can easily solve the equation and compute the generation constant by applying the boundary condition.

7.5 Application

$$A'(t) = Q_1 A(t) - Q_2 A(t)^3 \tag{7.5.1}$$

where $Q_1 = -\frac{a_2}{a_1}$ and $Q_2 = \frac{a_3}{a_1}$ according to nature of the GL equation, the initial solution may be taken in the form:

$$A_0(t) = c_1 + (a_0 - c_1)e^{\gamma t} \tag{7.5.2}$$

where $c_1 = \sqrt{\frac{Q_1}{Q_2}}$ and γ is as yet unspecified. The determination of γ can and will be dealt with at the time of seeking a series solution of the GL equation with a time-periodic coefficient. Quite obviously $A_0(t)$ has been so chosen that it satisfies the conditions $A_0(\infty) = c_1$ and $A_0(0) = a_0$. The choice of the form of $A_0(t)$ is most important in obtaining a

convergent series solution by HAM. Now introducing two notations to obtain the series solution of GL equation by HAM.

$$L[A(t)] = A'(t) + \gamma A(t) \tag{7.5.3}$$

$$N[A(t)] = A'(t) - Q_1 A(t) + Q_2 A(t)^3 \tag{7.5.4}$$

The required equation for $\varphi(t,q)$ can be constructed using $L[A(t)]$ and $N[A(t)]$. Also it is to be reminded at this point that $\varphi(t,q)$ varies from $A_0(t)$ to $A_{NL}(t)$ as q varies from 0 to 1. The required equation is as follows:

$$(1-q)L[\varphi(t,q) - A_0(t)] = qhN[\varphi(t,q)] \tag{7.5.5}$$

where h is a convergence-control parameter. Eq.(7.5.5) and $\varphi(t,0) = a_0$ are called the zeroth-order deformation equations. Now, in order to obtain the q-derivatives of $\varphi(t,q)$, differentiate m-times the zeroth-order deformation equations with respect to q. To make use of the notation $A_m(t)$ defined in Eq.(7.4.7) set $q = 0$ in the resulting equations and also divide by $m!$. The above procedure results in the following infinite system of linear equations:

$$L[A_m(t) - \chi_m A_{m-1}(t)] = hR_m\left(\tilde{A}_m(t)\right) \tag{7.5.6}$$

subject to the initial condition

$$A_m(0) = 0, \quad (m = 1, 2, 3....) \tag{7.5.7}$$

$$\tilde{A}_m(t) = \{A_0(t), A_1(t), A_2(t), A_3(t), ..., A_{m-1}(t)\}, m \geq 0 \tag{7.5.8}$$

and

$$R\left[\tilde{A}_{m-1}(t)\right] = A'_{m-1}(t) - Q_1 A_{m-1}(t) + Q_2 \sum_{k=0}^{m-1} A_{m-1-k}(t) \sum_{j=0}^{k} A_{k-j}(t) A_j(t), \quad (m = 1, 2, 3....) \tag{7.5.9}$$

After some simplification get recurrence relation as

$$A_m(t) = \chi_m A_{m-1}(t) + he^{-\gamma t} \int_0^t e^{\gamma\tau} R\left[\tilde{A}_{m-1}(\tau)\right] d\tau \tag{7.5.10}$$

In fact, the solution of Eq.(7.5.10) may be obtained with the aid of Mathematica. Some iterative solution are as follows.

$$\begin{aligned}
A_1(t) = {} & \frac{1}{2\gamma} e^{-3\gamma t} h \left\{ -\left(a_0 - c_1\right)^3 Q_2 - 6\left(a_0 - c_1\right)^2 c_1 e^{\gamma t} Q_2 + 2c_1 e^{3\gamma t}\left(-Q_1 + c_1^2 Q_2\right) + \right. \\
& \left. e^{2\gamma t}\left(2c_1 Q_1 + a_0^3 Q_2 + 3c_1\left(a_0^2 - 3a_0 c_1 + c_1^2\right) Q_2 - 2\left(a_0 - c_1\right)\gamma\left(\gamma + Q_1 - 3c_1^2 Q_2\right) t\right)\right\}
\end{aligned} \tag{7.5.11}$$

$$\begin{aligned}
A_2(t) = {} & \frac{1}{2\gamma} e^{-3\gamma t}\left\{ -\left(a_0 - c_1\right)^3 Q_2 - 6\left(a_0 - c_1\right)^2 c_1 e^{\gamma t} Q_2 + 2c_1 e^{3\gamma t}\left(-Q_1 + c_1^2 Q_2\right) + \right. \\
& \left. e^{2\gamma t}\left(2c_1 Q_1 + a_0^3 Q_2 + 3c_1\left(a_0^2 - 3a_0 c_1 + c_1^2\right) Q_2 - 2\left(a_0 - c_1\right)\gamma\left(\gamma + Q_1 - 3c_1^2 Q_2\right) t\right)\right\} h + \\
& \frac{1}{2} e^{-\gamma t}\left\{ \frac{\left(3\left(a_0 - c_1\right)^5\left(e^{-4\gamma t} - 1\right) Q_2^2\right)}{4\gamma^2} + \frac{\left(8\left(a_0 - c_1\right)^4 c_1\left(e^{-3\gamma t} - 1\right) Q_2^2\right)}{\gamma^2} + \right. \\
& \frac{6\left(a_0 - c_1\right) c_1 Q_2\left(-2a_0 Q_1 + 4c_1 Q_1 + a_0^3 Q_2 + 3a_0^2 c_1 Q_2 - 5a_0 c_1^2 Q_2 - c_1^3 Q_2\right)}{\gamma^2} + \\
& \frac{\left(a_0 - c_1\right)^2 Q_2\left(-2a_0 Q_1 + 8c_1 Q_1 + 3a_0^3 Q_2 + 9a_0^2 c_1 Q_2 - 57a_0 c_1^2 Q_2 + 39c_1^3 Q_2\right)}{2\gamma^2} - \\
& \frac{2c_1\left(e^{\gamma t} + 1\right)\left(Q_1^2 - 4c_1^2 Q_1 Q_2 + 3c_1^4 Q_2^2\right)}{\gamma^2} - \frac{1}{\gamma}\left(a_0^3 Q_2\left(\gamma + Q_1 - 3c_1^2 Q_2\right) + \right. \\
& 3a_0^2 c_1 Q_2\left(\gamma + Q_1 - 3c_1^2 Q_2\right) + c_1\left(-2\gamma^2 + 2Q_1^2 + 9c_1^2\gamma Q_2 - 15c_1^2 Q_1 Q_2 + 3c_1^4 Q_2^2\right) + \\
& \left. a_0\left(2\gamma^2 + \gamma\left(2Q_1 - 15c_1^2 Q_2\right) + 3c_1^2 Q_2\left(Q_1 + 5c_1^2 Q_2\right)\right)\right) t + \left(a_0 - c_1\right)\left(\gamma + Q_1 - 3c_1^2 Q_2\right)^2 t^2 + \\
& \left(1/\left(2\gamma^2\right)\right)\left(a_0 - c_1\right)^2 e^{-2\gamma t} Q_2\left(2a_0 Q_1 - 8c_1 Q_1 - 3a_0^3 Q_2 - 9a_0^2 c_1 Q_2 + 57a_0 c_1^2 Q_2 - 39c_1^3 Q_2\right. \\
& - 6\left(a_0 - c_1\right)\gamma\left(-\gamma - Q_1 + 3c_1^2 Q_2\right) t) + \left(1/\gamma^2\right) 6\left(a_0 - c_1\right) c_1 e^{-\gamma t} Q_2\left(2a_0 Q_1 - 4c_1 Q_1\right. \\
& \left. \left. - \; a_0^3 Q_2 - 3a_0^2 c_1 Q_2 + 5a_0 c_1^2 Q_2 + c_1^3 Q_2 - 2\left(a_0 - c_1\right)\gamma\left(-\gamma - Q_1 + 3c_1^2 Q_2\right) t\right)\right\} h^2
\end{aligned} \tag{7.5.12}$$

Other iterative solution were too long to be mentioned here, therefore, results are demonstrated graphically.

To determine an appropriate h, define a residual error in the form:

$$E_R(h) = \frac{1}{t_0}\int_0^{t_0} \left[A'(t) - Q_1 A(t) + Q_2 A(t)^3\right]^2 dt \tag{7.5.13}$$

where t_0 is time domain in which one wants to capture the error. The value of h is chosen in such a way, that error $E_R(h)$ is going to be minimum. Here, it is notice that h is a helpful parameter that influences the rate of convergence of the HAM solution but the convergent solution is independent of the choice of h , as proved by Liao (2009).

mth-order HAM solution can be written in the following form

$$A^m_{NL}(t) = \sum_{i=0}^{m} A_m(t), \quad m = 1, 2, 3..... \tag{7.5.14}$$

7.6 Results and Discussions

weakly nonlinear stability analysis for heat transfer has been performed in a horizontal nanofluid layer. The effects of Lewis number, modified thermophoresis to Brownian-motion diffusivity ratio, concentration Rayleigh number and Prandtl number on the heat transport has been obtained. Using power series expansion in terms of perturbation parameter, which is assumed to be small, the problem has been studied using the Ginzburg-Landau amplitude equation. Such an assumption will help in obtaining the amplitude equation of convection in a rather simple and elegant manner and is much easier to obtain than in the case of the Lorenz model. Obtained Ginzburg-Landau equation has been solved by using Homotopy Analysis Metohod considering fifteen terms.

From the expression of Rn, it is observed that Rn is defined as a typical nanofluid fraction instead of the difference of two fractions so that, Rn cannot be negative, the modified diffusion ratio N_A is positive, moreover, it is not necessary to take large values of Le. As there is no longer two opposing agencies which affect the instability, therefore, the oscillatory instability is not possible. One can observe that the solution of first order, second order and the Ginzburg-Landau equation is independent of modified particle-density increment N_B, therefore heat transfer is unaffected by modified particle-density increment

N_B, this happens due to orthogonality of the solution of the trial functions.

If one wants to quantify heat and mass transfer, which linear stability analysis is unable to do, this problem needs to perform the nonlinear analysis and hence the importance, thus the need for nonlinear stability analysis is justified.

It is difficult to control the nanoparticle fraction at the boundaries therefore, consider new set of boundary conditions are considered assuming that the normal component of the nanoparticle flux on boundaries is zero, such an assumption can be taken as more realistic and suits the real world problem. It is important to study the effect of nanoparticle concentration and modified diffusion ratio in nanofluid convection in fluid layer. The objective of this study is to consider nanoparticle concentration and modified diffusion ratio for either enhancing or inhibiting convective heat transport as is required by the real application.

At the critical wave number, the Eq.(7.2.35) can be expressed as

$$\mathrm{Ra}_{0,c} + N_A \mathrm{Rn}(\mathrm{Le}+1) = \frac{27\pi^4}{4}, \tag{7.6.1}$$

The Eq.(7.6.1) can be taken as a useful upper bound for the value of critical Rayleigh number in case of stationary convection.

Figures 7.1-7.4 show the effect of parameters on the heat transport. Initially, the value of Nusselt number is one, which shows that the heat transfer is by conduction alone and as time increases, the value of Nusselt number increases showing that the heat transport is effected by convection, Further more, after reaching a fixed value there is no change in the magnitude of Nusselt number with respect to time, showing the saturation state for heat transfer. Figures 7.1-7.4 show the effect of parameters on the heat transport for the base fluid, while Figures 7.5-7.8 show the effect of parameters on the heat transport for the nanoparticles. Values of the parameters are fixed at $\mathrm{Pr} = 1$, $\mathrm{Rn} = 1$, $N_A = 0.7$ and $\mathrm{Le} = 100$, except for the varying one.

Following results have been found from Figures 7.1-7.4 for the heat transport for base fluid

1. $[\mathrm{Nu}]_{N_A=0.9} < [\mathrm{Nu}]_{N_A=0.8} < [\mathrm{Nu}]_{N_A=0.7}$.

2. $[\mathrm{Nu}]_{Rn=1.2} < [\mathrm{Nu}]_{Rn=1.1} < [\mathrm{Nu}]_{Rn=1}$.

3. $[\mathrm{Nu}]_{Le=120} < [\mathrm{Nu}]_{Le=110} < [\mathrm{Nu}]_{Le=100}$.

4. $[\mathrm{Nu}]_{Pr=0.1} < [\mathrm{Nu}]_{Pr=0.2} < [\mathrm{Nu}]_{Pr=0.3}$.

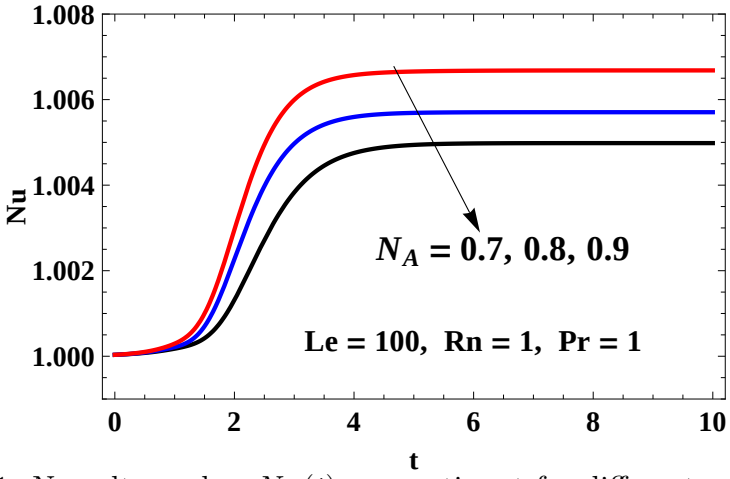

Figure 7.1: Nusselt number $Nu(t)$ versus time t for different values of N_A

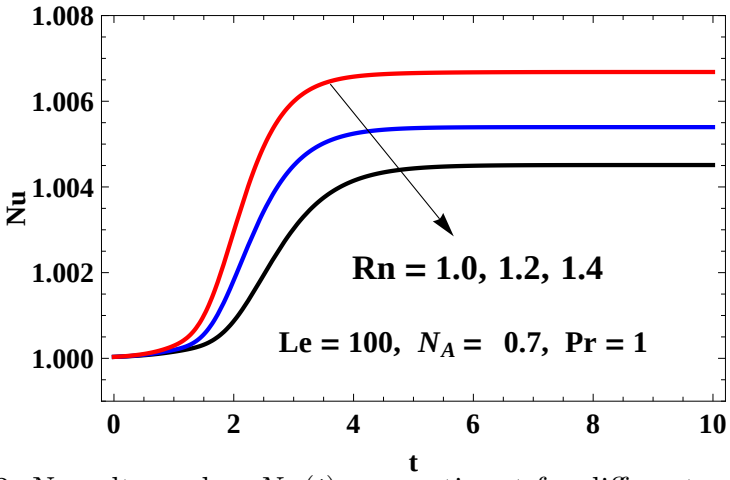

Figure 7.2: Nusselt number $Nu(t)$ versus time t for different values of Rn

The above results can be interpreted as, Figure 7.1 shows the effect of modified thermophoresis to Brownian-motion diffusivity ratio. It is is observed from the graph that on increasing the of values N_A heat transfer decreases. From figure 7.2, It is observe that for increasing values of concentration Rayleigh number heat transfer decreases. The effect of Lewis number is shown in Figure 7.3. It is found that on increasing value of Lewis number heat transfer decreases. Further, in Figure 7.4, the effect of Pr on Nu[τ] is felt only at small time.

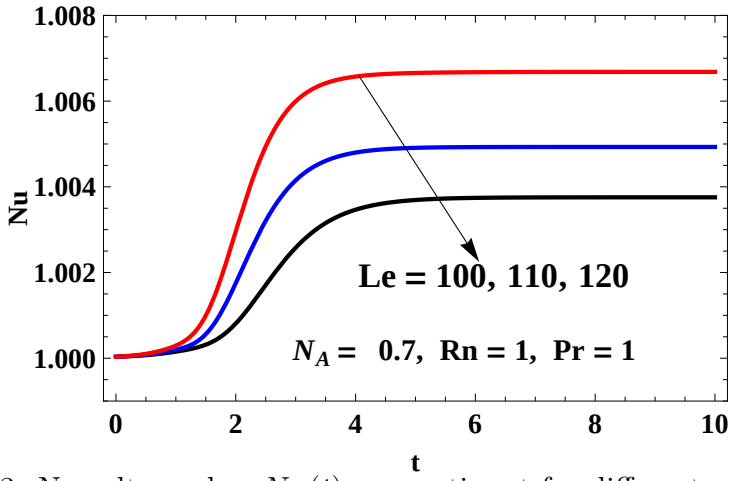

Figure 7.3: Nusselt number $Nu(t)$ versus time t for different values of Le

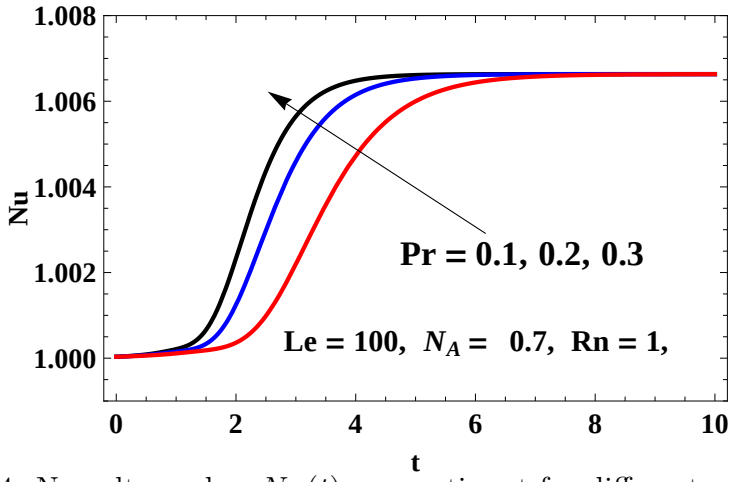

Figure 7.4: Nusselt number $Nu(t)$ versus time t for different values of Pr

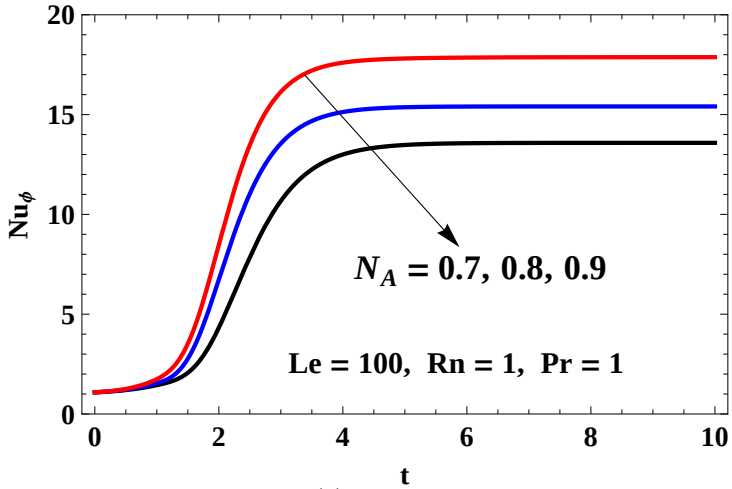

Figure 7.5: Nusselt number $Nu_\phi(t)$ versus time t for different values of N_A

Following results have been found from Figures 7.5, 7.6, 7.7, 7.8 for heat transport in the nanofluids

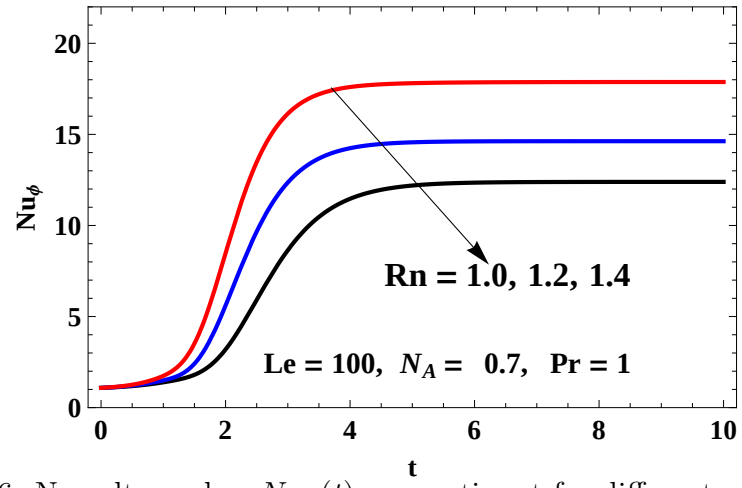

Figure 7.6: Nusselt number $Nu_\phi(t)$ versus time t for different values of Rn

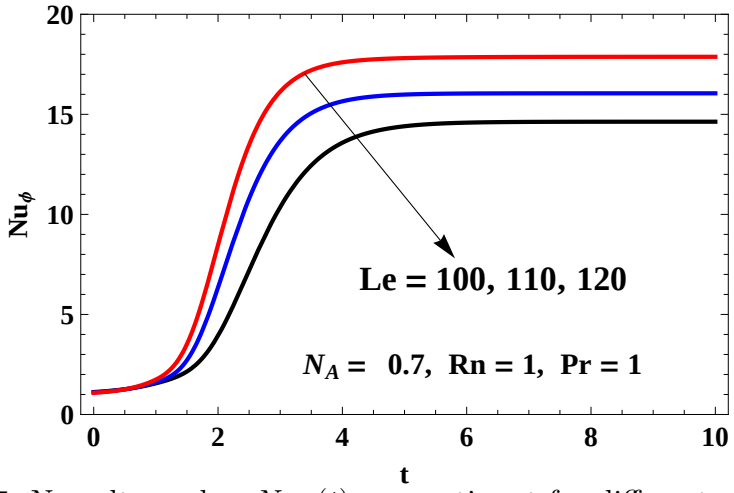

Figure 7.7: Nusselt number $Nu_\phi(t)$ versus time t for different values of Le

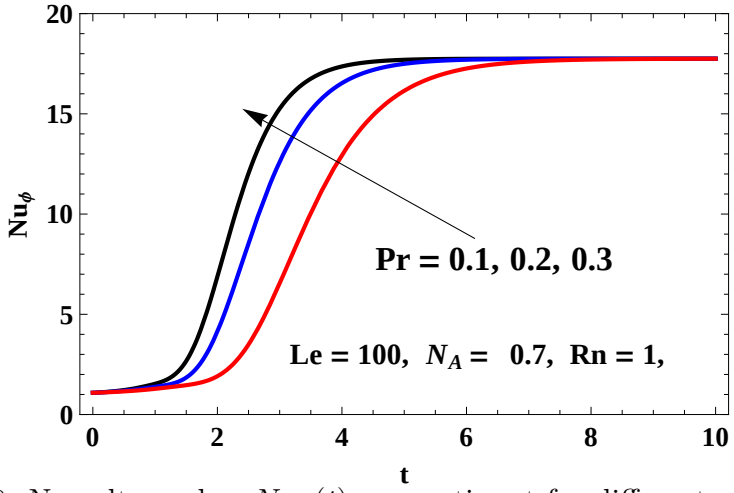

Figure 7.8: Nusselt number $Nu_\phi(t)$ versus time t for different values of Pr

1. $[\mathrm{Nu}_\Phi]_{N_A=0.9} < [\mathrm{Nu}_\Phi]_{N_A=0.8} < [\mathrm{Nu}_\Phi]_{N_A=0.7}$.

2. $[\mathrm{Nu}_\Phi]_{Rn=1.2} < [\mathrm{Nu}_\Phi]_{Rn=1.1} < [\mathrm{Nu}_\Phi]_{Rn=1}$.

3. $[\mathrm{Nu}_\Phi]_{Le=120} < [\mathrm{Nu}_\Phi]_{Le=110} < [\mathrm{Nu}_\Phi]_{Le=100}$.

4. $[\mathrm{Nu}_\Phi]_{Pr=0.1} < [\mathrm{Nu}_\Phi]_{Pr=0.2} < [\mathrm{Nu}_\Phi]_{Pr=0.3}$.

From Figure 7.5, it is clear that the effect of modified thermophoresis to Brownian-motion diffusivity ratio is to decrease, the heat transfer on increasing its values, From Figure 7.6, it is observed that for increasing values of concentration Rayleigh number heat transfer decreases. Figure 7.7 shows the effect of Lewis number, it is found that on increasing the value of Lewis number heat transfer decreases. Further, from Figure 7.8, it is found that the effect of Pr on $\mathrm{Nu}_\Phi[\tau]$ is felt only at small time.

Comparison of exact and Mathematica solutions with the fifteen-order HAM solution is depicted in Figure 7.9 and Figure 7.10. Figure 7.9 exhibits the plot of Nu verses t, on the other hand Figure 7.10 shows the plot of Nu_ϕ verses t. It is evident that the solution (for $h = 1.088$) of the fifteen-order HAM solution is convergent, for fixed values of parameters.

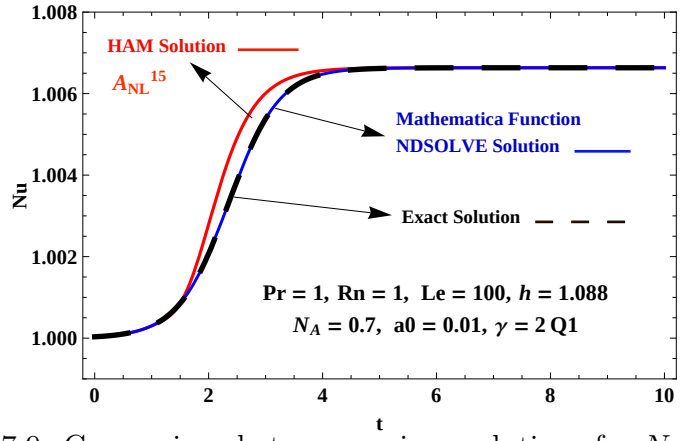

Figure 7.9: Comparison between various solutions for Nu verses t

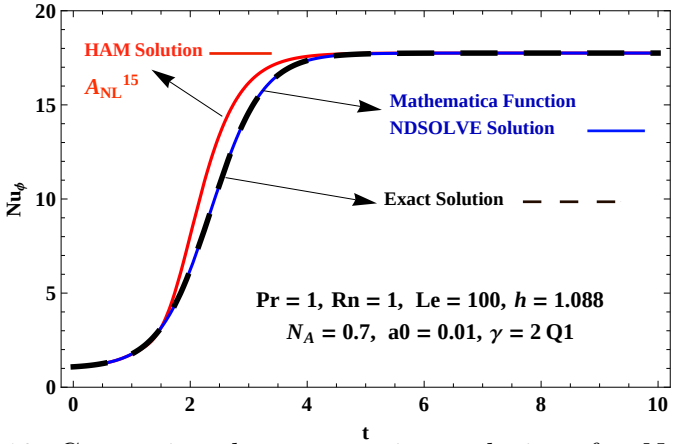

Figure 7.10: Comparison between various solutions for Nu_ϕ verses t

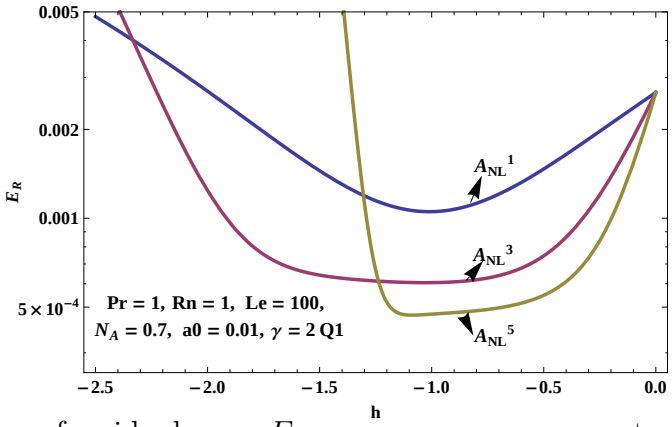

Figure 7.11: Curve of residual error E_R versus convergence controlling parameter h

When $h = -2.5$, increasing the order results in increasing the residual error, thus the series is divergent. Besides, choosing any a value of h in the region $-2.5 < h < -2.3$ results in divergent series. However, choosing any a value of h in the region $-1.3 < h < 0$ results in convergent series. Obviously, there exists such a region $h_B \leq h < 0$ where h_B is a constant, that choosing any a value of h in this region results in convergent HAM series. It is unnecessary to determine the exact value h_B of the boundary. For example, from Figure 7.11, it is obvious that the HAM series converges by choosing any value of h in the region $-1.3 < h < 0$. Besides, as proved by Liao (2004), all of these convergent HAM series converge to the same result for given physical parameters, although the convergence rate is dependent upon the chosen value of h

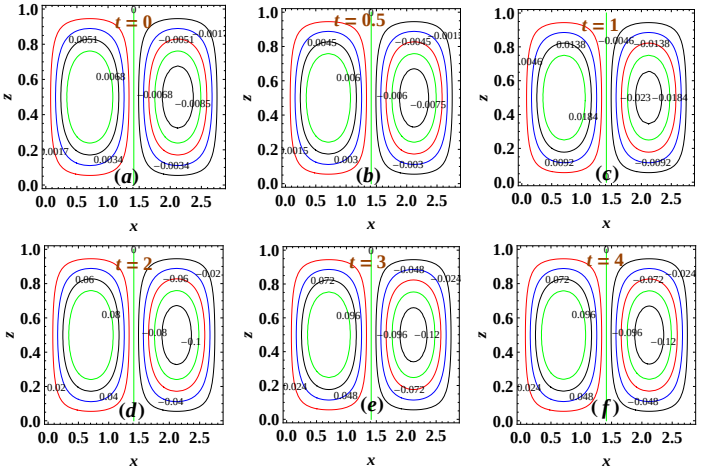

Figure 7.12: Streamlines at (a) $t = 0.0$, (b) $t = 0.5$, (c) $t = 1.0$, (d) $t = 2.0$, (e) $t = 3.0$, (f) $t = 4.0$.

Variation of stream lines, isotherms, isoconcentrations at different instant of time are depicted in Figure 7.12, Figure 7.13 and Figure 7.14 respectively. The magnitudes of

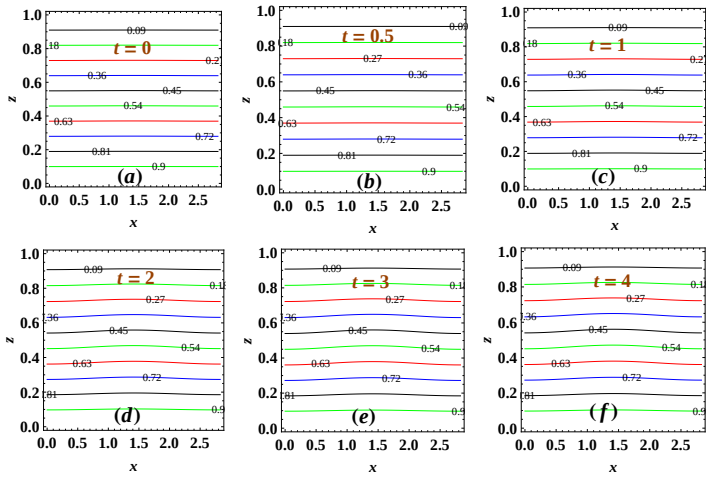

Figure 7.13: Isotherms at (a) $t = 0.0$, (b) $t = 0.5$, (c) $t = 1.0$, (d) $t = 2.0$, (e) $t = 3.0$, (f) $t = 4.0$.

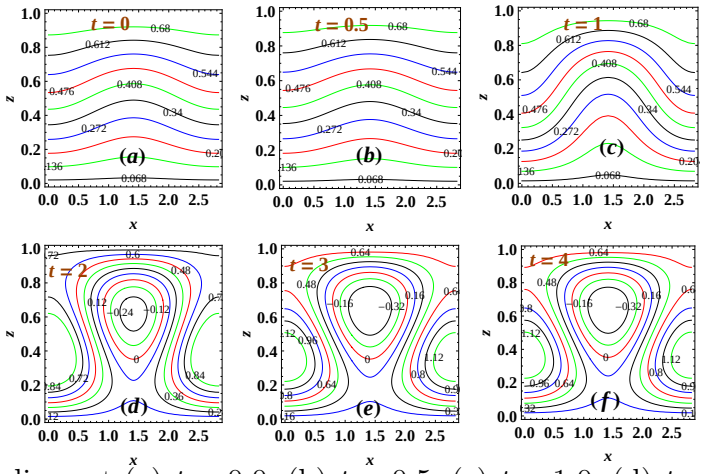

Figure 7.14: Streamlines at (a) $t = 0.0$, (b) $t = 0.5$, (c) $t = 1.0$, (d) $t = 2.0$, (e) $t = 3.0$, (f) $t = 4.0$.

stream lines increases as time increases, it is evident from Figure 7.12. Figure 7.13 shows the variation of isotherms at different instant of time. It is found that initially the isotherms are flat and parallel, showing that the heat transport is only by conduction alone and as time increases isotherms starts oscillating showing convective regime is in place. Figure 7.14 shows that initially the isoconcentrations are flat and parallel, thus heat transport is by conduction only. But as time increases isoconcentrations starts oscillating and form contours. It show that the convective regime became stronger. Further, it is clear from the Figure 7.12 to Figure 7.14 that after reaching at some instant, there is no changes in stream lines, isotherms, isoconcentrations on further elapses of time, which show that steady state has been achieved.

7.7 Conclusions

Weakly nonlinear stability analysis has been done to study the heat transfer in an infinite horizontal nanofluid layer using the Ginzburg-Landau equation. Effects of concentration Rayleigh number, modified thermophoresis to Brownian-motion diffusivity ratio, Lewis number and Prandtl number on the heat transfer have been studied for the stationary mode of convection. The following conclusions have been made from analysis, for the increasing values of parameter:

1. Prandtl number Pr : Only for short time.

2. Concentration Rayleigh number parameter Rn : heat transfer decreases for base fluid, heat transfer decreases for nanoparticles.

3. Lewis number Le : heat transfer decreases for base fluid, heat transfer increases for nanoparticles.

4. Modified thermophoresis to Brownian-motion diffusivity ratio N_A : heat transfer decreases for base fluid, heat transfer decreases for nanoparticles.

Bibliography

[1] Abu-Nada E., (2011); "Rayleigh-Bénard convection in nanofluids: Effect of temperature dependent properties.", *International Journal of Thermal Sciences* , **50**, 1720-1730.

[2] Abu-Nada E., Masoud Z., Hijazi A., (2008); "Natural convection heat transfer enhancement in horizontal concentric annuli using nanofluids. ", *Int. Commun. Heat Mass Transf*, **35**, 657-665.

[3] Agarwal S., (2014); "Natural convection in a nanofluid-saturated rotating porous layer: A More Realistic Approach. ", *Transp. Porous Media* , **104**, 581-592.

[4] Agarwal S., Bhadauria B.S., (2015); "Thermal instability of a nanofluid layer under local thermal non-equilibrium.", *Nano Convergence*, DOI: 10.1186/s40580-014-0037-z.

[5] Agarwal S., Bhadauria B.S., Siddheswar, P.G., (2011); "Thermal instability of a nanofluid saturating a rotating anisotropic porous medium. ", *Special Top. Rev. Porous Media*, **2(1)**, 53-64.

[6] Agarwal S., Bhadauria B.S., (2011); "Natural convection in a nanofluid saturated rotating porous layer with thermal nonequilibrium model.", *Transp. Porous Media*, **90**, 627-654.

[7] Agarwal S., Rana P., Bhadauria B.S., (2014); "Rayleigh-Bénard convection in a nanofluid layer using a thermal nonequilibrium model.", *ASME j.*, **136**, 122501-122514.

[8] Agarwal S., Sacheti N.M., Charan P., Bhadauria B.S., Singh A.K., (2012); "Nonlinear convective transport in a binary nanofluid saturated porous layer.", *Transp. Porous Media*, **93**, 29-49.

[9] Alchaar S., Vasseur P., Bilgen E., (1995a); "Effect of a magnetic field on the onset of convection in a porous medium.", *Heat and Mass Transfer* , **30**, 259-267.

[10] Alchaar S., Vasseur P., Bilgen E., (1995b); "Hydromagnetic natural convection in a tilted rectangular porous enclosure.", *Numerical Heat Transfer* , **27(A)**, 107-127.

[11] Alves L.S. de B., Barletta A., (2013); "Convective instability of the Darcy-Bénard problem with through flow in a porous layer saturated by a power-law fluid.", *International Journal of Heat and Mass Transfer*, **62**, 495-506.

[12] Ansari A., (2007); "Internal heat generation in a tall Cavity filled with a porous medium.", *J. Porous Med.*, **10**, 585-600.

[13] Barletta A., Celli M., Kuznetsov A.V., (2012); "Heterogeneity and onset of instability in Darcy's flow with a prescribed horizontal temperature gradient.", *J. Heat Transf. Trans. ASME* , **134**, 42602.

[14] Barletta A., Celli M., Kuznetsov A.V., (2011); "Transverse heterogeneity effects in the dissipation-induced instability of a horizontal porous layer.", *J. Heat Transf. Trans. ASME* , **133**, 122601.

[15] Barletta A., di Schio E.R., Storesletten L., (2011); "Convective roll instabilities of vertical throughflow with viscous dissipation in a horizontal porous layer.", *Transp. Porous Med.*, **81**, 461-477.

[16] Barletta A., Storesletten L., (2016); "Linear instability of the vertical throughflow in a horizontal porous layer saturated by a power-law fluid.", *International Journal of Heat and Mass Transfer*, **99**, 293-302.

[17] Bhadauria B.S, Sherani A., (2008b); "Onset of Darcy-convection in a magnetic-fluid saturated porous medium subject to temperature modulation of the boundaries.", *Transport in Porous Media*, **73**, 107-127 .

[18] Bhadauria B.S, Siddheshwar P.G., Suthar O.P., (2012); "Non-linear thermal instability in a rotating viscous fluid layer under temperature/gravity modulation.", *ASME J Heat Tranp* , **34**, 102-502.

[19] Bhadauria B.S, Srivastava A.K., (2010); "Magneto-double diffusive convection in an electrically conducting-fluid-saturated porous medium with temperature modulation of the boundaries.", *International Journal of Heat and Mass Transfer* , **53**, 2530-2538 .

[20] Bhadauria B.S., (2006); "Time-Periodic Heating of Rayleigh-Bénard Convection in a vertical Magnetic Field.", *Physica Scripta* , **73(3)**, 296-302.

[21] Bhadauria B.S., (2008a); "Effect of temperature modulation on Darcy convection in a rotating porous medium.", *J Porous Media* , **11(4)**, 361-75.

[22] Bhadauria B.S., (2008b); "Combined effect of temperature modulation and magnetic field on the onset of convection in an electrically conducting-fluid-saturated porous medium.", *ASME Journal of Heat Transfer* , **130**, 052601- 1-052601-9.

[23] Bhadauria B.S., (2012); "Double diffusive convection in a saturated anisotropic porous layer with internal heat source.", *Transp. Porous Media*, **92**, 299-320.

[24] Bhadauria B.S., Agarwal S., Kumar A., (2011); "Non-linear two-dimensional convection in a nanofluid saturated porous medium.", *Transp. Porous Media* , **90(2)**, 605-625.

[25] Bhadauria B.S., Agarwal S., (2011b); "Natural convection in a nanofluid saturated rotating porous layer : a nonlinear study.", *Transp. Porous Media*, **87(2)**, 585-602.

[26] Bhadauria B.S., Agarwal S., (2011a); "Convective transport in a nanofluid saturated porous layer with thermal nonequilibrium model.", *Transp. Porous Media*, **88**, 107-131.

[27] Bhadauria B.S., Hashim I., Siddheshwar P.G., (2012); "Study of heat transport in a porous medium under G-jitter and internal heating effects.", *Transp in Porous Media*, **93**, 21-37.

[28] Bhadauria B.S., Hashim I., Siddheshwar, P.G., (2013a); "Study of heat transport in a porous medium under G-jitter and internal heating effects.", *Transp. Porous Media*, **96**, 21-37.

[29] Bhadauria B.S., Hashim I., Siddheshwar, P.G., (2013b); "Effects of time-periodic thermal boundary conditions and internal heating on heat transport in a porous medium.", *Transp in Porous Media*, **97**, 185-200..

[30] Bhadauria B.S., Kiran P. and Belhaq, M., (2014); "Nonlinear thermal convection in a layer of nanouid under G-jitter and internal heating effects.", *MATEC Web of Conferences*, **16**, 9003.

[31] Bhadauria B.S., Kiran P., (2014a); "Effect of rotational speed modulation on heat transport in a fluid layer with temperature dependent viscosity and internal heat source.", *Ain Shams Eng J.*, **5**, 1287-1297 .

[32] Bhadauria B.S., Kiran P., (2014b); "Weak nonlinear analysis of magneto-convection under magnetic field modulation.", *Phys. Scr.*, **89**, 095209 (10pp) .

[33] Bhadauria B.S., Kiran P., (2015); "Chaotic and oscillatory magneto-convection in a binary viscoelastic fluid under G-jitter.", *Int. J Heat Mass Transf*, **84**, 610-624.

[34] Bhadauria B.S., Kumar A., Kumar J., Sacheti N.C., Chandran P., (2011); "Natural Convection in a Rotating Anisotropic Porous Layer with internal heat.", *Transp. Porous Media*, **90**, 687-705.

[35] Bhattacharjee J.K., (1989); "Rotating Rayleigh-Bénard convection with modulation.", *J Phys A Math Gen* , **22**, L1135-9.

[36] Bhattacharya S.P., Jena S.K., (1984); "Thermal instability of a horizontal layer of micropolar fluid with heat source.", *Proc. Indian Acad. Sci.(Math. Sci.)*, **93**, 13-26.

[37] Bian W., Vasseur P., Bilgen E., (1996b); "Effect of an electromagnetic field on natural convection in an inclined Porous layer.", *International Journal of Heat and Fluid Flow*, **17(A)**, 36-44.

[38] Bian W., Vasseur P., Bilgen E., (1996a); "Effect of an external magnetic field on buoyancy driven flow in a shallow porous cavity.", *Numerical Heat Transfer*, **29(A)**, 625-638.

[39] Brevdo L., Ruderman S., (2009); "On the convection in a porous medium with inclined temperature gradient and vertical throughflow. Part I. Normal modes.", *Transp. Porous Med.*, **80**, 137-151 .

[40] Brinkman H.C., (1952); "The viscosity of concentrated suspensions and solutions.", *J. Chem. Phys.*, **20**, 571571.

[41] Buongiorno J., (2006); "Convective transport in nanofluids.", *J. Heat Transf ASME* , **128**, 240-250.

[42] Buongiorno J., Hu W., (2005); "Nanofluid coolant for advanced nuclear power plants.", *In: Proceedings of ICAPP05, Seoul*, **Paper No. 5705**, May 15-19.

[43] Chand R., Rana G.C., (2012); "On the onset of thermal convection in rotating nanofluid layer saturating a Darcy-Brinkman porous medium.", *Int. J. Heat Mass Transf*, **55**, 5417-5424.

[44] Chand R., Rana G., (2015); "Magneto convection in a layer of nanofluid with soret effect.", *Acta mechanica acta mechanica et automatica*, **92**, .

[45] Chandrashekhar S., (1961); "Hydrodynamic and Hydromagnetic Stability.", *Oxford University Press, Oxford.*

[46] Chen G., (2001); "Ballistic-diffusive heat-conduction equations. Phys. Rev. Lett.", *Energy Technology Division, Argonne National Laboratory, Argonne*, **86**, 2297-2300.

[47] Choi S., (1999); "Nanofluid Technology: Current Status and Future Research.", *U.S. Department of Energy.*

[48] Choi, S., (1995); "Enhancing thermal conductivity of fluids with nanoparticles. In: Siginer DA, Wang HP (eds) Development and applications of Non-Newtonian Flows.", *ASME FED 231/MD*, **66**, 99-105.

[49] Das S.K., Putra N., Roetzel W., (2003b); "Pool boiling characteristics of nanofluids.", *Int. J. Heat Mass Transf.*, **46** , 851-862.

[50] Das S.K., Putra N., Thiesen P., Roetzel W., (2003a); "Temperature dependence of thermal conductivity enhancement for nanofluids.", *ASME J. Heat Transfer* , **125**, 567-574.

[51] Daungthongsuk W., Wongwise S., (2007); "A critical review of convective heat transfer of nanofluids.", *Renewable and Sustainable Energy Reviews.*, **11**, 797-817.

[52] Domairry G., Nadim N., (2008); "Assessment of homotopy analysis method and homotopy-perturbation method in non-linear heat transfer equation. ", *Int Commun Heat Mass Transfer* , **35**, 93-102.

[53] Drazin P.G., Reid W.H., (1981); "Hydrodynamic Stability.", *Cambridge University Press, Cambridge.*

[54] Eastman J.A., Choi S.U.S., Yu W., Thompson L.J., (2001); "Anomalously increased effective thermal conductivities of ethylene glycol-based nanofluids containing copper nanoparticles.", *Appl. Phys. Lett.*, **78**, 718-720.

[55] Eastman J.A., Choi S.U.S., Yu W., Thompson L.J., (2004); "Thermal transport in nanofluids.", *Annu. Rev. Mater.Res.*, **34**, 219-246.

[56] El-Hakiem M. A., Rashad A.M., (2007); "Effect of radiation on non-Darcy free convection from a vertical cylinder embedded in a fluid-saturated porous medium with a temperature-dependent viscosity.", *J. Porous Media* , **10**, 209-218.

[57] Gasser R., Kazimi M., (1976); "Onset of convection in a porous-medium with internal heat generation.", *J. Heat Transf. Trans. ASME* , **98**, 49-54.

[58] Gershuni G. Z., Zhukhovitskii E. M., (1976); "Convective stability in incompressible fluids.", *Jerusalem Keter Publishing House.*,.

[59] Givler R. C., Altobelli A., (1994); "A determination of the effective viscosity for Brinkman-Forchheimer model.", *J. Fluid Mech.*, **258**, 355-367 .

[60] Godson L., Raja B., Lal D.M., Wongwises S., (2010); "Enhancement of heat transfer using nanofluidsAn overview.", *Renewable and Sustainable Energy Reviews.*, **14**, 629-641.

[61] Gresho P.M., Sani R., (1970); "The effects of gravity modulation on the stability of a heated fluid layer ", *J. of Fluid Mech.* , **40**, 783-806.

[62] Gupta U., Ahuja j., Wanchoo R.K., (2013); "Magneto convection in a nanofluid layer.", *Int. J. Heat Mass Transf.*, **64**, 1163-1171.

[63] Hamilton R.L., Crosser O.K., (1962); "Thermal conductivity of heterogeneous two-component systems.", *Ind. Eng. Chem. Fund.*, **1**, 187191.

[64] Hayat T., Khan M., Ayub M., (2004); "On the explicit analytic solutions of an Oldroyd 6 - constant fluid.", *Int J Eng Sci.*, **42**, 123-135.

[65] Hayat T., Khan M., Ayub M., (2004); "Flow of a power-law nanofluid past a vertical stretching sheet with a convective boundary condition", *Journal of Applied Mechanics and Technical Physics*, **57 No. 1**, 173-179.

[66] Homsy G. M., Sherwood A. E., (1976); "Convective stability of incompressible fluids.", *Israel Program for Scientific Translations. AIChE J.*, **22**, 168-174.

[67] Jang S.P., Choi S.U.S., (2004); "Role of Brownian motion in the enhanced thermal conductivity of nanofluids.", *Appl. Phys. Lett.* , **84**, 4316-4318.

[68] Jones M. C., Persichetti J. M., (1986); "Convective instability in packed beds with through-flow.", *AIChE J.*, **32** , 1555-1557 .

[69] Joshi M.V., Gaitonde U.N., Mitra S.K., (2006); "Analytical study of natural convection in a cavity with volumetric heat generation.", *ASME J. Heat Transf.*, **128**, 176-182.

[70] Kakac S., Pramuanjaroenkij A., (2009); "Review of convective heat transfer enhancement with nanofluids.", *International Journal of Heat and Mass Transfer.*, **52**, 3187-3196.

[71] Keblinski P., Cahill D.G., (2005); "Comments on model for heat conduction in nanofluids.", *Phy. Rev. Lett.*, **95**, 209401 .

[72] Khalili A., Shivakumara I. S., (1998); "Onset of convection in a porous layer with net throughflow and internal heat generation, ", *Phys. of fluids* , **10**, 315-317 .

[73] Khalili A., Shivakumara I. S., (2003); "Non-Darcian effects on the onset of convection in a porous layer with through-flow.", *Transp. Porous Med.*, **53**, 245-263 .

[74] Khalili A., Shivakumara I. S., Huettel M., (2002); "Effects of through-flow and internal heat generation on convective instabilities in an anisotropic porous layer.", *J. Porous Media*, **5**, 187-198.

[75] Khalili A., Shivakumara I. S., Suma S. P., (2003); "Convective instability in superposed fluid and porous layers with vertical through flow. ", *Transp. Porous Med.*, **51**, Jan-18.

[76] Khanafer K, Vafai K, Lightstone M., (2003); "Buoyancy-driven heat transfer enhancement in a two-dimensional enclosure utilizing nanofluids. ", *Int. J. Heat Mass Transf.*, **46**, 3639-3653.

[77] Kim J., Kang Y.T., Choi C.K., (2004); "Analysis of convective instability and heat transfer characteristics of nanofluids.", *Phys. Fluids*, **16**, 2395-2401.

[78] Kleinstreuer C., Li J., Koo J., (2008); "Microfluidics of nano-drug delivery.", *Int. J. Heat Mass Transf.*, **51**, 5590-5597.

[79] Kloosterziel R.C., Carnevale G.F., (2003); "Closed-form linear stability conditions for rotating Rayleigh-Bénard convection with rigid stress-free upper and lower boundaries.", *J Fluid Mech*, **480**, 25-Apr.

[80] Kumar K., Bhattacharjee J.K., Banerjee K., (1986); "Onset of the first instability in hydrodynamic flows: effect of parametric modulation. ", *Phys Rev A*, **34**, 5000-6.

[81] Kuznetsov A.V., Nield D.A., (2010a); "Thermal instability in a porous medium layer saturated by a nanofluid : Brinkman model.", *Transp. Porous Media*, **81**, 409-422.

[82] Kuznetsov A.V., Nield D.A., (2010b); "Effect of local thermal non-equilibrium on the onset of convection in a porous medium layer saturated by a nanofluid.", *Transp. Porous Media*, **83**, 425-436.

[83] Kuznetsov A.V., Nield D.A., (2010c); "The onset of double-diffusive nanofluis convection in a layer of a saturated porous medium.", *Transp. Porous Media*, **85**, 941-951.

[84] Kuznetsov A.V., Nield D.A., (2011); "The effect of local thermal nonequilibrium on the onset of convection in a porous medium layer saturated by nanofluid: Brinkman model.", *J. Porous Media*, **14**, 285-293.

[85] Liao S.J., (2009); "Notes on the homotopy analysis method: Some definitions and theorems.", *Commun Non-linear Sci Numer Simulat.*, **14**, 983-97.

[86] Lee S., Choi S.U.S., Li S., Eastman J.A., (1999); "Measuring thermal conductivity of fluids containing oxide nanoparticles.", *Trans. ASME, J. Heat Transfer*, **121**, 280-289.

[87] Liao S.J., (2004); "On the homotopy analysis method for non-linear problems.", *Appl Math Comput.*, **47(2)**, 499-513.

[88] Liu Y., Ecke R.E., (1997); "Heat transport scaling in turbulent Rayleigh-Bénard convection: effects of rotation and Prandtl number.", *Phys Rev Lett.*, **79**, 2257-60.

[89] Malashetty M.S., Swamy M., (2007); "Combined effect of thermal modulation and rotation on the onset of stationary convection in porous layer. ", *Transp Porous Med.*, **69**, 313-330.

[90] Malashetty M.S., Swamy M., (2008); "Effect of thermal modulation on the onset of convection in rotating fluid layer.", *Int J Heat Mass Transp.*, **51**, 2814-23.

[91] Masuda H., Ebata A., Teramae K., Hishinuma N., (1993); "Alteration of thermal conductivity and viscosity of liquid by dispersing ultra fine particles.", *Netsu Bussei*, **7**, 227-233.

[92] Matura P. , Lcke M., (2009); "Thermomagnetic convection in a ferrofluid layer exposed to a time-periodic magnetic field.", *PHYSICAL REVIEW E*, **80**, 26314.

[93] Maxwell J. C., (1892); "A Treatise on Electricity and Magnetism.", *Oxford University Press, London.*

[94] Nield D. A., (1987); "Convective instability in porous medium with through-flow.", *AMSE J.*, **33**, 1222-1224.

[95] Nield D.A., Bejan A., (2013); "Convection in Porous Media.", *4th edn. Springer, New York*.

[96] Nield D.A., Kuznetsov A.V., (2009); "Thermal instability in a porous medium layer saturated by nanofluid.", *Int. J. Heat Mass Transf.*, **52**, 5796-5801.

[97] Nield D.A., Kuznetsov A.V., (2010a); "The onset of convection in a horizontal nanofluid layer of finite depth.", *Eur J Mech B Fluids*, **29**, 217-23.

[98] Nield D.A., Kuznetsov A.V., (2010b); "The effect of local thermal nonequilibrium on the onset of convection in a nanofluid.", *J. Heat Transf.*, **132**, 52405.

[99] Nield D.A., Kuznetsov A.V., (2011); "The effect of vertical throughflow on thermal instability in a porous medium layer saturated by a nanofluid.", *Transp. Porous Media*, **87**, 765-775.

[100] Nield D.A., Kuznetsov A.V., (2012); "The onset of convection in a layer of porous medium saturated by a nanofluid: effects of conductivity and viscosity variation and cross-diffusion.", *Trans. Porous Media*, **92**, 837-846.

[101] Nield D.A., Kuznetsov A.V., (2013); "Onset of convection with internal heating in a weakly heterogeneous porous medium.", *Transp Porous Media*, **98**, 543-552.

[102] Nield D.A., Kuznetsov A.V., (2014a); "The onset of convection in a horizontal nanofluid layer of finite depth: A revised model.", *International Journal of Heat and Mass Transfer*, **77**, 915-918.

[103] Nield D.A., Kuznetsov A.V., (2014b); "Thermal instability in a porous medium layer saturated by a nanofluid : A revised model.", *Int. J. Heat Mass Transf.*, **68**, 211-214.

[104] Nield D.A., Kuznetsov A.V., (2015); "The effect of vertical throughflow on thermal instability in a porous medium layer saturated by a nanofluid : A revised model.", *Journal of Heat Transfer ASME* , **137**, 052601-052605.

[105] Niemela J.J., Donnelly R.J., (1986); "Direct transition to turbulence in rotating-Bénard convection.", *Phys Rev Lett*, **57**, 2524-7.

[106] Patil R.P., Rudraiah N., (1973); "Stability of hydromagnetic thermoconvective flow through porous medium.", *Transactions of the ASME Journal of Applied Mechanics*, **40(E)**, 879-884 .

[107] Putra N., Roetzel W., Das SK., (2003); "Natural convection of nano-fluids.", *Heat Mass Transf.*, **39**, 775-784.

[108] Rauscher J.W., Kelly R.E., (1975); "Effect of modulation on the onset of thermal convection in a rotating fluid.", *Int J Heat Mass Transfer*, **18**, 1216-7.

[109] Roberts P.H. (1967); "Convection in horizontal layers with internal heat generation: Theory.", *J. Fluid Mech.*, **30** , 33-49.

[110] Rudraiah N., Shivkumara I.S., Friedrich R., (1986); "The effcet of rotation on linear and non-linear diffusive convection in sparsely packed porous medium.", *Int. J. of Heat Mass Transfer*, **299**, 1301-1371.

[111] Rudraiah N., Vortmeyer D., (1978); "Stability of finite-amplitude and overstable convection of a conducting fluid through fixed porous bed. ", *Warme-Stoffubertrag* , **11**, 241-254.

[112] Saidur R., Leong K. Y. , Mohammad H. A., (2011); "A review on applications and challenges of nanofluids.", *Renewable and Sustainable Energy Reviews*, **15**, 1646-1668.

[113] Sekar R., Vaidyanathan G., Ramanathan A., (1993); "The ferroconvection in fluids saturating a rotating densely packed porous medium.", *International Journal of Engineering Science*, **31**, 241-250 .

[114] Shivakumara I. S., (1999); "Boundary and inertia effects on convection in porous media with through-flow.", *Acta Mech.*, **137**, 151-165.

[115] Shivakumara I. S., Nanjundappa C. E., (2006); "Effects of quadratic drag and throughflow on double diffusive convection in a porous layer. ", *Int. Comm. Heat Mass Transfer*, **33**, 357-363.

[116] Shvartsblat D. L., (1969); "Steady convection motions in a plane horizontal fluid layer with permeable boundaries.", *Fluid Dyn.*, **4**, 54-59.

[117] Shvartsblat D. L., (1968); "The spectrum of perturbations and convective instability of a plane horizontal fluid layer with permeable boundaries.", *J. Appl. Mech. (PMM)*, **32**, 266-271.

[118] Siddheshwar P. G., (1995); "Suction-injection effects on Rayleigh-Bénard convection in a closely packed porous bed with general boundary condition on temperature ", *VI Asian Cong. of Fluid Mech., Singapore*, **1**, 590-594 .

[119] Srivastava A., Bhadauria B.S., Siddheshwar P.G., Hashim, I., (2013); "Heat transport in an anisotropic porous medium saturated with variable viscosity liquid under g-jitter and internal heating effects.", *Transp Porous Med.*, **99**, 359-376.

[120] Suthar O.P., Bhadauria B.S., Khan A., (2009); "Modulated centrifugal convection in a rotating vertical porous layer distant from the axis of rotation.", *Transp Porous Med.*, **79(2)**, 255-64 .

[121] Suthar O.P., Bhadauria B.S., Khan A., (2011); "Rotating Brinkman-Lapwood convection with modulation.", *Transp Porous Med.*, **88**, 369-83.

[122] Sutton F. M., (1970); "Onset of convection in a porous channel with net throughflow.", *Phys. of Fluids*, **13**, 1931-1942 .

[123] Takashima M., (1989); "The stability of natural convection in an inclined fluid layer with internal heat generation.", *J. Phys. Soc. Japan.*, **58**, 4431-4440.

[124] Tasaka Y., Takeda, Y., (2005); "Effects of heat source distribution on natural convection induced by internal heating.", *Int. J. Heat and Mass Transf.*, **48**, 1164-1174.

[125] Taylor R., Coulombe S., Otanicar T., Phelan P., Gunawan A., Lv W., Rosengarten G., Prasher R., Tyagi H., (2013); "Small particles, big impacts: A review of the diverse applications of nanofluids.", *Journal of Applied Physics* , **113**, doi: 10.1063/1.4754271.

[126] Trisaksria V., Wongwises S., (2007); "Critical review of heat transfer characteristics of nanofluids.", *Renewable and Sustainable Energy Reviews.*, **11**, 512-523..

[127] Tveitereid M., (1978); "Thermal convection in a horizontal fluid layer with internal heat sources.", *Int. J. Heat Mass Transf.*, **21**, 335-339.

[128] Tveitereid M., Palm E., (1976); "Convection due to internal heat sources.", *J. Fluid Mech.*, **76**, 481-499.

[129] Tzou D.Y., (2008a); "Instability of nanofluids in natural convection.", *ASME J Heat Transf.*, **130**, 72401.

[130] Tzou D.Y., (2008b); "Thermal instability of nanofluids in natural convection.", *Int. J. Heat Mass Transf.*, **51**, 2967-2979 .

[131] Umavathi J.C., (2013); "Effect of thermal modulation on the onset of convection in a porous medium layer saturated by a nanofluid.", *Transp Porous Media*, **98**, 59-79.

[132] Vadasz P. , (2006); "Heat conduction in nanofluid suspensions.", *ASME J. Heat Transf.*, **128**, 465-477.

[133] Vanishree R. K., Siddheshwar P. G., (2010); "Effect of rotation on thermal convection in an anisotropic porous medium with temperature-dependent viscosity.", *Transp. Porous Med.*, **81**, 73-87.

[134] Venezian, G., (1969); "Effect of modulation on the onset of thermal convection.", *Journal of Fluid Mechanics*, **35** , 243-254.

[135] Veronis G. (1966); "Motions at subcritical values of the Rayleigh number in a rotating fluid.", *Journal of Fluid Mechanics*, **24**, 545-554.

[136] Walsh T.J., Donnelly R.J., (1988); "Taylor-Couette flow with periodically corotated and counterrotated cylinders.", *Phys Rev Lett*, **60**, 700-703.

[137] Wang X.Q. , Mujumdar A.S., (2007); "Heat transfer characteristics of nanofluids: a review.", *International Journal of Thermal Sciences.*, **46**, 1-19.

[138] Wen D., Ding Y., (2006); "Natural convective heat transfer of suspensions of titanium dioxide nsnoparticles (nanofluids).", *IEEE Trans. Nanotechnol.*, **5**, 220-227.

[139] Wen D., Lin G., S. Vafaei, Zhang K., (2009); "Review of nanofluids for heat transfer applications.", *Particuology*, **7**, 141-150.

[140] Wooding, R. A., (1960); "Rayleigh instability of a thermal boundary layer in flow through porous medium.", *J. Fluid Mech.*, **9**, 183-192.

[141] Yadav D., Agrawal G.S., Lee J., (2015); "Thermal instability in a rotating nanofluid layer: A revised model.", *Ain Shams Eng J.*, http://dx.doi.org/10.1016/j.asej.2015.05.005.

[142] Yadav D., Bhargava R., Agrawal G.S., (2012); "Boundary and internal source effects on the onset of Darcy-Brinkman convection in a porous layer saturated by nanofluid.", *Int. J. Therm. Sci.*, **60**, 244-254.

[143] Yu C.P., Shih Y.D., (1980); "Thermal instability of an internally heated fluid layer in a magnetic field.", *Phys. Fluids*, **23**, 411.

[144] Yu W., Choi S.U.S., (2003); "The role of interfacial layers in the enhanced thermal conductivity of nanofluids: a renovated Maxwell model.", *J. Nanoparticle Res, 5*, **5**, 167-171.

[145] Yu W., France D.M., Choi S.U.S., Routbort J.L., (2007); "Review and assessment of nanofluid technology for transportation and other applications.", *Argonne National Laboratory, Argonne, IL*, **ANL/ESD/07-9**.

List of Publications

Published Article

1. Palle Kiran, B.S. Bhadauria, **Vineet Kumar**, "Thermal convection in a nanofluid saturated porous medium with internal heating and gravity modulation".
   Journal of nanofluid (American Scientific Publishers), Vol. 5, No. 3, pp. 328-339(12), (2016).

2. B.S. Bhadauria, **Vineet Kumar**, Brajesh K. Singh, "Weak nonlinear stability analysis of thermal convection in an electrically conducting nanofluid layer under magnetic field modulation".
   Recent Advances in Mathematical & Computational Science, Book Chapter in BBAU conference proceedings. ISBN : 9789384337674, (2015).

3. B.S. Bhadauria, **Vineet Kumar**, Brajesh K. Singh, I. Hashim, "Study of convective thermal instability in nanofluid saturated porous media in the presence of vertical throughflow, internal heat source and rotation".
   VIJNANA BHARATHI, Bangalore University Journal of Science, Vol. 1, No. 2, pp. 120-140, ISSN : 0971-6882, (2016).

4. Alok Srivastava, **Vineet Kumar**, B.S. Bhadauria, I. Hashim, "Study of heat transfer in a nanofluid layer using homotopy analysis method".
   International Journal of Science, Technology and Society, Vol 3, No. 1, pp. 27-39, (2017).

5. Alok Srivastava, **Vineet Kumar**, B.S. Bhadauria, I. Hashim, "Nonlinear study of

heat transfer in nanofluid saturated horizontal porous medium".

International Journal of Science, Technology and Society, Vol 3, No. 2, pp. 41-53, (2017).

6. B.S. Bhadauria, **Vineet Kumar**, "Convective motion in nanofluid under variable rotational speed".

   Advanced Science Engineering and Medicine(American Scientific Publishers), Vol. 10, 717-723, (2018).

Communicated Article

1. B.S. Bhadauria, **Vineet Kumar**, " Effect of Rotational Speed Modulation on Thermal Instability of Nanofluid Saturated Porous Medium". International Journal of Porous Media.

2. B.S. Bhadauria, **Vineet Kumar**, "The effect of vertical throughflow in a horizontal porous layer saturated by a power-law nanofluid ". Journal of nanofluid (American Scientific Publishers).

Papers presented in International / National Conferences

International conferences

1. Effect of throughflow and internal heat generation on thermal instability in nanofluid saturated porous medium. International conference on **Emerging Trends in Computational and Applied Mathematics**, ITM University, Gurgaon. June 2-4, 2014.

2. Effect of internal heat generation on nanofluid saturated porous medium with revised model. International conference on **Modelling and Computing**, BBAU, Lucknow. July 10-11, 2014.

3. Weak nonlinear stability analysis of thermal convection in an electrically conducting nanofluid layer under magnetic field modulation. International conference on **M3HPCST**, RKGIT Ghaziabad, December 27-29, 2015.

4. The effect of vertical throughflow in a horizontal porous layer saturated by a power-law nanofluid. International conference on **Fluid Dynamics and Its Applications**, BNMIT, Bengaluru. July 12-14, 2017.

5. Convective motion in nanofluid under variable rotational speed. International conference on **Nanoscience and Nanotechnology**, BBAU, Lucknow. September 22-24, 2017.

6. Study of thermal instability in power-law nanofluid in presence of vertical throughflow. International conference on **Science and Technology for Sustainable Future**, BBAU, Lucknow. January 10-11, 2018.

National conferences

1. Effect of internal heat generation on nanofluid saturated porous medium with more realistic model. National conference on **Recent Advances in Mathematics and Applications**, BBAU, Lucknow. October 30-31, 2014.

2. Effect of throughflow and internal heat generation on thermal instability in nanofluid saturated porous medium. National conference on **Mathematical Analysis and Application**, BHU, Varanasi. January 30-31, 2015.

3. Effect of throughflow in an electrically conducting nanofluid saturated porous medium. National conference on **Mathematical Techniques in Engineering and Technology**, BBAU, Lucknow. March 30-31, 2016.

4. Weakly nonlinear analysis of convective motion in nanofluid under rotational speed modulation. National conference on **Mathematical Modelling-Modern Approaches**, DITU, Dehradun. October 13-14, 2017.

Workshop

1. A Mini workshop on **Biomathematics**, BHU, Varanasi. March 28-30, 2015.

AMERICAN SCIENTIFIC PUBLISHERS

Journal of Nanofluids
Vol. 5, pp. 1–12, 2016
(www.aspbs.com/jon)

ARTICLE

Thermal Convection in a Nanofluid Saturated Porous Medium with Internal Heating and Gravity Modulation

Palle Kiran[1,*], B. S. Bhadauria[2], and Vineet Kumar[3]

[1]*Department of Mathematics, Rayalaseema University, Kurnool 518002, Andhra Pradesh, India*
[2]*Department of Mathematics, Faculty of Sciences, Banaras Hindu University, Varanasi 221005, India*
[3]*Department of Applied Mathematics, School for Physical Sciences, Babasaheb Bhimrao Ambedkar University, Lucknow 226025, India*

We present thermal convection in a nanofluid saturated porous medium under the effects of gravity modulation and internal heating. The non-uniform vertical vibrations, which can be realized by oscillating the system vertically is considered to vary sinusoidally with time. Linear and nonlinear stability analysis have been performed to investigate onset and heat/mass transfer in the system. Linear stability analysis is made using Venezian approach, nonlinear stability analysis is made using truncated Fourier series expansions. The effects of various physical parameters have been investigated on heat and mass transfer. Linear model shows there is a particular range of frequency of modulation, where the system stabilizes and destabilizes. The duel effect of this nature is due to the presence of internal heating of the system. It is found that gravity modulation can be used effectively to regulate heat/mass transfer in the system. Further, the effect of internal heating is to destabilize the system, as a consequence enhances the heat/mass transfer.

KEYWORDS: Thermal Instability, Gravity Modulation, Internal Heating, Darcy Model.

1. INTRODUCTION

The advanced concepts of nanofluids offer absorbing heat transfer characteristics compared to conventional heat transfer fluids. Applications of nanofluids in industries such as heat exchanging devices appear promising with these characteristics. Common fluids have limited heat transfer capabilities while some of the metals have very high thermal conductivity in comparison to these fluids. Therefore, the basic idea behind nanofluids was to make a substance by combining these two, which would behave like a fluid and have thermal conductivity of a metal, thus nanofluids were made by suspending the nanoparticles in the common fluids, called base fluids. Presence of these nanoparticles in the base fluids may increase the thermal conductivity of the fluids by 15–40%. The following features (a) abnormal enhancement of thermal conductivity, (b) stability, (c) small concentration and (d) Newtonian behavior, motivates research in nanofluids, with the expectation that, these fluids will play an important role in developing the next generation of cooling technology. The fundamental applications of nanofluids in industries such as heat exchanging devices appear promising with these characteristics. Some of them are: heat-transfer nanofluids, tribological nanofluids, pollution cleaning nanofluids, surfactant and coating nanofluids, chemical nanofluids, process/extraction nanofluids, Bio pharmaceutical nanofluids, Medical nanofluids (drug delivery and functional tissue cell interaction) etc.

A significant feature of nanofluids is thermal conductivity enhancement which was first reported by Masuda et al.[1] Nanofluids are mixtures of base fluid such as water or ethylene-glycol along with small amount of nanoparticles such as metallic or metallic oxide particles (Cu, Cuo, Al_2O_3), having dimensions from 1 to 100 nm. Choi[2] was the first, who proposed this term "nanofluid." Natural convection or buoyancy driven convection, is the heat removal strategy adopted in a wide variety of industries ranging from transportation (heating, ventilation, and air conditioning), energy production and supply to electronics, textiles and paper production, geophysical problems, nuclear reactors to name a few Choi.[3] The ballistic nature of heat transport within nanoparticles was analyzed by Chen.[4] Eastman et al.[5] reported an increase of 40% in the effective thermal conductivity of ethylene-glycol with 0.3% volume of copper nanoparticles of 10 nm diameter. These reports led

*Author to whom correspondence should be addressed.
Email: kiran40p@gmail.com
Received: xx Xxxx xxxx
Accepted: xx Xxxx xxxx

ARTICLE

Buongiorno and Hu[6] to suggest the possibility of using nanofluids in advanced nuclear systems. Another application of the nanofluid flow is in the delivery of nano-drug as suggested by Kleinstreuer et al.[7]

Khanafer et al.[8] reported an increase in concentration of suspended nanoparticles, is to increase in heat transfer in Cu-water nanofluids in a two-dimensional rectangular enclosures. Ballistic nature of heat transport within nanoparticles by Keblinski and Cahill[9] and thermal lagging in nanoparticles with a large surface area to volume ratio by Vadász.[10] A comprehensive review of heat transport in nanofluids is due to Eastman et al.[11] In spite of several reported studies, it is a fact that no satisfactory explanation could be found so far, for abnormal enhancement in the thermal conductivity and viscosity of the fluid due to the presence of nano-particles. Abu-Nada et al.[12] reported the enhancement of heat transfer in nanofluids at higher values of the Rayleigh number in comparison to clear fluid. Buongiorno[13] has given an extensive study to account for the unusual behavior of nanofluids based on inertia, Brownian diffusion thermophoresis, diffusiophoresis, Magnus effects, fluid drainage and gravity settling, and proposed a model incorporating the effects of Brownian diffusion and the thermophoresis. With the help of these equations, studies were conducted by Kim et al.,[14] Tzou[15] and Nield and Kuznetsov.[16, 17]

Bhadauria and Agarwal[18] studied nonlinear thermal instability in a horizontal porous layer saturated by a nanofluid. Agarwal and Bhadauria[19] studied thermal instability in a rotating porous layer saturated by a nanofluid for top and bottom-heavy suspension for Darcy model. Chand and Rana[20] studied the onset of thermal convection in a rotating nanofluid saturated porous medium. Boundary and internal heat source effects on the onset of Darcy-Brinkman convection in a porous layer saturated by nanofluid was studied by Yadav et al.[21] No study in the above literature is available in which the work has been carried out under modulation. Recently Umavathi[22] studied temperature modulation, gravity modulation by Pranesh et al.,[23] of convection in a nanofluid saturated porous medium, using linear stability analysis with Venezian[24] approach. Bhadauria and Kiran[25] investigated g-jitter effects on thermal convection. Bhadauria and Kiran[26] investigated heat transfer in nonofluid saturate porous medium under gravity modulation using truncated Fourier series model. This is first model which presents g-jitter effects on nanofluid convection. It is found that modulation enhances or diminishes heat transfer in the medium depending on amplitude and frequency of modulation. The similar mode was extended for viscoelastic nanofluids by Kiran[27] Linear as well as non-linear study for Rayleigh-Bènard convection in a nanofluid under thermal non-equilibrium with new boundary condition is studied by Agarwal et al.[28] Nield and Kuznetsov[29] has been done a tremendous work in the area of throughflow subjecting to another revised boundary conditions, where they consider the fact that the total nanoparticle flux is the sum of diffusive, convective and thermophoretic terms. Since the particles are transported in the fluid phase only, and so, the intrinsic velocity is involved in the convective terms. Puneet and Agarwal[30] studied the thermal instability of a binary nanofluid saturated porous medium in presence of rotation.

The heat and mass transfer characteristic for MHD threedimensional water-based nanofluid due to an exponentially stretching sheet subjected to a magnetic field is presented by Baag and Mishra.[31] Three types of nanofluid, namely Cu-water, Al_2O_3-water and TiO_2-water is studied. The governing nonlinear partial differential equations are reduced into ordinary differential equations by employing similarity variables and then solved numerically by Runge-Kutta method along with shooting technique. The effects of various physical parameters on the flow, heat and mass profiles are presented graphically. The rotational effects on two competent nanofluid saturating porous medius is investigated by Puneet and Shilpi.[32] The porus medium of Darcy model and the nanofluid incorporates the effects of Brownian motion and thermophoresis. Thermorheological effect on the onset of convection in a horizontal nanofluid layer heated from below is studied for rigid-rigid, freefree and rigidfree boundaries by incorporating the effects of Brownian motion and thermophoresis by Shivakumara et al.[33] It is found that stability characteristics of the system are strongly dependent on the viscosity parameter while the viscosity of nanofluid is allowed to vary exponentially with temperature. The uniform vertical magnetic field effect on thermal convection in a nanofluid saturated porous medium is investigated for more realistic boundary conditions by Chand and Rana.[35] The onset of convection under magnetic fiels is presented using linear stability analysis based upon normal mode technique.

It appears that all of the above studies deal with the case of uniform heating from below, and the case of internal heating has been largely neglected. There are numerous situations of great practical importance where the material offers its own source of heat. It is due to the internal heating of the earth that there exists a thermal gradient between the interior and exterior of the earth's crust, saturated by multi-components fluids, which helps convective flow, thereby transferring the thermal energy towards the surface of the earth. Therefore, the role of internal heat generation becomes very important in several applications that include geophysics, reactor safety analyses, metal waste form development for spent nuclear fuel, fire and combustion studies, and storage of radioactive materials. However, there are relatively very few studies available in which the effect of internal heating on convective flow has been investigated. Some of these studies are: Bhattacharya and Jena,[35] Tasaka and Takeda[36] and Bhadauria et al.[37] and Srivastava et al.[38]

Internal heating in porous media or gravity modulation of the system or a combination of both can be used as effective mechanism to control the convective flow

by suppressing or advancing it. However, to the best of authors' knowledge, there is no study available in the literature in which the effect of vertical vibrations on the Darcy-Bénard convection in a nanofluid has been studied under internal heating effect using linear and nonlinear analysis. It is with this motive that we have made linear and nonlinear analysis of thermal instability in a nanofluid saturated porous medium under gravity modulation, and studied the effect of internal heating on the system. We follow Venezian approach for linear theory, and five mode Lorenz model for nonlinear theory, and in the process stability is discussed, heat and mass transport quantified in terms of Nusselt numbers.

2. MATHEMATICAL FORMULATION

We consider a porous layer saturated by nanofluid, confined between two horizontal boundaries, respectively at $z = 0$ and $z = d$, heated from below and cooled from above. The boundaries are impermeable and perfectly thermally conducting. The porous layer is extended infinitely in x and y-directions, and z-axis is taken vertically upward with the origin at the lower boundary. In addition, the local thermal equilibrium between the fluid and solid has been considered, thus the heat flow has been described using one equation model. T_h and T_c are the temperatures at the lower and upper walls respectively such that $T_h > T_c$. Employing the Oberbeck-Boussinesq approximation, the governing equations to study the thermal instability in a nanofluid saturated porous medium are:[13, 39, 40]

$$\nabla \cdot \mathbf{v_D} = 0 \tag{1}$$

$$\frac{\rho_f}{\varepsilon_p}\frac{\partial \mathbf{v_D}}{\partial \tau} + \nabla p = -\frac{\mu}{K}\mathbf{v}_D + [\phi\rho_p + (1-\phi)\{\rho(1-\beta(T-T_c))\}]\vec{g} \tag{2}$$

$$\gamma\frac{\partial T}{\partial \tau} + \mathbf{v}_D \cdot \nabla T = \kappa_T \nabla^2 T + \varepsilon_p \frac{(\rho c)_p}{(\rho c)_f}\left[D_B \nabla\phi \cdot \nabla T + \frac{D_T}{T_c}\nabla T \cdot \nabla T\right] + Q(T - T_c) \tag{3}$$

$$\frac{\partial \phi}{\partial \tau} + \frac{1}{\varepsilon_p}\mathbf{v}_D \cdot \nabla\phi = D_B \nabla^2\phi + \frac{D_T}{T_c}\nabla^2 T \tag{4}$$

$$\vec{g} = g_0(1 + \epsilon\cos(\Omega\tau))\vec{k} \tag{5}$$

where $\mathbf{v}_D$ is the Darcy velocity. The physical variables have their usual meanings, given in nomenclature. We suppose that the upper and lower boundaries are both impermeable. We also assume that the temperature and the volumetric fraction of the nanoparticles are constant on the boundaries, and one has thermal equilibrium there.[39] Thus, the boundary conditions are as:[18, 19, 25, 26]

$$\mathbf{v} = 0, \quad T = T_h, \quad \phi = \phi_0 \quad \text{at } z = 0 \tag{6}$$

$$\mathbf{v} = 0, \quad T = T_c, \quad \phi = \phi_1 \quad \text{at } z = d \tag{7}$$

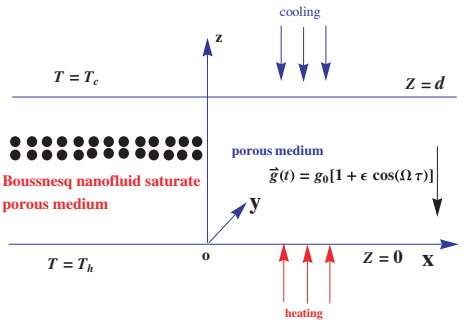

Fig. 1. A sketch of the physical problem.

where nanoparticle concentration ϕ_1 at upper plate is greater than nanoparticle concentration ϕ_0 at lower plate. The dimensionless variables are considered as given below:

$$(x^*, y^*, z^*) = (x, y, z)/d, \quad \tau^* = \tau\kappa_T/\gamma d^2$$

$$(u^*, v^*, w^*) = (u, v, w)d/\kappa_T, \quad p^* = pK/\mu\kappa_T$$

$$\phi^* = \frac{\phi - \phi_0}{\phi_1 - \phi_0} \quad \text{and} \quad T^* = \frac{T - T_c}{T_h - T_c}$$

where $\kappa_T = k_m/(\rho c)_f$, $\gamma = (\rho c_p)_m/(\rho c_p)_f$. The non-dimensionalized governing equations along with boundary conditions are (after dropping the asterisk for simplicity)

$$\nabla \cdot \mathbf{v} = 0 \tag{8}$$

$$\frac{1}{Va}\frac{\partial \mathbf{v}}{\partial \tau} = -\nabla p - \mathbf{v} - g_m(Rm - Ra\ T + Rn\phi)\hat{e}_z \tag{9}$$

$$\frac{\partial T}{\partial \tau} + \mathbf{v}\cdot\nabla T = (\nabla^2 + R_i)T + \frac{N_B}{Le}\nabla\phi\cdot\nabla T + \frac{N_A N_B}{Le}\nabla T\cdot\nabla T \tag{10}$$

$$\frac{1}{\gamma}\frac{\partial \phi}{\partial \tau} + \frac{1}{\varepsilon_p}\mathbf{v}\cdot\nabla\phi = \frac{1}{Le}\nabla^2\phi + \frac{N_A}{Le}\nabla^2 T \tag{11}$$

$$\mathbf{v} = 0, \quad T = 1, \quad \phi = 0 \quad \text{at } z = 0 \quad \text{and} \quad \mathbf{v} = 0, \quad T = 0, \quad \phi = 1 \quad \text{at } z = 1 \tag{12}$$

where $g_m = (1 + \epsilon\cos(\Omega t))$. The non-dimensionlized parameters in the above equations are given in nomenclature, N_A is the modified diffusivity ratio, which is similar to the Soret parameter that arises in cross diffusion in thermal instability.

2.1. Conduction State

At the basic state, the nanofluid is assumed to be at rest, therefore the quantities at the basic state will vary only in z-direction, and are given by:

$$\mathbf{v} = 0, \quad p = p_b(z), \quad T = T_b(z), \quad \phi = \phi_b(z) \tag{13}$$

Substituting Eq. (13) in Eqs. (10) and (11), we get:

$$\frac{d^2T_b}{dz^2}+R_iT_b+\frac{N_B}{Le}\frac{d\phi_b}{dz}\frac{dT_b}{dz}+\frac{N_AN_B}{Le}\left(\frac{dT_b}{dz}\right)^2=0 \quad (14)$$

Using order magnitude analysis, Tzou[15, 16] showed that the second and third terms in Eq. (14) are small, and hence we have:

$$\frac{d^2T_b}{dz^2}+R_iT_b=0, \quad \frac{d^2\phi_b}{dz^2}=0 \quad (15)$$

The boundary conditions for solving Eq. (15) can be obtained from Eq. (12) as:

$$T_b=1, \quad \phi_b=0 \quad \text{at } z=0 \quad (16)$$

$$T_b=0, \quad \phi_b=1 \quad \text{at } z=1 \quad (17)$$

Solving the Eq. (15), subject to the conditions, Eqs. (16) and (17), we obtain:

$$T_b=\frac{\sin\sqrt{R_i}(1-z)}{\sin\sqrt{R_i}} \quad (18)$$

$$\phi_b=z \quad (19)$$

2.2. Perturbed State/Dimensionless Governing Equations

We now superimpose perturbations on the basic state given in Eq. (13):

$$\mathbf{v}=\mathbf{v}', \quad p=p_b+p', \quad T=T_b+T', \quad \phi=\phi_b+\phi' \quad (20)$$

Substituting the above expression (20) in Eqs. (8)–(11) and using the expressions (18) and (19), eliminating the pressure and introducing the stream functions, we obtain:[25, 26]

$$\frac{1}{Va}\frac{\partial}{\partial\tau}(\nabla^2\psi)+\nabla^2\psi=\left(Rn\frac{\partial\phi}{\partial x}-Ra\frac{\partial T}{\partial x}\right)g_m\vec{k} \quad (21)$$

$$-\frac{\partial T_b}{\partial z}\frac{\partial\psi}{\partial x}-(\nabla^2+Ri)T=-\frac{\partial T}{\partial\tau}+\frac{\partial(\psi,T)}{\partial(x,z)} \quad (22)$$

$$-\frac{1}{\varepsilon_p}\frac{\partial\psi}{\partial x}-\frac{N_A}{Le}\nabla^2T=\frac{1}{Le}\nabla^2\phi-\frac{1}{\gamma}\frac{\partial\phi}{\partial\tau}+\frac{1}{\varepsilon_p}\frac{\partial(\psi,\phi)}{\partial(x,z)} \quad (23)$$

3. LINEAR STABILITY

Here we study the linear stability analysis considering marginal and over-stable states. To perform linear stability analysis we neglect nonlinear term in Eqs. (21) to (23) thus we get linear system of equations.

$$\frac{1}{Va}\frac{\partial}{\partial\tau}(\nabla^2\psi)+\nabla^2\psi=\left(Rn\frac{\partial\phi}{\partial x}-Ra\frac{\partial T}{\partial x}\right)g_m\vec{k} \quad (24)$$

$$-\frac{\partial T_b}{\partial z}\frac{\partial\psi}{\partial x}-(\nabla^2+Ri)T=-\frac{\partial T}{\partial\tau} \quad (25)$$

$$-\frac{1}{\varepsilon_p}\frac{\partial\psi}{\partial x}-\frac{N_A}{Le}\nabla^2T=\frac{1}{Le}\nabla^2\phi-\frac{1}{\gamma}\frac{\partial\phi}{\partial\tau} \quad (26)$$

Eliminating T and ϕ from Eqs. (24) to (26) after elimination process we get single equation for ψ in the form

$$\left(\frac{1}{Va}\frac{\partial}{\partial\tau}+1\right)\left(\nabla^2+Ri-\frac{\partial}{\partial\tau}\right)\left(\frac{1}{Le}\nabla^2-\frac{1}{\gamma}\frac{\partial}{\partial\tau}\right)\nabla^2\psi$$
$$=-\frac{\partial^2}{\partial x^2}Rn\left[\frac{1}{\varepsilon_p}\left(\nabla^2+Ri-\frac{\partial}{\partial\tau}\right)-\frac{N_A}{Le}\nabla^2\frac{\partial T_b}{\partial z}\right]g_m\psi$$
$$+Ra\frac{\partial^2}{\partial x^2}\left[\left(\frac{1}{Le}\nabla^2-\frac{1}{\gamma}\frac{\partial}{\partial\tau}\right)\frac{\partial T_b}{\partial z}\right]g_m\psi \quad (27)$$

3.1. Method of Solution

We obtain the perturbation technique to obtain eigen functions ψ and eigen values Ra by introducing a small perturbation parameter ϵ.[23, 24]

$$\begin{cases}\psi=\psi_0+\epsilon\psi_1+\epsilon^2\psi_2+\cdots\\ Ra=Ra_0+\epsilon^2Ra_2+\cdots\end{cases} \quad (28)$$

Substituting the Eq. (28) into Eq. (27) and equating like powers of ϵ on both sides, we get:

$$L\psi_0=0 \quad (29)$$

$$L\psi_1=Rn\frac{\partial^2}{\partial x^2}\left[-\frac{1}{\varepsilon_p}\left(\nabla^2+Ri-\frac{\partial}{\partial\tau}\right)+\frac{N_A}{Le}\nabla^2\frac{\partial T_b}{\partial z}\right]$$
$$\times\psi_0\cos(\Omega\tau)+Ra_0\frac{\partial^2}{\partial x^2}\left[\left(\frac{1}{Le}\nabla^2-\frac{1}{\gamma}\frac{\partial}{\partial\tau}\right)\frac{\partial T_b}{\partial z}\right]$$
$$\times\psi_0\cos(\Omega\tau) \quad (30)$$

$$L\psi_2=Rn\frac{\partial^2}{\partial x^2}\left[-\frac{1}{\varepsilon_p}\left(\nabla^2+Ri-\frac{\partial}{\partial\tau}\right)+\frac{N_A}{Le}\nabla^2\frac{\partial T_b}{\partial z}\right]$$
$$\times\psi_1\cos(\Omega\tau)+\frac{\partial^2}{\partial x^2}\left[\left(\frac{1}{Le}\nabla^2-\frac{1}{\gamma}\frac{\partial}{\partial\tau}\right)\frac{\partial T_b}{\partial z}\right]$$
$$\times(Ra_0\psi_1\cos(\Omega\tau)+Ra_2\psi_0) \quad (31)$$

where

$$L=\left(\frac{1}{Va}\frac{\partial}{\partial\tau}+1\right)\left(\nabla^2+Ri-\frac{\partial}{\partial\tau}\right)\left(\frac{1}{Le}\nabla^2-\frac{1}{\gamma}\frac{\partial}{\partial\tau}\right)\nabla^2$$
$$-\frac{\partial^2}{\partial x^2}Rn\left[-\frac{1}{\varepsilon_p}\left(\nabla^2+Ri-\frac{\partial}{\partial\tau}\right)+\frac{N_A}{Le}\nabla^2\frac{\partial T_b}{\partial z}\right]$$
$$-Ra_0\frac{\partial^2}{\partial x^2}\left[\left(\frac{1}{Le}\nabla^2-\frac{1}{\gamma}\frac{\partial}{\partial\tau}\right)\frac{\partial T_b}{\partial z}\right] \quad (32)$$

3.2. Zeroth Order System

We now assume the marginally stable solutions for Eq. (29) in the form

$$\psi_0=\sin(\alpha x)\sin(\pi z) \quad (33)$$

Since ψ is independent of y therefore α is the wave number in x direction, the corresponding eigen values are given by

$$Ra_0=\left(\frac{\delta^2(\delta^2-Ri)(4\pi^2-Ri)}{4\pi^2\alpha^2}\right)$$
$$-Rn\left(\frac{Le(\delta^2-Ri)(4\pi^2-Ri)}{\varepsilon_p4\pi^2\delta^2}+N_A\right) \quad (34)$$

where $\delta^2 = \pi^2 + \alpha^2$. In the absence of internal heat, the expression of Ra_0 similar with the result of Umavathi.[22] We note that Ra_0 attains its critical value, Ra_{0c} at $\alpha = \pi$.

3.3. First Order System

Using Eq. (33) in Eq. (30) we have,

$$L\psi_1 = Rn\alpha^2\left[\left(\frac{Ri-\delta^2}{\varepsilon_p}+\frac{N_A}{Le}I_1\delta^2\right)\cos(\Omega\tau) + \frac{\Omega}{\varepsilon_p}\sin(\Omega\tau)\right]\sin(\alpha x)\sin(\pi z) + Ra_0\alpha^2 I_1\left[\left(\frac{\delta^2}{Le}\cos(\Omega\tau)-\frac{\Omega}{\gamma}\sin(\Omega\tau)\right)\right] \times \sin(\alpha x)\sin(\pi z) \quad (35)$$

where $I_1 = \int_0^1\int_0^{\pi/\alpha}(\partial T_b/\partial z)\sin^2(\alpha x)\sin^2(\pi z)\,dx\,dz = -(\pi^3/\alpha)/(4\pi^2 - Ri)$. The solution of the homogeneous equation corresponding to the Eq. (35), one must have a term which is orthogonal to $\sin(\alpha x)\sin(\pi z)$. Note that we already apply the theory of minimal Rayleigh number therefore right hand side of Eq. (35) is complete orthogonal function to $\sin(\alpha x)\sin(\pi z)$. Using (32) we find that

$$L[\sin(\pi z)\exp^{(i\alpha x - i\Omega\tau)}] = L(\Omega)\sin(\pi z)\exp^{(i\alpha x - i\Omega\tau)} \quad (36)$$

where $L(\Omega) = A + iB$

$$A = \Omega^2\left(\frac{\delta^2}{\gamma}\left(1+\frac{\delta^2-Ri}{Va}\right)+\frac{\delta^4}{LeVa}\right) + Rn\alpha^2\left(\frac{\delta^2-Ri}{\varepsilon_p}-\frac{N_A}{Le}I_1\delta^2\right) - Ra_0\alpha^2\frac{1}{Le}I_1\delta^2 - \frac{\delta^4}{Le}\left(\delta^2-Ri\right)$$

$$B = \Omega\left[Ra_0\alpha^2\frac{I_1}{\gamma} - Rn\frac{\alpha^2}{\varepsilon_p} + \frac{\delta^2}{\gamma}\left(\delta^2 - Ri - \frac{\Omega^2}{Va}\right) + \frac{\delta^4}{Le}\left(1+\frac{\delta^2-Ri}{Va}\right)\right]$$

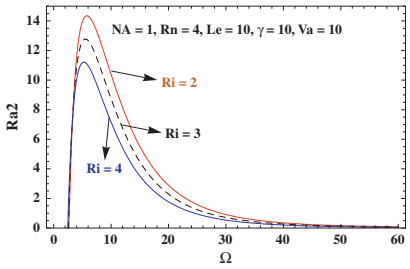

Fig. 2. Ra_2 versus Ω for different values of Ri.

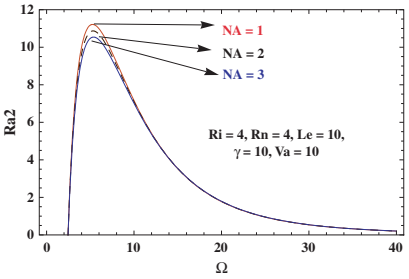

Fig. 3. Ra_2 versus Ω for different values of NA.

Hence we obtain ψ_1, by inverting the operator L in the following form

$$\psi_1 = Re\left[\frac{L^*(\Omega)}{|L(\Omega)|^2}F_1(\tau)\sin(\alpha x)\sin(\pi z)\right] \quad (37)$$

where $L^*(\Omega)$ is the complex conjugate of $L(\Omega)$.

$$F_1(\tau) = Rn\alpha^2\left\{\left(\frac{Ri-\delta^2}{\varepsilon_p}+\frac{N_A}{Le}I_1\delta^2\right)\cos(\Omega\tau)+\frac{\Omega}{\varepsilon_p}\sin(\Omega\tau)\right\} + Ra_0\alpha^2 I_1\left\{\left(\frac{\delta^2}{Le}\cos(\Omega\tau)-\frac{\Omega}{\gamma}\sin(\Omega\tau)\right)\right\}$$

3.4. Second Order System

From the Eq. (31) we get:

$$L\psi_2 = \left[Ra_0\alpha^2 I_1\frac{\delta^2}{Le} - Rn\alpha^2\left(\frac{\delta^2-Ri}{\varepsilon_p}-\frac{N_A}{Le}I_1\delta^2\right)\right] \times \psi_1\cos(\Omega\tau) + \left[Ra_0\alpha^2\frac{1}{\gamma} - Rn\frac{\alpha^2}{\varepsilon_p}\right] \times (\psi_1\cos(\Omega\tau))' + Ra_2\alpha^2 I_1\frac{\delta^2}{Le}\psi_0 \quad (38)$$

We will not solve the Eq. (38), but using this equation we determine Ra_2. For the existence of a solution of the

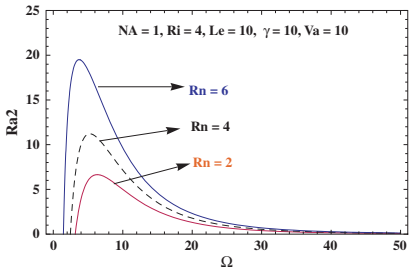

Fig. 4. Ra_2 versus Ω for different values of Rn.

ARTICLE

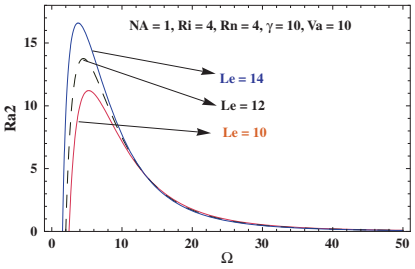

Fig. 5. Ra_2 versus Ω for different values of Le.

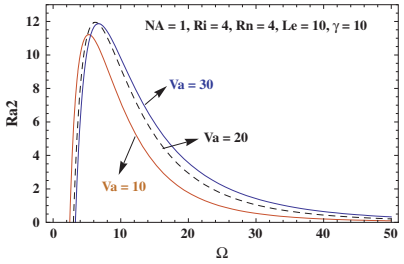

Fig. 7. Ra_2 versus Ω for different values of Va.

Eq. (38), it is necessary that, the steady part of its right hand side must orthogonal to $\sin(\alpha x)\sin(\pi z)$. This gives,

$$\int_0^1\int_0^{\pi/\alpha}\left[\left\{Ra_0\alpha^2 I_1\frac{\delta^2}{Le}-Rn\alpha^2\left(\frac{\delta^2-Ri}{\varepsilon_p}-\frac{N_A}{Le}I_1\delta^2\right)\right\}\times\overline{\psi_1\cos(\Omega\tau)}+\left\{Ra_0\alpha^2\frac{1}{\gamma}-Rn\frac{\alpha^2}{\varepsilon_p}\right\}\times\overline{(\psi_1\cos(\Omega\tau))'}+Ra_2\alpha^2 I_1\frac{\delta^2}{Le}\psi_0\right]\times\sin(\alpha x)\sin(\pi z)\,dx\,dz \quad (39)$$

where the upper bar denotes the time average.

$$Ra_2=-\left(LeA\alpha^2\left[Ra_0 I_1\frac{\delta^2}{Le}-Rn\left(\frac{\delta^2-Ri}{\varepsilon_p}-\frac{N_A}{Le}I_1\delta^2\right)\right]^2\right)\times(2I_1\delta^2(A^2+B^2))^{-1} \quad (40)$$

4. NONLINEAR STABILITY

Assuming Fourier expressions (following the studies of Bhadauria and Agarwal,[18] Agarwal et al.[44]) for the physical variables such as stream function, temperature and nanoparticle fraction, a local nonlinear stability analysis is performed. We take the modes (1, 1) for stream function, and (0, 2) and (1, 1) for temperature and nanoparticle concentration, thus using a severely truncated representation of Fourier series for stream function, temperature and nanoparticle concentration.[41,42] This study will help in understanding the physics of the problem with minimum mathematical expressions. Further, the results can be used as starting point to generalize it for full nonlinear problem. Also, it is to be noted that the effect of nonlinearity is to distort the temperature and concentration fields through the interaction of ψ and T, and ψ and ϕ respectively. As a result a component of the form $\sin(2\pi z)$ will be generated. Therefore the minimal expression which describes the finite amplitude convection is of the form

$$\psi=A_{11}(\tau)\sin(\alpha x)\sin(\pi z) \quad (41)$$

$$T=B_{11}(\tau)\cos(\alpha x)\sin(\pi z)+B_{02}(\tau)\sin(2\pi z) \quad (42)$$

$$\phi=C_{11}(\tau)\cos(\alpha x)\sin(\pi z)+C_{02}(\tau)\sin(2\pi z) \quad (43)$$

where the amplitudes $A_{11}(\tau)$, $B_{11}(\tau)$, $B_{02}(\tau)$, $C_{11}(\tau)$ and $C_{02}(\tau)$ are functions of time and to be determined. Substituting Eqs. (41)–(43) in Eqs. (21)–(23), taking the orthogonality condition with the eigenfunctions associated with the considered minimal mode, we get:

$$\frac{dA_{11}(\tau)}{d\tau}=\frac{Va}{\delta^2}[\alpha(1+\epsilon\cos(\Omega t))\times[RnC_{11}(\tau)-RaB_{11}(\tau)]-\delta^2A_{11}(\tau)] \quad (44)$$

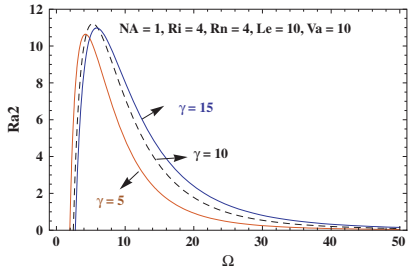

Fig. 6. Ra_2 versus Ω for different values of γ.

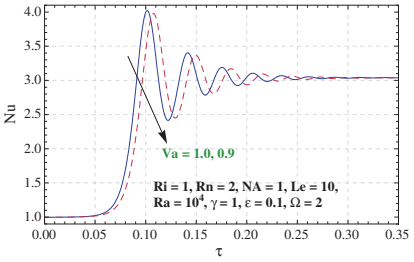

Fig. 8. Nu versus τ for different values of Va.

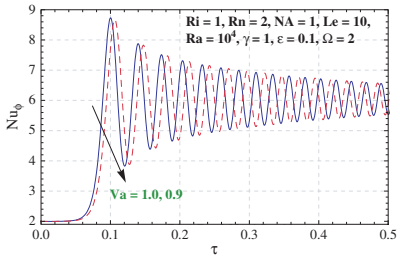

Fig. 9. Nu_ϕ versus τ for different values of Va.

$$\frac{dB_{11}(\tau)}{d\tau} = -\left[\frac{4\pi^2 a}{(4\pi^2 - Ri)}A_{11}(\tau) + (\delta^2 - Ri)B_{11}(\tau) + \pi\alpha A_{11}(\tau)B_{02}(\tau)\right] \quad (45)$$

$$\frac{dB_{02}(\tau)}{d\tau} = \frac{\pi\alpha}{2}A_{11}(\tau)B_{11}(\tau) - (4\pi^2 - Ri)B_{02}(\tau) \quad (46)$$

$$\frac{1}{\gamma}\frac{dC_{11}(\tau)}{d\tau} = -\left[\frac{\alpha}{\varepsilon_p}A_{11}(\tau) + \frac{1}{Le}\delta^2 C_{11}(\tau) + \frac{\pi\alpha}{\varepsilon_p}A_{11}(\tau)C_{02}(\tau) + \frac{N_A}{Le}\delta^2 B_{11}(\tau)\right] \quad (47)$$

$$\frac{1}{\gamma}\frac{dC_{02}(\tau)}{d\tau} = \frac{\pi\alpha}{2\varepsilon_p}A_{11}(\tau)C_{11}(\tau) - \frac{4\pi^2}{Le}[C_{02}(\tau) + N_A B_{02}(\tau)] \quad (48)$$

The above system of simultaneous autonomous ordinary differential equations can be subsequently solved numerically using Mathematica NDSolve.

5. HEAT AND NANOPARTICLE CONCENTRATION TRANSPORT

The thermal Nusselt number, $Nu(\tau)$ is defined as

$$Nu(\tau) = \frac{\text{Heat transport by (conduction + convection)}}{\text{Heat transport by conduction}} = 1 + \left[\frac{\int_0^{2\pi/\alpha_c}(\partial T/\partial z)\,dx}{\int_0^{2\pi/\alpha_c}(\partial T_b/\partial z)\,dx}\right]_{z=0} \quad (49)$$

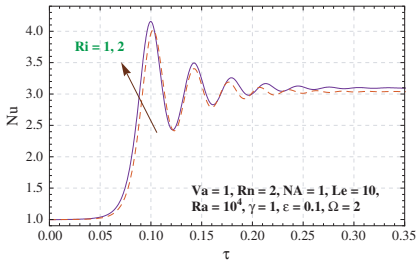

Fig. 10. Nu versus τ for different values of Ri.

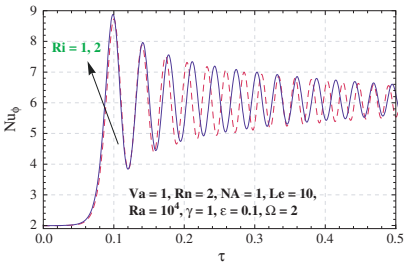

Fig. 11. Nu_ϕ versus τ for different values of Ri.

Substituting Eqs. (18) and (42) in Eq. (49), we get

$$Nu(\tau) = 1 - 2\pi B_{02}(\tau) \quad (50)$$

The nanoparticle concentration Nusselt number, $Nu_\phi(\tau)$ is defined similar to the thermal Nusselt number.

$$Nu_\phi(\tau) = (1 - 2\pi C_{02}(\tau)) + N_A(1 - 2\pi B_{02}(\tau)) \quad (51)$$

6. RESULTS AND DISCUSSION

The increasing effect of thermal conductivity are important in improving the heat transfer behavior of fluids. In this scenario it is also important to regulate heat transfer. A number of other variables also play key roles. For example, the heat transfer coefficient for convection depends on many physical quantities related to the fluid or the geometry of the system through which the fluid is flowing. This geometry of the flow ultimate cause of flow models and its external applied modulations too. These quantities include constitutional properties of the fluid such as its thermal conductivity, density, specific heat, and viscosity, along with system parameters such as diameter and length, modulation parameters and average fluid velocity. Therefore, it is important to measure the heat transfer performance of nanofluids directly under flow conditions. With this concept the present article investigate such a parameters which control heat transfer fluctuations in the medium. Especially the effect of modulation and internal heating of

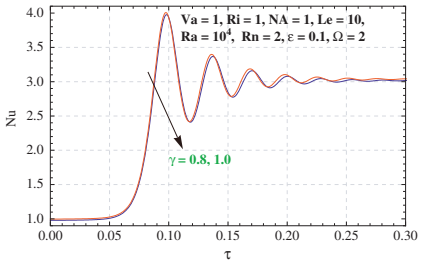

Fig. 12. Nu versus τ for different values of γ.

ARTICLE

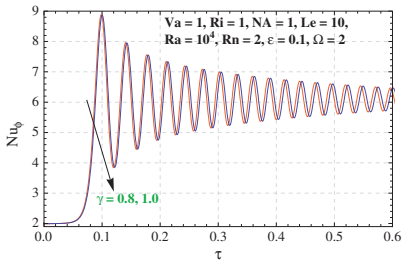

Fig. 13. Nu_ϕ versus τ for different values of γ.

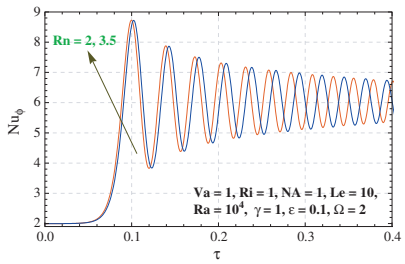

Fig. 15. Nu_ϕ versus τ for different values of Rn.

the medium on heat and concentration transport is investigated. Linear and nonlinear models being considered to see both onset and transport phenomenon in the medium. The linear stability solutions obtained Venezian approach. The expressions for the critical Rayleigh number for different realistic values of the non dimensional parameters such as Lewis number, concentration Rayleigh number, Vadász number, heat capacity ratio, internal Rayleigh number and modified diffusivity ratio are computed, and the results are depicted in Figures 2–7.

The Darcy model was employed for the porous medium while considering top heavy porus layer. A linear theory has been investigated by Umavathi,[22] concerning temperature modulation, Pranesh et al.[23] performed gravity modulation using Venezian model.[24] It is well known that, we make a nonlinear theory to analyze heat/mass transport, which is not possible by linear stability theory. Moreover external regulations of convection is important in the study of thermal instability, therefore, the gravity modulation is considered for either enhancing or inhibiting the convective heat/mass transport as is required by a real life application. According to Buongiorno,[13] for most of the nanofluids investigated so far with Le is large, but as per Bhadauria and Agarwal[18] and Umavathi,[22] we have considered $Le = 10$. The reason behind this may be to get proper results corresponding to the parameters of nonlinear model. The effect of gravity modulation on heat/mass transport has been depicted in Figures 8–23. The following parameters Va, Rn, N_A, Le, γ, ϵ and Ω are occurred in the present study, and influence the convective heat/mass transport. The first five parameters are related to the porous layer and the next two parameters concern the modulation. Because of small amplitude of modulation, the values of ϵ are considered to be small. Further, the gravity modulation assumed to be of low frequency, as at low range of frequencies, the effect of frequency on onset of convection as well as on heat/mass transport is maximum. The coefficient of heat transport, i.e., thermal Nusselt number and the coefficient of nanoparticle concentration transport, i.e., concentration Nusselt number are calculated as functions of time and other parameters of the system. The obtained results are depicted in the Figures 8–23 for $Nu(\tau)$ and $Nu_\phi(\tau)$ versus time τ. In the figures, the values of $Nu(\tau)$ and $Nu_\phi(\tau)$ start with 1 and 2 respectively, and remains constant for a quite some time, showing the conduction state. Then the values of $Nu(\tau)$ and $Nu_\phi(\tau)$ increase as time passes, thus showing that the convection is taking place. These values oscillates and then approach constant values thus showing that the steady state has been achieved.

Let us present results corresponding to linear stability, for this we have derived correction in Rayleigh number

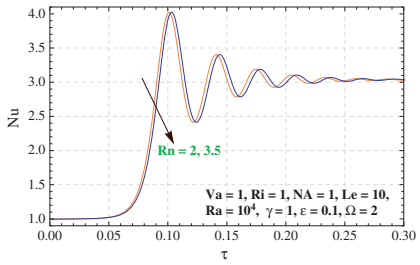

Fig. 14. Nu versus τ for different values of Rn.

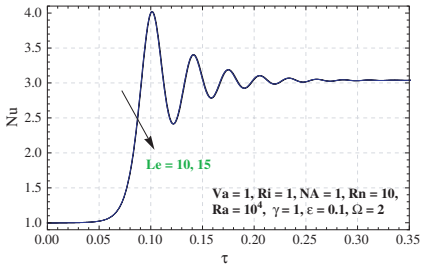

Fig. 16. Nu versus τ for different values of Le.

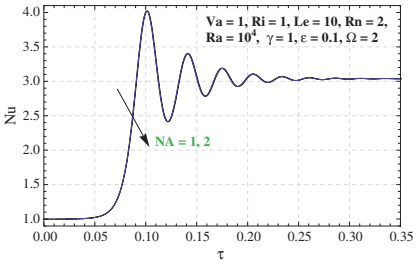

Fig. 17. *Nu* versus τ for different values of *NA*.

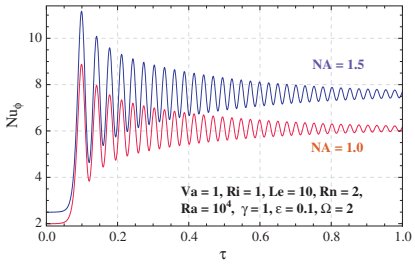

Fig. 19. Nu_ϕ versus τ for different values of *NA*.

as a function modulation frequency. It is examined that, how this correction Rayleigh number Ra_2 affected by the modulation frequency Ω. Figure 2 presents result corresponding to Ri, as Ri increases, $|Ra_2|$ decreases. The increment in Ri implies entropy of the system will increase. Thus, increase in Ri destabilizes the system. Figure 3 is the plot of Ra_2 versus Ω for different values of modified diffusivity ratio N_A. Upon increasing the value of N_A signifies that thermophoresis effect will increase, in result the value of $|Ra_2|$ decreases, thus destabilize the system. The Figure 4 show the effect of Rn. An increment in Rn represents an increment in concentration of suspended nanoparticles. We find that upon increasing Rn, the values of $|Ra_2|$ increases and thereby it stabilizes the system. This means that the fluids with suspended nanoparticles are more helpful to stabilization by modulation than ordinary fluids. Figure 5 is the plot of Ra_2 versus Ω for different values of Lewis number Le. We find from the figure that as Le increases $|Ra_2|$ increases and thus stabilizes the system. From the Figure 6 we observed that, for certain range of modulation frequency as γ increases Ra_2 increases but out of that range, the effect is reverse. Which shows γ has duel effect on thermal instability. For higher value of Ω the variation in heat capacity ratio is small and hence it stabilizes the system. Figure 7 is the plot of Ra_2 versus Ω for different values of Vadász number Va. It is observed that effect of Vadász number is similar to γ. From the above one may conclude that, the system destabilizes for lower values of Ω and stabilizes for larger values of Ω. The results of the present model may be compared with the studies of Umavathi,[22] Pranesh et al.[23] and Bhadauria et al.[25, 26]

Now let us discuss the results related to nonlinear system. From the Figures 8 and 9, we find that initially when time τ is small, the vibrations become of high amplitudes as the value of Va increases, and so thermal Nusselt (Nu) and concentration Nusselt numbers (Nu_ϕ) increase, thus increasing the rate of heat and mass (nanoparticle concentration) transport. But at large values of time τ, the vibrations become smaller and subsequently the values of Nu and Nu_ϕ approach steady state values showing the system achieved it saturating stage. From the Figures 10 and 11, we observe that, the effect of internal Rayleigh number Ri is to enhance the heat/mass transport. This confirms the results obtained by Bhadauria et al.,[37] where internal heating of the system enhances the heat transfer. Also, we observed from the Figures 12 and 23 that the rates of mass transfer are more than the rate of heat transfer across the porous medium.

However, from the Figures 12 and 13, we find that as the value of thermal capacity ratio γ increases, the values of thermal Nusselt and concentration Nusselt numbers

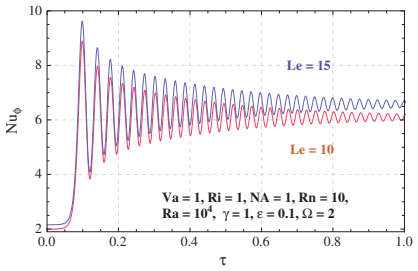

Fig. 18. Nu_ϕ versus τ for different values of *Le*.

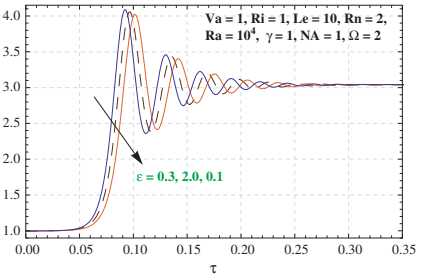

Fig. 20. *Nu* versus τ for different values of ϵ.

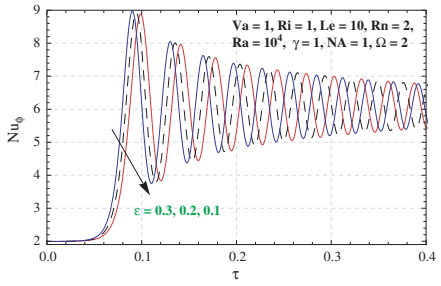

Fig. 21. *Nu* versus τ for different values of ϵ.

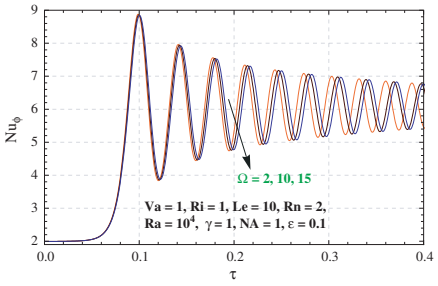

Fig. 23. *Nu* versus τ for different values of Ω.

decrease, thus decreasing the rate of heat and mass transport. Further, the influence of concentration Rayleigh number *Rn* on both thermal and concentration Nusselt number is found to enhance the heat and mass transport as given in Figures 14 and 15, which is due to the fact that the nanoparticle concentration is more at the top. From the Figures 16 and 17 it is found that effect of *Le* and N_A do not have significant effect on heat transport since these two parameters are related to nanofluid and conforms the results of Bhadauria et al.[18, 25, 26] On the contrary in the case of concentration Nusselt number, the effect of *Le* and N_A enhances mass transfer upon increasing them given in the Figures 18 and 19. The above corresponding results may be compared with the studies of Agarwal et al.[28] and Puneet et al.[30, 32]

Let us now discuss the effect of amplitude and frequency of modulation on heat and mass transfer. Figures 20 and 21 show that, the effect of amplitude of modulation ϵ on heat and concentration transport is to increase the values of *Nu* and Nu_ϕ and hence enhances the transport phenomena. Figures 22 and 23 show that, upon increasing the value of modulation frequency is to decrease heat and nanoparticle concentration upon increasing *Nu* and Nu_ϕ, and hence stabilize the system. Thus, we obtain the classical results as per Bhadauria and Kiran,[25, 26] Gresho and Sani.[43] It is observed in most of the cases that

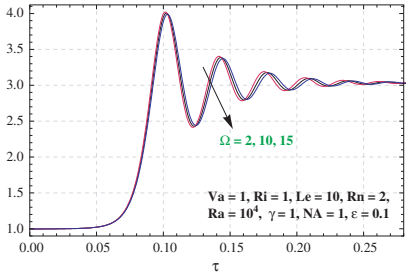

Fig. 22. *Nu* versus τ for different values of Ω.

there is much effect of parameters on *Nu* and Nu_ϕ at low values of time, but less effect at large values of time, since vibrations become smaller in magnitude, and disappears as *Nu*, Nu_ϕ reach steady state. Finally, the parameters *Va*, *Rn*, ϵ have destabilizing effects on the system, while γ, Ω have stabilizing effects. The parameters N_A, *Le* do not show any effect on *Nu*, but increases the value of Nu_ϕ. Also for heat/mass transfer results the reader may see the studies of Bhadauria et al.[26] and Kiran.[27]

7. CONCLUSIONS

We have investigated the effects of internal heating and gravity modulation on Bénard-Darcy convection in a horizontal porous layer saturated by a nanofluid, which is heated from below and cooled from above. Incorporating the effect of Brownian motion along with thermophoresis the linear and nonlinear theories being analyzed. The following conclusions are drawn from the previous analysis:

1. Low frequency of modulation show destabilization effect but, high frequency stabilize the system for *Va* and γ.
2. The effect of internal heating is to increase (destabilizes) the heat transport as well as nanoparticle concentration transport in the system.
3. Increment in concentration Rayleigh number *Rn*, modified diffusivity ratio N_A and Lewis number *Le* increases the effect of gravity modulation.
4. An increment in *Va* is to increase the values of $Nu(\tau)$ and $Nu_\phi(\tau)$ at small values of time τ but no effect at large time τ.
5. There is no significant effect of N_A and *Le* on heat transport.
6. Increasing *Le*, ϵ, N_A and *Rn* is to increase the concentration Nusselt number, whereas an increase in Ω decreases the same, and so the concentration transport.
7. Gravity modulation can be used to regulate the system effectively, whereas internal heating destabilize the system.

NOMENCLATURE

Latin Symbols		Unit
D_B	Brownian diffusion coefficient	m^2/sec
D_T	Thermophoretic diffusion coefficient	m^2/sec
Da	Darcy number, $Da = \frac{\bar{\mu}K}{\mu d^2}$	
$\mathbf{v}_D$	Darcy velocity	m/sec
d	Dimensional layer depth	m
Ri	Internal Rayleigh number, $R_i = \frac{Qd^2}{\kappa_T}$	
Rm	Basic density Rayleigh number, $Rm = \frac{[\rho_p\phi_0 + \rho(1-\phi_0)]g_0Kd}{\mu\kappa_T}$	
Rn	Concentration Rayleigh number, $Rn = \frac{(\rho_p - \rho)(\phi_1 - \phi_0)g_0Kd}{\mu\kappa_T}$	
Le	Lewis number, $Le = \frac{\kappa_T}{D_B}$	
(x^*, y^*, z^*)	Cartesian coordinates	m
N_A	Modified diffusivity ratio, $N_A = \frac{D_T(T_h - T_c)}{D_B T_c(\phi_1 - \phi_0)}$	
N_B	Modified particle-density increment, $N_B = \frac{(\rho c)_p(\phi_1 - \phi_0)}{(\rho c)_f}$	
$\vec{g}$	Modulated gravity field	m/sec^2
$\mathbf{v}$	Nanofluid velocity	m/sec
Pr	Pradtl number, $Pr = \frac{\mu}{\rho_f\ \kappa_T}$	
p	Pressure	kg/(m sec^2)
T	Temperature	K
T_h	Temperature at the lower wall	K
T_c	Temperature at the upper wall	K
k_m	Thermal conductivity of porous medium	W/mK
K	Permeability of porous medium	m^2
Ra	Thermal Rayleigh-Darcy number, $Ra = \frac{\rho g_0 \beta K d(T_h - T_c)}{\mu\kappa_T}$	
τ	Time	sec
Va	Vadász number, $Va = \frac{\varepsilon_p Pr}{Da}$	

Greek Symbols		Unit
ϵ	Amplitude of modulation	m
$(\rho c)_m$	Effective heat capacity of the porous medium	J/kgK
$(\rho c)_p$	Effective heat capacity of the nanoparticle material	J/kgK
$\bar{\mu}$	Effective viscosity of the porous medium	mPa s
ρ_f	Fluid density	kg/m^3
Ω	Frequency of modulation	sec^{-1}
$(\rho c)_f$	Heat capacity of the fluid	J/kgK
α	Horizontal wave number	
ρ_p	Nanoparticle mass density	kg/m^3
ε_p	Porosity	
β	Proportionality factor	K^{-1}
μ	Viscosity of the fluid	mPa sec
κ_T	Effective thermal diffusivity of the fluid	m^2/sec
γ	Heat capacity ratio $\frac{(\rho c)_m}{(\rho c)_f}$	
ν	Kinematic viscosity μ/ρ_f	m^{4}Pa sec/kg
ϕ	Nanoparticle volume fraction	
ψ	Stream function	m^2/sec

Subscripts

b Basic

Superscripts

$*$ Dimensional variable
$'$ Perturbation variable

Operators

$\nabla^2 \quad \frac{\partial^2}{\partial x^2} + \frac{\partial^2}{\partial y^2} + \frac{\partial^2}{\partial z^2}$

References and Notes

1. H. Masuda, A. Ebata, K. Teramae, and N. Hishinuma, *Netsu Bussei* 7, 227 (**1993**).
2. S. Choi, Development and Applications of Non-Newtonian Flows, edited by D. A. Siginer and H. P. Wang (**1995**), ASME FED 66, pp. 99–105.
3. S. Choi, Energy Technology Division, Argonne National Laboratory, Argonne (**1999**).
4. G. Chen, *Phys. Rev. Lett.* 86, 2297 (**2001**).

5. J. A. Eastman, S. U. S. Choi, W. Yu, and L. J. Thompson, *Appl. Phys. Lett.* 78, 718 (**2001**).
6. J. Buongiorno and W. Hu, *Proceedings of ICAPP05*, Seoul (**2005**), Vol. 15, p. 19.
7. C. Kleinstreuer, J. Li, and J. Koo, *Int. J. Heat Mass Transf.* 51, 5590 (**2005**).
8. K. Khanafer, K. Vafai, and M. Lightstone, *Int. J. Heat Mass Transf.* 46, 3639 (**2003**).
9. P. Keblinski and D. G. Cahill, *Phy. Rev. Lett.* 95, 209401 (**2005**).
10. P. Vadász, *ASME J. Heat Transf.* 128, 465 (**2006**).
11. J. A. Eastman, S. U. S. Choi, W. Yu, and L. J. Thompson, *Annu. Rev. Mater. Res.* 34, 219 (**2004**).
12. E. Abu-Nada, Z. Masoud, and A. Hijazi, *Int. Commun. Heat Mass Transf.* 35, 657 (**2008**).
13. J. Buongiorno, *ASME J. Heat Transf.* 128, 240 (**2006**).
14. J. Kim, Y. T. Kang, and C. K. Choi, *Phys. Fluids* 16, 2395 (**2004**).
15. D. Y. Tzou, *ASME J. Heat Transf.* 130, 072401 (**2008**).
16. D. Y. Tzou, *Int. J. Heat Mass Transf.* 51, 2967 (**2008**).
17. D. A. Nield and A. V. Kuznetsov, *J. Heat Transf.* 132, 052405 (**2010**).
18. B.S. Bhadauria and S. Agarwal, *Transp. Porous Media* 87, 585 (**2011**).
19. S. Agarwal, B. S. Bhadauria, and P. G. Siddheswar, *Special Top. Rev. Porous Media* 2, 53 (**2011**).
20. R. Chand and G. C. Rana, *Int. J. Heat Mass Transf.* 55, 5417 (**2012**).
21. D. Yadav, R. Bhargava, and G. S. Agrawal, *Int. J. Therm. Sci.* 60, 244 (**2012**).
22. J. C. Umavathi, *Transp. Porous Media* 98, 59 (**2013**).
23. S. Pranesh, S. Tarannum, and T. V. Joseph, *Journal of Advances in Mathematics* 3, 2347 (**2014**).
24. G. Venezian, *J. Fluid Mech.* 35, 243 (**1969**).
25. B. S. Bhadauria, P. Kiran, and M. Belhaq, *MATEC Web of Conferences* (**2014**), Vol. 16, p. 09003.
26. B.S. Bhadauria and P. Kiran, *Adv. Sci. Lett.* 20, 903 (**2014**).
27. P. Kiran, *Ain Shams Engineering Journal* (**2015**), doi:10.1016/j.asej.2015.06.005.
28. S. Agarwal, P. Rana, and B. S. Bhadauria, *ASME J. of Heat Transf.* 136, 122501 (**2014**).
29. D. A. Nield and A. V. Kuznetsov, *ASME J. of Heat Transf.* 137, 052601 (**2015**).
30. R. Puneet and S. Agarwal, *J. of Nanofluids* 4, 59 (**2015**).
31. S. Baag and S. R. Mishra, *J. of Nanofluids* 4, 352 (**2015**).
32. R. Puneet and A. Shilpi, *J. of Nanofluids* 4, 59 (**2015**).
33. I. S. Shivakumara and M. Dhananjaya, *J. of Nanofluids* 4, 402 (**2015**).
34. R. Chand and G. C. Rana, *J. of Nanofluids* 4, 196 (**2015**).
35. S. P. Bhattacharya and S. K. Jena, *Proceedings of ICAPP05*, Seoul (**2005**), p. 15.
36. Y. Tasaka and Y. Takeda, *Int. J. Heat and Mass Transf.* 48, 1164 (**2005**).
37. B. S. Bhadauria, I. Hashim, and P. G. Siddheshwar, *Transp. in Porous Media* 93, 21 (**2012**).
38. A. Srivastava, B. S. Bhadauria, P. G. Siddheshwar, and I. Hashim, *Transp. Porous Media* 99, 359 (**2013**).
39. A. V. Kuznetsov and D. A. Nield, *Transp. Porous Media* 81, 409 (**2010**).
40. D. A. Nield and A. V. Kuznetsov, *Transp. Porous Media* 98, 543 (**2013**).
41. G. Veronis, *J. of Fluid Mech.* 24, 545 (**1966**).
42. N. Rudraiah, I. S. Shivkumara, and R. Friedrich, *Int. J. of Heat Mass Transfer* 299, 1301 (**1986**).
43. P. M. Gresho and R. Sani, *J. of Fluid Mech.* 40, 783 (**1970**).
44. S. Agarwal and B. S. Bhadauria, *Transp. Porous Media* 90, 627 (**2011**).

Article

Advanced Science, Engineering and Medicine
Vol. 10, 1–8, 2018
www.aspbs.com/asem

Convective Motion in Nanofluid Under Variable Rotational Speed

B. S. Bhadauria* and Vineet Kumar

Department of Mathematics, School of Physical and Decision Sciences, Babasaheb Bhimrao Ambedkar University, Lucknow 226025, UP, India

This article deals with linear stability analysis of the convective motion in nanofluid saturated porous layer, under rotational speed modulation rotating about a vertical axis. The revised boundary conditions are used as they are more realistic because the values of temperature at the boundaries can be adjusted but not the concentration of nanoparticles, and so, the flux of nano-particle concentration is assumed to be constant at the boundaries. G. Venezian, *J. Fluid Mech.* 35, 243 (1969) approach has been adopted to execute the linear stability analysis. An alteration has been noticed in the critical Rayleigh number due to rotational speed modulation. The obtain results are depicted graphically, and discussed in details. It is observed that the modulated rotational speed inhibited to the rate of advection for different values of the modulation frequency.

Keywords: Nanofluid, Nusselt Numbers, Perturbation Method, Rotational Speed Modulation.

1. INTRODUCTION

During the last two decades, the nanofluids (the suspensions of nanometre size particles in the base fluid) are being used as heat transfer media due to their smart thermal conductivity over ordinary fluids as heat trafficking. The presence of very little quantity of nanoparticles in base fluids gives a drastic enhancement in the heat transfer characteristics of the fluids. This virtue of nanofluids highly depends on the thermo-physical properties of the base fluid and the suspended nanoparticles. Industrial, commercial, residential, medical and transportation are sectors where nanofluids are widely used.

The main aim of using nanofluids is the better thermal conductivity over regular fluid, which was first introduced by Masuda et al.[1] Choi[2] was the first to propose the term "nanofluid." Das et al.[3] reported 1–4% increment in the effective thermal conductivity in alumina/water nanofluids with 1–4% concentration of alumina. According to these reports, Buongiorno and Hu[4] suggested that the nanofluids can be used in advanced nuclear systems as a coolant.

Vadász[5] studied thermal lagging in nanoparticles to improve the surface area to the same volume ratio. For large amount of nanoparticles Wen and Ding[6] suggested a reduction in heat transfer in a nanofluid.

Buongiorno[7] develop a model for convective motion in nanofluids incorporating the effects of thermophoresis and Brownian diffusion. Further Nield and Kuznetsov[8] was revisited this problem based on convective motion in nanofluid for different types of non-dimensional parameters. Also Nield and Kuznetsov[9] and Chand and Rana[10] investigated the heat transfer mechanism in porous medium for different configuration. A study has been performed for the onset of convection in a rotating fluid layer under temperature modulation by Rauscher and Kelly.[11] Rotation speed modulation was the similar concept of the temperature-gravity modulation, but this is rare in literature. The effect of temperature modulation on the Rayleigh-Bénard instability and the effect of rotational speed modulation in the Taylor-Couette instability have been studied theoretically and experimentally by Walsh and Donnelly.[12] The most of studies, related with the rotating porous media saturated with a nanofluid, were rectified by Agarwal et al.,[13] Bhadauria and Agarwal[14] and Chand and Rana.[10]

Recently, Nield and Kuznetsov[15] in their revised model adopted a new set of boundary conditions, where it was assumed that at the boundaries nanoparticle flux is zero, and the nanoparticle fraction adjusts accordingly. Due to the absence of two opposing forces oscillatory mode of convection was ruled out. Agarwal[16] studied the convective

*Author to whom correspondence should be addressed.

motion in a porous layer saturated by a nanofluid rotating about z-axis, additional with new boundary conditions for nanoparticle fraction. Similar work has been done by Yadav et al.[17] for free–free, rigid–rigid and free-rigid boundaries. Linear as well as nonlinear stability analysis has been performed by Agarwal et al.[18] for the case of thermal non-equilibrium with same boundary conditions.

The present article is concerning with the study of the effect of rotational speed modulation on thermal instability in a porous medium saturated by a nanofluid and in place of fixed nanopartical fraction boundary conditions, the thermo-nanopartical flux boundary conditions have been introduced. The impact of the different parameters such as ω, ξ, Pr, Ta, Rn, Le, N_A, N_B, ε, and Da on thermal instability has been studied, and the modification in the critical Rayleigh number due to rotational speed modulation has been investigated. The physical behavior of these parameters has been depicted graphically.

2. GOVERNING EQUATION

Consider an infinite extent nanofluid saturated porous layer, having H distance apart heated from below. The boundaries are assumed to be impermeable and perfectly thermally conducting, the system is rotating periodically about z-axis with angular velocity Ω while the z-axis is extending vertically upward. The Coriolis effect has been taken into account by including the Coriolis force term in the momentum equation. In addition, the local thermal equilibrium between the fluid and solid has been considered, in addition to the Oberbeck-Boussinesq approximation has been employed, the governing equations to study the thermal instability in a nanofluid-saturated rotating porous medium are[15]

$$\nabla \cdot v_D = 0$$

$$\frac{\rho_f}{\varepsilon}\frac{\partial v_D}{\partial t} + \nabla p = \overline{\mu}\nabla^2 v_D - \frac{\mu}{K}v_D + \frac{2\rho_f}{\varepsilon}v_D \times \Omega + [\phi\rho_p + (1-\phi)\{\rho(1-\beta(T-T_c))\}]\vec{g} \quad (1)$$

$$\frac{(\rho c)_f}{(\rho c)_p}\left(\frac{\partial T}{\partial t} + v\cdot\nabla T\right) = \frac{\kappa_m}{(\rho c)_p}\nabla^2 T + \left[D_B\nabla\phi + \frac{D_T}{T_c}\nabla T\right].\nabla T$$

$$\frac{\partial \phi}{\partial t} + v\cdot\nabla\phi = D_B\nabla^2\phi + \frac{D_T}{T_c}\nabla^2 T$$

The Darcy velocity is denoted by v_D, T_h and T_C are the temperatures at the lower and upper walls respectively, such that $T_h > T_C$. The considered rotational speed, which is varying sinusoidally with respect to time, is defined as:

$$\Omega = \Omega_0(1 + \xi\cos(\omega t))\hat{k} \quad (2)$$

In Eq. (1), both Brownian transport and thermophoresis coefficients are time-independent. Let the temperature and flux of the nanoparticles to be constant at the boundaries, the boundary conditions are taken as

$$v = 0, \quad T = T_h, \quad D_B\frac{\partial\phi}{\partial z} + \frac{D_T}{T_c}\frac{\partial T}{\partial z} = 0, \quad \text{at } z = 0 \quad (3)$$

$$v = 0, \quad T = T_c, \quad D_B\frac{\partial\phi}{\partial z} + \frac{D_T}{T_c}\frac{\partial T}{\partial z} = 0, \quad \text{at } z = H \quad (4)$$

The dimensionless variables are considered as given below:

$$(x^*, y^*, z^*) = \frac{(x, y, z)}{H}, \quad (u^*, v^*, w^*) = \frac{(u, v, w)H}{\kappa_T},$$
$$t^* = t\frac{\kappa_T}{\sigma H^2}, \quad p^* = p\frac{K}{\mu\kappa_T}, \quad \phi^* = \frac{\phi - \phi_0}{\phi_0}$$
$$\text{and } T^* = \frac{T - T_c}{T_h - T_c}$$

where $\kappa_T = \kappa_m/(\rho c)_f$, $\sigma = (\rho c_p)_m/(\rho c_p)_f$, ϕ_0 is reference value for nanoparticle volume fraction. The non-dimensionalized governing equations along with boundary conditions are (after dropping the asterisk for simplicity)

$$\nabla\cdot v = 0 \quad (5)$$

$$\frac{Da}{\text{Pr}}\frac{\partial v}{\partial t} = -\nabla p + v + Da\nabla^2 v - (Rm - RaT + Rn\phi)\vec{k} + \sqrt{Ta}(1 + \xi\cos(\omega t))(v\times\hat{k}) \quad (6)$$

$$\frac{\partial T}{\partial t} + v\cdot\nabla T = \nabla^2 T + \frac{N_B}{Le}\nabla\phi\cdot\nabla T + \frac{N_A N_B}{Le}\nabla T\cdot\nabla T \quad (7)$$

$$\frac{1}{\sigma}\frac{\partial\phi}{\partial t} + \frac{1}{\varepsilon}v\cdot\nabla\phi = \frac{1}{Le}\nabla^2\phi + \frac{N_A}{Le}\nabla^2 T \quad (8)$$

$$\left.\begin{aligned} v = 0, \quad T = 1, \quad \frac{\partial\phi}{\partial z} + N_A\frac{\partial T}{\partial z} = 0, \quad \text{at } z = 0 \\ v = 0, \quad T = 0, \quad \frac{\partial\phi}{\partial z} + N_A\frac{\partial T}{\partial z} = 0, \quad \text{at } z = 1 \end{aligned}\right\} \quad (9)$$

The non-dimensionlized parameters in the above equations are as given below,

$$Rn = \frac{(\rho_p - \rho_f)gKH\phi_0}{\mu\kappa_T}, \quad Rm = \frac{\{\rho_p\phi_0 - \rho_f(1-\phi_0)\}gKH}{\mu\kappa_T},$$
$$Ra = \frac{\rho_f g\beta KH(T_h - T_c)}{\mu\kappa_T}, \quad Le = \frac{\kappa_T}{D_B},$$
$$N_A = \frac{D_T(T_h - T_c)}{D_B T_c\phi_0}, \quad N_B = \frac{\varepsilon(\rho c)_p}{(\rho c)_f}\phi_0,$$
$$\text{Pr} = \frac{\overline{\mu}\varepsilon(\rho c)_m}{\rho_f\kappa_m}, \quad Ta = \left(\frac{2K\Omega_0}{\nu\varepsilon}\right)^2, \quad Da = \frac{\overline{\mu}K}{\mu H^2}$$

2.1. Basic Solution

At the basic state the nanofluid is assumed to be at rest, and hence, the temperature and nanoparticle volume fraction vary in z-direction only. Therefore we have

$$v = 0, \quad p = p_B(z), \quad T = T_b(z), \quad \phi = \phi_B(z) \tag{10}$$

Using Eq. (10), Eqs. (7) and (8) reduce to

$$\frac{d^2T_b}{dz^2} + \frac{N_B}{Le}\frac{d\phi_b}{dz}\frac{dT_b}{dz} + \frac{N_AN_B}{Le}\left(\frac{dT_b}{dz}\right)^2 = 0 \tag{11}$$

$$\frac{d^2\phi_b}{dz^2} + N_A\frac{d^2T_b}{dz^2} = 0 \tag{12}$$

After integrating Eq. (12), subject to the boundary condition Eq. (9), we obtain

$$\frac{d\phi_b}{dz} + N_A\frac{dT_b}{dz} = 0 \tag{13}$$

Using Eq. (13), Eq. (11) reduces to

$$\frac{d^2T_b}{dz^2} = 0 \tag{14}$$

The solutions of Eqs. (13) and (14) subject to the boundary condition (9) are as follows

$$T_b = 1 - z \tag{15}$$

$$\phi_b = \phi_0 + N_A z \tag{16}$$

2.2. Stability Analysis

We now slightly perturb the all physical quantities on the basic state as given below:

$$v = v', \quad p = p_B + p', \quad T = T_b + T', \quad \phi = \phi_B + \phi' \tag{17}$$

substituting the expressions (17) into the Eqs. (5)–(9), and using (15) and (16), we obtain

$$\nabla \cdot v' = 0 \tag{18}$$

$$\left(\frac{Da}{\mathrm{Pr}}\frac{\partial}{\partial t} - Da\nabla^2 + 1\right)v' = -\nabla p' + RaT'\hat{k} - Rn\phi\hat{k} + \sqrt{Ta}(1 + \xi\cos(\omega t)) \times (v' \times \hat{k}) \tag{19}$$

$$\frac{\partial T'}{\partial t} + \frac{dT_b}{dz} + v' \cdot \nabla T' = \nabla^2 T' + \frac{N_B}{Le}(N_A\nabla(T' + T_b) \cdot \nabla(T' + T_b) + \nabla(T' + T_b) \cdot \nabla(\phi' + \phi_b)) \tag{20}$$

$$\frac{1}{\sigma}\frac{\partial \phi'}{\partial t} + \frac{1}{\varepsilon}\frac{d\phi_b}{dz}w' + \frac{1}{\varepsilon}v' \cdot \nabla\phi' = \frac{1}{Le}\nabla^2\phi' + \frac{N_A}{Le}\nabla^2 T' \tag{21}$$

$$v' = 0, \quad T' = 0, \quad \frac{\partial \phi'}{\partial z} + N_A\frac{\partial T'}{\partial z} = 0, \quad \text{at } z = 0, \quad \text{and at } z = 1 \tag{22}$$

The parameter Rm is absorbed in pressure term due to hydrostatic equilibrium. The nanoparticle flux is assuming zero at the boundaries indicates the absence of the two opposing forces responsible for the occurrence of the oscillatory mode of convection, hence oscillatory convection has been abdicated.

We consider the all physical quantities to be independent of y for two-dimensional convective rolls, we introduce the stream function ψ as $u = \partial\psi/\partial z$, $u = \partial\psi/\partial z$, $w = -\partial\psi/\partial x$, and taking curl of the momentum equation twice to eliminate the pressure term, the system of nonlinear perturbed equations is obtained as

$$-\left(\frac{Da}{\mathrm{Pr}}\frac{\partial}{\partial t} - Da\nabla^2 + 1\right)^2\frac{\partial \psi}{\partial x} = \left(\frac{Da}{\mathrm{Pr}}\frac{\partial}{\partial t} - Da\nabla^2 + 1\right)\nabla_1^2(RaT' - Rn\phi) + Ta(1 + \xi\cos(\omega t))^2\frac{\partial^2}{\partial z^2}\frac{\partial \psi}{\partial x} \tag{23}$$

$$\frac{\partial T}{\partial t} + \frac{\partial \psi}{\partial x} = \nabla^2 T + \frac{\partial(\psi, T)}{\partial(x, z)} \tag{24}$$

$$\frac{1}{\sigma}\frac{\partial \phi}{\partial t} - \frac{N_A}{\varepsilon}\frac{\partial \psi}{\partial x} = \frac{1}{Le}\nabla^2\phi + \frac{N_A}{Le}\nabla^2 T + \frac{1}{\varepsilon}\frac{\partial(\psi, \phi)}{\partial(x, z)} \tag{25}$$

$$\psi = \frac{\partial^2 \psi}{\partial z^2} = 0, \quad T = 0, \quad \frac{\partial \phi}{\partial z} + N_A\frac{\partial T}{\partial z} = 0 \quad \text{at } z = 0, \quad \text{and at } z = 1 \tag{26}$$

2.2.1. Linear Stability Analysis

The linear stability analysis is performed to bifurcate the stability, instability region and the marginal states. For this, we neglect nonlinear terms in Eqs. (23)–(25), thus we get a linear system of equations

$$-\left(\frac{Da}{\mathrm{Pr}}\frac{\partial}{\partial t} - Da\nabla^2 + 1\right)^2\frac{\partial \psi}{\partial x} = \left(\frac{Da}{\mathrm{Pr}}\frac{\partial}{\partial t} - Da\nabla^2 + 1\right)\nabla_1^2(RaT' - Rn\phi) + Ta(1 + \xi\cos(\omega t))^2\frac{\partial^2}{\partial z^2}\frac{\partial \psi}{\partial x} \tag{27}$$

$$\frac{\partial T}{\partial t} + \frac{\partial \psi}{\partial x} = \nabla^2 T + \frac{\partial(\psi, T)}{\partial(x, z)} \tag{28}$$

$$\frac{1}{\sigma}\frac{\partial \phi}{\partial t} - \frac{N_A}{\varepsilon}\frac{\partial \psi}{\partial x} = \frac{1}{Le}\nabla^2\phi + \frac{N_A}{Le}\nabla^2 T + \frac{1}{\varepsilon}\frac{\partial(\psi, \phi)}{\partial(x, z)} \tag{29}$$

$$\psi = \frac{\partial^2 \psi}{\partial z^2} = 0, \quad T = 0, \quad \frac{\partial \phi}{\partial z} + N_A\frac{\partial T}{\partial z} = 0 \quad \text{at } z = 0, \quad \text{and at } z = 1 \tag{30}$$

Eliminating T and ϕ from Eqs. (27)–(29), we get a single equation for ψ in the form and further we have

$$\left(\frac{\partial}{\partial t}-\nabla^2\right)\left(\frac{1}{\sigma}\frac{\partial}{\partial t}-\frac{1}{Le}\nabla^2\right)\times\left(\frac{Da}{\mathrm{Pr}}\frac{\partial}{\partial t}-Da\nabla^2+1\right)^2\nabla^2 w = Ra\left(\frac{Da}{\mathrm{Pr}}\frac{\partial}{\partial t}-Da\nabla^2+1\right)\left(\frac{1}{\sigma}\frac{\partial}{\partial t}-\frac{1}{Le}\nabla^2\right)\nabla_1^2 w + RnN_A\left(\frac{Da}{\mathrm{Pr}}\frac{\partial}{\partial t}-Da\nabla^2+1\right)\times\left(\frac{1}{\varepsilon}\frac{\partial}{\partial t}-\left(\frac{1}{Le}+\frac{1}{\varepsilon}\right)\nabla^2\right)\nabla_1^2 w + Ta\left(\frac{\partial}{\partial t}-\nabla^2\right)\times\left(\frac{1}{\sigma}\frac{\partial}{\partial t}-\frac{1}{Le}\nabla^2\right)(1+\xi\cos(\omega t))^2\frac{\partial^2 w}{\partial z^2} \quad (31)$$

The perturbation technique is applied to obtain eigen functions w and the corresponding eigenvalues Ra by introducing a small perturbation parameter ξ as follows[24]

$$w = w_0+\xi w_1+\xi^2 w_2+\cdots$$
$$Ra = Ra_0+\xi Ra_1+\xi^2 Ra_2+\cdots \quad (32)$$

Using expressions (32) into Eq. (31), and then equating the like powers of ξ on both sides, we get

$$\xi^0 : Lw_0 = 0 \quad (33)$$

$$\xi^1 : Lw_1 = Ra_1\left(\frac{Da}{\mathrm{Pr}}\frac{\partial}{\partial t}-Da\nabla^2+1\right)\left(\frac{1}{\sigma}\frac{\partial}{\partial t}-\frac{1}{Le}\nabla^2\right)\times\nabla_1^2 w_0 - 2Ta\left(\frac{\partial}{\partial t}-\nabla^2\right)\left(\frac{1}{\sigma}\frac{\partial}{\partial t}-\frac{1}{Le}\nabla^2\right)\times\cos(\omega t)\frac{\partial^2}{\partial z^2}w_0 \quad (34)$$

$$\xi^2 : Lw_2 = Ra_2\left(\frac{Da}{\mathrm{Pr}}\frac{\partial}{\partial t}-Da\nabla^2+1\right)\left(\frac{1}{\sigma}\frac{\partial}{\partial t}-\frac{1}{Le}\nabla^2\right)\times\nabla_1^2 w_0 - Ta\left(\frac{\partial}{\partial t}-\nabla^2\right)\left(\frac{1}{\sigma}\frac{\partial}{\partial t}-\frac{1}{Le}\nabla^2\right)\times\cos^2(\omega t)\frac{\partial^2}{\partial z^2}w_0 + Ra_1\left(\frac{Da}{\mathrm{Pr}}\frac{\partial}{\partial t}-Da\nabla^2+1\right)\times\left(\frac{1}{\sigma}\frac{\partial}{\partial t}-\frac{1}{Le}\nabla^2\right)\nabla_1^2 w_1 - 2Ta\left(\frac{\partial}{\partial t}-\nabla^2\right)\times\left(\frac{1}{\sigma}\frac{\partial}{\partial t}-\frac{1}{Le}\nabla^2\right)\cos(\omega t)\frac{\partial^2}{\partial z^2}w_1 \quad (35)$$

where

$$L = \left(\frac{\partial}{\partial t}-\nabla^2\right)\left(\frac{1}{\sigma}\frac{\partial}{\partial t}-\frac{1}{Le}\nabla^2\right)\times\left(\frac{Da}{\mathrm{Pr}}\frac{\partial}{\partial t}-Da\nabla^2+1\right)^2\nabla^2 - Ra\left(\frac{Da}{\mathrm{Pr}}\frac{\partial}{\partial t}-Da\nabla^2+1\right)\left(\frac{1}{\sigma}\frac{\partial}{\partial t}-\frac{1}{Le}\nabla^2\right)\nabla_1^2 - RnN_A\left(\frac{Da}{\mathrm{Pr}}\frac{\partial}{\partial t}-Da\nabla^2+1\right)\times\left(\frac{1}{\varepsilon}\frac{\partial}{\partial t}-\left(\frac{1}{Le}+\frac{1}{\varepsilon}\right)\nabla^2\right)\nabla_1^2 + Ta\left(\frac{\partial}{\partial t}-\nabla^2\right)\times\left(\frac{1}{\sigma}\frac{\partial}{\partial t}-\frac{1}{Le}\nabla^2\right)(1+\xi\cos(\omega t))^2\frac{\partial^2}{\partial z^2}$$

In the following sections, the above system is solved for different orders of ξ.

a. Lowest order system

Since, two dimensional dynamics is assumed to be independent of y direction, so, we take $w_0 = \sin(\alpha x)\sin(\pi z)$ for the marginally stable solutions, and the corresponding eigen values are obtained by using Eq. (33)

$$Ra_0 = \left(\frac{\delta^2(Da\delta^2+1)^2+Ta\pi^2\delta^2}{\alpha^2(Da\delta^2+1)}\right)-RnN_A Le\left(\frac{1}{Le}+\frac{1}{\varepsilon}\right) \quad (36)$$

where $\delta^2 = \pi^2+\alpha^2$.

b. First order system

We have

$$Lw_1 = Ra_1(Da\delta^2+1)\left(\frac{\delta^2}{Le}\right)\alpha^2 w_0 + 2Ta\pi^2(h_1\cos(\omega t)-h_2\sin(\omega t))w_0 \quad (37)$$

where $h_1 = (\delta^2/Le-\omega^2/\sigma)$ and $h_2 = \delta^2\omega(1/Le-1/\sigma)$. The solution of the homogeneous equation corresponding to Eq. (37) must have a term orthogonal to null space of operator L. Now, we apply the theory of minimal Rayleigh number, taking $Ra_1 = 0$, so that time dependent term on right hand side of equation Eq. (35) is complete orthogonal function to $\sin(\alpha x)\sin(\pi z)$. Using $w_0 = \sin(\alpha x)\sin(\pi z)$, we obtain

$$L[\sin(\pi z)\exp^{(i\alpha x+i\omega t)}] = L(\omega)\sin(\pi z)\exp^{(i\alpha x+i\omega t)} \quad (38)$$

where

$$L(\omega) = S_1+iS_2$$

$$S_1 = \frac{\delta^2}{Le}\left\{(Da\delta^2+1)\left(RnN_A Le\left(\frac{1}{Le}+\frac{1}{\varepsilon}\right)\right)-\delta^4(Da\delta^2+1)^2-Ta\pi^2\delta^2\right\} + \omega^2\left\{\frac{Da^2}{\mathrm{Pr}}\frac{\delta^2}{Le}+(Da\delta^2+1)^2\frac{\delta^2}{\sigma}+\frac{Ta\pi^2}{\sigma}+2\delta^2(Da\delta^2+1)\frac{Da}{\mathrm{Pr}}\left(\frac{1}{Le}+\frac{1}{\varepsilon}\right)-\alpha^2\frac{Da}{\mathrm{Pr}}\left(\frac{Ra_0}{\sigma}+\frac{RnN_A}{\varepsilon}\right)\right\}$$

$$S_1 = \omega\Bigg[\left(\delta^4(Da\delta^2+1)+Ta\pi^2\delta^2\right)\left(\frac{1}{Le}+\frac{1}{\varepsilon}\right) + 2\frac{Da}{\mathrm{Pr}}\frac{\delta^6}{Le}\times(Da\delta^2+1) - Ra_0\alpha^2\left(\frac{(Da\delta^2+1)}{\sigma}\frac{Da}{\mathrm{Pr}}\frac{\delta^2}{Le}\right) - RnN_A\alpha^2\left(\frac{Da\delta^2}{\mathrm{Pr}}\left(\frac{1}{Le}+\frac{1}{\varepsilon}\right)+\frac{(Da\delta^2+1)}{\varepsilon}\right) \times\omega^2\left\{\frac{Da^2\delta^2}{\mathrm{Pr}^2}\left(\frac{1}{Le}+\frac{1}{\varepsilon}\right)+2\frac{Da}{\mathrm{Pr}}\frac{(Da\delta^2+1)}{\sigma}\right\}\Bigg]$$

Now, w_1 is obtained by inverting the operator L term by term as follows

$$w_1 = 2Ta\pi^2 Re\left[\frac{L^*(\omega)}{|L(\omega)|^2}\{h_1\cos(\omega t) - h_2\sin(\omega t)\}\sin(\alpha x)\sin(\pi z)\right] \quad (39)$$

c. Second order system

From Eq. (35), we obtain

$$Lw_2 = Ra_2\alpha^2(Da\delta^2+1)\left(\frac{\delta^2}{Le}\right)w_0 + Ta\pi^2\left(\frac{\delta^4}{Le}\cos^2(\omega t)+\frac{\omega^2}{\sigma}\cos(2\omega t) - 2\omega\delta^2\left(\frac{1}{Le}-\frac{1}{\sigma}\right)\sin(2\omega t)\right)w_0 + 2Ta\pi^2\Bigg[H_1\frac{\delta^4}{Le}+\left\{H_2\left(\frac{\delta^4}{Le}-\frac{4\omega^2}{\sigma}\right) + 2H_1\delta^2\omega\left(\frac{1}{Le}-\frac{1}{\sigma}\right)\right\}\sin(2\omega t) \times\left\{H_1\left(\frac{\delta^4}{Le}-\frac{4\omega^2}{\sigma}\right)+2H_2\delta^2\omega\left(\frac{1}{Le}-\frac{1}{\sigma}\right)\right\} \times\cos(2\omega t)\Bigg]w_0 \quad (40)$$

where

$$H_1 = Ta\pi^2 Re\left[\frac{L^*(\omega)}{|L(\omega)|^2}h_1\right],$$

$$H_2 = -Ta\pi^2 Re\left[\frac{L^*(\omega)}{|L(\omega)|^2}h_2\right]$$

We shall not solve Eq. (40), but use it to determine Ra_2. For the existence of the solution of Eq. (40), it is necessary that the steady part of its right hand side is orthogonal to $\sin(\alpha x)\sin(\pi z)$, which yields

$$\int_0^1\int_0^{\pi/\alpha}\Bigg[Ra_2\alpha^2(Da\delta^2+1)\left(\frac{\delta^2}{Le}\right)w_0 + Ta\pi^2 \times\left(\frac{\delta^4}{Le}\overline{\cos^2(\omega t)}+\frac{\omega^2}{\sigma}\overline{\cos(2\omega t)} - 2\omega\delta^2\left(\frac{1}{Le}-\frac{1}{\sigma}\right)\overline{\sin(2\omega t)}\right)w_0 + 2Ta\pi^2 \times\Bigg[H_1\frac{\delta^4}{Le}+\left\{H_2\left(\frac{\delta^4}{Le}-\frac{4\omega^2}{\sigma}\right)+2H_1\delta^2\omega\left(\frac{1}{Le}-\frac{1}{\sigma}\right)\right\} \times\overline{\sin(2\omega t)}\left\{H_1\left(\frac{\delta^4}{Le}-\frac{4\omega^2}{\sigma}\right)+2H_2\delta^2\omega\left(\frac{1}{Le}-\frac{1}{\sigma}\right)\right\} \times\overline{\cos(2\omega t)}\Bigg]w_0\Bigg]\times\sin(\alpha x)\sin(\pi z)dxdz = 0 \quad (41)$$

where $\overline{f(t)}$ denotes the time average of $f(t)$. Simplifying the above equation, we obtain

$$Ra_2 = \frac{Ta\pi^2\delta^2}{2\alpha^2(Da\delta^2+1)}\left[1+2Ta\pi^2\left(\frac{\delta^4}{Le}+\frac{\omega^2}{\sigma}\right) \times Re\left[\frac{L^*(\omega)}{|L(\omega)|^2}\right]\right] \quad (42)$$

3. RESULTS AND DISCUSSION

In this article, we have studied the impact of rotational speed modulation on the onset of convection and estimated the heat transport in a nanofluid saturated porous medium by means of a linear stability analysis. The rotational speed modulation with revised boundary conditions has been considered for either increasing or decreasing the convective flow and heat transport as it is required in many real life applications in different fields of sciences and engineering.

The variation of the critical thermal Rayleigh number Ra_2 with frequency ω for different values of parameters is depicted in the Figures 2–9, it is found that the effect of rotation speed modulation is less at low frequency as the value of Ra_2 is small. The value of Ra_2 increases for intermediate values of ω, so the effect of modulation is more at intermediate values of the frequency. Thus, at intermediate values of the frequency, the onset of convection takes place a little late, and so the system is stabilized

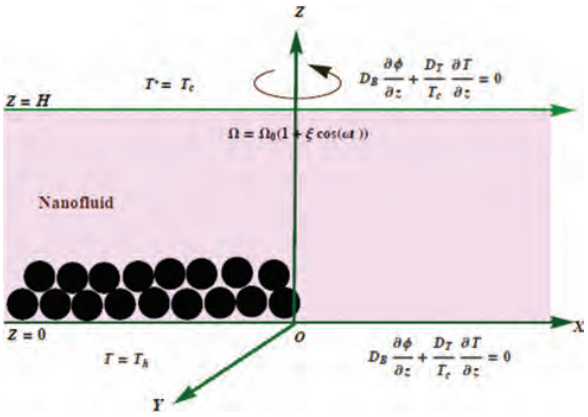

Figure 1. A sketch is showing physical configuration of problem.

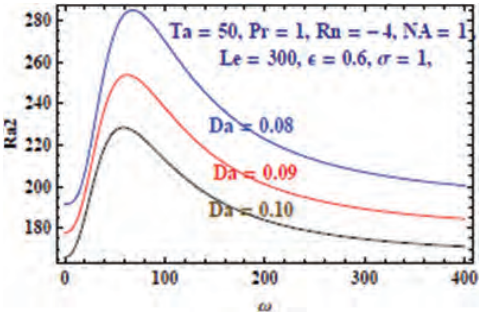

Figure 2. Ra_2 versus ω for different values of Da.

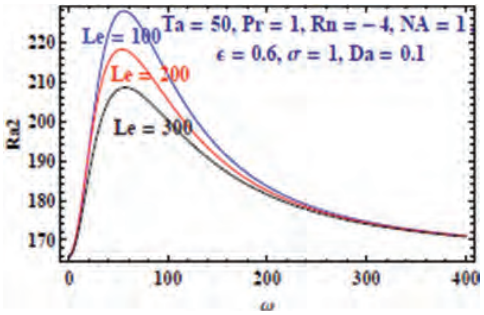

Figure 3. Ra_2 versus ω for different values of Le.

more in this range of frequency. Further, as the frequency ω increases, the effect of modulation diminishes and disappears altogether at very large values of ω. These results are compatible with the results of Venezian[24] in which the effect of thermal modulation at the boundaries has been studied, and where the variation in the critical value of the Rayleigh number due to temperature modulation becomes almost zero at high frequencies.

Figure 2 is the plot of Ra_2 versus ω for different values of Darcy number Da. It shows that Ra_2 decreases as Da increases, therefore the critical Rayleigh number decreases, and the onset of convective motion occur little early. Thus the system becomes less stabilized on increasing Da. Figure 3 shows the plot of Ra_2 versus ω for different values of Lewis number Le. It evident that as the value of Lewis number increases, the correction to thermal

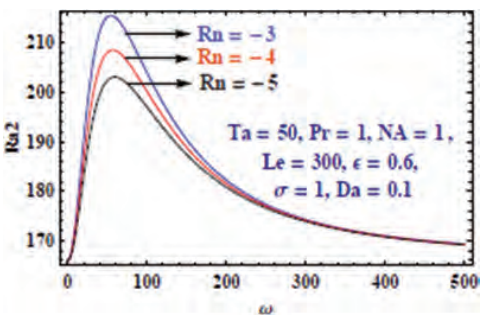

Figure 4. Ra_2 versus ω for different values of Rn.

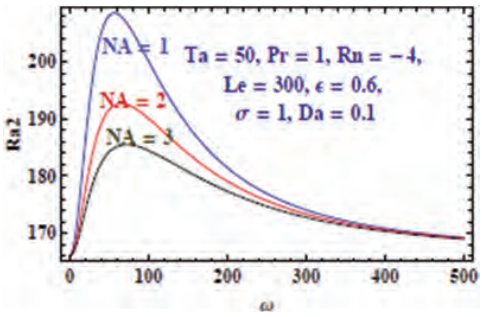

Figure 5. Ra_2 versus ω for different values of N_A.

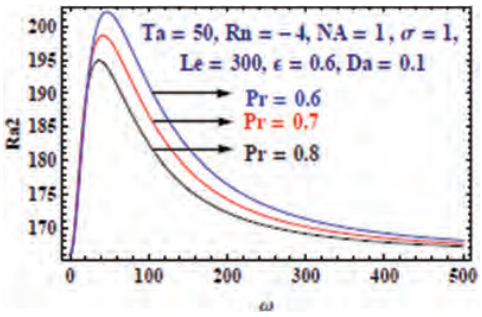

Figure 6. Ra_2 versus ω for different values of Pr.

Rayleigh number decreases, so convective motion occur at lower value of Ra_2, thus system is less stabilized. But this effect diminishes for the large number of frequency of modulation. In Figure 4 we depict Ra_2 versus ω for different values of nanoparticle Rayleigh number Rn. It is clear that as Rn increases, the concentration of suspended nanoparticles will increase, so the onset of convection will take place at higher value of Ra_2. Thus, we find that an increment in Rn increases Ra_2, thereby stabilizes the system more. This means that the fluids with suspended nanoparticles are more helpful to stabilization than ordinary fluids. Figure 5 is the plot for Ra_2 versus ω for different values of modified diffusivity ratio N_A. Increase in N_A signifies that the thermophoresis effect will increase. Now, when the thermophoresis effect increases, the onset of convection will occour early and so Ra_2 decreases as

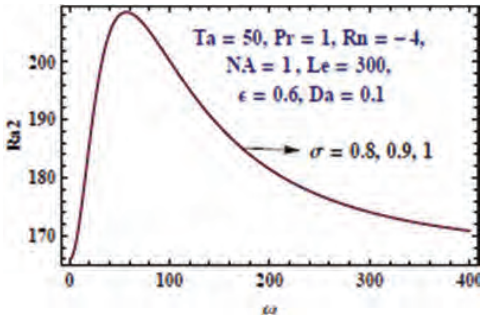

Figure 7. Ra_2 versus ω for different values of σ.

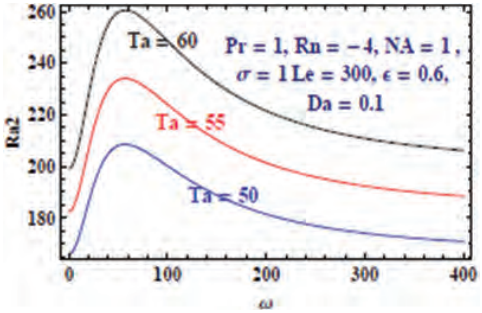

Figure 8. Ra_2 versus ω for different values of Ta.

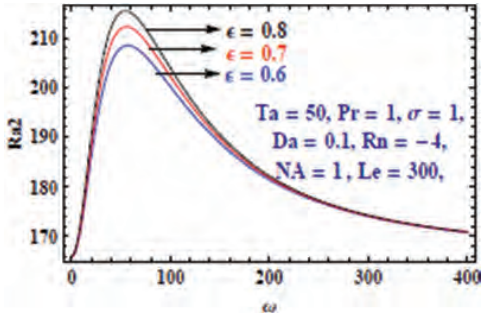

Figure 9. Ra_2 versus ω for different values of ε.

N_A increases, thus the system becomes less stabilizing. Figure 6 depicts variation of Ra_2 with ω for different values of the Prandtl Pr. This figure confirms that Ra_2 decreases as Prandtl number increases, thus onset of convection is advanced due to higher thermal conductivity. In Figure 7, Ra_2 versus ω is shown for different values of heat capacity ratio σ. As there is no significant change in the value of Ra_2, on increasing heat capacity ratio, therefore, the system is not much effected by this parameter. Figure 8 depicts Ra_2 versus ω for different values of Taylor number Ta. It is evident that as Taylor number increases, the correction in thermal Rayleigh number, Ra_2 also increases, implying that the effect of an increment in Ta is more stabilizing on the system. Figure 9 depicts the plot of Ra_2 versus ω for different values of porosity ε, which confirms that as porosity of the system increases, the thermal Rayleigh number also increases, so the convective motion is little late, and the system is stabilized.

4. CONCLUSION

In this article, we have studied convective motion in a horizontal porous layer saturated by a nanofluid, rotating about z-axis with time periodic angular velocity Ω. Darcy-Brinkman model with more realistic boundary conditions is considered, which intertwines the effects of Brownian motion along with thermophoresis. The results have been obtained in terms of thermal Rayleigh number. The obtained results for the various parameters depicted graphically. We have the following observations.

1. It is found that the rotational speed modulation can be used to regulate the heat and mass transports effectively.
2. The new boundary conditions has significant role on heat and mass transport due to this one can investigate heat and mass transfer in naofluid in precise way.
3. The obtained outcome for the concentration Rayleigh number Rn, Lewis number Le, modulation amplitude ξ, heat capacity ratio σ, modified diffusivity ratio N_A and Prandtl number Pr, is destabilizing for the system.
4. The effect of the porosity ε, modulation frequency ω, Taylor number Ta, and Darcy number Da stabilize the system.

Acknowledgments: Author Vineet Kumar gratefully acknowledges the financial assistance from UGC, New Delhi as a junior research fellowship (Award Letter "F 17-1/2006 (SA-1)").

References and Notes

1. H. Masuda, A. Ebata, K. Teramae, and N. Hishinuma, *Netsu Bussei* 7, 227 (**1993**).
2. S. Choi, *ASME FED 231/MD* 66, 99 (**1995**).
3. S. K. Das, N. Putra, P. Thiesen, and W. Roetzel, *ASME J. Heat Transfer* 125, 567 (**2003**).
4. J. Buongiorno and W. Hu, *Proceedings of ICAPP05*, Seoul, May (**2005**), p. 5705.
5. P. Vadász, *ASME J. Heat Transf.* 128, 465 (**2006**).
6. D. Wen and Y. Ding, *IEEE Trans. Nanotechnol.* 5, 220 (**2006**).
7. J. Buongiorno, *ASME J. Heat Transf.* 128, 240 (**2006**).
8. D. A. Nield and A. V. Kuznetsov, *Eur. J. Mech. B Fluids.* 29, 217 (**2010**).
9. D. A. Nield and A. V. Kuznetsov, *Int. J. Heat Mass Transf.* 52, 5796 (**2009**).
10. R. Chand and G. C. Rana, *Int. J. Heat Mass Transf.* 55, 5417 (**2012**).
11. J. W. Rauscher and R. E. Kelly, *Int. Heat Mass Transfer* 18, 1216 (**1975**).
12. T. J. Walsh and R. J. Donnelly, *Phys. Rev. Lett.* 60, 700 (**1988**).
13. S. Agarwal, B. S. Bhadauria, and P. G. Siddheshwar, *Spec. Top. Rev. Porous Med.* 2, 53 (**2011**).
14. B. S. Bhadauria and S. Agarwal, *Transp. Porous Med.* 87, 585 (**2011**).
15. D. A. Nield and A. V. Kuznetsov, *A Revised Model. Int. J. Heat Mass Transf.* 68, 211 (**2014**).
16. S. Agarwal, *Transp. Porous Media* 104, 581 (**2014**).
17. G. S. Agrawal, J. Lee, and Yadav, *Ain Shams Eng. J.* (**2015**), http://dx.doi.org/10.1016/j.asej.2015.05.005
18. S. Agarwal, P. Rana, and B. S. Bhadauria, *ASME J.* 136, 122501 (**2014**).
19. D. A. Nield and A. Bejan, Convection in Porous Media, 4th edn., Springer, New York (**2013**).
20. S. Chandrashekhar, Oxford University Press, Oxford (**1961**).
21. P. G. Drazin and W. H. Reid, Cambridge University Press, Cambridge (**1981**).
22. B. S. Bhadauria and P. Kiran, *Ain Shams Eng. J.* 5, 1287 (**2014**).
23. K. Khanafer, K. Vafai, and M. Lightstone, *Int. J. Heat Mass Transf.* 46, 3639 (**2003**).
24. G. Venezian, *J. Fluid Mech.* 35, 243 (**1969**).

Received: 25 August 2017. Accepted: 19 December 2017.